Collège Doctoral du Languedoc-Roussillon

THÈSE

Pour obtenir le grade de

Docteur

Délivré par l'Université Montpellier II

Préparée au sein de l'école doctorale Sciences Chimiques ED459
Et de l'unité de recherche UMR 5253

Spécialité : Chimie et Physico-Chimie des Matériaux

Présentée par Etienne LABALME

SYNTHESIS AND CHARACTERIZATIONS OF NEW FLUORINATED MEMBRANES BEARING PENDANT PHOSPHONIC ACID GROUPS FOR PEMFC APPLICATION

Va être soutenue le 17 décembre 2013 devant le jury composé de

M. J.P. HABAS, Professeur, UM2	Président du Jury
M. P. JANNASCH, Professeur, Université de Lund	Rapporteur
M. L. FONTAINE, Professeur, Université du Maine	Rapporteur
M. L.GUBLER, Chargé de Recherche, Paul Scherrer Institut	Examinateur
M. P.BUVAT, Docteur, CEA, Le Ripault	Examinateur
M. G. DAVID, Maître de Conférences, ENSCM	Directeur de Thèse

UNIVERSITÉ MONTPELLIER 2
SCIENCES ET TECHNIQUES

Table of Contents

General Introduction

The requirement of the world energy consumption is constantly evolving. The increase in short-term pollution, as well as the long-term depletion of fossil fuels such as oil, coal and uranium, mainly used today, must make a deep energy change. The ideal generator must be efficient, low-emission, adaptable to different uses, compact and quiet. The fuel cell is an electrochemical generator capable of converting chemical energy of a fuel gas (hydrogen, natural gas, methanol, ethanol, oil, biomass, or hydrides, for example) in the presence of an oxidant (oxygen of air) directly into electrical energy by way of a redox reaction. Thus fuel cell system occurs as a potential solution. During recent years, many research works have been carried out on the new technology development in order to use fuel cell as a new energy source. One of the main subjects of research was the amelioration of the proton exchange membrane performance, which is the heart of the fuel cell. Nowadays, the most used membranes are perfluorosulfonic polymers (Nafion®, Aquavion®…), which allow to reach the best performances in moderate range of temperatures between 25 and 80°C and high level of hydration with a required high relative humidity (more than 50% RH).

Nevertheless, in the automotive sector, fuel cell specifications were defined to be used nominally at 120°C with 30% RH and low pressure. Under these conditions, perfluorosulfonic membrane performances fall drastically due to loss of water. This implies the necessity to develop membranes with novel protogenic groups able to give proton conduction in low hydration condition and at 120°C. In these conditions, membranes bearing phosphonic acid groups seem to be a good potential candidate [1, 2].

Indeed, the proton conductivity of phosphonic acid polyelectrolytes was better than sulfonated polymers at elevated temperatures and in a dry state. This higher proton conductivity demonstrates the amphoteric character of the acid phosphonic groups associated to a proton transport by a Gröthuss mechanism [3]. Furthermore, phosphonic acid-functionalized polyelectrolytes permit to obtain material with low water swelling, which improve the mechanical stability during cycle of use.

Previous work performed by our team [4-6] involved the synthesis of partially fluorinated copolymer bearing phosphonic acid groups: poly(chlorotrifluoroethylene-*alt*-vinyl ether phosphonic acid) (Figure 1).

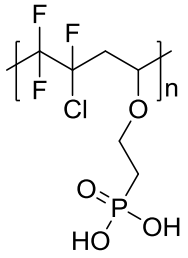

Figure 1 : poly(chlorotrifluoroethylene-alt-vinyl ether phosphonic acid) (poly(CTFE-alt-VEPA)

The polymer synthesis requires a multi-step pathway. Thanks to the acceptor/donor character of monomers used for the polymerization, the copolymer obtained showed an alternated structure[7] between fluorinated and phosphonic acid units, which allows the presence of phosphonic acid groups distributed along the copolymer. Interestingly, this polymer was used as proton exchange membrane fuel cell (PEMFC) and showed a very good thermal stability (up to 200°C). Furthermore, when decreasing relative humidity (RH) from 95 to 25%, the conductivity values decreased of only 1 order of magnitude, while the Nafion® conductivity drops of about 3 orders of magnitude in the same range. Furthermore, an increase of the temperature (from 90 to 120°C) leads to an increase of the proton conductivity by twice in the same range of RH. This result indicates that water molecules and phosphonic acid hydrogen bonding are involved in the proton conduction mechanism. Finally, the proton conductivity increases by 3 orders of magnitude by increasing ionic exchange capacity (IEC) (from 2.5 to 7 meq.g^{-1}) to reach 20 mS.cm^{-1} at 25°C and 95% RH. It was concluded that the high IEC is the key factor to significantly change the water sorption and, as a consequence, to increase the proton conductivity.

However, these membranes present some drawbacks. Indeed, the mechanical properties are too weak, especially at low RH where membranes are very brittle. And at high RH, the swelling of membranes is too high, therefore a breakdown of the membrane was observed. So, an improvement of the mechanical properties and a control of the swelling are necessary to consider the use of these membranes in a fuel cell. Thus, “MEMbranes FluorophOSniques pour PEMFC hautes temperatures” (MemFOS) project has been implemented. This project financially supported by the “Agence Nationale pour la Recherche” (ANR), gathers different coworkers:

-“Institut Européen des Membranes (IEM)”, which aims at developing phosphonated polymer membranes from plasma techniques.

-“Ingenierie et Architectures Macromoléculaires (IAM)”: The aim of researches consists to develop new fluoro-phosphonated membrane from the poly(CTFE-*alt*-VEPA), but also to perform the synthesis of structured (block or graft) copolymer.

-“Commissariat à l'énergie atomique et aux énergies alternatives (CEA) »: The main task of CEA concerns both the casting and the characterization, notably the proton conductivities and fuel cell test, of the different membranes performed by the IAM and IEM laboratories.

The aim of this PhD work is, to be used different methods in order to improve the physico-chemical performance of poly(CTFE-*alt*-VEPA), but also to propose synthetic routes for obtaining polymer block.

To do this, Chapter 1 of this manuscript will be dedicated to the literature review of techniques that will be used: cast of blend membranes and crosslinked membranes. We will also discuss the contribution of the use of block copolymer or graft on the physico-chemical properties of the membranes.

The second chapter will present the work carried out on the casting of blend membranes from a mixture of poly(CTFE-*alt*-VEPA) and a commercially available fluorinated copolymer. This chapter is mainly illustrated by a scientific article, which is currently being submitted to the journal "Journal of power sources."

The third chapter will present the work to implement a new technique for crosslinking fluorinated copolymer by a simple heat treatment. This new technique is illustrated by the crosslinking of model terpolymer. The fourth chapter will be devoted to the use of this new technique to achieve crosslinking of fluorinated copolymer carrying phosphonic acid groups. Characterization of the resulting membranes obtained from this fluoro-phosphonated crosslinkable copolymer and a commercially available fluoropolymer will be presented in this chapter.

The fifth and last chapter will be devoted to the synthesis of block copolymers from a RAFT strategy. This block copolymer will be obtained from a pre-synthesized phosphonated monomer and a commercially available fluorinated monomer.

References

1. Schuster, M.; Rager, T.; Noda, A.; Kreuer, K. D.; Maier, J., About the Choice of the Protogenic Group in PEM Separator Materials for Intermediate Temperature, Low Humidity Operation: A Critical Comparison of Sulfonic Acid, Phosphonic Acid and Imidazole Functionalized Model Compounds. *Fuel Cells* **2005,** *5* (3), 355-365.
2. Paddison, S. J.; Kreuer, K. D.; Maier, J., About the choice of the protogenic group in polymer electrolyte membranes: Ab initio modelling of sulfonic acid, phosphonic acid, and imidazole functionalized alkanes. *Physical chemistry chemical physics : PCCP* **2006,** *8* (39), 4530-42.
3. Parvole, J.; Jannasch, P., Poly(arylene ether sulfone)s with phosphonic acid and bis(phosphonic acid) on short alkyl side chains for proton-exchange membranes. *J. Mater. Chem.* **2008,** *18* (Copyright (C) 2013 American Chemical Society (ACS). All Rights Reserved.), 5547-5556.
4. Tayouo, R.; David, G.; Ameduri, B.; Roualdes, S.; Galiano, H.; Bigarre, J. Copolymers comprising phosphonates and/or phosphonic acid groups useful for fuel-cell membrane constituents. WO2011048076A1, 2011.
5. Tayouo, R.; David, G.; Ameduri, B., New fluorinated polymers bearing pendant phosphonic groups for fuel cell membranes: Part 1 synthesis and characterizations of the fluorinated polymeric backbone. *Eur. Polym. J.* **2010,** *46* (Copyright (C) 2013 American Chemical Society (ACS). All Rights Reserved.), 1111-1118.
6. Tayouo, R.; David, G.; Ameduri, B.; Roziere, J.; Roualdes, S., New Fluorinated Polymers Bearing Pendant Phosphonic Acid Groups. Proton Conducting Membranes for Fuel Cell. *Macromolecules (Washington, DC, U. S.)* **2010,** *43* (Copyright (C) 2013 American Chemical Society (ACS). All Rights Reserved.), 5269-5276.
7. Boutevin, B.; Cersosimo, F.; Youssef, B., Studies of the alternating copolymerization of vinyl ethers with chlorotrifluoroethylene. *Macromolecules* **1992,** *25* (11), 2842-2846.

Chapter I

Bibliographic review

1 Introduction

This bibliographic chapter will present the strategies that will be used in order to optimize the use of poly(CTFE-*alt*-VEPA). In the general introduction of this manuscript, we have seen that the work previously performed in the laboratory allowed to obtain proton conducting membranes with good potential for application in fuel cell. Indeed, this membrane is cast from an alternated copolymer carrying phosphonic acid groups and this copolymer possesses a high ionic exchange capacity (IEC) of 7 $meq.g^{-1}$. But, the synthesis used does not afford high molecular weight values for the copolymer. This low molecular weight is the result of transfer reaction which implies dead chain formation. Thus, membrane cast from this copolymer, with low molecular weight, leads to materials with low mechanical properties. These low mechanical properties are restrictive factors for the final application. Indeed, membrane plays a very important role in the heart of the fuel cell. Membrane allows the protons transport from the anode to the cathode, but it also plays the barrier role between the hydrogen and oxygen (or air) respectively present at the anode and the cathode. The existence of a pressure difference on either side of the membrane up to 1 bar requires that the membrane has the mechanical properties that allow to resisting at this pressure variation. In order to obtain membrane which possesses the sufficient mechanical properties, other synthetic strategies are therefore to be investigated. A technique based on the mixture of two or more different species of polymer to obtain a macroscopically homogeneous membrane, namely blend membrane, will be considered. Each of the polymers possesses special properties that we will find in the final material. In our case, we will use two polymers, the phosphonated copolymer for the proton conductivity properties and a fluorinated copolymer for the mechanical properties. So, the first part of this bibliographic review will be dedicated to the study of the scientific articles concerning the cast of blend membranes for a PEMFC use in order to improve the mechanical properties.

The water uptake and the swelling of the materials used as proton exchange membranes are an essential characteristic for the good operating of the fuel cell. As a reminder, the water molecules play a crucial role in the proton transport. Indeed, the water molecules will be assuring the proton transport between the acid groups via a vehicular mechanism. So, the membranes used need to possess a sufficient water uptake to assure the

transport of the proton. The water uptake implies a swelling of the membranes. Excessive swelling of a water uptake capacity can lead to a breakdown of the membrane and loss of mechanical properties. Always in the goal to improve physical-chemical properties of the membrane casting from the poly(CTFE-*alt*-VEPA), it may be interesting to control the ability of water uptake therefore, the swelling phenomena. Indeed, this copolymer possesses a high water uptake value of about 60%. In order to control the water uptake and the swelling of the membrane, cross-linking the polymeric membrane can be a solution. The crosslinking of a material will ensure a densification of the polymer network. This material densification is proportional to the crosslinking rate. So, with a judicious variation of the crosslinking rate, we can regulate the two essentials properties: the water uptake and the swelling. Lot of crosslinking reactions are possible and different activation methods exist to allow the crosslinking reaction. Thus, a bibliographic research combining the two key words “polymer and crosslinking “resulted in more than 2,500 articles. This is why the second part of this chapter will be devoted only to the description of different thermal crosslinking methods for PEMFC application

The third and final part of this chapter is devoted to the use of controlled polymer architecture. This part does not concern the optimization of the properties of the poly(CTFE-*alt*-VEPA). However, in the continuity of this work, we focus on the polymer having a part made of a fluorinated monomer, and another one from a phosphonated monomer. The use of a polymer having controlled architecture will induce a self-assembly of the material during the casting of the membrane. We will see in detail the impact of the structure on the transport of protons and thus the electrochemical performance of the membranes. For this, two types of architecture are commonly used: the block and graft copolymers. In both cases, the self-assembly of the material is due to a difference of hydrophobic / hydrophilic characters between different parts of the polymer. As the crosslinking of the polymer, the syntheses of block and grafted copolymers are widely used in the field of polymer chemistry. We are therefore only interested in describing the various works devoted to the synthesis of polymer for a fuel cell use with a fluorinated part or phosphonated part. This bibliographic review on the synthesis of structured copolymer will allow us to develop a strategy for obtaining model copolymer.

2 PEMCF produced from a blend strategy

2.1 Introduction

The element blend is commonly used in the material chemistry field in order to refer to the technique which consists in mixing the two polymers, to obtain a new material. This technique is used in order to optimize the performance of a material with good potential. By performing polymer blends wisely selected based on their properties, a final material with all the required properties for the intended application can be obtained. In the case of PEMFC, the blend technique is used to improve the mechanical properties but also the thermal properties or the proton conductivity.

2.2 Conductor polymer/fluorinated polymer blend

Fluorinated polymers are widely used in the field of materials because they are to their high value added polymers. In fact, they have very good chemical, thermal and mechanical properties that are essential for use in PEMFC. Therefore, they appear interesting to make membranes with on the one hand polymer bearing protogenic groups that will allow proton transportation through the membrane and on the other hand a fluoropolymer that will give the final material all the other required features.

The polyvinylidene fluoride ($(CH_2\text{-}CF_2)_n$) is the most used fluorinated polymer for the realization of PEMFC membranes. Various categories of polyvinylidene fluoride (poly(VDF)) are commercialized with a wide range of molar masses, but also as a copolymer with a few percent of other fluorinated monomers such as chlorotrifluoroethylene, hexafluoropropylene. Indeed, poly(VDF) is a highly crystalline polymer which implies very low solubility in common organic solvents. The addition of a second monomer has the direct effect of reducing the crystallinity rate and thus to promote its solubility.

The poly(VDF) has been widely used for the casting of “Direct Methanol Fuel Cell” (DEMFC) membranes. In this kind of fuel cell, methanol is the combustive and the

membrane's methanol permeability is a major problem. So, the blend technique is used in order to reduce this permeability.

The poly(VDF) is used to improve the performance of the reference membrane as Nafion®[1-3]. So as to decrease the methanol permeability of Nafion 117, Cho et al.[1] deposited a thin film of poly(VDF)/Nafion® onto the surface of a Nafion 117 membrane. The thin film deposition is performed by a simple immersion of the membrane in a solution of the two polymers. After the immersion, the membrane possesses a surface coating around 1µm thick which reduces considerably the methanol permeability but also improves the life time (Figure 2).

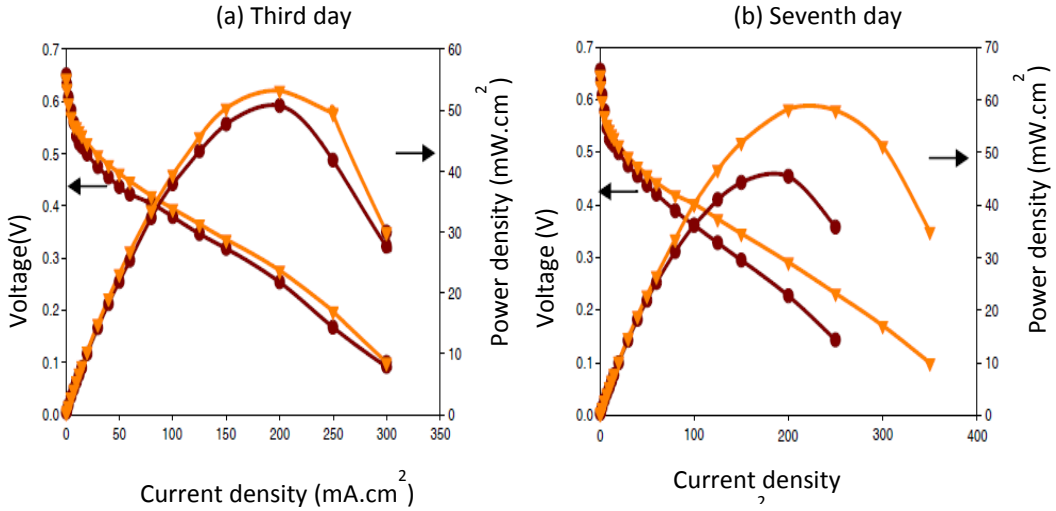

Figure 2: Polarization curves of coated Nafion (▼) and native Nafion 117 (●) at 30°C[1]

Many publications speak about the realization of proton exchange membrane (PEM) from a blend strategy with a conducting polymer and poly(VDF)[4-9]. It is the case of Wootthikanokkhan and co.[5] who performed blend membranes with poly(VDF) and sulfonated poly(ether ether ketone) (SPEEK). The results obtained (Table 1) demonstrate clearly the interest of this kind of membrane. Indeed, with 50% of poly(VDF) in the membrane composition, the methanol permeability is naught. On the other hand, the proton conductivity value is decreased by a factor 0.3 only, whereas the amount of conductor polymer is decreased by a factor of 2.

Table 1 :Proton conductivity and methanol permeability of various membranes SPEEK/PVDF[5]

Membranes	Proton conductivity (10^{-3} S.cm^{-1})	Methanol permeability (cm^2.sec^{-1})
PVDF	-	0
SPEEK/PVDF(50/50)	7.18	0
SPEEK/PVDF(70/30)	9.10	$5.34.10^{-9}$
SPEEK/PVDF(90/10)	8.99	$5.66.10^{-9}$
SPEEK	10.34	$2.35.10^{-7}$

In order to improve the miscibility between the poly(VDF) and the conducting polymer, a compatibilizer[4, 7, 10, 11] can be used. This compatibilizer is a block copolymer with one block highly miscible with the poly(VDF) and the other block highly miscible with the conducting polymer. The compatibilizer mostly used to make PEM with the poly(VDF) is the poly(methyl methacrylate) (PMMA) which is totally miscible with it[12]. From this result, different block copolymers such as the poly(styrene)-b-poly(methyl methacrylate)[4], or poly(methyl methacrylate-butylacrylate-methyl methacrylate) block copolymer (MAM)[11] were used to improve the membranes homogeneity. Indeed, from Figure 3, we can clearly observe the homogeneity difference between a blend membrane without and with a compatibilizer block copolymer. This is explained by the fact that the addition of compatibilizer reduces the interfacial tension existing between the PVDF and sulfonated polystyrene.

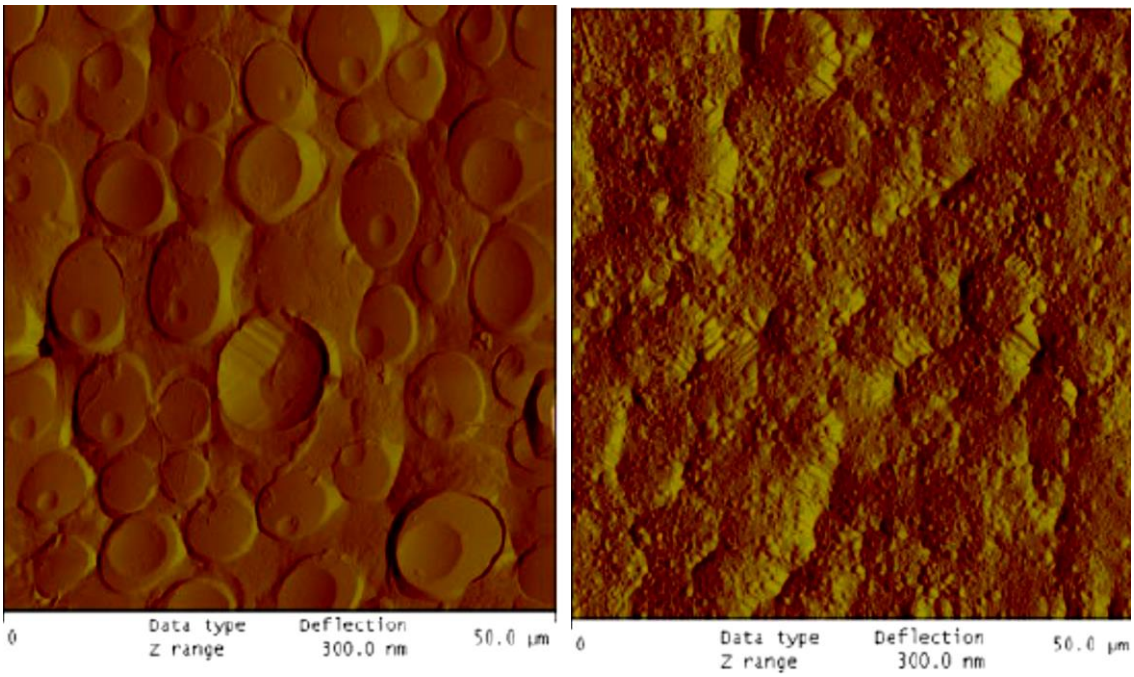

Figure 3 : Atomic force micrograph of the sulfonated polystyrene/PVDF blend membrane (40/60%) (left) and of the blend membrane compatibilized with PS-b-PMMA block copolymer(right)[4].

On the basis that poly(methyl methacrylate) allows to obtain an homogenous material with the poly(VDF), block copolymers having a poly(methyl methacrylate) block and a sulfonated poly(styrene) block were synthetized in order to be blended with the poly(VDF)[13, 14]. However, methacrylates are not stable in acidic conditions at high temperatures. So, for a PEMFC, which operates around 100°C, utilization of this polymer is limited.

Nevertheless, a blend membrane with a low poly(VDF) content, can be homogeneous without using any compatibilizer. Although the amount of poly(VDF) added is low (below 20%), effects on properties such as water uptake and swelling are clearly detectable. This kind of result are obtained for the blend between poly(VDF) and SPPESK (Sulfonated poly(phthalazinone ether sulfone ketone))[15] (Figure 4).

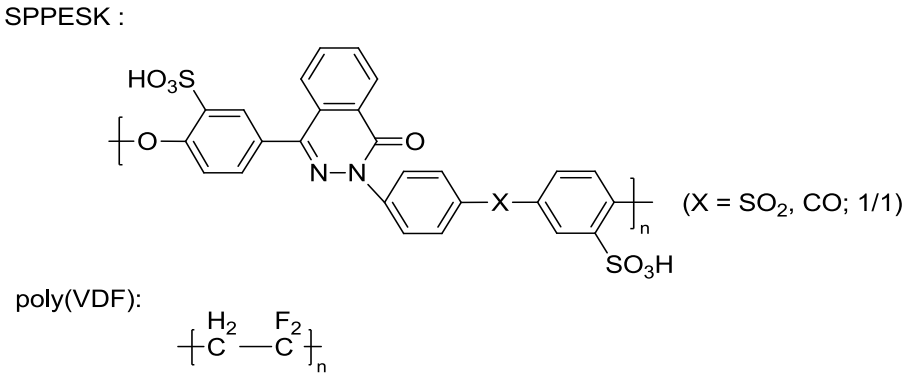

Figure 4: Chemical structure of poly(VDF) and SPPESK.

The most interesting results with this kind of blend were obtained with the membrane compositions of poly(VDF)/SPPESK 10/90 and 15/85. These content allow to have the best compromise between a low swelling to limit the physical breakdown of the membrane, and an interesting proton conductivity, around 4.10^{-2} S.cm^{-1}.

The poly(VDF) can be used as a matrix support to disperse organic microsphere bearing sulfonic acid groups[16, 17]. In order to ensure a good homogeneity of the membrane, a third polymer was added, i.e. the poly(vinyl pyrrolidone). Cohesion between the different polymers is achieved by hydrogen bonding between the various groups (Figure 5).

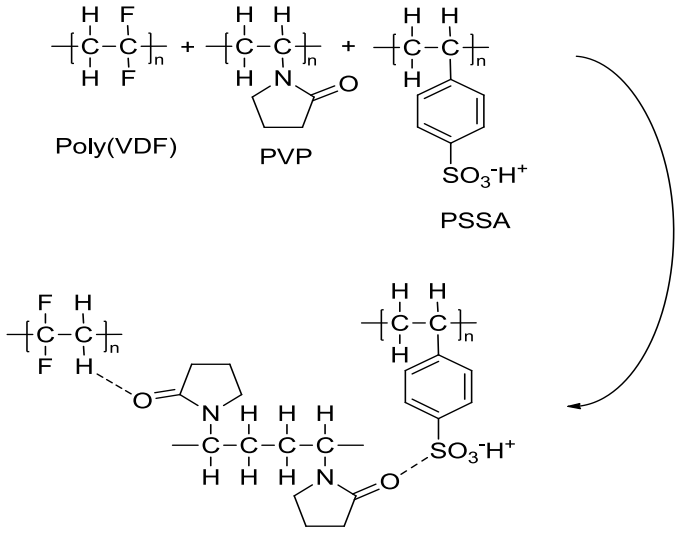

Figure 5: Chemical structure of poly(VDF)/PVP/PSSA membrane[17]

This type of membrane provides conductivities comparable to Nafion® 117 (0,012 $S.cm^{-1}$)[16] at room temperature.

The development of blend membrane from the poly(VDF) also allow to obtain a final material where the mechanical properties will be increased. Hofmann and co[18] thus demonstrated that the addition of poly(VDF), about 25%wt, during the casting of membrane realized from a polyphosphazenes bearing sulfonimide groups increased the mechanical properties. More recently, Hazarika and co[19] made blend membranes from poly(VDF-co-HFP) and poly(benzimidazole). The results of the mechanical analyses clearly show an increase of the blend membrane properties. Indeed, the elongation at break increases up to 25% with an addition of 10%wt of poly(VDF).

2.3 Conclusion

In order to highlight a conductive polymer with interesting properties but not sufficient to be used as PEMFC, the realization of blend membrane appears as a simple method. In addition, the use of commercial fluorinated polymers such as poly(VDF) improves performance at lower cost. Indeed, a price decrease of PEMFC membranes compared to Nafion® remains fundamental. However, one of the major difficulties of this technique is to obtain a homogeneous membrane, due to the highly hydrophobic nature of fluorinated polymers.

3 PEMFC from a crosslinking strategy

3.1 Introduction

Recall that the membranes used as separators and gas and too high gas permeability and low mechanical properties could result in a mixture of gas and cause a danger of explosion in the use of the battery. So, despite good properties (thermal stability, chemical stability, high conductivity), the use of a material can be limited by poor mechanical properties.

The crosslinking seems a very interesting technique to overcome this problem. Indeed, the crosslinking consists in reacting different chemical groups present on the main polymer chain in order to create links between the polymer chains. This generally results in the creation of thicker materials. So, the crosslinking is commonly used in the polymers area with the aim to improve the inherent material properties (thermic, mechanical, and physico-chemical). Different methods can be used in order to create inter-chains bonds: the formation of covalent bonds, ionic bonds or physical bonds (Van der Wasls or hydrogen bonds). In this bibliographic review, we only focus on the covalent bonds because they are the most stable.

3.2 The different crosslink techniques

The formations of the chemical bonds between the polymers chains can be activated and controlled by different methods:

- The use of different irradiation types (plasma neutral gas, UV rays, gamma rays ...);
- Thermal activation of the crosslinking reaction;
- The use of external reagent such as oxygen or water.

We only focus on the first two techniques mentioned above, which are the most commonly used especially in crosslinking of polymers for a PEMFC application.

3.2.1 *Crosslinking by irradiation technique*

The various techniques of irradiation crosslinking are shown below:

-Physically crosslinked membranes by implementation of a plasma neutral gas such as argon, helium or neon. In the ANR MemFOS project, which has funded this thesis, a work is accomplished in close collaboration with the European Membrane Institute (EMI) in Montpellier, consisting in membranes modification by plasma treatment. Indeed, this technique is used to obtain a modification of the surface properties of materials. We can cite, for example, the work of Follain and co[20] using the plasma treatment on commercial polymers to modify the water transport properties;

-The UV exposure is also used to perform crosslinking reactions. In this case, UV rays will allow the formation of radicals within the membrane that will be able to react with other functional groups present on the polymer chain, thereby forming inter-chain bonds. We can cite for example the work of Soulès and co.[21] who managed to crosslink membranes through the photo-polymerization of sulfonated polystyrene functionalized with two terminal azido groups with 1,10-diazide-1H, 1H, 2H, 2H, 9H, 9H, 10H, 10H-perfluorodecane (Figure 6).

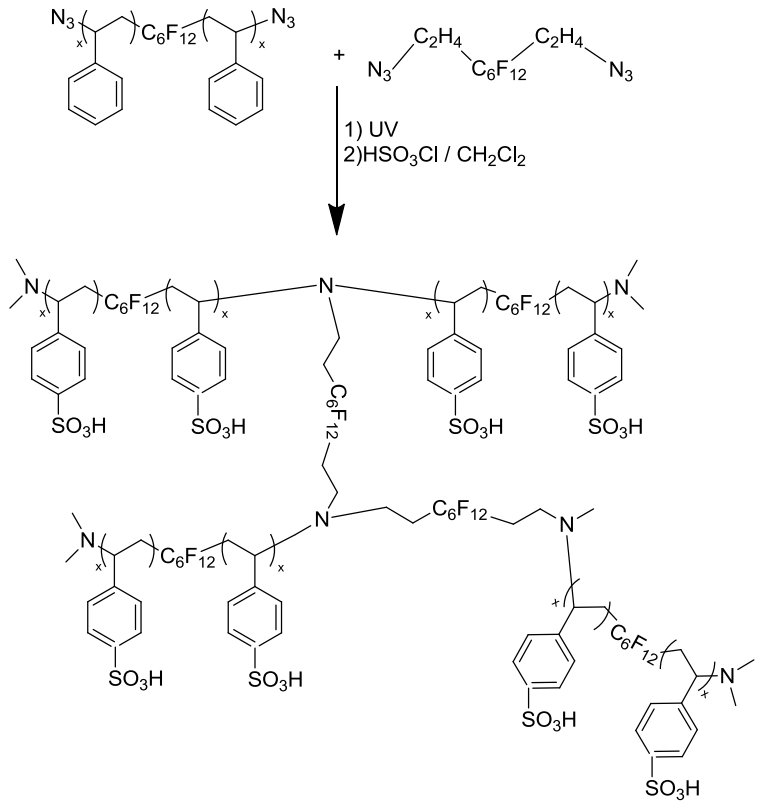

Figure 6 : Preparation of sulphonated fluorinated poly(styrene)-crosslinked electrolyte membranes from the photopolymerization of 1,10-diazido-1H,1H,2H,2H,9H,9H,10H,10H-perfluorodecane and telechelic diazido polystyrene, followed by sulphonation[21].

-as the last example of polymer crosslinking by irradiation, we can cite the work of Nikolic and co.[22] who performed the crosslinking of polyvinyl alcohol (PVA) by gamma irradiation. During the irradiation, there is a formation of radicals (-CH•-, -•COH-) which react with each other via recombination reactions and / or disproportionation to form inter or intra-chain bonds. The formation of these bonds generates a three-dimensional polymer network. This

technique, with a percentage of crosslinker between 3 and 5%, allows to annihilate the hydrophilic characters of PVA membranes.

We have seen that the radiation crosslinking provides materials which physical and chemical properties been irreversibly altered. However, this type of technique requires precise instrumentation that is complex to implement, especially for plasma treatment and gamma irradiation. For potential industrial development of the materials resulting from this thesis, it is necessary to develop easily implementable methods. Crosslinking by heating seems to be the best solution.

3.2.2 *Crosslinking by thermal activation*

Polymers crosslinking can also, and in most cases, occur via a thermal treatment. For this kind of crosslinking, we will draw up a state of the art of the different techniques used for the crosslinking polymer earmarked for a PEMFC application. All this techniques will be sorted according to the kind of chemical group used for the reaction. However, for all of them, the protocol is the same, the polymer is solubilized with or without a crosslinking agent, then the solution is casted on a support (glass plate, Teflon plate…), and placed in an oven to be treated appropriately.

3.2.2.1 Crosslinking by the protogenic groups

The polymer crosslinking can be realized by the protogenic groups present on the polymer chain. This kind of crosslinking is the most easier to implement, because the reactive group is already present on the polymer. Thus, it is not necessary to modify the polymer synthesis. However, the crosslinking by the protogenic groups has as direct effect to decrease their number, decreasing also the ionic exchange capacity (IEC). So, this sort of crosslinking is only to the polymers possessing a high IEC.

This reaction is used to crosslink the sulfonated poly(ether ether ketone)[23-25] (SPEEK). The crosslinking is the result of a simple thermal treatment. Indeed with temperature increase, a condensation of sulfonic groups is observed, leading to the formation of sulfone bridges (R-SO_2-R). The crosslinking degree can be easily controlled by

the duration and the temperature of the treatment. The result is then a decrease in water uptake, and methanol permeability. About the mechanical properties, the crosslinking reaction allows to increase the tensile strength, but also the material rigidity. So the elongation at break is lower. It is necessary to control crosslinking reaction in order to obtain a membrane with the mechanical properties required to resist to the difference in gas pressure on each side of the membrane. In contrast, a too high crosslinking degree annihilates the polymer proton conductivity.

The crosslinking can be also realized by a condensation reaction between sulfonic groups and polyols[26] (glycol ethylene or glycerol) (Figure 7). Such a reaction requires a heat treatment to obtain a sufficient level of crosslinking in order to significantly reduce the water uptake. Indeed, even if the swelling of the membrane is required especially in the case of sulfonated membrane, excessive water uptake causes an exfoliation phenomenon. The heating time must be between 48 and 60 hours at temperatures ranging from 125 to 150 ° C. The use of a low amount of crosslinking agent allows cross-linked membranes to have enough sulfonic groups available for the transport of protons and thus to obtain values for the proton conductivity around 2.10^{-2} $S.cm^{-1}$ at 25°C.

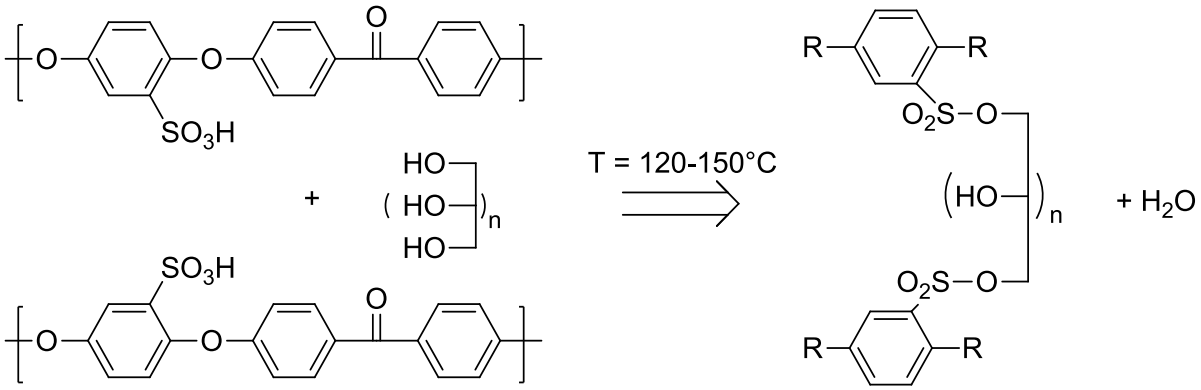

Figure 7: Possible reaction of SPEEK cross-linking[26].

The poly (arylene ether sulfone) (PSU) can be synthesized through a S-alkylation reaction between the sulfinic groups and the crosslinkers. This crosslinker is a dihaloalkane (diiodoalkane, dibromoalkane...)[27, 28](Figure 8). The length of the crosslinker carbon chain will influence the swelling values. Indeed, the higher the chain length the higher the space

between the polymers chains, thus allowing a higher solvent absorption. For this kind of reaction, the use of diodoalkane is more effective since it is more reactive.

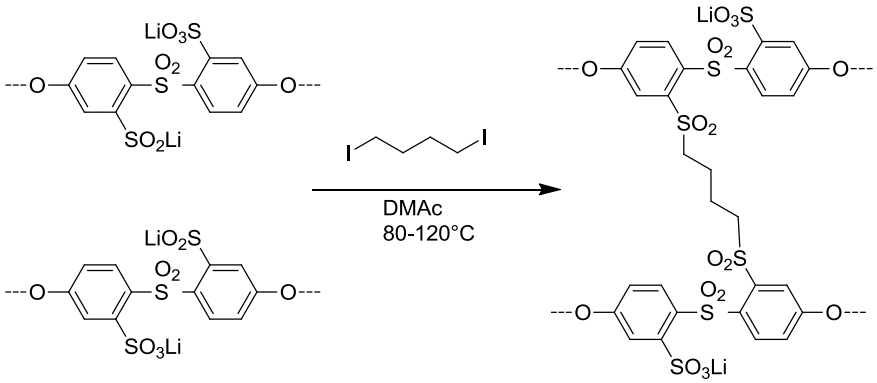

Figure 8:Covalent crosslinking of sulfinated-sufonated PSU membranes by S-alkylation of sulfinic units using 1,4-diiodobutane[28].

Given the reaction between the sulfonic acid groups an the 1-4,diphenoxybenzene, it is possible to crosslink the sulfonated poly(ether sulfone)[29](SPES). This crosslinking reaction occurs in the presence of phosphorus pentoxide-methanesulfonic acid (PPMA) which allows the formation of the R-SO_2^+ group (Figure 9). This kind of polysulfone with a high IEC (about 3,5meq.g^{-1}) possesses very low mechanical properties, especially in the dry state[30], while the mechanical properties of the crosslinked membranes are better. Indeed, the loss modulus (E') and the elastic modulus (E'') are stable up to 160°C, and this in a dry state.

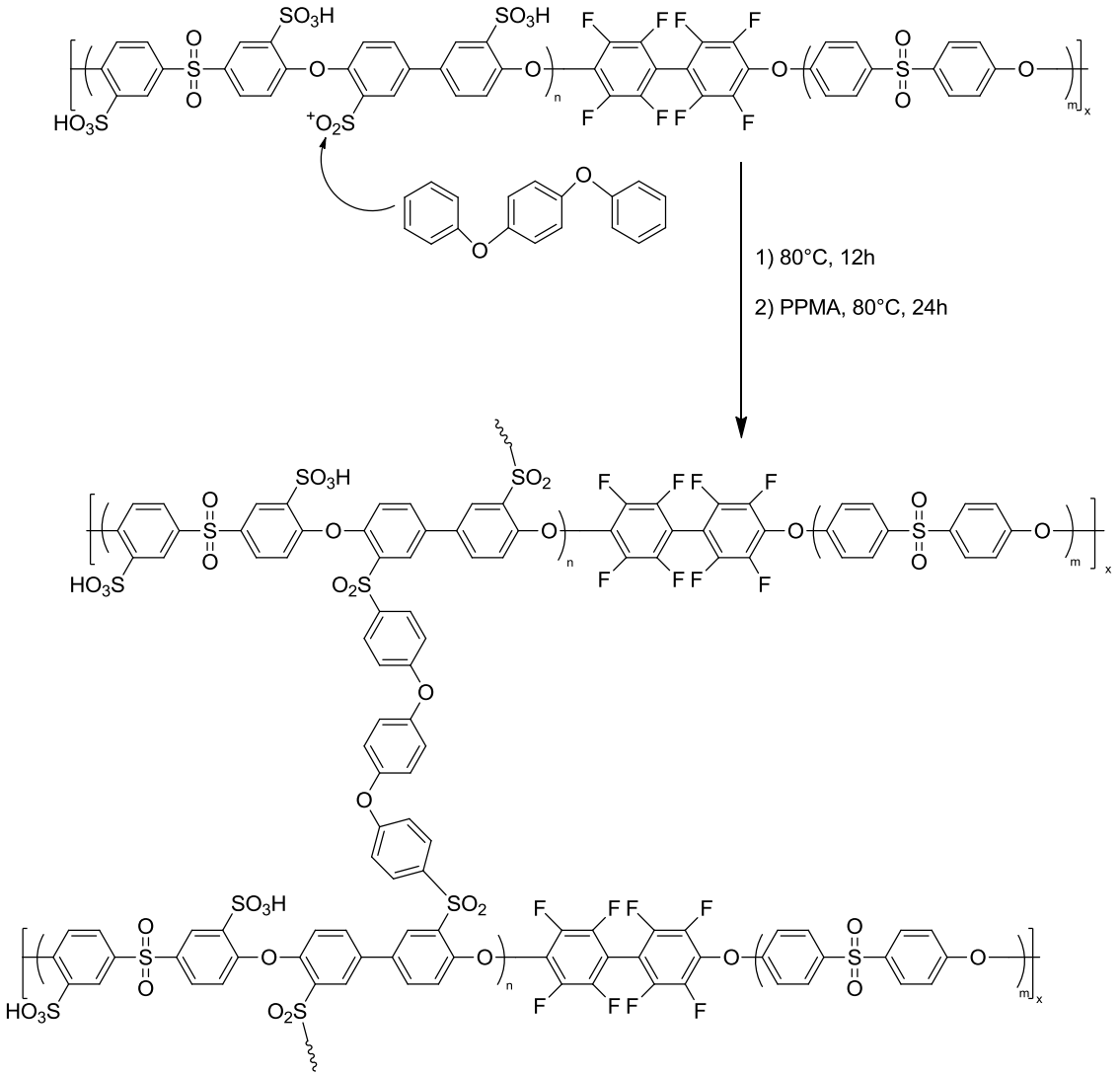

Figure 9: Crosslinking of SPES with 1,4-diphenoxybenzene[29]

3.2.2.2 Crosslinking reaction by other reactive groups

In order to not reduce the number of available protogenic groups, the crosslinking of the polymer can be achieved through another reactive function present on the polymer, it is therefore necessary to introduce this function during the polymer synthesis.

3.2.2.2.1 With a crosslinker bearing a protogenic group

Polymer crosslinking may be carried out by adding a crosslinker bearing a protogenic group. This crosslinking method has the advantage of increasing the number of protogenic groups within the polymer unlike the previous method (3.2.2.1).

For example, the poly(vinyl alcohol) (PVA) crosslinking can be performed via the use of sulfosuccinic acid[31-33] (Figure 10). The formation of bridges between the polymer chains occurs through the esterification reaction between the carboxylic acid groups of the crosslinking agent and the alcohol groups of the polymer. This crosslinking technique allows the suppression of the PVA hydrophilic nature and the addition of more sulfonic acid groups. The presence of such functions will allow to reach conductivity values of about 10^{-2} S.cm^{-1}. It is important to note that the heat treatment temperature as well as the amount of crosslinking agent have both a great influence on the final properties of the material. Thus, a significant amount of sulfosuccinic acid groups generates a high crosslinking degree, which will directly reduce the amount of water absorbed by the membrane and thus decrease the ability to conduct protons even if the number of protogenic groups is important.

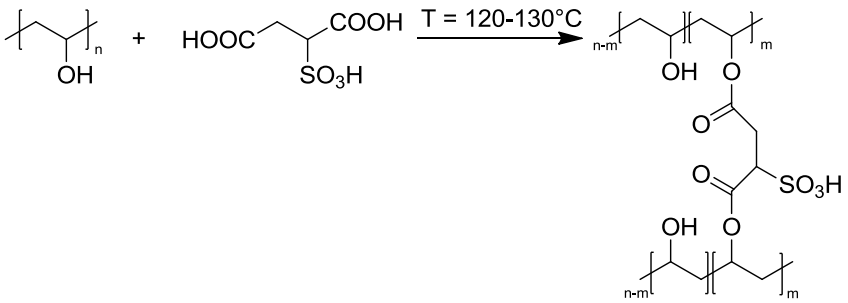

Figure 10: PVA-SSA crosslinking reaction scheme.[31]

The poly(arylene ether ketone) (PAEK) can be crosslinked by crosslinkers bearing a protogenic group[34] too. To do that, several steps are required. After these different steps, once the PAEK bearing of N-Hydroxysuccinimide groups will be synthetized, the crosslinking can be realized with 2,2'-benzidinesulfonic acid. The crosslinking reaction is illustrated on the Figure 11. Crosslinking the polymer with a crosslinker carrying two sulfonic acid groups does not affect the IEC or the proton conductivity of the different membranes. On the contrary, a

controlled crosslinking degree (between 0 and 20%) had a positive impact on the structure of the membrane. The Small Angle X-ray Scattering (SAXS) analyses show a decrease in the size of water clusters ionic domains. This will reduce the water uptake, and the methanol permeability and thus improve performances in terms of proton conductivity. Indeed, with the 20% crosslinking degree membrane fuel cell tests showed a power density of 71mW.cm^{-2}, a value slightly higher than the Nafion117 ® (66.5 mW.cm^{-2}).

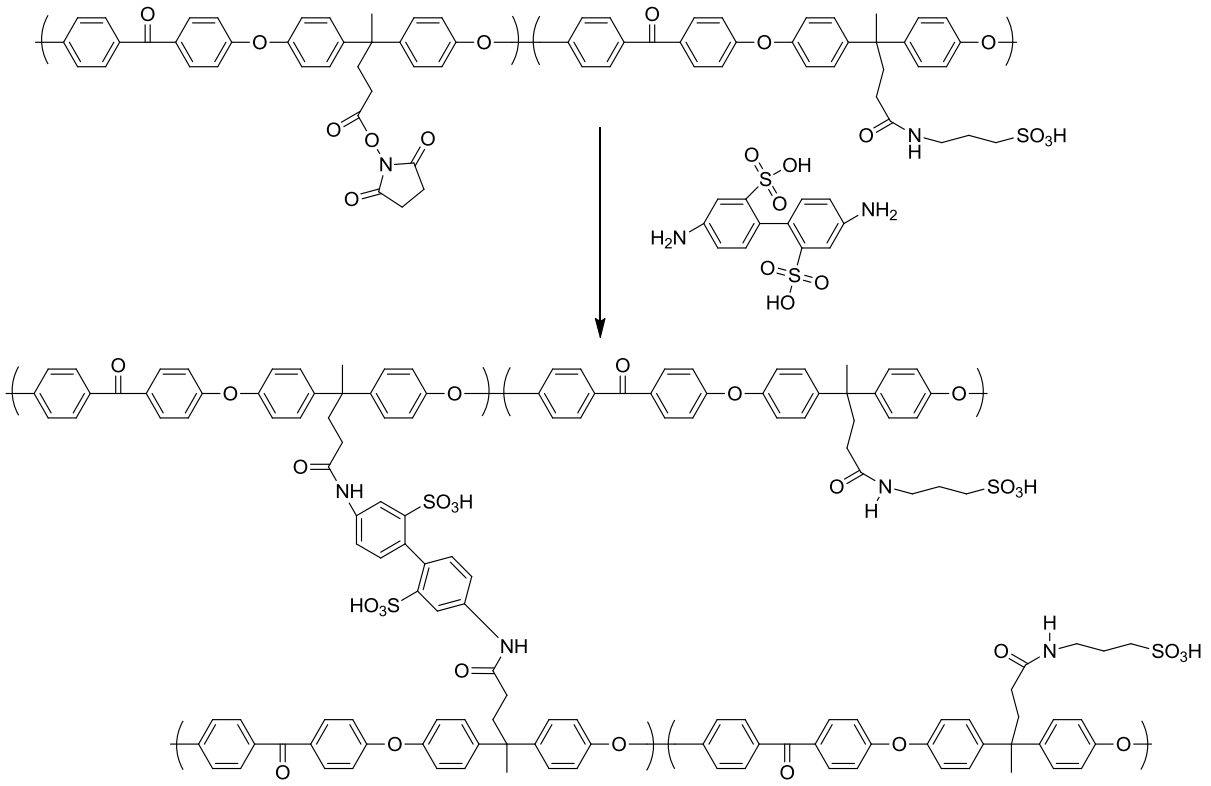

Figure 11: PAEK Crosslinking reaction with the 2,2'-benzidinedisulfonic acid[34].

Furthermore, Zhang and co[35] realized the crosslinking of PAEKs bearing fluorophenyl group. In this work, the crosslinker used is a poly (arylene ether sulfone) (SPAES) functionalized with two terminal phenolic groups. The crosslinking of the two polymers takes place through a substitution reaction between the phenolic groups and the fluoro groups (see Figure 12). Typically, polymers with many sulfonic groups have high swelling ratios and poor mechanical properties. This type of crosslinking eliminates these problems.

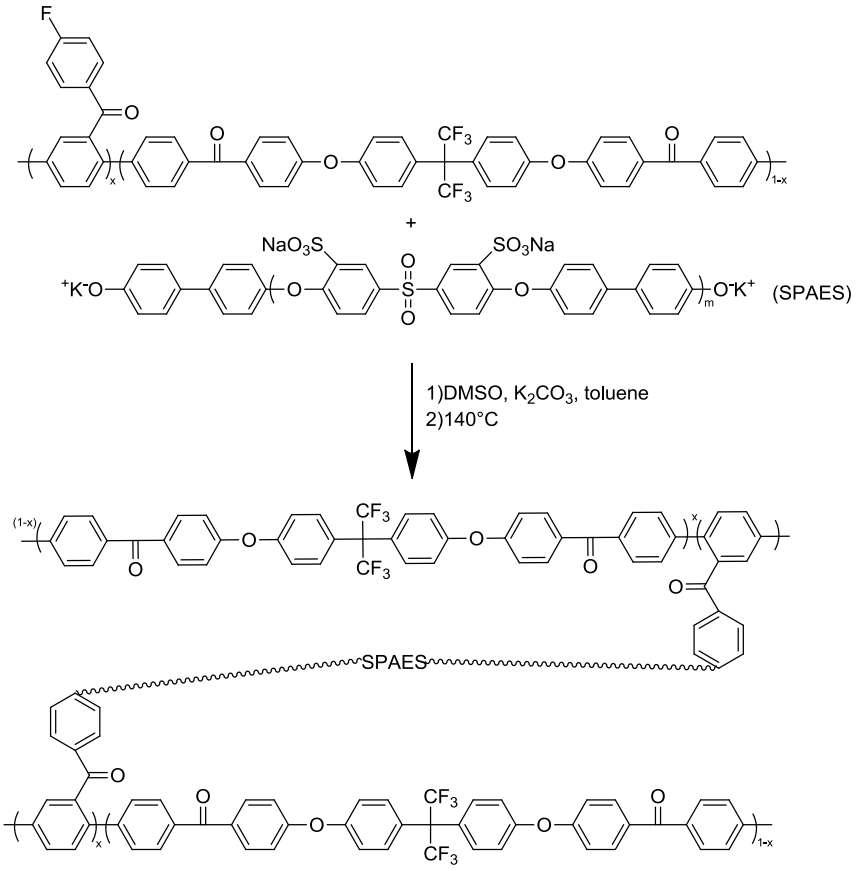

Figure 12:Crosslinking reaction of PAEK with the SPAES[35]

3.2.2.2.2 Crosslinkers without protogenic groups

This cross-linking technique is by far the most widely used, because a lot of molecules (mostly commercially available) can play the role of crosslinkers. Thereafter, we will describe succinctly the synthesis methods allowing the crosslinking, as well as its effect on the membranes properties.

Carboxylic acids are groups allowing crosslink. Indeed, Park and co[36] use this function to crosslink a SPAES. During the casting of the membrane, 5%wt of hydroquinone was added in order to promote an esterification reaction, which allows the inter-chain bridges formation (Figure 13). Although the crosslinking does not usually impact directly the conductivity values, in this case an increase of the cell test performances for high

temperature (120°C) is observed. Indeed, a high temperature increases the solubility of the polymer which inevitably affects the conductivity value; crosslinking can decrease the solubility of the polymer, leading to better performances.

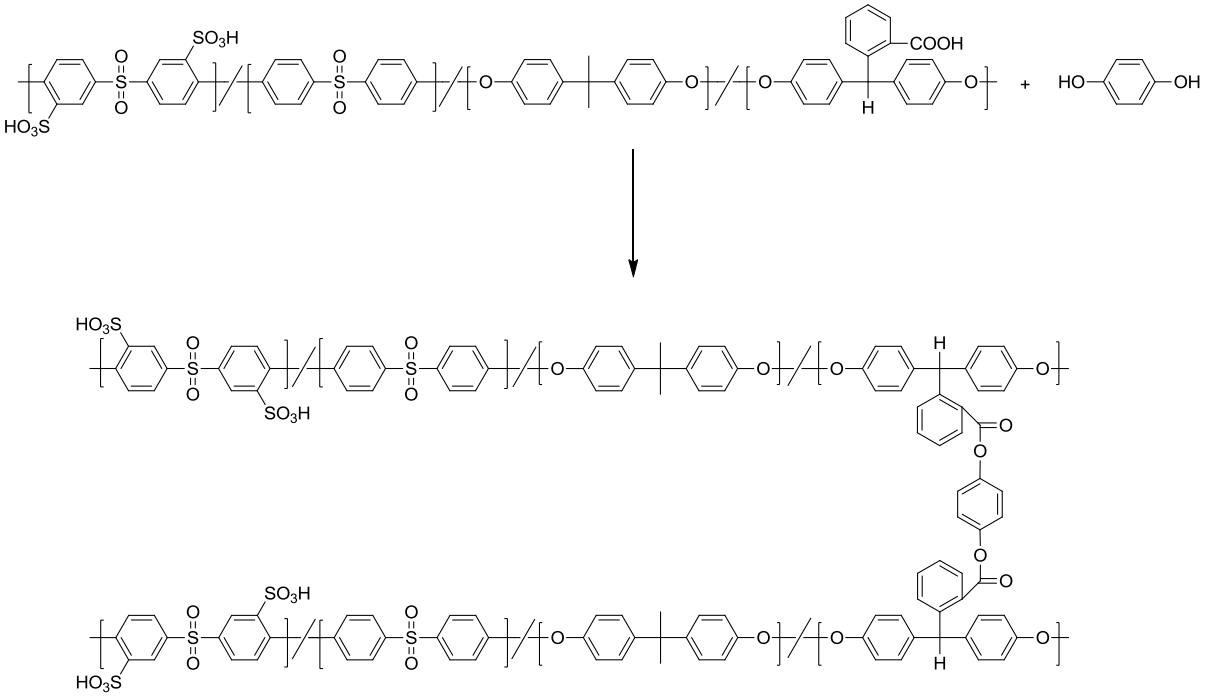

Figure 13: SPAES crosslinking reaction

SPEEK crosslinking can be achieved through the reaction between an epoxy and a hydroxyl group[37] (Figure 14). However, it is necessary to introduce the hydroxyl functions on the polymer chain. This is done by the reduction of the benzophenone groups. Once the hydroxyl groups are present, the crosslinking reaction is performed with a tetra epoxy molecule through a nucleophilic substitution reaction catalyzed by the triphenylphosphine (TTP). After the crosslinking, a clear drop in swelling value and methanol permeability is observed. Thus, the selectivity value, defined by the proton conductivity on the methanol permeability, is about three times higher than that of Nafion® 117.

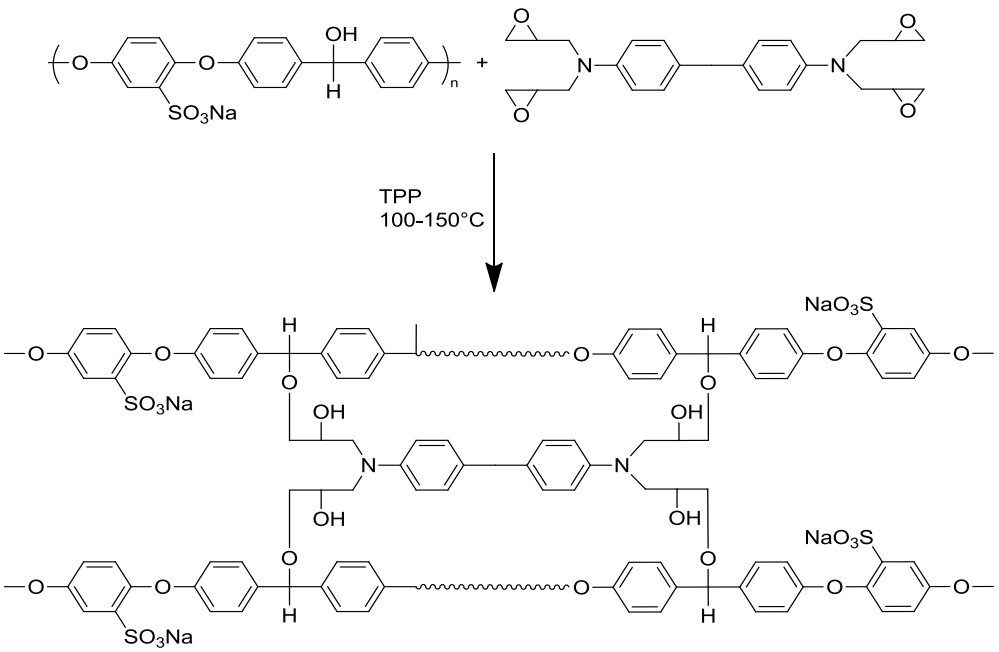

Figure 14: Crosslinking scheme of SPEEK with MY721[37]

Epoxy groups can also react with the carboxylic acid groups[38]. This kind of reaction is used to crosslink the SPAEK (Figure 15). However, it is necessary to introduce COOH group on the polymer. To do this, during the synthesis, 4,4-bis (4-hydroxyphenyl) valeric acid is added to the other monomers. The crosslinking reaction is achieved by simple heating treatment (150°C). After crosslinking, the characterizations carried out on the materials having different crosslinking degrees show improved mechanical strength, reduced swelling and therefore better proton conductivity at high temperatures.

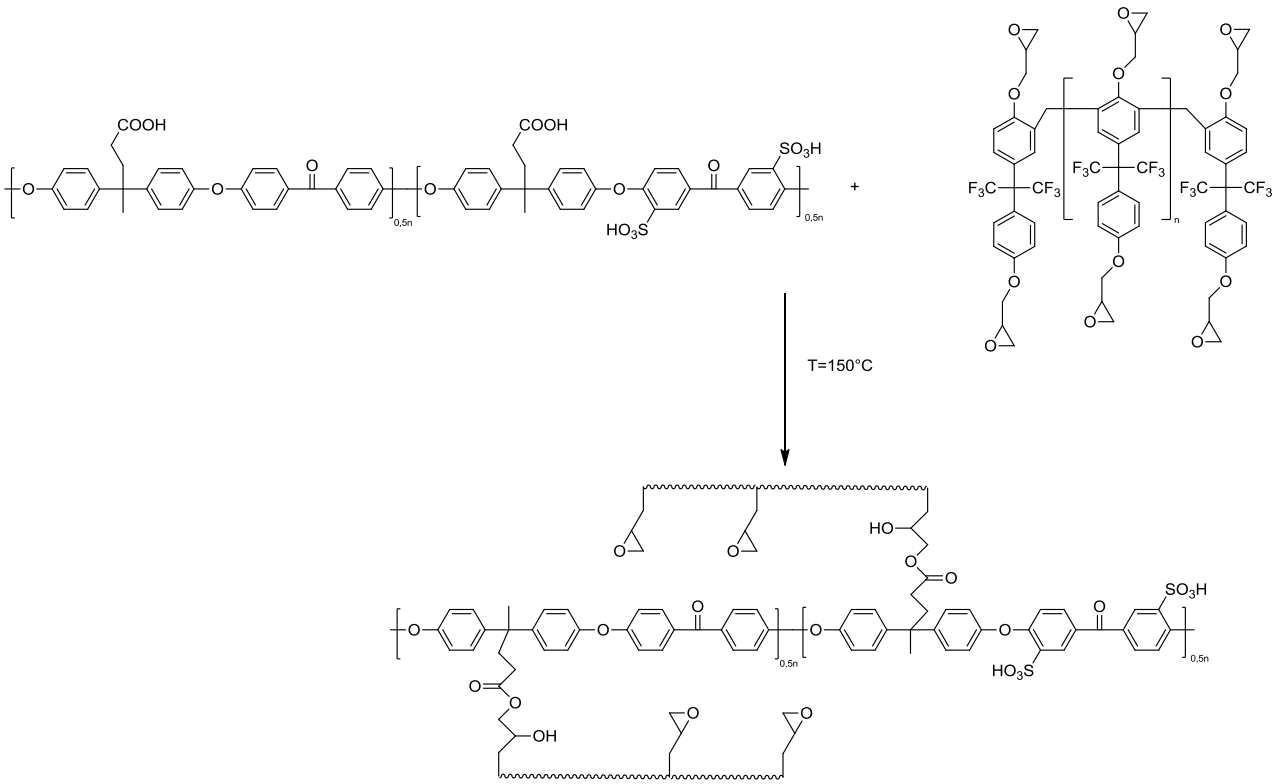

Figure 15: Possible schematic representation of crosslinked sulfonated poly(arylene ether ketone)s[38].

The use of Huisgen cycloaddition reaction, that is to say, the coupling between the alkyne and azide functions (Figure 16) allows the functionalization and crosslinking of poly (sulfone). However, before the crosslinking reaction, it is necessary to introduce the azide functions ($R\text{-}N_3$) onto the polymer chains[39].

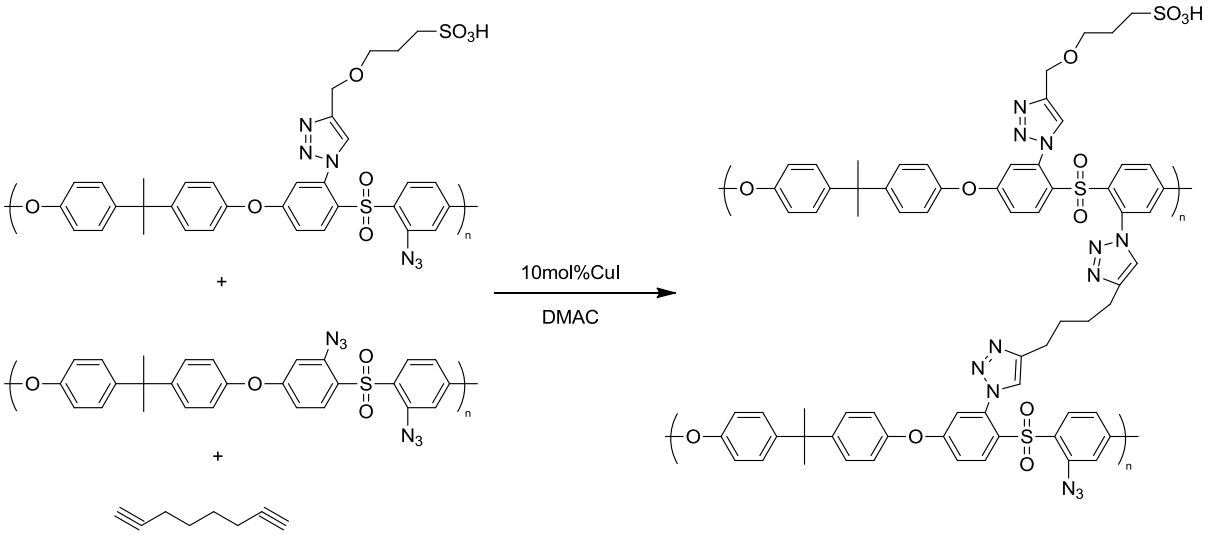

Figure 16:Polysulfone crosslinking via the click chemistry[39]

The crosslinking of SPAEK can be done using 3,3-diaminobenzidine (DAB)[40]. To do so, it is necessary to add to the synthesis of SPAEK the monomer 2,6-difluorobenzil. This monomer carrying two carbonyl functions will allow crosslinking via a condensation (Figure 17). Although the value of proton conductivity for the crosslinked membrane is slightly lower than the initial membrane, the mechanical properties are significantly improved.

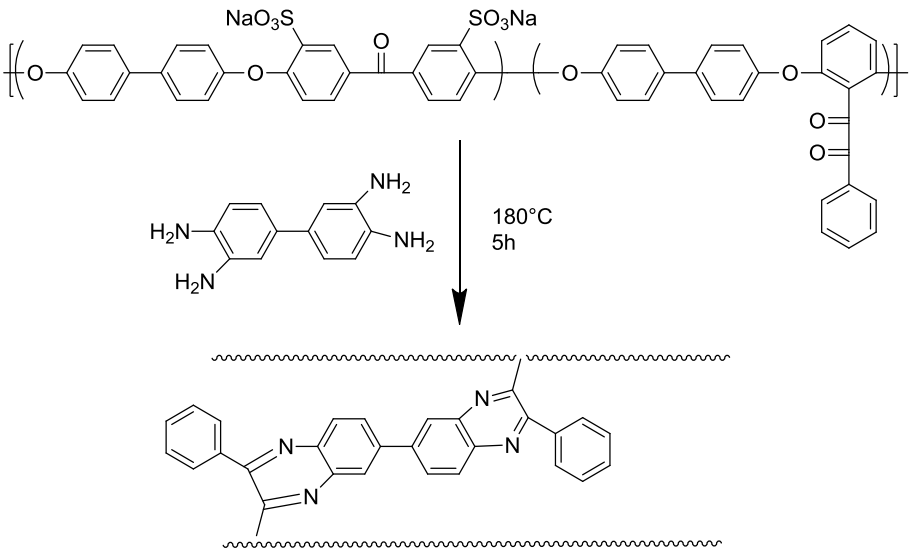

Figure 17 :Crosslinking scheme of SPAEK with DAB.

The 3,3'-diaminobenzidine (DABI) was also used to crosslink the poly(2,5-benzimidazole)[41]. This crosslinking is based on the reaction between the carboxylic acid terminal groups of the polymer and the primary amine of the crosslinker (Figure 18). The use of the benzimidazole groups for PEMFC requires a proton acid contribution. This contribution is realized by a phosphoric acid doping. To this end, the membrane is immersed in a phosphoric acid solution, and for the membrane cast from a linear polymer a high adsorption rate (above 80%wt) resulted in a progressive dissolution of the membrane. On the contrary, with the crosslinked membrane, the adsorption rate can be higher thant 90%wt coupledwith very good mechanical properties. This increase of the phosphoric acid amount in the membrane allows a small increase of the conductivity value.

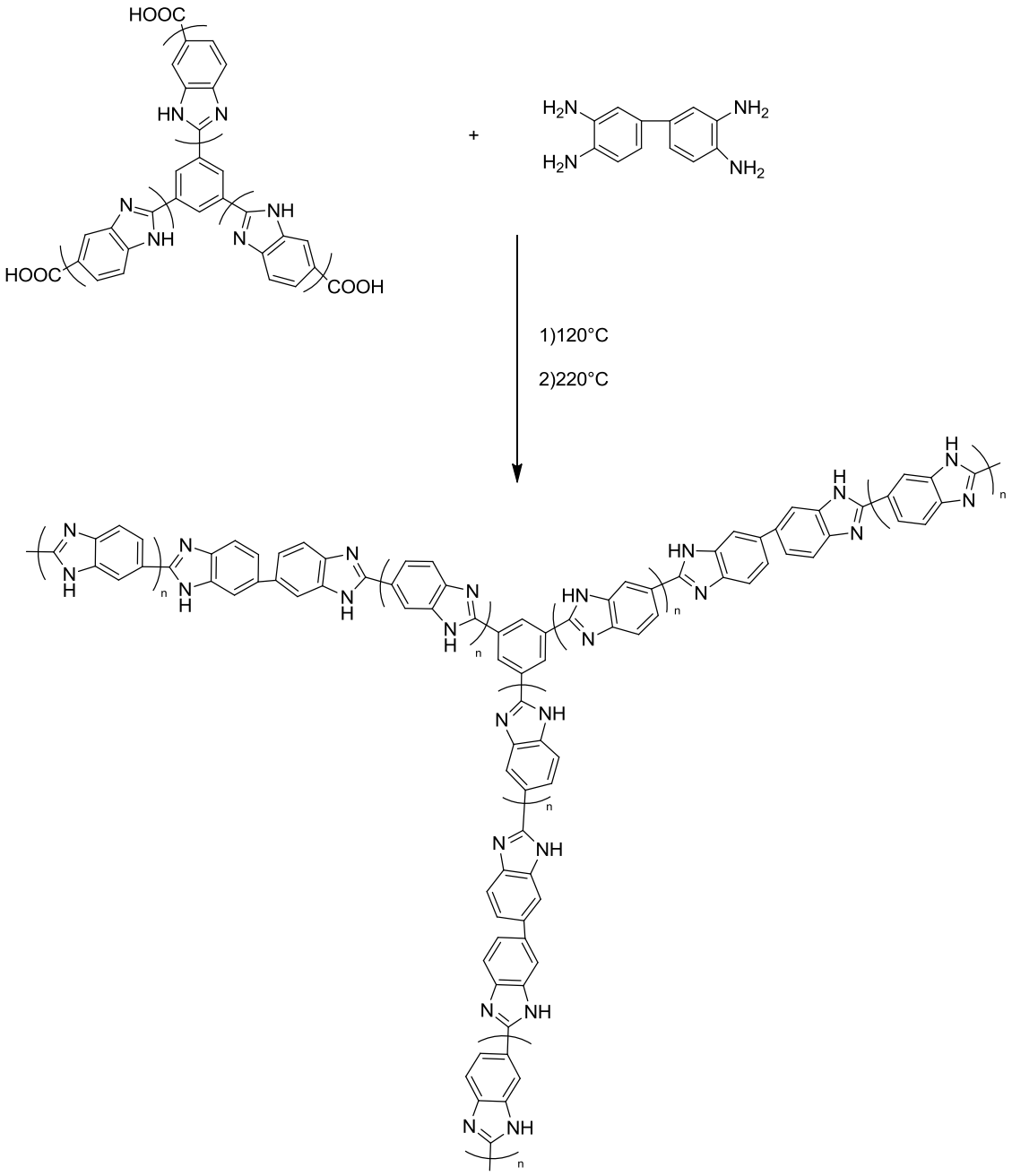

Figure 18: Crosslinking of poly(2,5-benzimidazole) with DABI[41]

The crosslinking of poly(benzimidazole) (PBI) can be realized by the nitrogen atom from the heterocyclic. Indeed, the presence of the reactive proton of the R-**NH**-R group allows different crosslinking reactions. For instance Lin and co. [42] crosslinked the PBI with the epoxy resin diglycidyl ether of Bisphenol A (Figure 20). The mechanism of this reaction is illustrated Figure 19[43]. This crosslinking technique allows to reach the same mechanical properties that non crosslinked membrane, and for a membrane twice less thick. In this way,

the membrane with a smaller thickness leads to a decrease in the resistivity during the proton transport in the membrane, leading to better performances during the cell tests.

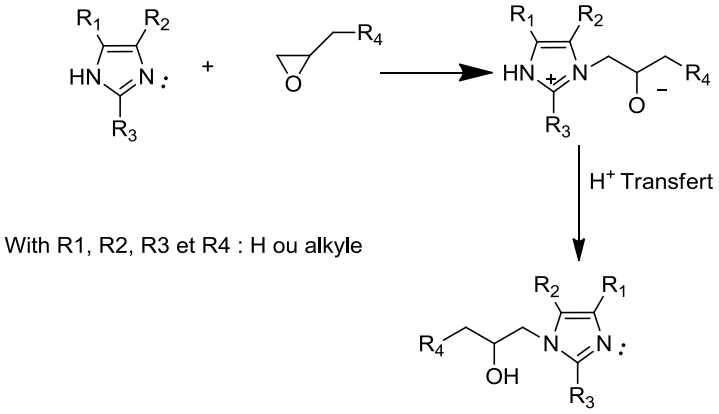

Figure 19: Mechanism of the reaction between the epoxy and imidazole groups[43]

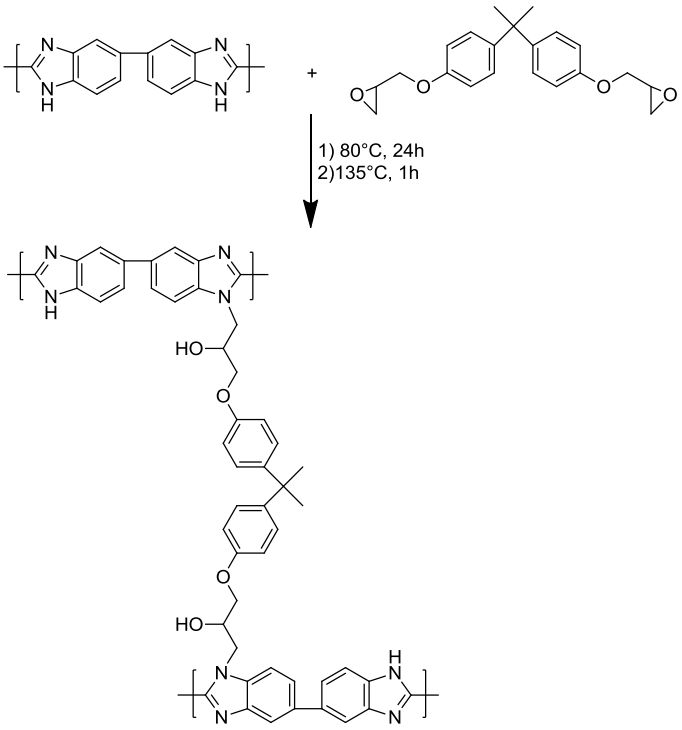

Figure 20: Crosslinked PBI with the diglycidyl ether Bisphenol A[42]

PBI can be crosslinked by using the p-xylene dichloride[44] (Figure 21). This crosslinking reaction is achieved by a simple heating treatment (120°C, 2h). This type of crosslinking leads to the casting of a porous membrane. This porosity helps to increase the

amount of phosphoric acid during doping. As discussed above, an increase in the amount of phosphoric acid leads to higher proton conductivity values.

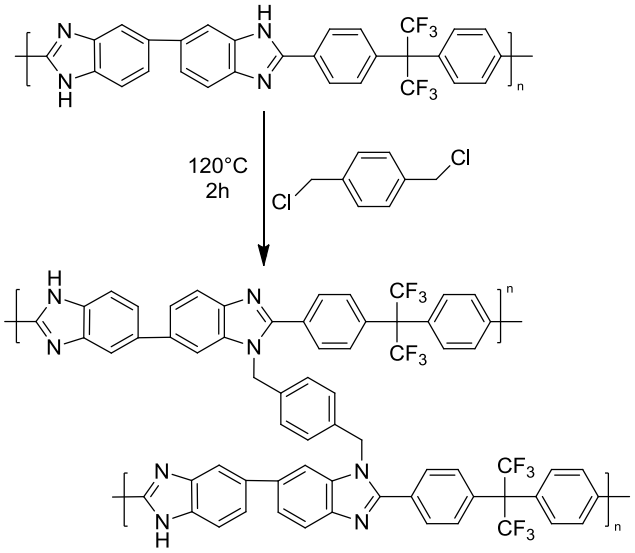

Figure 21 : Crosslinking of PBI with p-xylylene dichloride[44]

PBI may also be crosslinked using the divinylsulfone[45](Figure 22). This type of crosslinking greatly increases the thermal stability but also the chemical stability. Indeed, the Fenton test was applied to this kind of membrane. This test allows to evaluate the resistance of the membrane to radicals. With a crosslinking rate of 48% , the membrane is not deteriorated even after 440h of testing.

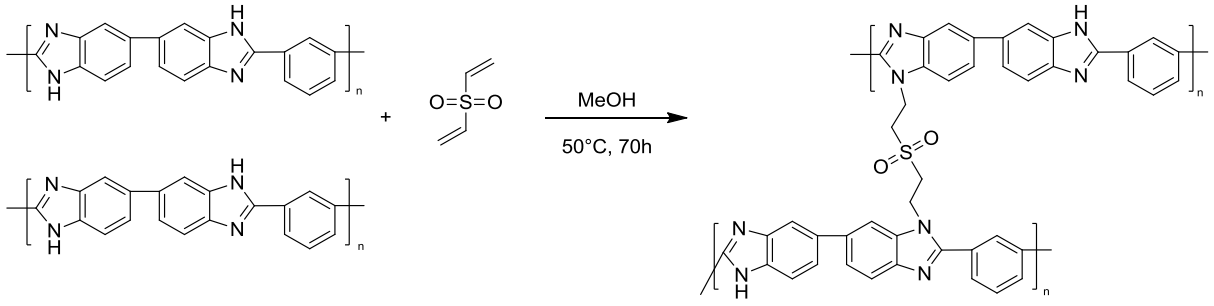

Figure 22: PBI crosslinking with the divinylsulfone[45]

Furthermore, the PBI crosslinking can also be accomplished by performing the radical polymerization between N-vinylimidazole and vinyl benzene grafted beforehand on PBI[46] (Figure 23). A major problem for doping of phosphoric acid is the release of the acid over time during use of the battery. Such crosslinking can halve the rate of acid leached over time.

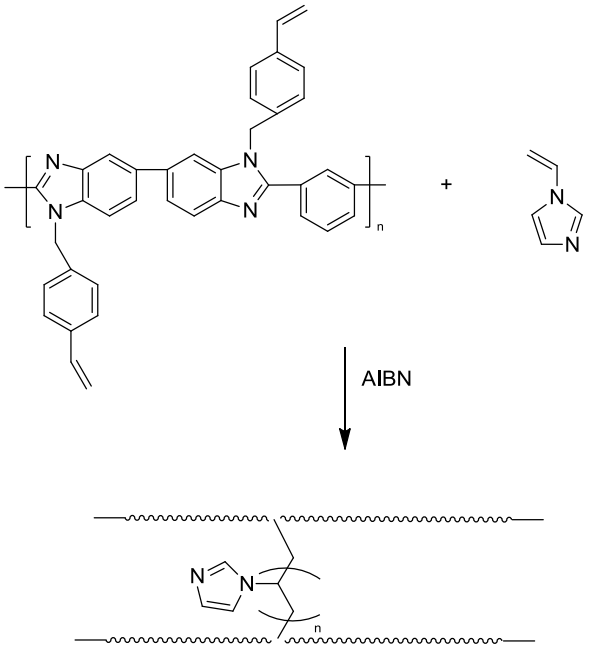

Figure 23: Crosslinking of PBI via N-vinylimidazole[46]

Han and co.[47] achieved SPEEK crosslinking by using a crosslinker compound such as benzimidazole groups bearing of COOH terminal group (Figure 24). Once the membrane is casted, it is heat-treated (180°C under vacuum for 12h) to condensate the R-COOH groups on the aromatic cycle (Friedel-Crafts reaction). This reaction is favored by the sulfonic acid functions, as well as by the elimination of the water molecules during the heat treatment, which is done under reduced atmosphere. The study of the proton conductivity as a function of the crosslinking degree shows an increase in conductivity to a threshold crosslinking value. Beyond this value, a drop in conductivity is observed due to excessive consumption of sulfonic groups during the crosslinking. Interestingly, even for a crosslinking ratio of 6.5%, the IEC of the membrane is decreased, which should lead to a decrease in conductivity values. However, the crosslinking of the membrane changes its structure. These changes result in phase segregation between the hydrophobic domains and hydrophilic domains.

Thus, a hydrophilic network is formed, composed of ion clusters, within the membrane, enabling the transport of protons. The impact of the membrane structure on the proton conductivity will be discussed in the next section.

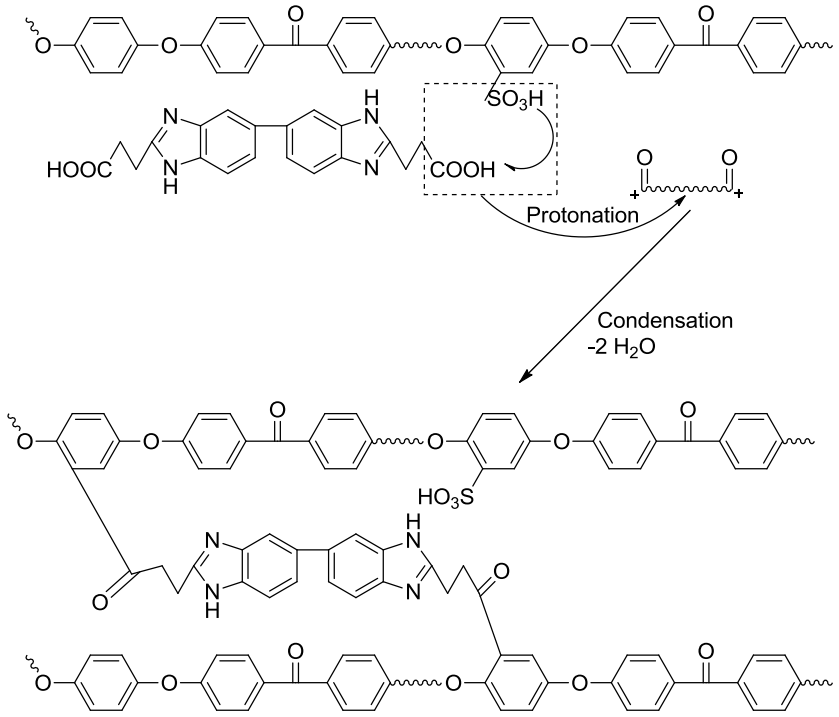

Figure 24 : Crosslinking scheme of SPEEK with l'alkyl-BI dimer[47]

The crosslinking of polymers can also be done by the reaction between an aldehyde and a hydroxyl group. The use of molecules bearing two aldehyde functions, such as glutaraldehyde, will allow the creation of inter-chain bridges through the acetalization reaction between aldehyde and alcohol functional groups[48, 49]. This reaction is favored at high temperatures, and is catalyzed in the presence of acid (HCl). Although the acetalization reaction is reversible in concentrated acid environment (pH = 0), the tests on this type of crosslinked polymer show that the proton conductivity does not decrease over time, this over a period of 240 and 120 hours respectively at temperatures of 25 and 50°C[48].

One of the few examples of phosphonated polymer crosslinking is the crosslinking of phosphonated poly (N-phenylacrylamide) (PDPAA)[50]. For this, the crosslinker used is hexamethoxymethylmelamine (CLYMEL). This is an electrophilic substitution reaction

between the aromatic moiety of PDPAA and carbocation from CYMEL, created in the presence of methane sulfonic acid (Figure 25). Although this kind of membrane provides good conductivity values at high RH, a drop of these values was observed when the RH decreases, being due to the sharp decrease of water swelling after curing.

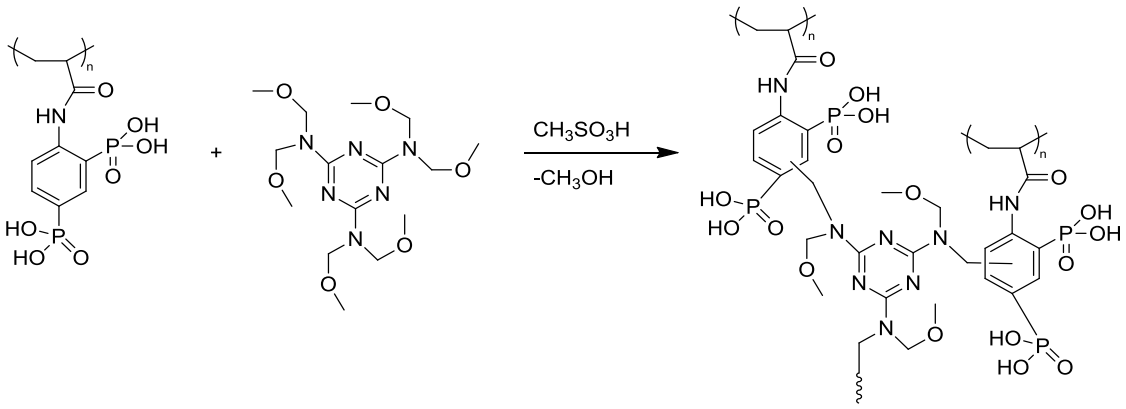

Figure 25 : Crosslinking scheme of PDPAA with CLYMEL in presence of methane sulfonic acid.

3.2.2.3 Polymer crosslinking without crosslinker

Some reactive functions can lead to crosslinking reactions by a simple heat treatment. During the synthesis of the polymer, it is only required to introduce the reactive group, and heat treatment for the casting of the membrane will also allow crosslinking.

Crosslinking of the polymer can be achieved by reaction of functional groups present at the chain end. This technique has the advantage of not changing the initial polymer synthesis since the functionalization is ensured by the chain end.

Presence of alkene functions at the chain end also allows the polymer crosslinking. For example, coupling of alkene/azide functions is used to obtain crosslinked polymers. This technique was used for the crosslinking of sulfonated poly (ether sulfone)[51]. The presence of hydroxy groups at the chain end, due to the polycondensation reaction, allows the introduction of allyl functions through a Williamson reaction. The crosslinking technique is based on the use of a crosslinking agent bearing, at least, two azide functions to form of

interchain bridges. Crosslinking of the polymer provides a better proton conductivity at high temperatures (50-100°C), due to a better internal structure of the material.

We can also include the coupling of alkyne functions, situated in alpha position of an aromatic group to form an aromatic ring. This technique is used for the crosslinking of sulfonated poly (fluorinated aromatics)[52, 53]. The coupling of the alkyne function requires a simple heat treatment (250°C for 100 min) (Figure 26).

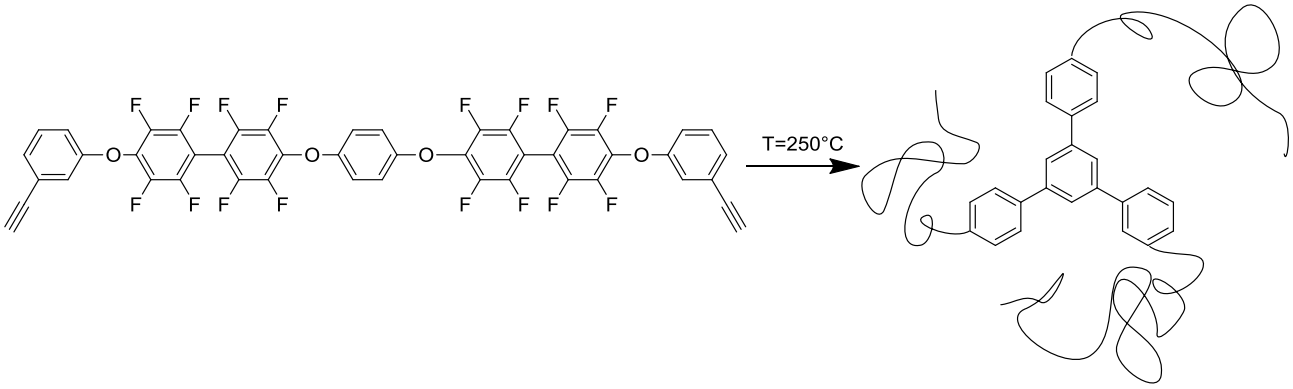

Figure 26: Crosslinking scheme of alkyne functions[53]

Vinyl groups allow also to perform the crosslinking without any additional compound. Indeed, in the presence of these functions, crosslinking can be done by introducing a thermal initiator such as benzoyl peroxide (BPO)[54] and heating. This is the case for example of poly (arylene ether sulfone) for which a monomer bearing allyl functions (3,3-diallyl-4,4-dihydroxybiphenyl) was added during the copolymerization (Figure 27). To do this, the BPO is added to the solution prior to the casting and the crosslinking reaction is activated by heating (about 120°C for 48h). This type of crosslinking reduces the swelling and methanol permeability without sacrificing conductivity values.

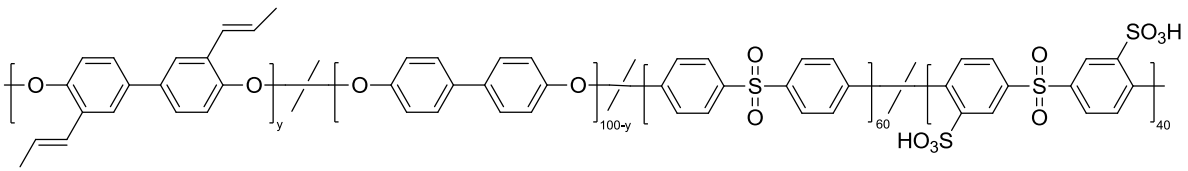

Figure 27: poly(arylene ether sulfone) bearing allyl functions[54]

Coupling reaction between two perfluorinated vinyl ether functions also enable polymer crosslinking. It is used in the case crosslinking aromatic fluorinated polyether[55]. The crosslinking scheme is as follows (Figure 28).

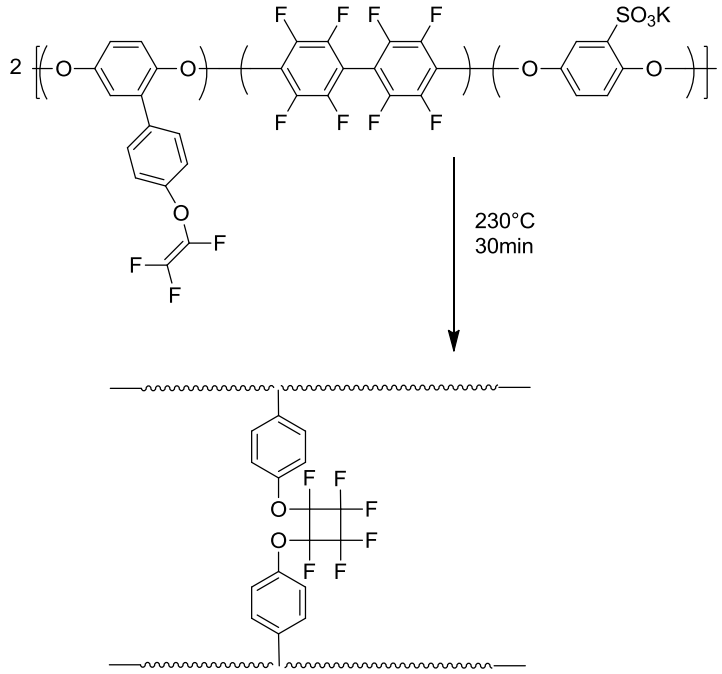

Figure 28 : Crosslinking by vinyl perfluoronated functions coupling[55]

SPEEK was also crosslinked by a simple heat treatment[56] (Figure 29). To this end, it is necessary to have the presence of hydroxyl functions on the polymer chain. This hydroxyl functions were obtained by benzophenone groups reduction. Once the benzhydol groups are present, the crosslinking is done via an electrophilic substitution in acidic conditions. Two kinds of mechanism are possible.

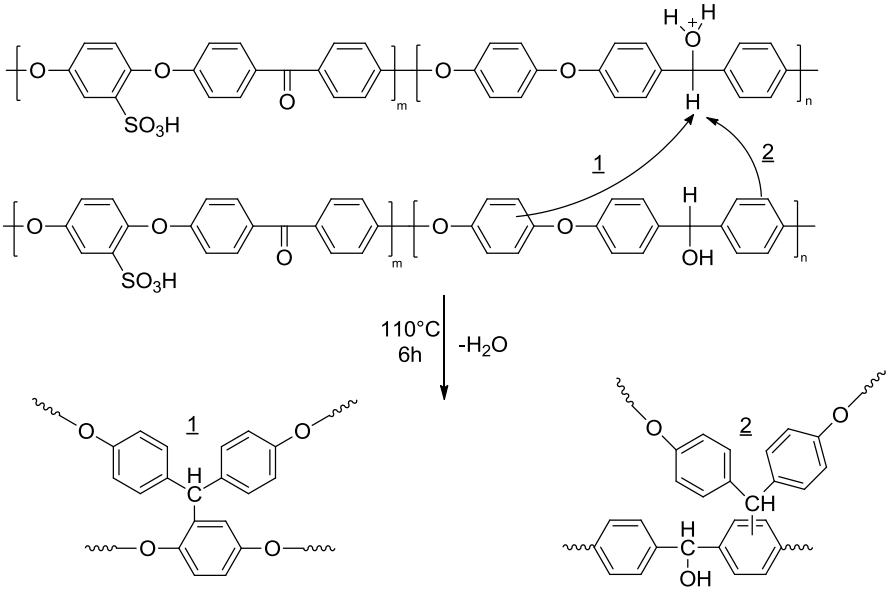

Figure 29 :Schematic representation of the postulated crosslinked structure[56]

3.3 **Conclusion**

Many techniques to crosslink polymers for a PEMFC application are available in the literature. The crosslinking will allow the modification of essential properties such as the polymer solubility, the degree of swelling or the water uptake. However, it is important to realize that the crosslinking of the polymer must remain moderate and controlled to make sure that it is not at the expense of other properties. In fact, a too high crosslinking degree will, for example, have an adverse effect on the mechanical properties due to an increase degree of membrane rigidity. A drastic reduction in the conductivity is also observed if the crosslinking is through protogenic groups.

4 PEMFC from structured polymers

4.1 Introduction

One of the main problems limiting the development of membranes for PEMFC is the low level of proton conductivity on the temperature range used, namely 50°C to 130°C. In order to improve the proton conductivity of the membranes, it is necessary to improve the proton transport within the membrane. As a reminder, the proton transport in the membrane takes place via two mechanisms:

-a proton hopping mechanism, where the transport is realized through the acid groups;

-a vehicular mechanism, where the transport is realized through water molecules.

It is therefore necessary to synthesize polymers whose architecture will help to promote these mechanisms. In this goal, the polymer needs to possess a hydrophilic and a hydrophobic part. In this way, during the casting, phase segregation will take place allowing the formation of hydrophilic and hydrophobic areas.

This segregation phenomenon is found in the Nafion® type membranes. Indeed, membranes possess a perfluorinated main chain on which are grafted fluorinated pendant chains bearing terminal sulfonic acid groups (Figure 30).

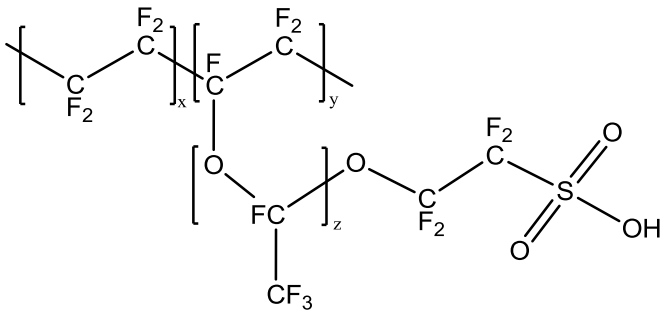

Figure 30: Nafion® structure

When the Nafion® membrane is in a hydrated state, the water molecules join together around the sulfonic acid groups to form a hydration sphere. Large numbers of water molecules constitutive of these hydration spheres will form clusters and the juxtaposition of the acid groups will allow to create a network of water channels in the membrane. The clusters size can be determined by SAXS analyses, and thereby define a network model of the water cluster (Figure 31) thus promoting the transport of protons. The presence of three areas can be noted on the Figure 31 :

-the area A, which corresponds to the hydrophobic area composed of the fluorinated material;

-the area B, which corresponds to the channels connected the ionic clusters. This region is often considered as poor ionic species;

-the area C, which corresponds to the ionic clusters constituted by the sulfonic acid groups and the water molecules.

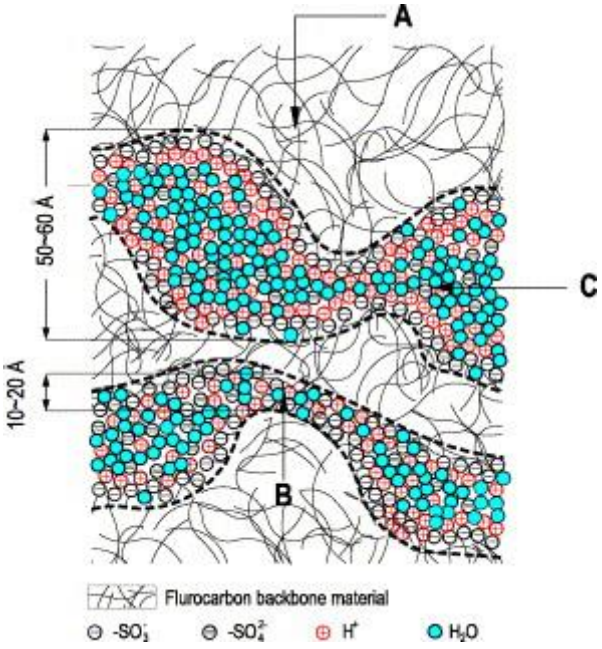

Figure 31 : Representation of the water cluster networks in the membrane Nafion®[57]

However, recent studies demonstrated the importance of controlling the formation of this network because the properties are highly dependent on the type of network that is

formed. Indeed, Beers and co[58] show that the size of the different areas (B and C) involve significant differences in the conduction properties of the membrane.

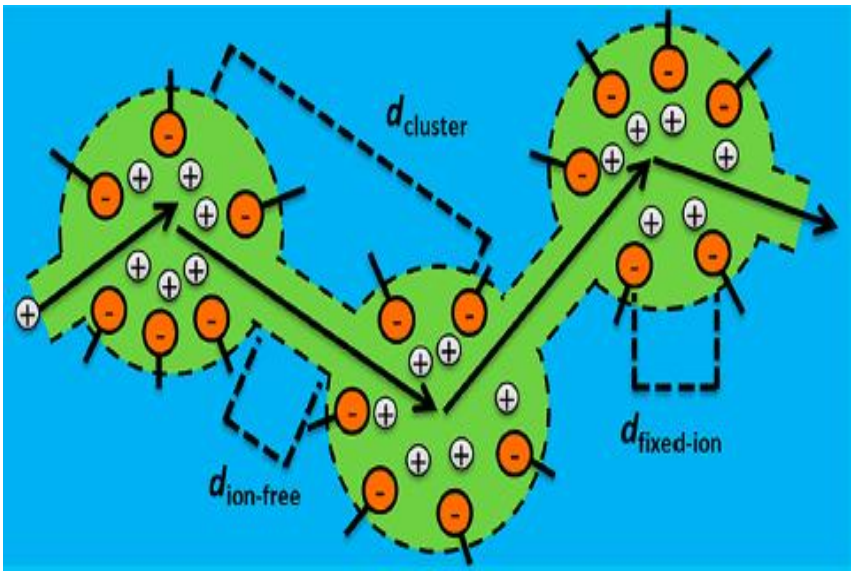

Figure 32 : network ionic cluster schematization[58]

Proton transport is necessarily from a cluster to another, so the protons must cross areas composed mainly of water molecules (Area B). However, having to cross an ion-free zone requires crossing a high energy barrier. So, it seems interesting to make membranes without these ion-free channels resulting from clustering phenomena within the membrane. These results are based on the work of Manning[59], showing that the distance between two ions from a pair in a hydrated PEM is 0.7 nm, this distance is called the Bjerrum distance. In order to overcome the energy barrier due to the lack of ions in the inter cluster channels, structuration of the membrane is required to obtain an inter-cluster distance of the order of 1 nm. In order to synthesize a polymer that can provide this structuration to the membrane, two types of polymers having a controlled architecture can be used, i.e. graft polymers and block polymers (Figure 33).

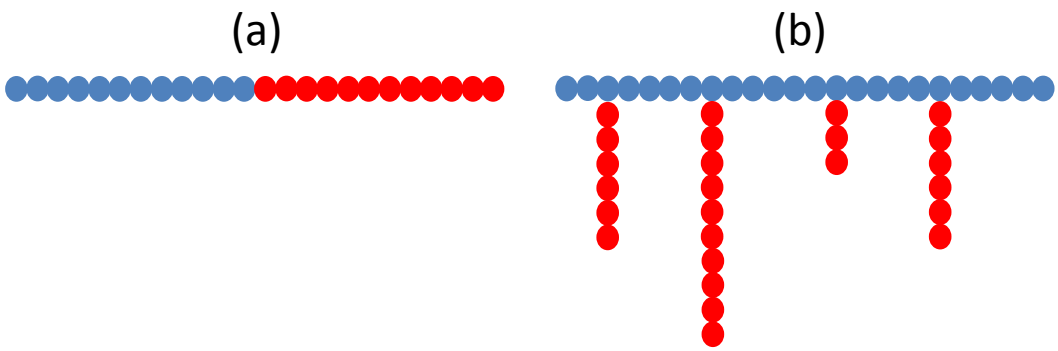

Figure 33: Representation of block copolymer (a) and graft copolymer (b)

With this kind of polymers, the thermal, mechanical and chemical properties can be related to the properties of the blocks or the grafts pendent chains which compose the polymer. To provide all the required final membrane properties, we focus only on:

-the block polymers having a fluorinated block or a block bearing phosphonic group;

-the polymers having a fluorinated main chain bearing phosphonated pendent chains;

-the polymers having a main chain functionalized with phosphonic acid groups bearing fluorinated graft.

4.2 Block copolymers

4.2.1 *Block copolymers with a phosphonated block*

In the literature, only few examples report the synthesis of block copolymers possessing a block with phosphonic acid groups. Among these few publications, we can cite the work of Jannasch and co[60] who synthesized poly(styrene-b-vinylphosphonic acid) via sequential anionic polymerization. The structure of the obtained polymer is shown Figure 34.

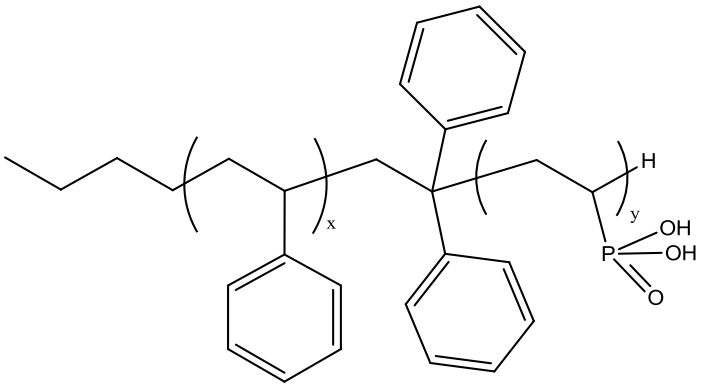

PS_x-*b*-$PVPA_y$

Figure 34: PS-b-PVPA[60] diblock copolymer structure.

Various diblock copolymers were synthesized with block sizes ranging from 8000 to 20000 $g.mol^{-1}$ and 5000 to 15000 $g.mol^{-1}$ for PS block and PVPA block, respectively. AFM observations showed an increase in the size of the nano areas with the block size. However, this increase has little influence on the values of proton conductivity, all between 1.10^{-2} and 20.10^{-2} $S.cm^{-1}$ for temperatures between 0 and 140°C.

Styrene monomers and their derivatives are highly reactive; they are polymerizable through various controlled polymerizations technique. Thus, they can be used in order to obtain block polymers. For example, Cho and co[61] made a PEM from a polymer having a styrene block (PS) and a phosphonic acid bearing styrene block, the poly(vinylbenzyl phosphonic acid) (PVBPA). The structure of this polymer is shown in Figure 35.

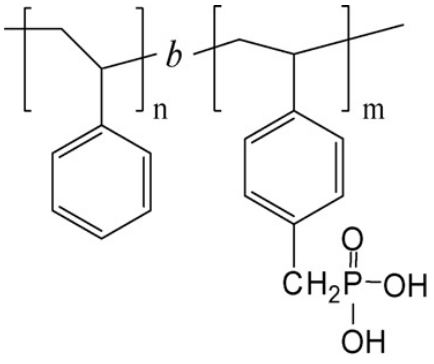

Figure 35 :PS-b-PVBPA structure.

However, a weak point of the membranes obtained from styrene polymers lies in their very poor mechanical properties. Indeed, when casting the membranes, the PS-b-PVBPA is dispersed in a matrix of poly (2,6-dimethyl-1,4-phenylene oxide) (PPO) in order to provide the necessary mechanical strength. When mixed with the PPO (a very hydrophobic polymer) there is a good miscibility with the formation of micro-domains in the hydrophilic membrane as shown in AFM images (Figure 36). The size of these areas increases with the percentage of PS-b-PVBPA present, to form a network of hydrophilic channels which will enable the transport of protons in the membrane.

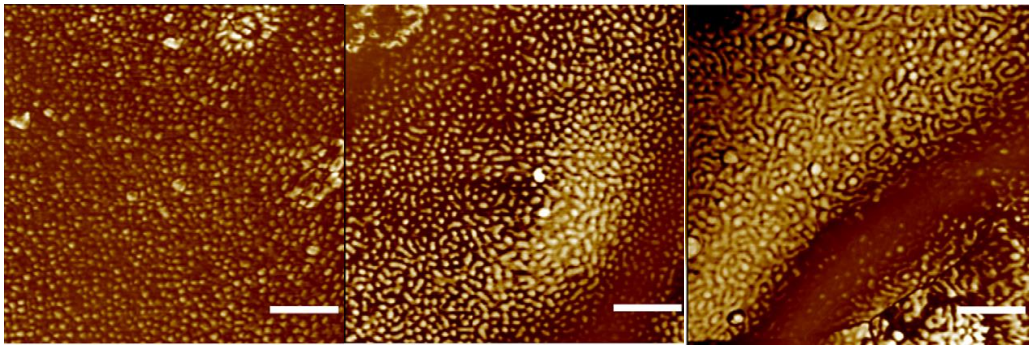

(a) (b) (c)

Figure 36: AFM images of the PS-b-PVBPA/PPO blend membranes with 90 (a), 70 (b) and 50 % (c) of PPO[61]

Low IEC values of these membranes (ranging from 0.5 to 1.8 meq.g^{-1}) are then balanced by the presence of hydrophilic regions within the membrane which allows to obtain reasonable conductivity values ranging from 1.10^{-3} to 2.10^{-2} S.cm^{-1} at temperatures of 25 and 140°C respectively and at 100% RH.

To overcome the brittleness of styrenic polymers, Markova[62] achieved the synthesis of triblock polymer type (BAB) using polyether ether ketone (PEEK) as a central block, which has good mechanical properties. To do this, they realized the polymerization of diethyl-vinylbenzyl phosphonate (DEVBP) by ATRP from functionalized PEEK. The polymer obtained is shown in Figure 37

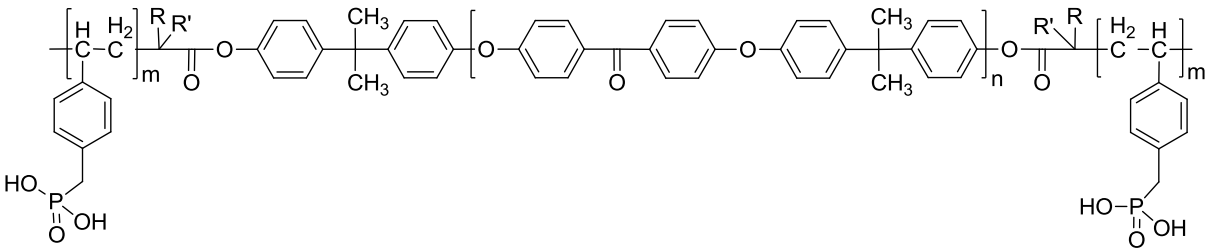

Figure 37: Structure of tribloc polymer PVBPA/PEEK/PVBPA[62]

Proton conductivity values of this type of polymers are between 1.10^{-5} and 5.10^{-5} $S.cm^{-1}$ for temperatures ranging from 100 to 160°C, under anhydrous conditions. Although these values of conductivity are low, they highlighted the amphoteric nature of the phosphonic acid groups and thus demonstrate the possibility of using these groups at temperature higher than 100°C and at low RH (<40%). However, morphology studies of these polymers, achieved by simulation methods such as "Dissipative Particle Dynamics"[63] used to determine the dynamic rheological properties of complex fluid, showed that the phase segregation between the two blocks was not sufficient. Indeed, the possible formation of hydrogen bonds between phosphonic acid groups and ketone groups of PEEK results in a partial compatibility of polymers. To overcome this problem, the synthesis of diblock polymer was performed using a hydrophobic block poly (phenylene oxide)[64] (PPO) (Figure 38). Like the previous example, the polymerization of DEVBP is performed by ATRP from functionalized PPO. Although the structure of the final material seems more distinct, values of proton conductivity measured in dry conditions are of the same order of magnitude as the membranes layouts from PVBPA-b-b-PVBPA PEEK polymer, namely a maximum of 5.10^{-5} $S.cm^{-1}$ at 160°C.

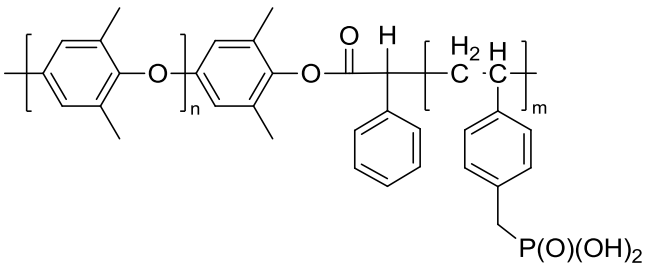

Figure 38 : Representation of PPO-b-PVBPA block copolymers obtained via ATRP by applying a mono-functional PPO macroinitiator for polymerizing diethyl p-vinylbenzyl phosphonate[64].

4.2.2 *Block copolymers with a fluorinated block*

4.2.2.1 Aromatic polymers: use of DodecaFluoroBiPhenyle (DFBP)

The polycondensation reaction is widely used in the fuel cell membranes area in order to obtain polymers with a polyarylene main chain. Indeed, polyarylene polymers possess a very good thermal stability but also a high glass transition temperature. This last property is very interesting to obtain membrane for fuel cell. In addition, this type of synthesis provides polymers having a reactive chain end, thus enabling the synthesis of block polymers.

In the aim to obtain a fluorinated block, several kinds of monomers have been used :

-monomers having fluorine atom directly on the aromatic ring;

-monomers having fluorinated groups on the carbon atom between the aromatic rings.

As monomers having fluorine atom directly on the aromatic ring, dodecaFluoroBiPhenyle (DFBP) is widely employed (Figure 39).

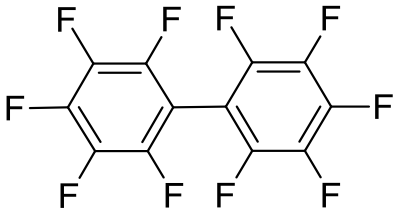

Figure 39: DodecaFluoroBiPhenyle (DFBP)

The first example concerns the use of multiblock copolymers[65] whose structures are showed in Figure 40. Polymers were obtained by the polycondensation reaction of bifunctional oligomers. They have been synthesized with different molar masses for each block.

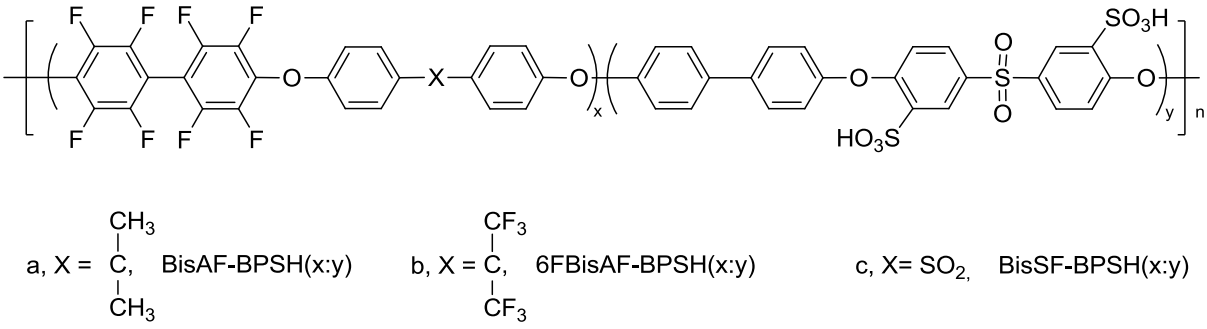

Figure 40: Structures of sulfonated-fluorinated multiblock copolymers[65]

From the Figure 41, we observe that the block copolymers show higher proton conductivity than the random polymers. Furthermore, for the same IEC values, 1.3 meq.g^{-1}, proton conductivity values of polymers having the highest molar masses are better. This difference in conductivity, despite identical IEC, indicates that higher molecular weights tend to promote phase segregation and thus promote the transport of protons in the membrane.

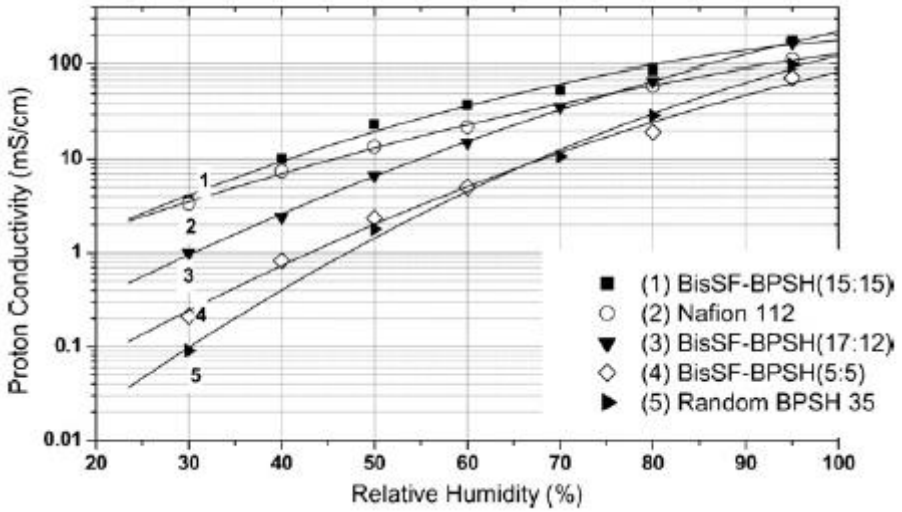

Figure 41 : Influence of block length on proton conduction under partially hydrated conditions at 80°C for the BisSF-BPSH multiblocks at similar IECs[65].

The 2nd example presents the synthesis of diblock copolmyers having one hydrophilic segment with sulfonic groups and one hydrophobic segment synthetized from the DFBP[66]. Reaction scheme is shown in Figure 42.

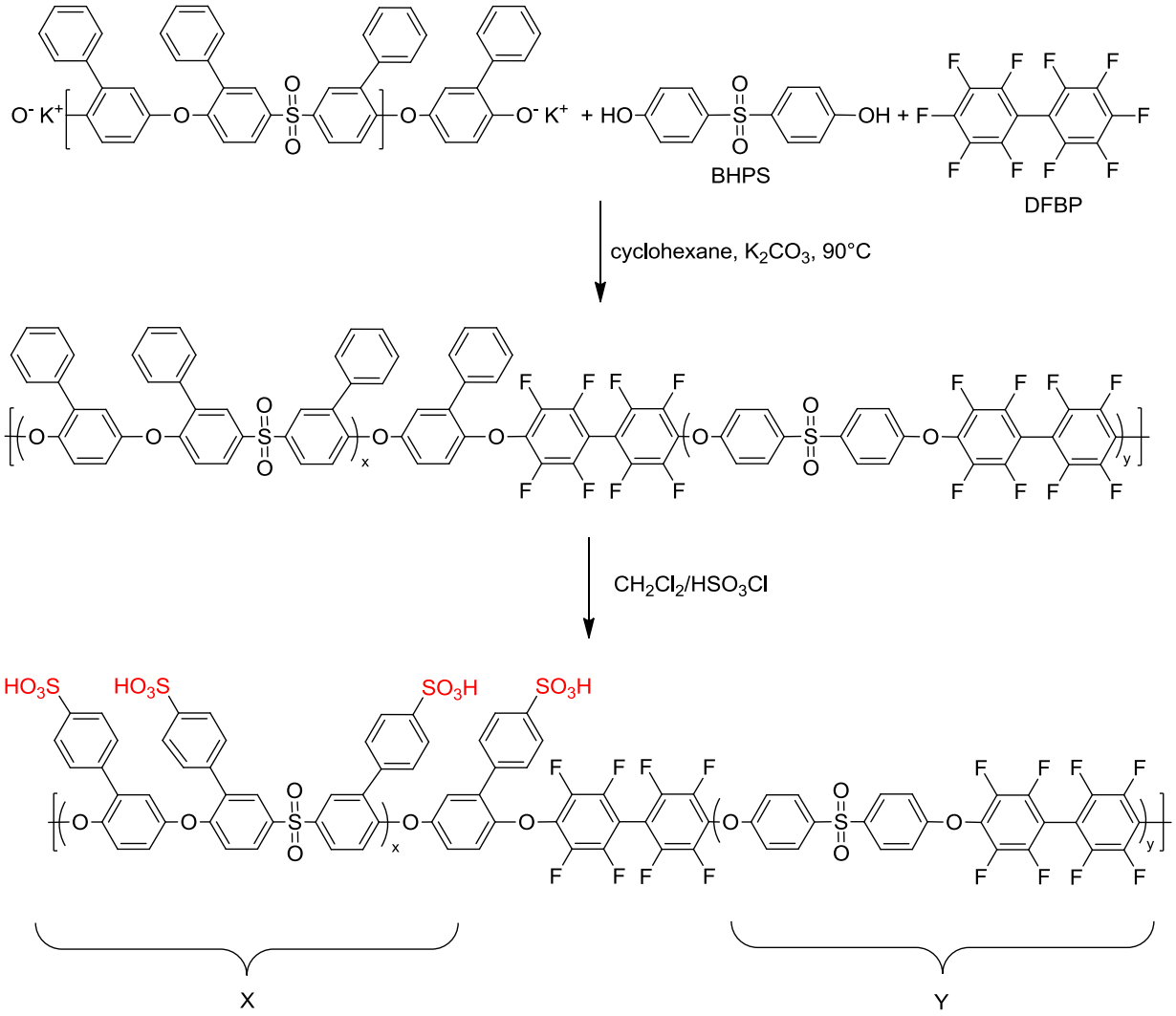

Figure 42: Structures and synthesis of the segmented sulfonated copolymers X_x-Y_y[66]

Different membranes have been synthesized with different molecular weight values for the 2 segments. The proton conductivity values were determined at 80°C versus RH and are showed in Figure 43. Overall, there is a strong dependence of conductivity with RH and the performances are below Nafion® when RH is low.

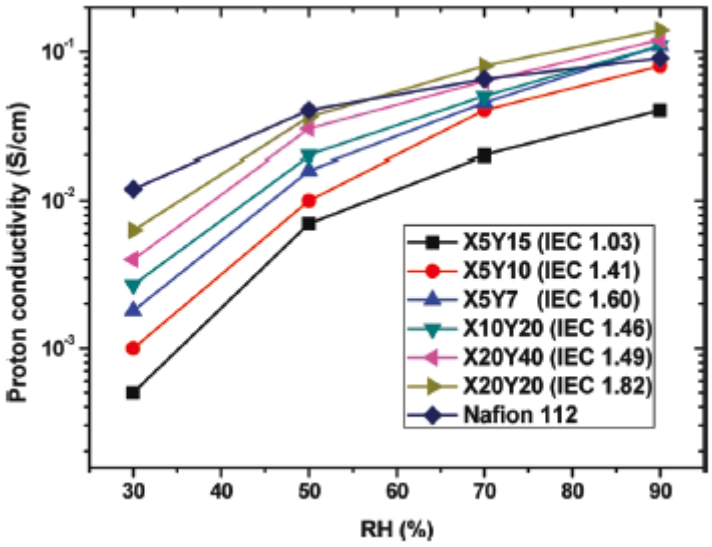

Figure 43: Dependence of proton conductivity on RH of Nafion 112 and copolymers membranes at 80°C

The use of DFBP allows to obtain block polymers, however, the polycondensation reaction does not allow proper control of the molar masses. Indeed, the polydispersity index is higher than two. It is therefore more appropriate to use techniques of controlled radical polymerization to synthesize polymers with a polydispersity index less than 1.5.

4.2.2.2 Use of 4,4-Hexafluoroisopropylidenediphenol (6F-BPA)

As another monomer bearing fluorinated groups, used for the production of diblock or multiblock copolymer, we can cite the 4,4 '-Hexafluoroisopropylidenedophenol (6F-BPA) [67-69] (Figure 44). As before, the polymerization technique used is the polycondensation reaction.

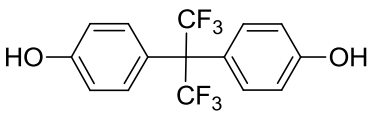

Figure 44: Structure of 4,4'-Hexa fluoroisopropylidenedophenol (6F-BPA)

In the work of Lee and co[69], the influence of the size of blocks on the physicochemical properties was studied. For this, they synthesized multiblock copolymers

possessing variable molars masses from two oligomers, the disulfonated poly(arylene ether sulfone) (BPSH) and the partially fluorinated poly-(arylene ether ketone) (6FK). The polymer structure obtained as well as the reaction conditions are illustrated Figure 45.

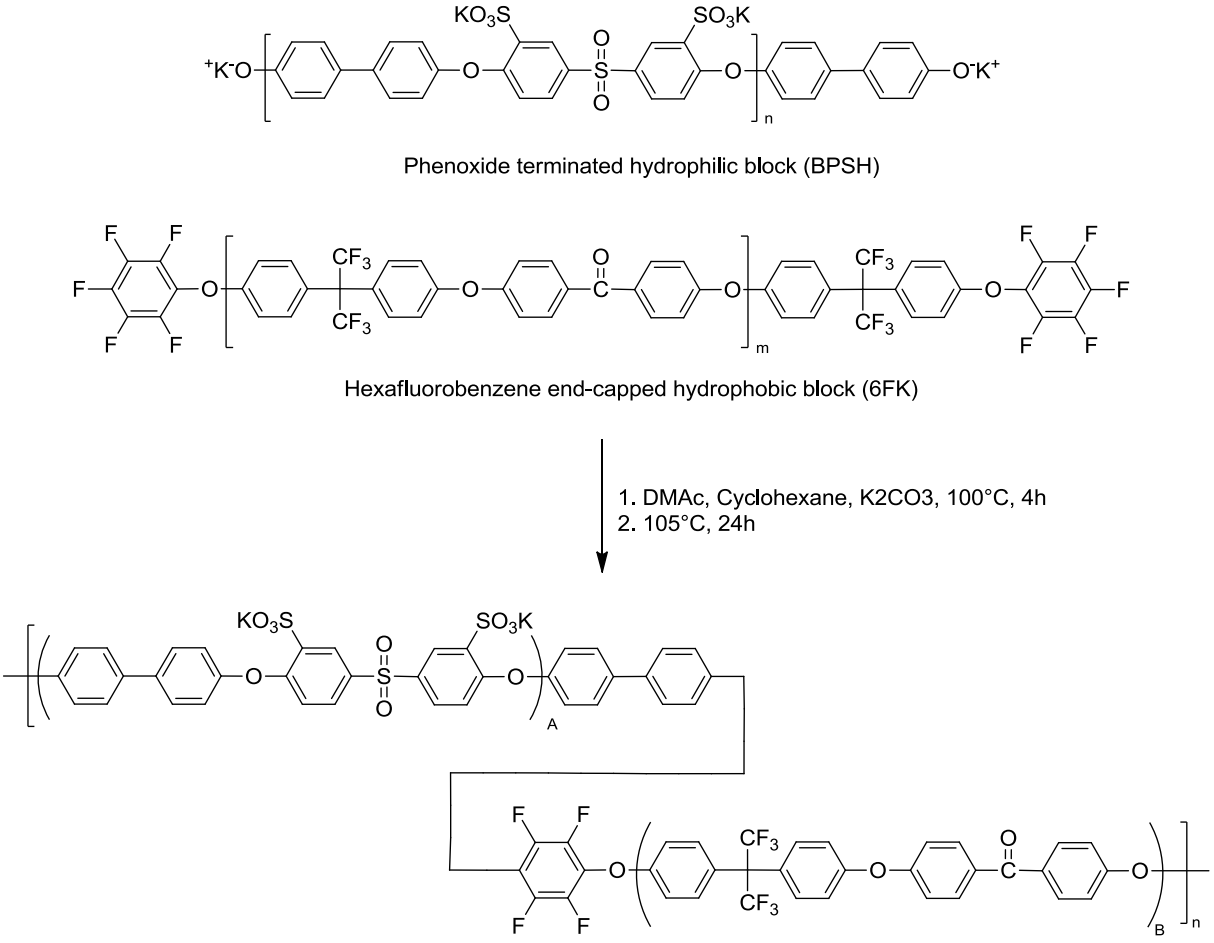

Figure 45 : Synthesis of segmented sulfonated multiblock copolymers (BPSHA-6FKB) with HFP linkage group[69]

To investigate the effect of molecular weight on the structure of the polymer, different membranes structures were observed by TEM. The results are shown inFigure 46. From these images, we can observe the evolution of phase segregation with the molar mass of the different blocks. It is clear that a higher molar mass greatly facilitates the structuration of the membrane. The results highlight the importance of obtaining polymers with high molecular weights to obtain sufficient phase segregation in order to facilitate the transport of protons in the membrane.

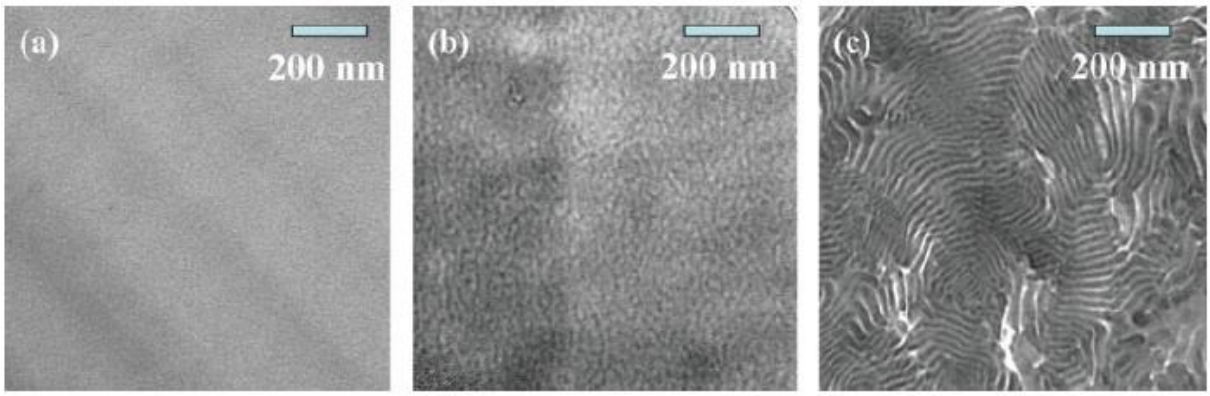

Figure 46 : TEM phase image of BPSH-6FK multiblock copolymers. BPSH5000-6FK5000 (a), BPSH10000-6FK10000 (b), BPSH15000-6FK15000 (c)[69]

From Figure 47 which shows the evolution of the proton conductivity as a function of HR at 80°C, we see that for RH below 80%, the values of the proton conductivity is higher for membranes obtained from polymers having high molecular weights. Indeed, a greater molar mass promotes the structuration of the membrane which in turn promotes the transport of protons in the membrane and thus provides better proton conductivity.

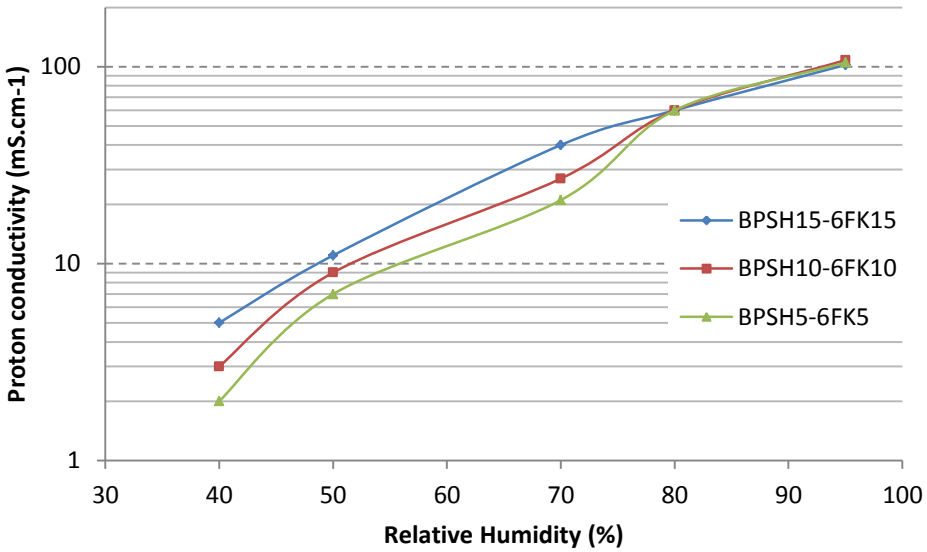

Figure 47: Proton conductivities of BPSH-6FK under partially hydrated conditions at 80°C.

4.2.2.3 Use of Pentafluorostyrene (PFS)

Styrene monomers allow the use of different techniques of controlled radical polymerization, with high conversion rates and relatively high yields. The PFS is used in the work of Matsumoto and co[70] to achieve the synthesis of a diblock structure from "NMP" (Nitroxide Mediated Polymerization) illustrated (Figure 48). The AFM observation of this type of membrane shows surface roughness probably due to a phase segregation between the fluorinated block and the sulfonic acid block. However, the realization of such membranes requires the incorporation of a third monomer to obtain homogeneous membranes. That is why they use the 4-1-methylsilicacyclobutyl styrene. It allows, through a palladium-catalyzed reaction, the crosslinking of the polymer and thus ensures the homogeneity of the final membrane.

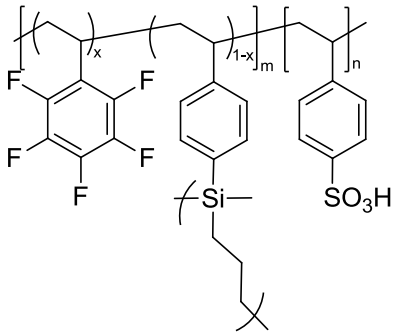

Figure 48 : Diblock polymer structure 2,3,4,5,6-pentafluorostyrene (PFS)/4-(1-methylsilacyclobutyl)styrene (SBS) and neopentyl styrenesulfonate (SSPen) (poly(PFS-co-SBS)-b-polySSPen)s[70]

4.2.2.4 Use of vinylidene fluoride (VDF)

In order to study the influence of the incorporation of fluorinated block on film morphology and proton conductivity over a wide range of IEC, Yang and co[71] compared a sulfonated polysulfone and a sulfonated polysulfone witn a poly (vinylidene fluoride) block grafted. This segment was previously synthesized by free radical telomerization using di-tert-butyl peroxide as an initiator and 1,2-dibromo-tetrafluoroethane as bi-functional agent[72].

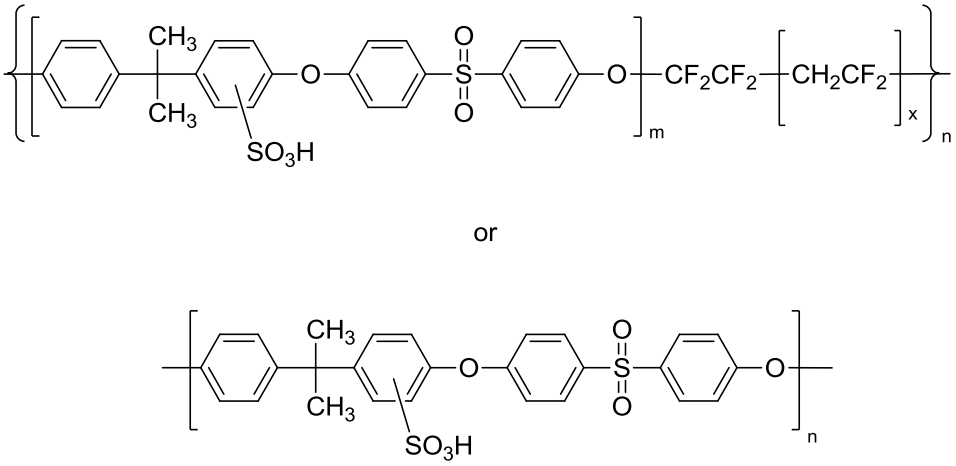

Figure 49: Sulfonated Bisphenol A Polysulfone-b-PVDF and Sulfonated Bisphenol A Polysulfone[71]

Both kinds of polymers were synthesized with varying degrees of sulfonation and proton conductivity values were measured at 30 ° C and 95% RH. The results are shown in Figure 50. We clearly see in this figure that the proton conductivity of the block copolymer is higher than the homopolymer one at low IEC, that is to say for smaller hydration numbers. Therefore when the percolation network is not saturated with water because of too low IEC, the presence of a fluorinated block increases the phase segregation, allowing the formation of a network consisting of ionic groups.

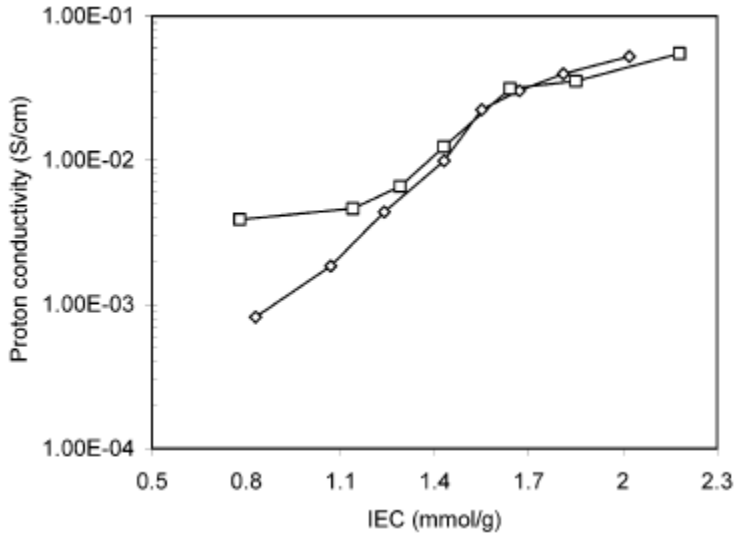

Figure 50: Proton conductivity versus IEC for Sulfonated Bisphenol A Polysulfone-b-PVDF (□) and Sulfonated Bisphenol A Polysulfone (◊) [71]

The diversity of techniques used for the polymerization of VDF (ITP[73-75], RAFT/MADIX[76, 77]) allows the realization of block polymers with reactive chain ends. This is the case, for example, for the polymerization of VDF/HFP in emulsion and in the presence of chloroform used as a chain transfer agent[78]. The presence of the -CCl_3 group at the chain end can then initiate the ATRP polymerization of styrene (Figure 51).

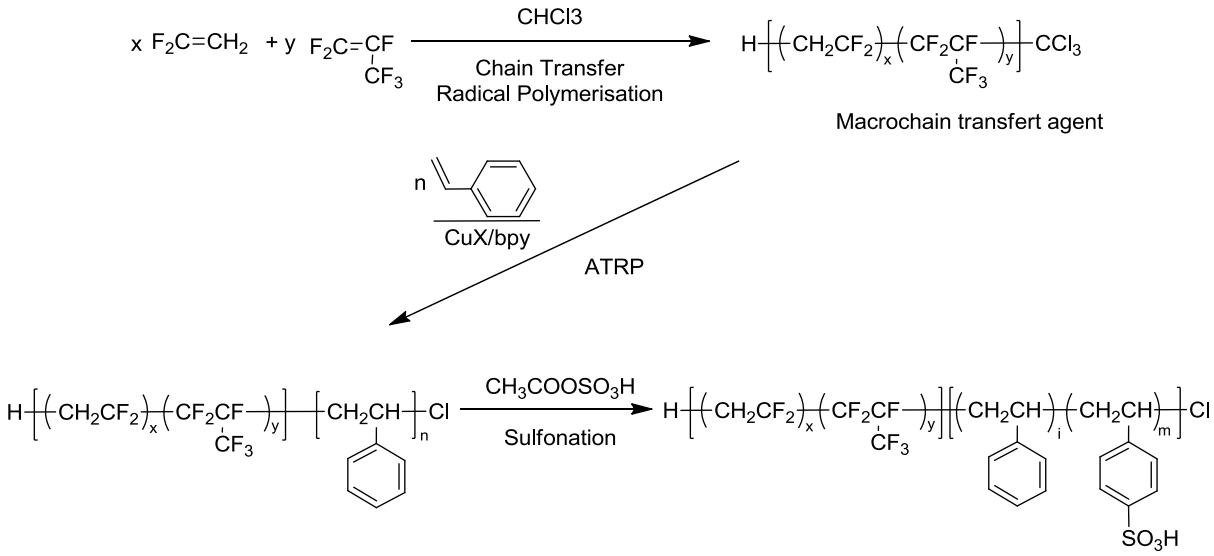

Figure 51: Synthesis poly(VDF-co-HFP)-b-SPS[78]

The conductivity values obtained with this type of polymer are higher by one order of magnitude compared to the conductivities obtained with partially sulfonated polystyrene (which can be considered as a random polymer) with the same values of IEC.

These results clearly put forward the advantage of using block copolymers having a fluorinated block because the highly hydrophobic nature of fluorinated polymer increases the phase segregation. This then allows an improvement in the structuration of the membrane, which has a direct impact on its conduction properties.

4.3 **Graft copolymers**

The membranes realized from graft copolymers have all the same structure, namely a fluorinated main chain on which polymers bearing protogenic groups (sulfonic acid or phosphonic acid) are grafted. Different grafting methods are then possible.

Numerous works use the irradiation technique in order to synthesize graft polymers. Indeed, by subjecting the main chain of the polymer to irradiations, it is possible to carry out the polymerization of various monomers from radicals which will be created along the main chain. The main chain used in this work is generally a commercial fluorinated (co)polymer (PVDF[79-83], ETFE[80, 83-87]) which is subjected to an electron-beam or to gamma rays… Then irradiated membrane was then placed in a solution containing the monomers. Commonly used monomers are styrene monomers which are functionalized with sulfonic acid groups[79-88] or phosphonic acid groups[84]. Although the results obtained with this kind of synthesis lead to PEM with interesting properties, we decided to focus thereafter only on the PEM with a controlled architecture obtained by conventional radical and anionic polymerization.

The use of phosphonic acid groups, in graft copolymers is not widely described. We can cite the work of Parvole and co[89] who did the anionic polymerization of diethyl vinyl phosphonate (DEVEP) from polysulfone (PSU) by a “grafting from” technique. The structure of the grafted copolymer obtained is shown Figure 52.

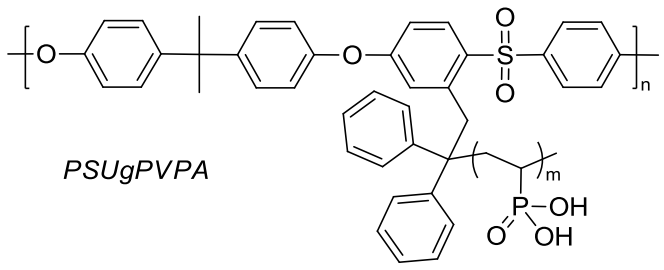

Figure 52 : Structure of PSU-g-PVPA graft copolymer[89]

The difference between the hydrophobic character of the main chain end the hydrophilicity of the grafted PVPA, as well as the strong hydrogen bonding allows good

phase segregation and thus the formation of ionic cluster. As a reminder, these clusters are absolutely necessary in order to obtain high proton conductivity in a dry state. This kind of polymer reaches reasonable proton conductivity values in a dry state (about 5 $mS.cm^{-1}$) but also in fully hydrated state (10^{-1} $S.cm^{-1}$ at 120°C). However, one must take into account that this system is limited by condensation between phosphonic acid groups, which then decreases the performances of the membranes.

In the Dimitrov and co[90] work, the synthesis of the graft copolymer is carried out using a technique of "grafting onto", namely the grafting of poly(pentafluorostyrene) on a commercial polysulfone through a Huisgen cycloaddition followed by a post phosphonation. The polymer obtained is shown in Figure 53.

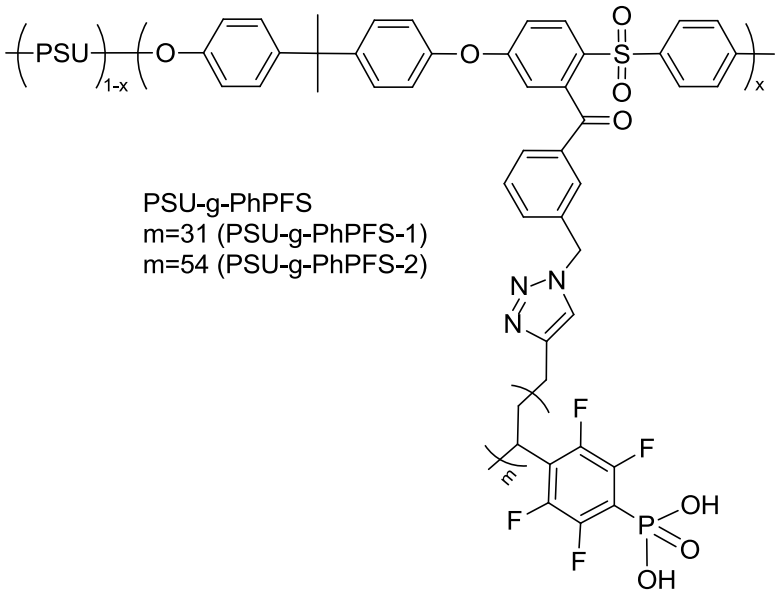

Figure 53: PSU-g-PhPFS graft copolymer structure[90]

With this type of polymer, although the phosphonic acid group is situated in the para position of a fluorinated styrene group, significant swelling was observed for the high IEC value (188% for an IEC=4.8 meq.g-1). This swelling causes large deformations; however, the conductivity values remain attractive, with a maximum of 80 $mS.cm^{-1}$ in submerged conditions at 100°C.

To achieve the synthesis of a grafted fluoropolymer through a radical polymerization reaction, the method used by Ameduri et al. was ATRP[91]. In this work, the fluorinated copolymer used was poly(VDF-co-CTFE) (Figure 54), which allowed the use of the ATRP polymerization by the presence of chlorine. However, the implementation of this method is difficult, because the reactivity of the chlorine atom of CTFE units is very low. In addition, after polymerization, the presence of the chlorine atom at the chain end is not demonstrated. The identification of this type of graft copolymer is mainly demonstrated by thermal characterizations such as the modification of the glass transition temperature.

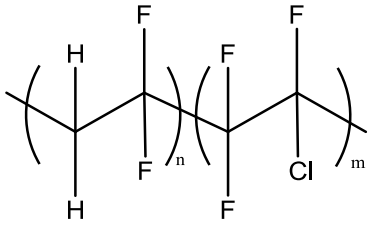

Figure 54: Representation of poly(VDF-co-CTFE)

We can cite the work of Tsang and co[92] who made the ATRP of styrene from poly(VDF-co-CTFE) followed by sulfonation, performing graft sizes with varying degrees of sulfonation (Figure 55). They were able to study the influence of the size of the graft and the IEC on the different properties of the membrane.

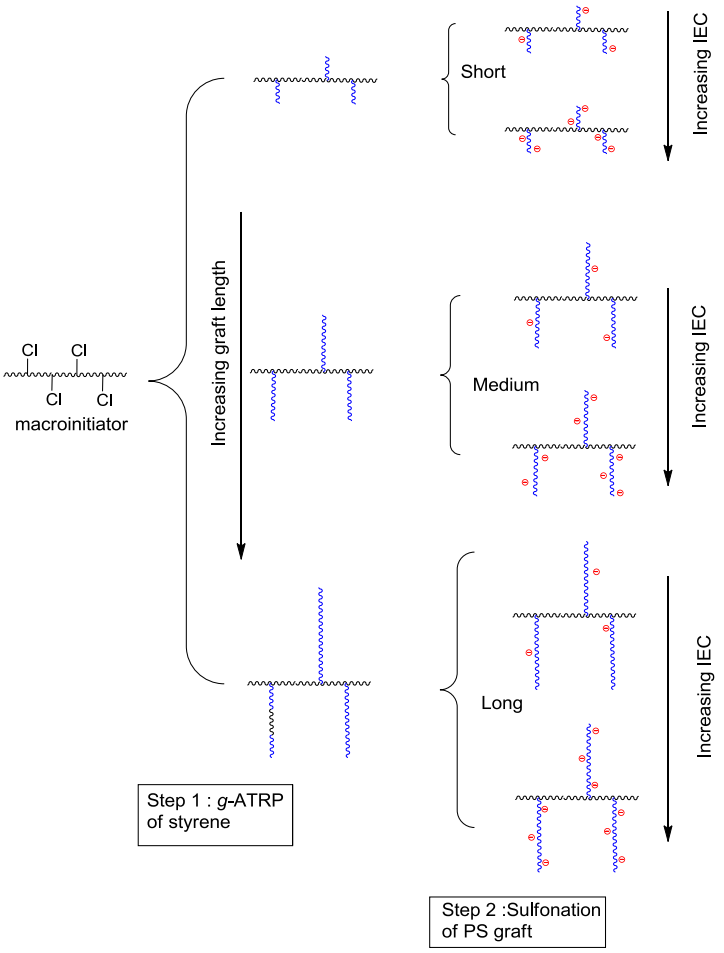

Figure 55:Structure relationships between the various series of P(VDF-co-CTFE)-g-SPS[92]

It shows that for each size of graft, the proton conductivity is proportional to the IEC up to a maximum value from which a drop in proton conductivity is observed. This drop is due to the dilution because of too high IEC leads to an excessive water uptake. In addition, the length of the grafts will also play an important role. The grafting of long chains will help to form, at sufficient IEC, a percolation network involving most ionic clusters formed by the acid groups. On the contrary, short chains will promote the formation of ionic cluster of larger size, but that cannot be linked together, pendant chains being too small. The principle is illustrated in Figure 56.

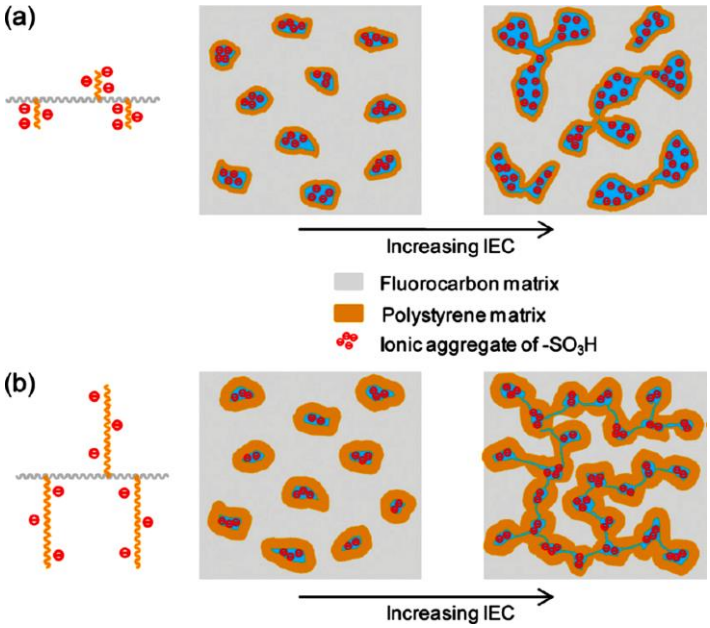

Figure 56 :Schematic representation of the postulated ionic aggregation in P(VDF-co-CFE)-g-SPS membranes with (a) short and (b) long graft length at different ion contents[92].

Up to this day, only one example shows the synthesis of copolymer with a fluorinated grafted chain and a backbone with acid groups. This work[93] describes the synthesis of poly(phenylene oxide) sulfonated (PPOS) with the grafting of poly(4-fluorostyrene). The influence of the size of the fluorinated graft on proton conductivity is studied. A comparison of the proton conductivities in submerged conditions was performed between PPOS with 56% and 67% of poly (4-fluorostyrene) grafted sulfonated graft polymer I and sulfonated graft polymer II, respectively). The results are shown in Figure 57.

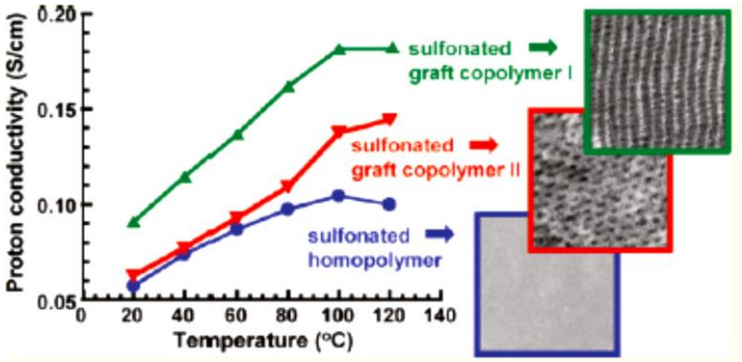

Figure 57 : Proton conductivity of PPOS, PPOS-PFS1, et PPOS-PPS2 in submerged conditions[93].

From Figure 57, we note that :

-the fluorinated graft chain gives proton conductivity values much higher than the linear polymer;

- the structural arrangement depends on the size of the graft, which impacts the conductivity values, and lamellar structures should be preferred.

4.4 Conclusion

In the light of the different works on the synthesis of polymers having block or grafted architecture, it is clear that these types of polymers provide membranes with interesting and superior properties to membranes made out of polymers with a random architecture. However, graft polymers and block polymers provide different benefits. In the works studying the comparison between these two types of architectures[94, 95] it appears that the block copolymers improve the conductivity while grafted copolymers impacts primarily the mechanical stability. This is mainly due to the different polymer organization patterns. Thus, a characteristic block polymer lamellar structure leads to greater swelling and better proton transport. Concerning the graft copolymer, a bi-continuous structure can withstand the swelling phenomenon, but is not as favorable to proton transport. It appears interesting to develop polymers with more complex structures such as tri-block copolymers that could be used to obtain cylindrical type architectures, and to combine the different advantages.

5 Final Conclusion

In order to improve the performances and properties of membranes cast from poly(CTFE-*alt*-VEPA), the blend technique can be considered The interest of achieving blends lies in the fact that the mechanical properties will be improved and the applying of this technique is very simple. To do this, the blend with the poly(VDF) will be considered, and the effect on the mechanical properties will be analyzed. In addition, the fluorine intake within the membrane could improve the structure and allow improved electrochemical

performances. Indeed, the structuration of the membrane has a great influence on the properties.

Still with the aim of improving the properties of the first generation membranes, namely to increase the mechanical strength and control water uptake, the crosslinking is very interesting. It will nevertheless be necessary to use a technique that will maintain a sufficient amount of phosphonic acid groups (as a high IEC is essential to obtain high values of proton conductivity) and easy to implement in order not to change the synthesis of the copolymer, which is already well established. The most appropriate solution would be the synthesis of fluoro copolymer with phosphonic acid moieties containing a few percent of vinyl monomer bearing a curable group. This appears to be a significant technical challenge, because to the best of our knowledge, no work reported the crosslinking of a fluorinated polymer bearing phosphonic acid groups.

The last parameter to improve the properties of a PEMFC is the structure of the copolymer A new synthetic strategy is necessary to combine a fluorinated part and a phosphonated part. Although many studies describe the use of block copolymers and graft copolymers, we found that very little work combine the synthesis of block copolymers having a fluorinated and a phosphonated block. Even less work deal with a graft architecture where the backbone is bearing of phosphonic acid units and the grafted polymer consists of fluorinated groups.

6 References

1. Cho, K.; Jung, H.; Choi, N.; Sung, S.; Park, J.; Choi, J.; Sung, Y., A coated Nafion membrane with a PVdF copolymer/Nafion blend for direct methanol fuel cells (DMFCs). *Solid State Ionics* **2005,** *176* (39-40), 3027-3030.
2. Song, M.-K.; Kim, Y.-T.; Fenton, J. M.; Kunz, H. R.; Rhee, H.-W., Chemically-modified Nafion®/poly(vinylidene fluoride) blend ionomers for proton exchange membrane fuel cells. *Journal of Power Sources* **2003,** *117* (1-2), 14-21.
3. Nazir, N. A.; Kim, N.; Iglesias, W. G.; Jakli, A.; Kyu, T., Conductive behavior in relation to domain morphology and phase diagram of Nafion/poly(vinylidene-co-trifluoroethylene) blends. *Polymer* **2012,** *53* (1), 196-204.
4. Piboonsatsanasakul, P.; Wootthikanokkhan, J.; Thanawan, S., Preparation and characterizations of direct methanol fuel cell membrane from sulfonated polystyrene/poly(vinylidene fluoride) blend compatibilized with poly(styrene)-b-poly(methyl methacrytlate) block copolymer. *Journal of Applied Polymer Science* **2008,** *107* (2), 1325-1336.
5. Wootthikanokkhan, J.; Seeponkai, N., Methanol permeability and properties of DMFC membranes based on sulfonated PEEK/PVDF blends. *Journal of Applied Polymer Science* **2006,** *102* (6), 5941-5947.
6. Xue, S.; Yin, G., Proton exchange membranes based on poly(vinylidene fluoride) and sulfonated poly(ether ether ketone). *Polymer* **2006,** *47* (14), 5044-5049.
7. Seeponkai, N.; Wootthikanokkhan, J., Proton exchange membranes for a direct methanol fuel cell based on sulfonated styrene-(ethylene-butylene)-styrene/polyvinylidene fluoride blends. *Journal of Applied Polymer Science* **2010**, NA-NA.
8. Ren, S.; Sun, G.; Li, C.; Wu, Z.; Jin, W.; Chen, W.; Xin, Q.; Yang, X., Sulfonated poly (ether ether ketone)/polyvinylidene fluoride polymer blends for direct methanol fuel cells. *Materials Letters* **2006,** *60* (1), 44-47.
9. Subramanian, M. S.; Sasikumar, G., Sulfonated polyether sulfone-poly(vinylidene fluoride) blend membrane for DMFC applications. *Journal of Applied Polymer Science* **2010,** *117* (2), 801-808.
10. Mokrini, A.; Huneault, M. A., Proton exchange membranes based on PVDF/SEBS blends. *Journal of Power Sources* **2006,** *154* (1), 51-58.
11. Mokrini, A.; Huneault, M. A.; Gerard, P., Partially fluorinated proton exchange membranes based on PVDF–SEBS blends compatibilized with methylmethacrylate block copolymers. *Journal of Membrane Science* **2006,** *283* (1-2), 74-83.
12. Moussaif, N.; Jérôme, R., Compatibilization of immiscible polymer blends (PC/PVDF) by the addition of a third polymer (PMMA): analysis of phase morphology and mechanical properties. *Polymer* **1999,** *40* (14), 3919-3932.
13. Erdogan, T.; Unveren, E. E.; Inan, T. Y.; Birkan, B., Well-defined block copolymer ionomers and their blend membranes for proton exchange membrane fuel cell. *Journal of Membrane Science* **2009,** *344* (1-2), 172-181.
14. Choi, W. H.; Jo, W. H., Preparation of new proton exchange membrane based on self-assembly of Poly(styrene-co-styrene sulfonic acid)-b-poly(methyl methacrylate)/Poly(vinylidene fluoride) blend. *Journal of Power Sources* **2009,** *188* (1), 127-131.

15. Gu, S.; He, G.; Wu, X.; Hu, Z.; Wang, L.; Xiao, G.; Peng, L., Preparation and characterization of poly(vinylidene fluoride)/sulfonated poly(phthalazinone ether sulfone ketone) blends for proton exchange membrane. *Journal of Applied Polymer Science* **2010,** *116* (2), 852-860.
16. Chen, N.; Hong, L., Proton-conducting membrane composed of sulfonated polystyrene microspheres, poly(vinylpyrrolidone) and poly(vinylidene fluoride). *Solid State Ionics* **2002,** *146* (3,4), 377-385.
17. Panwar, V.; Cha, K.; Park, J.-O.; Park, S., High actuation response of PVDF/PVP/PSSA based ionic polymer metal composites actuator. *Sensors and Actuators B: Chemical* **2012,** *161* (1), 460-470.
18. Hofmann, M. A.; Ambler, C. M.; Maher, A. E.; Chalkova, E.; Zhou, X. Y.; Lvov, S. N.; Allcock, H. R., Synthesis of Polyphosphazenes with Sulfonimide Side Groups. *Macromolecules* **2002,** *35* (Copyright (C) 2013 American Chemical Society (ACS). All Rights Reserved.), 6490-6493.
19. Hazarika, M.; Jana, T., Novel proton exchange membrane for fuel cell developed from blends of polybenzimidazole with fluorinated polymer. *European Polymer Journal* **2013,** *49* (6), 1564-1576.
20. Follain, N.; Roualdes, S.; Marais, S.; Frugier, J.; Reinholdt, M.; Durand, J., Water Transport Properties of Plasma-Modified Commercial Anion-Exchange Membrane for Solid Alkaline Fuel Cells. *The Journal of Physical Chemistry C* **2012,** *116* (15), 8510-8522.
21. Soulès, A.; Améduri, B.; Boutevin, B.; David, G.; Perrin, R.; Gebel, G., Proton Conducting Sulphonated Fluorinated Poly(Styrene) Crosslinked Electrolyte Membranes. *Fuel Cells 11* (5), 611-619.
22. Nikolic, V. M.; Krkljes, A.; Popovic, Z. K.; Lausevic, Z. V.; Miljanic, S. S., On the use of gamma irradiation crosslinked PVA membranes in hydrogen fuel cells. *Electrochemistry Communications* **2007,** *9* (11), 2661-2665.
23. Zhao, C.; Wang, Z.; Bi, D.; Lin, H.; Shao, K.; Fu, T.; Zhong, S.; Na, H., Blend membranes based on disulfonated poly(aryl ether ether ketone)s (SPEEK) and poly(amide imide) (PAI) for direct methanol fuel cell usages. *Polymer* **2007,** *48* (11), 3090-3097.
24. Brunetti, A.; Fontananova, E.; Donnadio, A.; Casciola, M.; Di, V. M. L.; Sgreccia, E.; Drioli, E.; Barbieri, G., New approach for the evaluation of membranes transport properties for polymer electrolyte membrane fuel cells. *J. Power Sources 205*, 222-230.
25. Di Vona, M. L.; Sgreccia, E.; Tamilvanan, M.; Khadhraoui, M.; Chassigneux, C.; Knauth, P., High ionic exchange capacity polyphenylsulfone (SPPSU) and polyethersulfone (SPES) cross-linked by annealing treatment: Thermal stability, hydration level and mechanical properties. *Journal of Membrane Science 354* (1-2), 134-141.
26. Mikhailenko, S. D.; Wang, K.; Kaliaguine, S.; Xing, P.; Robertson, G. P.; Guiver, M. D., Proton conducting membranes based on cross-linked sulfonated poly(ether ether ketone) (SPEEK). *Journal of Membrane Science* **2004,** *233* (1-2), 93-99.
27. Kerres, J.; Cui, W.; Junginger, M., Development and characterization of crosslinked ionomer membranes based upon sulfinated and sulfonated PSU crosslinked PSU blend membranes by alkylation of sulfinate groups with dihalogenoalkanes. *Journal of Membrane Science* **1998,** *139* (2), 227-241.
28. Jannasch, P., Fuel Cell Membrane Materials by Chemical Grafting of Aromatic Main-Chain Polymers. *Fuel Cells* **2005,** *5* (2), 248-260.

29. Nakabayashi, K.; Higashihara, T.; Ueda, M., Polymer Electrolyte Membranes Based on Cross-Linked Highly Sulfonated Multiblock Copoly(ether sulfone)s. *Macromolecules 43* (13), 5756-5761.
30. Schuster, M.; de Araujo, C. C.; Atanasov, V.; Andersen, H. T.; Kreuer, K.-D.; Maier, J., Highly Sulfonated Poly(phenylene sulfone): Preparation and Stability Issues. *Macromolecules* **2009,** *42* (8), 3129-3137.
31. Morancho, J. M.; Salla, J. M.; Cadenato, A.; Fernandez-Francos, X.; Colomer, P.; Calventus, Y.; Ramis, X.; Ruiz, R., Thermal analysis of enhanced poly(vinyl alcohol)-based proton-conducting membranes crosslinked with sulfonation agents for direct methanol fuel cells. *J. Appl. Polym. Sci. 124* (S1), E57-E65.
32. Boroglu, M. S.; Celik, S. U.; Bozkurt, A.; Boz, I., The synthesis and characterization of anhydrous proton conducting membranes based on sulfonated poly(vinyl alcohol) and imidazole. *Journal of Membrane Science 375* (1-2), 157-164.
33. Rhim, J.-W.; Park, H. B.; Lee, C.-S.; Jun, J.-H.; Kim, D. S.; Lee, Y. M., Crosslinked poly(vinyl alcohol) membranes containing sulfonic acid group: proton and methanol transport through membranes. *Journal of Membrane Science* **2004,** *238* (1-2), 143-151.
34. Kim, J.-e.; Kim, D., Pendant-sulfonated poly(arylene ether ketone) (PAEK) membranes cross-linked with a proton conducting reagent for fuel cells. *J. Membr. Sci. 405-406*, 176-184.
35. Zhang, X.; Hu, Z.-X.; Luo, L.-Q.; Chen, S.-S.; Liu, J.-M.; Chen, S.-W.; Wang, L.-J., Graft-crosslinked Copolymers Based on Poly(arylene ether ketone)-gc-sulfonated Poly(arylene ether sulfone) for PEMFC Applications. *Macromol. Rapid Commun. 32* (14), 1108-1113.
36. Park, K. T.; Chun, J. H.; Kim, S. G.; Chun, B.-H.; Kim, S. H., Synthesis and characterization of crosslinked sulfonated poly(arylene ether sulfone) membranes for high temperature PEMFC applications. *International Journal of Hydrogen Energy 36* (2), 1813-1819.
37. Feng, S.; Shang, Y.; Wang, Y.; Liu, G.; Xie, X.; Dong, W.; Xu, J.; Mathur, V. K., Synthesis and crosslinking of hydroxyl-functionalized sulfonated poly(ether ether ketone) copolymer as candidates for proton exchange membranes. *Journal of Membrane Science 352* (1-2), 14-21.
38. Zhang, Y.; Fei, X.; Zhang, G.; Li, H.; Shao, K.; Zhu, J.; Zhao, C.; Liu, Z.; Han, M.; Na, H., Preparation and properties of epoxy-based cross-linked sulfonated poly(arylene ether ketone) proton exchange membrane for direct methanol fuel cell applications. *International Journal of Hydrogen Energy* **2010,** *35* (12), 6409-6417.
39. Norris, B. C.; Li, W.; Lee, E.; Manthiram, A.; Bielawski, C. W., Click-functionalization of poly(sulfone)s and a study of their utilities as proton conductive membranes in direct methanol fuel cells. *Polymer 51* (23), 5352-5358.
40. Chen, X.; Chen, P.; An, Z.; Chen, K.; Okamoto, K., Crosslinked sulfonated poly(arylene ether ketone) membranes bearing quinoxaline and acidâ€“base complex cross-linkages for fuel cell applications. *Journal of Power Sources 196* (4), 1694-1703.
41. Kim, S.-K.; Kim, T.-H.; Ko, T.; Lee, J.-C., Cross-linked poly(2,5-benzimidazole) consisting of wholly aromatic groups for high-temperature PEM fuel cell applications. *Journal of Membrane Science 373* (1-2), 80-88.
42. Lin, H.-L.; Chou, Y.-C.; Yu, T. L.; Lai, S.-W., Poly(benzimidazole)-epoxide crosslink membranes for high temperature proton exchange membrane fuel cells. *Int. J. Hydrogen Energy 37* (1), 383-392.

43. Guhan, S.; Muruganantham, R.; Sangeetha, D., Development of a solid polymer electrolyte membrane based on sulfonated poly(ether ether) ketone and polysulfone for fuel cell applications. *Can. J. Chem. 90* (2), 205-213.
44. Wang, S. J.; Luo, J. J.; Xiao, M.; Han, D. M.; Shen, P. K.; Meng, Y. Z., Design, synthesis and properties of polyaromatics with hydrophobic and hydrophilic long blocks as proton exchange membrane for PEM fuel cell application. *International Journal of Hydrogen Energy* **2012,** *37* (5), 4545-4552.
45. Aili, D.; Li, Q.; Christensen, E.; Jensen, J. O.; Bjerrum, N. J., Crosslinking of polybenzimidazole membranes by divinylsulfone post-treatment for high-temperature proton exchange membrane fuel cell applications. *Polymer International 60* (8), 1201-1207.
46. Guan, Y. S.; Pu, H. T.; Jin, M.; Chang, Z. H.; Wan, D. C., Preparation and Characterisation of Proton Exchange Membranes Based on Crosslinked Polybenzimidazole and Phosphoric Acid. *Fuel Cells 10* (6), 973-982.
47. Han, M.; Zhang, G.; Li, M.; Wang, S.; Zhang, Y.; Li, H.; Lew, C. M.; Na, H., Considerations of the morphology in the design of proton exchange membranes: Cross-linked sulfonated poly(ether ether ketone)s using a new carboxyl-terminated benzimidazole as the cross-linker for PEMFCs. *International Journal of Hydrogen Energy 36* (3), 2197-2206.
48. Tripathi, B. P.; Saxena, A.; Shahi, V. K., Phosphonic acid grafted bis(4-Î³-aminopropyldiethoxysilylphenyl)sulfone (APDSPS)-poly(vinyl alcohol) cross-linked polyelectrolyte membrane impervious to methanol. *Journal of Membrane Science* **2008,** *318* (1-2), 288-297.
49. Qiao, J.; Hamaya, T.; Okada, T., New highly proton conductive polymer membranes poly(vinyl alcohol)-2-acrylamido-2-methyl-1-propanesulfonic acid (PVA-PAMPS). *Journal of Materials Chemistry* **2005,** *15* (41), 4414-4423.
50. Fukuzaki, N.; Nakabayashi, K.; Nakazawa, S.; Murata, S.; Higashihara, T.; Ueda, M., Highly phosphonated poly(N-phenylacrylamide) for proton exchange membranes. *Journal of Polymer Science Part A: Polymer Chemistry 49* (1), 93-100.
51. Oh, Y.-S.; Lee, H.-J.; Yoo, M.; Kim, H.-J.; Han, J.; Kim, T.-H., Synthesis of novel crosslinked sulfonated poly(ether sulfone)s using bisazide and their properties for fuel cell application. *Journal of Membrane Science* **2008,** *323* (2), 309-315.
52. Lee, K.-S.; Jeong, M.-H.; Lee, J.-S.; Pivovar, B. S.; Kim, Y. S., Optimizing end-group cross-linkable polymer electrolytes for fuel cell applications. *Journal of Membrane Science 352* (1-2), 180-188.
53. Lee, K.-S.; Jeong, M.-H.; Lee, J.-P.; Lee, J.-S., End-Group Cross-Linked Poly(arylene ether) for Proton Exchange Membranes. *Macromolecules* **2009,** *42* (3), 584-590.
54. Feng, S.; Shang, Y.; Xie, X.; Wang, Y.; Xu, J., Synthesis and characterization of crosslinked sulfonated poly(arylene ether sulfone) membranes for DMFC applications. *Journal of Membrane Science* **2009,** *335* (1-2), 13-20.
55. Lee, K.-S.; Jeong, M.-H.; Kim, Y.-J.; Lee, S.-B.; Lee, J.-S., Fluorinated Aromatic Polyether Ionomers Containing Perfluorocyclobutyl as Cross-Link Groups for Fuel Cell Applications. *Chemistry of Materials* **2012,** *24* (8), 1443-1453.
56. Li, H.; Zhang, G.; Wu, J.; Zhao, C.; Jia, Q.; Lew, C. M.; Zhang, L.; Zhang, Y.; Han, M.; Zhu, J.; Shao, K.; Ni, J.; Na, H., A facile approach to prepare self-cross-linkable sulfonated poly(ether ether ketone) membranes for direct methanol fuel cells. *Journal of Power Sources 195* (24), 8061-8066.
57. Karimi, G.; Li, X., Electroosmotic flow through polymer electrolyte membranes in PEM fuel cells. *Journal of Power Sources* **2005,** *140* (1), 1-11.

58. Beers, K. M.; Balsara, N. P., Design of Cluster-free Polymer Electrolyte Membranes and Implications on Proton Conductivity. *ACS Macro Letters* **2012,** *1* (10), 1155-1160.
59. Manning, G. S., Limiting Laws and Counterion Condensation in Polyelectrolyte Solutions I. Colligative Properties. *The Journal of Chemical Physics* **1969,** *51* (3), 924-933.
60. Perrin, R.; Elomaa, M.; Jannasch, P., Nanostructured Proton Conducting Polystyrene−Poly(vinylphosphonic acid) Block Copolymers Prepared via Sequential Anionic Polymerizations. *Macromolecules* **2009,** *42* (14), 5146-5154.
61. Cho, C. G.; Kim, S. H.; Park, Y. C.; Kim, H.; Park, J.-W., Fuel cell membranes based on blends of PPO with poly(styrene-b-vinylbenzylphosphonic acid) copolymers. *Journal of Membrane Science* **2008,** *308* (1-2), 96-106.
62. Markova, D.; Kumar, A.; Klapper, M.; Müllen, K., Phosphonic acid-containing homo-, AB and BAB block copolymers via ATRP designed for fuel cell applications. *Polymer* **2009,** *50* (15), 3411-3421.
63. Roy, S.; Markova, D.; Kumar, A.; Klapper, M.; Müller-Plathe, F., Morphology of Phosphonic Acid-Functionalized Block Copolymers Studied by Dissipative Particle Dynamics. *Macromolecules* **2009,** *42* (3), 841-848.
64. Kumar, A.; Pisula, W.; Markova, D.; Klapper, M.; Müllen, K., Proton-Conducting Poly(phenylene oxide)–Poly(vinyl benzyl phosphonic acid) Block Copolymers via Atom Transfer Radical Polymerization. *Macromolecular Chemistry and Physics* **2012,** *213* (5), 489-499.
65. Roy, A.; Yu, X.; Dunn, S.; McGrath, J. E., Influence of microstructure and chemical composition on proton exchange membrane properties of sulfonated-fluorinated, hydrophilic-hydrophobic multiblock copolymers. *J. Membr. Sci.* **2009,** *327* (Copyright (C) 2013 American Chemical Society (ACS). All Rights Reserved.), 118-124.
66. Li, N.; Hwang, D. S.; Lee, S. Y.; Liu, Y.-L.; Lee, Y. M.; Guiver, M. D., Densely Sulfophenylated Segmented Copoly(arylene ether sulfone) Proton Exchange Membranes. *Macromolecules* **2011,** *44* (12), 4901-4910.
67. Li, Y.; Roy, A.; Badami, A. S.; Hill, M.; Yang, J.; Dunn, S.; McGrath, J. E., Synthesis and characterization of partially fluorinated hydrophobic-hydrophilic multiblock copolymers containing sulfonate groups for proton exchange membrane. *J. Power Sources* **2007,** *172* (Copyright (C) 2013 American Chemical Society (ACS). All Rights Reserved.), 30-38.
68. Chu, J. Y.; Kim, A. R.; Nahm, K. S.; Lee, H.-K.; Yoo, D. J., Synthesis and characterization of partially fluorinated sulfonated poly(arylene biphenylsulfone ketone) block copolymers containing 6F-BPA and perfluorobiphenylene units. *Int. J. Hydrogen Energy* (Copyright (C) 2013 American Chemical Society (ACS). All Rights Reserved.), Ahead of Print.
69. Lee, H.-S.; Roy, A.; Lane, O.; Lee, M.; McGrath, J. E., Synthesis and characterization of multiblock copolymers based on hydrophilic disulfonated poly(arylene ether sulfone) and hydrophobic partially fluorinated poly(arylene ether ketone) for fuel cell applications. *Journal of Polymer Science Part A: Polymer Chemistry* **2010,** *48* (1), 214-222.
70. Matsumoto, K.; Ozaki, F.; Matsuoka, H., Synthesis of proton-conducting block copolymer membranes composed of a fluorinated segment and a sulfonic acid segment. *J. Polym. Sci., Part A: Polym. Chem.* **2008,** *46* (Copyright (C) 2013 American Chemical Society (ACS). All Rights Reserved.), 4479-4485.
71. Yang, Y.; Shi, Z.; Holdcroft, S., Synthesis of Sulfonated Polysulfone-block-PVDF Copolymers: Enhancement of Proton Conductivity in Low Ion Exchange Capacity Membranes. *Macromolecules* **2004,** *37* (5), 1678-1681.

72. Yang, Y.; Shi, Z.; Holdcroft, S., Synthesis of poly[arylene ether sulfone-b-vinylidene fluoride] block copolymers. *European Polymer Journal* **2004,** *40* (3), 531-541.
73. Boyer, C.; Valade, D.; Sauguet, L.; Ameduri, B.; Boutevin, B., Iodine Transfer Polymerization (ITP) of Vinylidene Fluoride (VDF). Influence of the Defect of VDF Chaining on the Control of ITP. *Macromolecules* **2005,** *38* (25), 10353-10362.
74. Durand, N.; Ameduri, B.; Boutevin, B., Synthesis and characterization of functional fluorinated telomers. *J. Polym. Sci., Part A: Polym. Chem. 49* (1), 82-92.
75. Valade, D.; Boyer, C.; Ameduri, B.; Boutevin, B., Poly(vinylidene fluoride)-b-poly(styrene) Block Copolymers by Iodine Transfer Polymerization (ITP): Synthesis, Characterization, and Kinetics of ITP. *Macromolecules* **2006,** *39* (25), 8639-8651.
76. Girard, E.; Marty, J.-D.; Ameduri, B.; Destarac, M., Direct Synthesis of Vinylidene Fluoride-Based Amphiphilic Diblock Copolymers by RAFT/MADIX Polymerization. *ACS Macro Lett.* **2012,** *1* (Copyright (C) 2013 American Chemical Society (ACS). All Rights Reserved.), 270-274.
77. Patil, Y.; Ameduri, B., First RAFT/MADIX radical copolymerization of tert-butyl 2-trifluoromethacrylate with vinylidene fluoride controlled by xanthate. *Polym. Chem.* **2013,** *4* (Copyright (C) 2013 American Chemical Society (ACS). All Rights Reserved.), 2783-2799.
78. Shi, Z.; Holdcroft, S., Synthesis and Proton Conductivity of Partially Sulfonated Poly([vinylidene difluoride-co-hexafluoropropylene]-b-styrene) Block Copolymers. *Macromolecules* **2005,** *38* (10), 4193-4201.
79. Lehtinen, T.; Sundholm, G.; Holmberg, S.; Sundholm, F.; Björnbom, P.; Bursell, M., Electrochemical characterization of PVDF-based proton conducting membranes for fuel cells. *Electrochimica Acta* **1998,** *43* (12–13), 1881-1890.
80. Shen, M.; Roy, S.; Kuhlmann, J. W.; Scott, K.; Lovell, K.; Horsfall, J. A., Grafted polymer electrolyte membrane for direct methanol fuel cells. *Journal of Membrane Science* **2005,** *251* (1–2), 121-130.
81. Flint, S. D.; Slade, R. C. T., Investigation of radiation-grafted PVDF-g-polystyrene-sulfonic-acid ion exchange membranes for use in hydrogen oxygen fuel cells. *Solid State Ionics* **1997,** *97* (1–4), 299-307.
82. Soresi, B.; Quartarone, E.; Mustarelli, P.; Magistris, A.; Chiodelli, G., PVDF and P(VDF-HFP)-based proton exchange membranes. *Solid State Ionics* **2004,** *166* (3–4), 383-389.
83. Chen, J.; Asano, M.; Maekawa, Y.; Yoshida, M., Suitability of some fluoropolymers used as base films for preparation of polymer electrolyte fuel cell membranes. *Journal of Membrane Science* **2006,** *277* (1–2), 249-257.
84. Schmidt-Naake, G.; Böhme, M.; Cabrera, A., Synthesis of Proton Exchange Membranes with Pendent Phosphonic Acid Groups by Irradiation Grafting of VBC. *Chemical Engineering & Technology* **2005,** *28* (6), 720-724.
85. Scott, K.; Taama, W. M.; Argyropoulos, P., Performance of the direct methanol fuel cell with radiation-grafted polymer membranes. *Journal of Membrane Science* **2000,** *171* (1), 119-130.
86. Ben, Y. H.; Gubler, L.; Guersel, S. A.; Henkensmeier, D.; Wokaun, A.; Scherer, G. G., Novel ETFE based radiation grafted poly(styrene sulfonic acid-co-methacrylonitrile) proton conducting membranes with increased stability. *Electrochem. Commun.* **2009,** *11* (Copyright (C) 2013 American Chemical Society (ACS). All Rights Reserved.), 941-944.
87. Ben, y. H.; Gubler, L.; Yamaki, T.; Sawada, S.-i.; Gursel, S. A.; Wokaun, A.; Scherer, G. G., Cross-Linker Effect in ETFE-Based Radiation-Grafted Proton-Conducting Membranes. *J.*

Electrochem. Soc. **2009,** *156* (Copyright (C) 2013 American Chemical Society (ACS). All Rights Reserved.), B532-B539.
88. Büchi, F. N.; Gupta, B.; Haas, O.; Scherer, G. G., Study of radiation-grafted FEP-G-polystyrene membranes as polymer electrolytes in fuel cells. *Electrochimica Acta* **1995,** *40* (3), 345-353.
89. Parvole, J.; Jannasch, P., Polysulfones Grafted with Poly(vinylphosphonic acid) for Highly Proton Conducting Fuel Cell Membranes in the Hydrated and Nominally Dry State. *Macromolecules* **2008,** *41* (11), 3893-3903.
90. Dimitrov, I.; Takamuku, S.; Jankova, K.; Jannasch, P.; Hvilsted, S., Polysulfone Functionalized With Phosphonated Poly(pentafluorostyrene) Grafts for Potential Fuel Cell Applications. *Macromolecular Rapid Communications* **2012,** *33* (16), 1368-1374.
91. Bruno, A., Controlled Radical (Co)polymerization of Fluoromonomers. *Macromolecules* **2010,** *43* (24), 10163-10184.
92. Tsang, E. M. W.; Zhang, Z.; Yang, A. C. C.; Shi, Z.; Peckham, T. J.; Narimani, R.; Frisken, B. J.; Holdcroft, S., Nanostructure, Morphology, and Properties of Fluorous Copolymers Bearing Ionic Grafts. *Macromolecules* **2009,** *42* (24), 9467-9480.
93. Ingratta, M.; Jutemar, E. P.; Jannasch, P., Synthesis, Nanostructures and Properties of Sulfonated Poly(phenylene oxide) Bearing Polyfluorostyrene Side Chains as Proton Conducting Membranes. *Macromolecules* **2011,** *44* (7), 2074-2083.
94. Peckham, T. J.; Holdcroft, S., Structure-morphology-property relationships of non-perfluorinated proton-conducting membranes. *Adv Mater* **2010,** *22* (42), 4667-90.
95. Tsang, E. M. W.; Zhang, Z.; Shi, Z.; Soboleva, T.; Holdcroft, S., Considerations of Macromolecular Structure in the Design of Proton Conducting Polymer Membranes: Graft versus Diblock Polyelectrolytes. *Journal of the American Chemical Society* **2007,** *129* (49), 15106-15107.

CHAPTER II

A new PEMFC composed of a high fluorinated polymer blended with a fluorinated polymer containing phosphonic acid

Chlorotrifluoroethylene (CTFE)

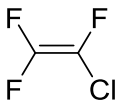

2-Chloroethylvinylether (CEVE)

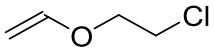

poly(CTFE-*alt*-CEVE)

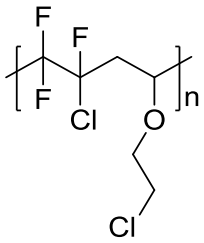

poly(CTFE-*alt*-IEVE)

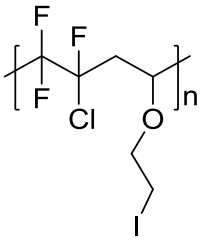

poly(CTFE-*alt*-DEVEP)

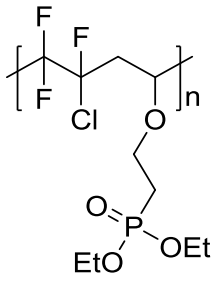

poly(CTFE-*alt*-VEPA)

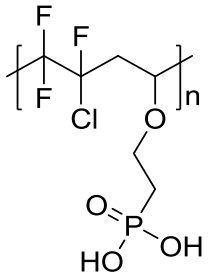

poly(VDF-*co*-*CTFE*)

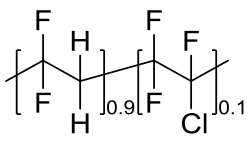

1 Introduction

One of the main goal of this work is the improvement of the physical, mechanical properties and the achievement of the first generation membrane previously synthesized in the laboratory during the Dr TAYOUO's [1] thesis. This first generation of polymer, with phosphonic acid groups, led to the publication of two scientific articles [2, 3], and one patent [4]. On the one hand the proton conductivity are rather low (about 0.25mS.cm^{-1} at 120°C), on the other hand the poor mechanical properties of the polymer greatly limit its use. That is why it is necessary to develop new strategies of membranes' synthesis in order to maximize the potential of this material.

We have already seen in Chapter 1 the interests of forming blend membranes to improve the mechanical properties of a material. This strategy will therefore be used to make new membranes through the blending of phosphonated polymer with a commercial fluorinated copolymer (Figure 58).

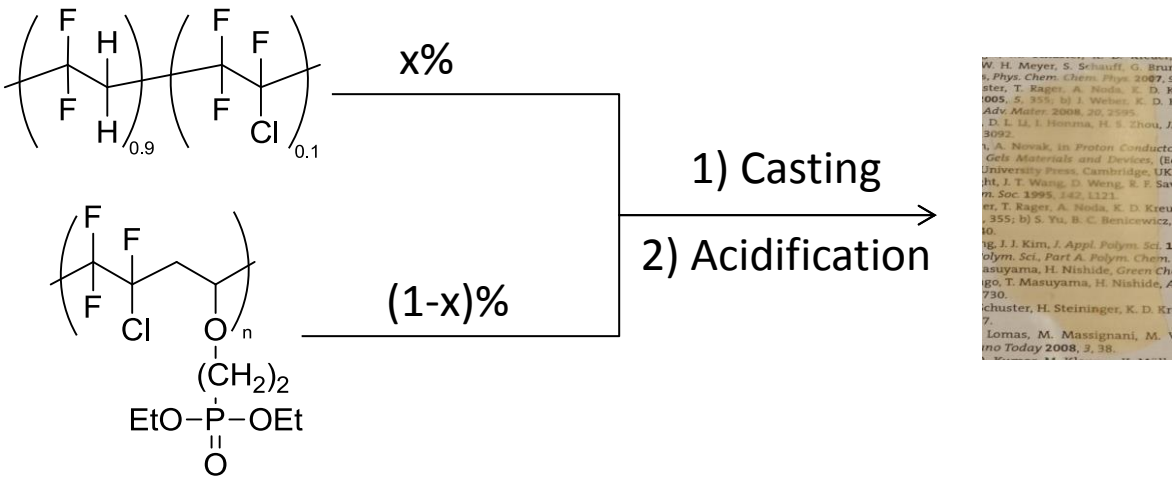

Figure 58 : Schematic representation for the casting of blend membranes

The fluorinated polymer will allow to improve the mechanical properties of the final membranes, but also to give a high chemical stability in a hard environment, such as an acid or an oxidant environment. This commercial polymer was synthesized from two fluorinated

monomers, the vinyl difluoride (VDF) and the chlorotrifluoroethylene (CTFE), with only few percent of the latter.

The fluorinated copolymer bearing phosphonic acid groups will allow the presence of protogenic groups which will permit the transport of protons through the composite membrane. The presence of CTFE in the two polymers used in a view to realizing these membranes should enable a better affinity and membranes will be much more homogeneous. The synthesis of the conductor polymer has been widely described in the work of Tayouo and co [2-5].

This chapter will be divided in two parts, the first part will deal with a brief description of the synthesis of phosphonated copolymer and the strategy to achieve the membranes. Then, the second part will be dedicated to the formation of composite membranes and their physico-chemical characterizations. This second part will be illustrated by the scientific article submitted to Journal of Power Sources.

2 Synthesis of the phosphonated copolymer poly(CTFE-*alt*-DEVEP)

This copolymer synthesis is based on the radical copolymerization of a fluorinated monomer, which is a good electron-accepting one as the CTFE and a strong electron-donating monomer as the 2-chloroethyl vinyl ether (CEVE). Thus, this radical copolymerization leads to alternated copolymers[3]. Then, after the chemical modification, the copolymer will be functionalized with phosphonic acid groups. Since both the electron-donating /electron-accepting characters of CTFE and CEVE will afford an alternated structure, the phosphonic acid groups will be situated throughout the copolymer chain.

2.1 Copolymerization of CTFE with the CEVE

The copolymer poly(CTFE-*alt*-DEVEP) was obtained by a three steps reaction. The first step corresponds to the radical copolymerization between the CTFE and the CEVE (Figure 59a).

As the CTFE is a gaseous monomer, the polymerization reaction was carried out in a Hastelloy autoclave. The reaction was initiated by the *tert*-butyl peroxypivilate (TBPPI) (1% in mole compared to the monomers) with the reaction was carried out in 1,1,1,3,3-pentafluorobutane (solkane®) used as solvent, with the presence of potassium carbonate (3% molar compared to the CEVE), to prevent the cationic homopolymerization of the vinyl ether. The reaction was performed at 75°C for 12h. The alternated poly(CTFE-*alt*-CEVE) copolymer was obtained with a mass yield of 75%. Molecular weight of the poly(CTFE-*alt*-CEVE) is 25,000 $g.mol^{-1}$ with a polydispersity index (PDI) of 3. These results were determined by size exclusion chromatography (SEC) measurement calibrated with monodispersed polystyrene standard.

The second step corresponds to a chemical modification of the poly(CTFE-*alt*-CEVE) that will allow us to achieve a direct phosphonation. This chemical modification is based on the Finkelstein reaction and realized by a nucleophilic substitution of the chloride atom into an iodide atom [6] (Figure 59b).

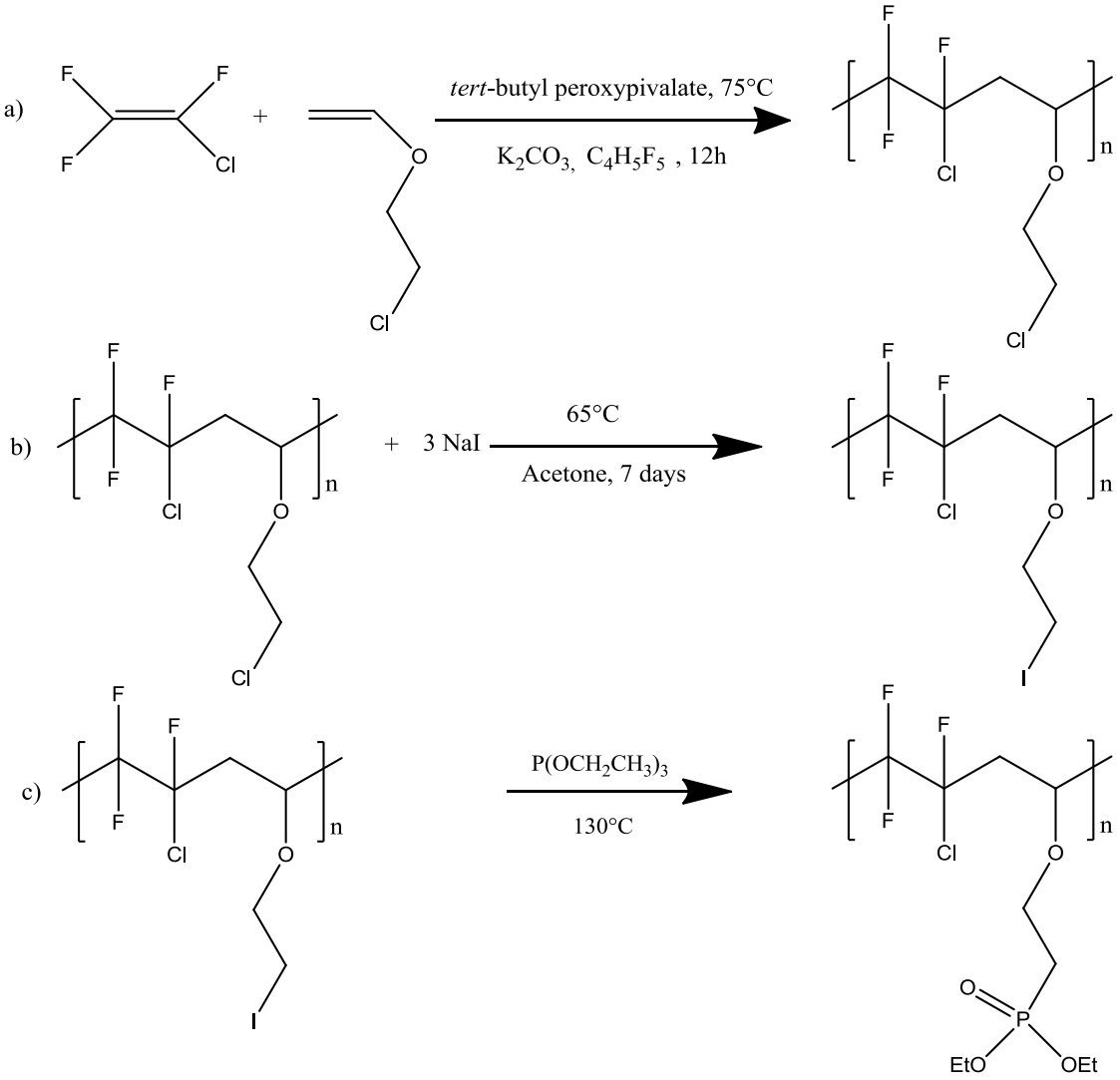

Figure 59 : Synthesis of poly(CTFE-alt-DEVEP) phosphonated copolymer : a) Radical copolymerization of CTFE with CEVE, b) Finkelstein reaction, c) Michaelis-Arbuzov reaction.

The direct phosphonation of the iodine copolymer is performed during the third step of the synthesis via the Michaelis-Arbuzov [7-9] reaction (Figure 59c). This reaction, between a trialkyl phosphite and a halogenated derivative, is a SN_2 nucleophilic substitution. The trialkyl chosen for this reaction is the triethyl phosphite. It is also used as the solvent. The Michaelis-Arbuzov reaction gives secondary products resulting from the decomposition of triethyl phosphite and iodoethane. Thus, the presence of a large excess of triethyl phosphite enables to substitute iodoethane by the diethyl phosphonate. These secondary products and solvent are removed by distillation under reduced pressure. The poly(CTFE-*alt*-DEVEP) is obtained with a final mass yield of 60% and has been characterized by ^{1}H, ^{31}P and ^{19}F NMR

spectroscopies (Figure 60, Figure 61 and Figure 62 respectively) in order to confirm the expected structure.

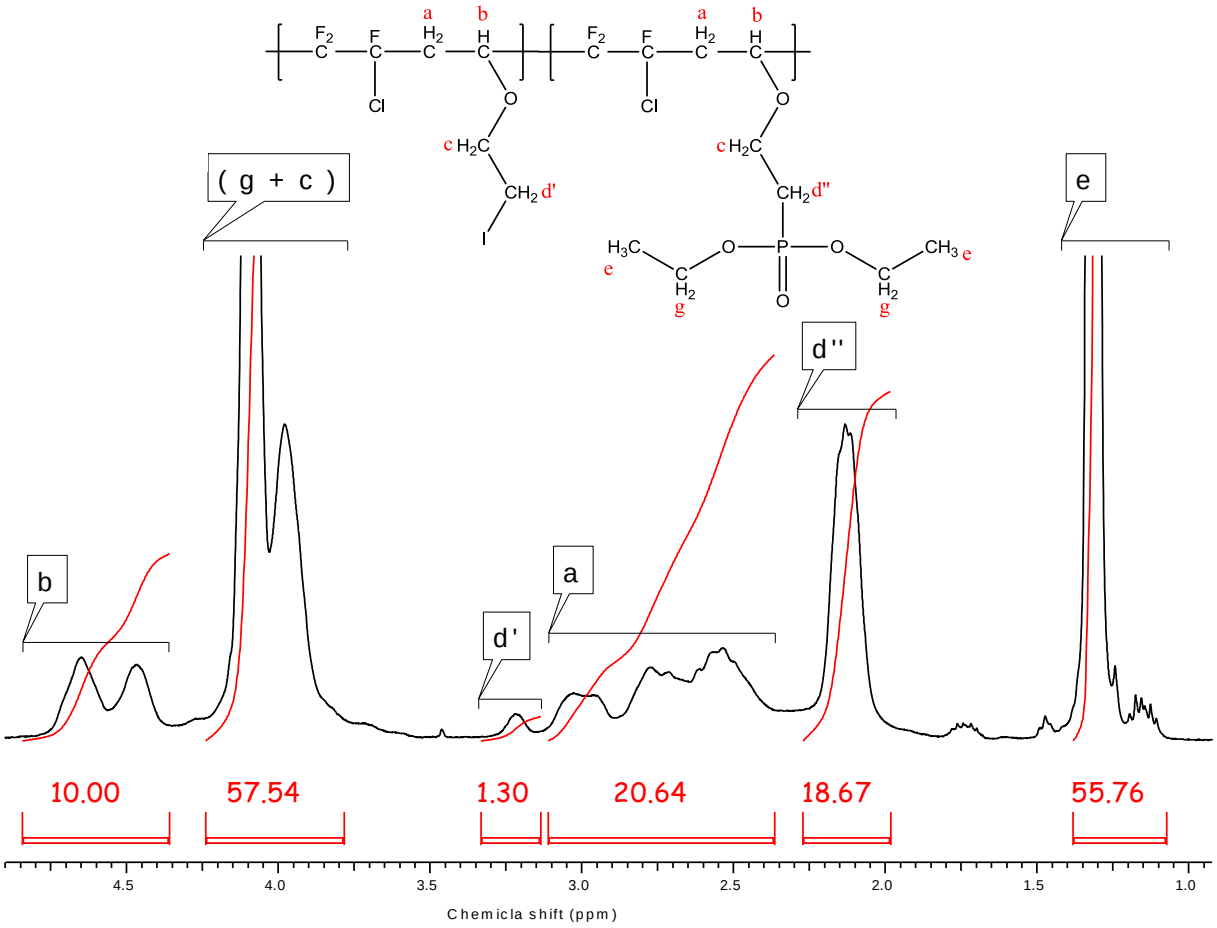

Figure 60 : ^{1}H NMR spectrum of poly(CTFE-alt-DEVEP) (recorded in $CDCl_3$)

From Figure 60, we can see a triplet centered at 1.32 ppm, and also a multiplet centered at 4.09 ppm corresponding respectively to the –C**H$_3$** (*e*) and the –C**H$_2$**- (*g*) assigned to the phosphonic ester functions. Furthermore, the iodine substitution by the phosphonate groups is confirmed by the decrease of the intensity signal assigned of the –C**H$_2$**-I (*d'*) and the occurrence of the signal of the –C**H$_2$**-P-(*d''*) groups centered at 3.22 and 2.13ppm, respectively.

The phosphonation rate is calculated from ^{1}H NMR spectroscopy by using the equation 1.

$$\propto DEVEP = \frac{\int CH_2P}{\int CH_2P + \int CH_2I}$$

with DEVEP: diethyl-2-vinylethyl ether phosphonated.

Equation 1: Calculation of phosphonated rate into the poly(CTFE-alt-DEVEP) copolymer

The content of phosphonation was then assessed to 93 mol%.

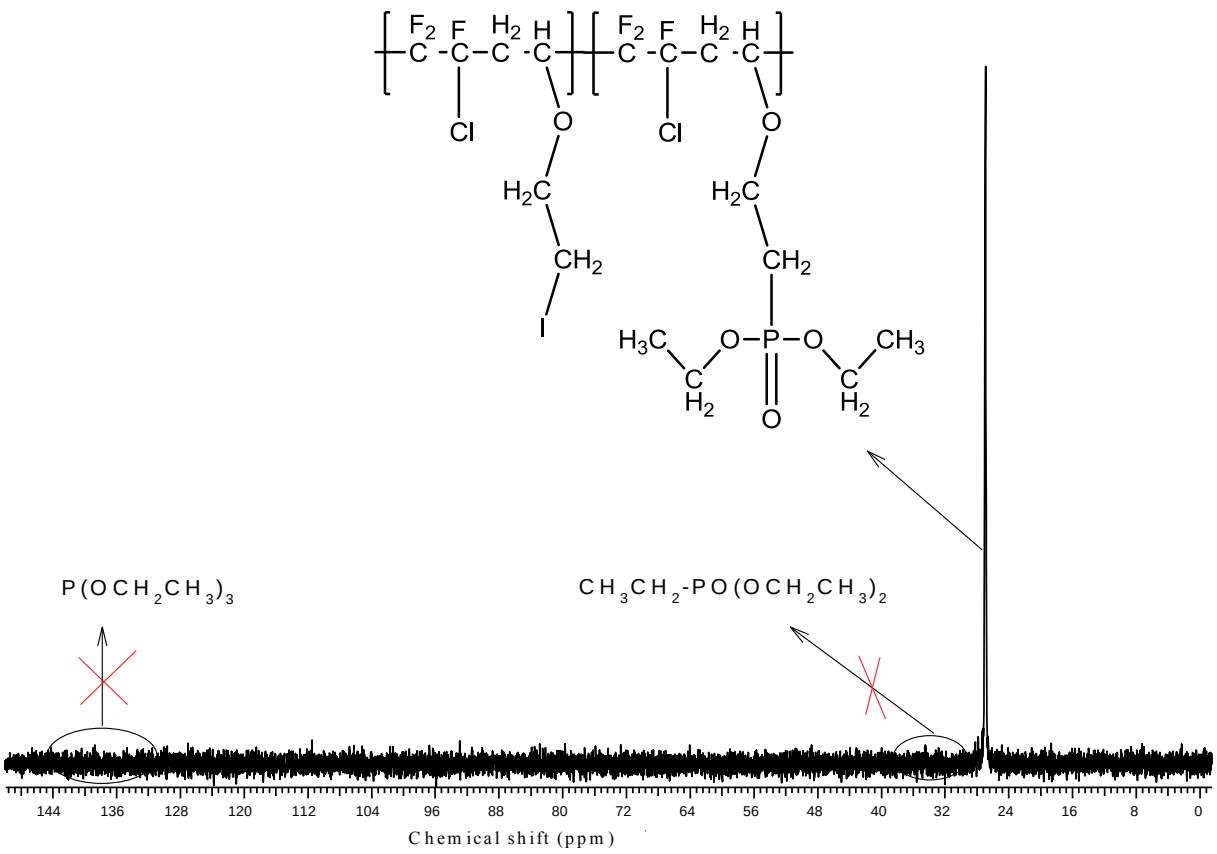

Figure 61 : ^{31}P NMR spectrum of poly(CTFE-alt-DEVEP) copolymer (recorded in $CDCl_3$)

The ^{31}P NMR spectrum of poly(CTFE-*alt*-DEVEP) is shown Figure 61, and allows to confirm the direct phosphonation reaction. Furthermore, we can observe the absence of

peaks at 33 and 104ppm, corresponding to the ethyl phosphonate and the triethyl phosphite, respectively.

The ^{19}F NMR spectrum is showed Figure 62. The presence of the four signals significant of the fluorine atom of the polymer main chain can be observed. Concerning the -C**F**$_2$- groups, the large signals are range between -108 at -112, -115 at -119, and -120.7 at -123 ppm and for the -C**F**Cl- the signal is centered at -120 ppm.

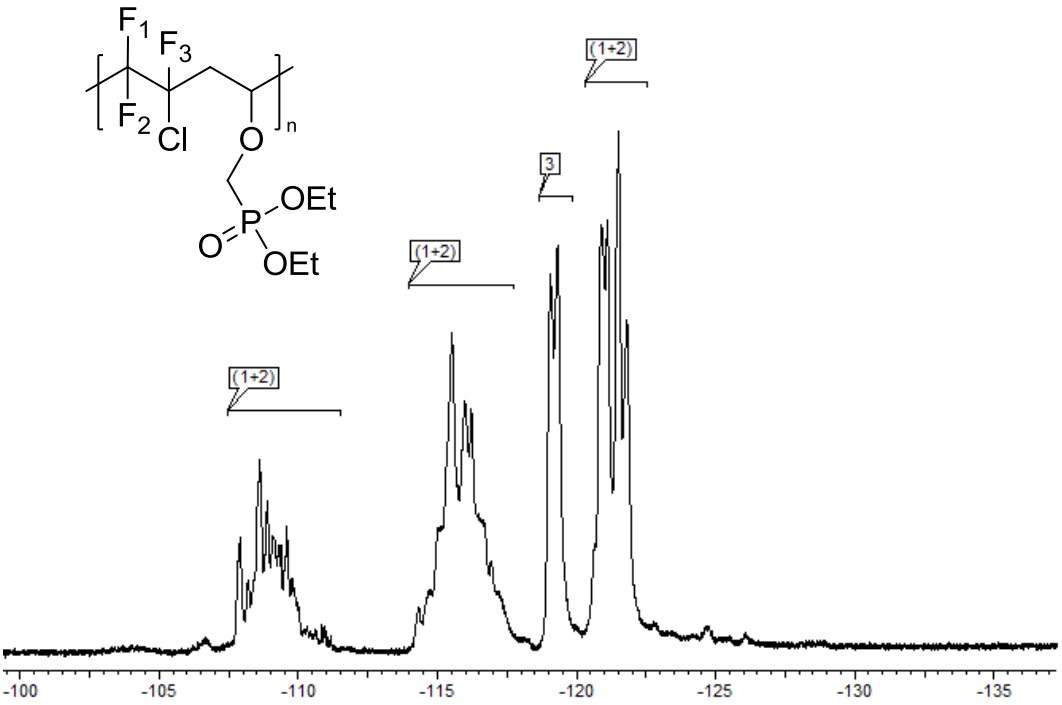

Figure 62 : 19F NMR spectrum of poly(CTFE-alt-DEVEP) (realized in $CDCl_3$)

Thermal properties of the copolymer were then determined from thermogravimetric analysis (TGA) and differential scanning calorimetry (DSC).

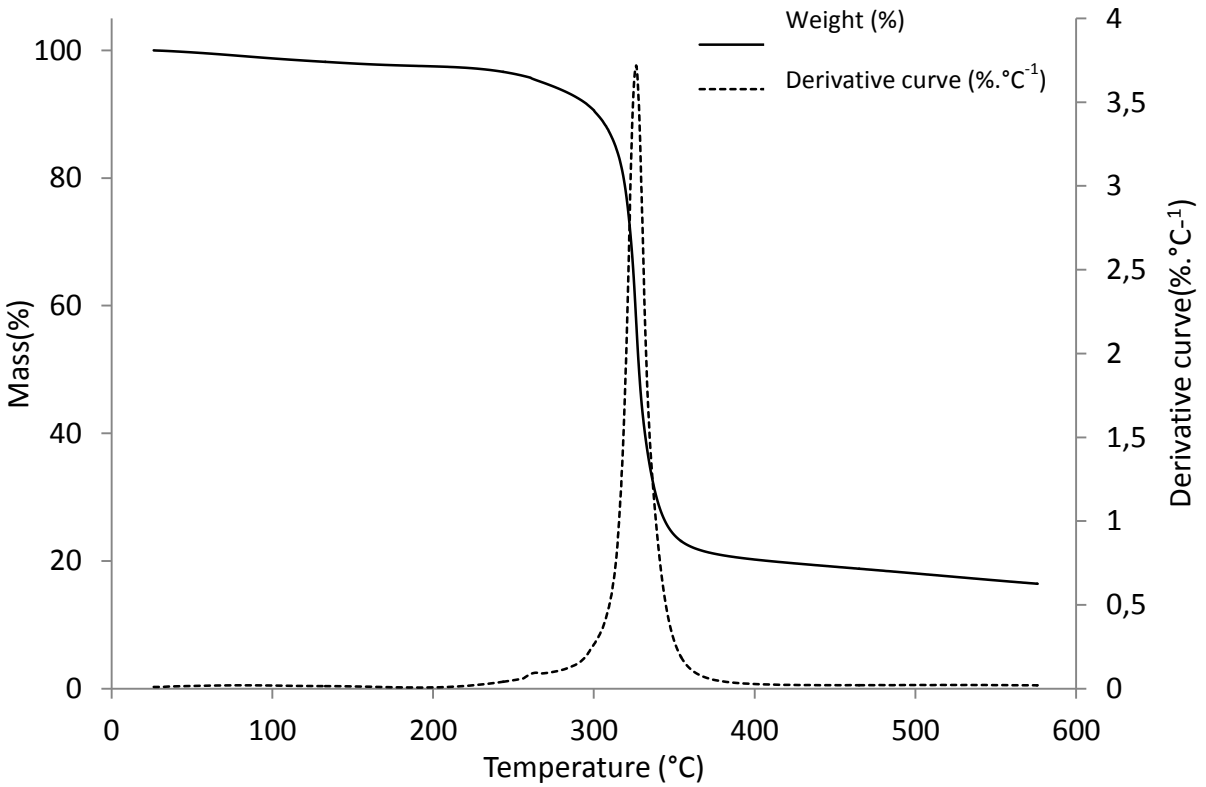

Figure 63 : Thermogravimetric analysis recorded under nitrogen in dynamic mode at 10°C.min^{-1} of poly(CTFE-alt-DEVEP)

Figure 63 represents the thermogram obtained by TGA of the poly(CTFE-*alt*-DEVEP). This analysis has been realized under nitrogen atmosphere at 10°C.min^{-1}. We can observe that the starting temperature for the main polymer degradation is about 250°C, and the temperature corresponding at the 5 % of weight loss is 268°C. However, the weight loss between 250 and 300°C can be attributed to the loss of diethyl ester groups via the formation of ethylene and phosphonic acid [10].

The glass transition temperature (Tg) of the poly(CTFE-*alt*-DEVEP) has been determined by DSC. It is equal at 3°C. We can note that the Tg of poly(CTFE-*alt*-DEVEP) is much lower than that of poly(CTFE-*alt*-IEVE) and poly(CTFE-*alt*-CEVE). This is explained by the difference of the free volume occupied by these two types of terminal groups. Indeed, the phosphonate groups are much larger, which has the effect of increasing the distance between the polymer chains. The results of both thermal analyses are listed in Table 2.

Table 2 : thermal properties of poly(CTFE-alt-CEVE), poly(CTFE-alt-IEVE) and poly(CTFE-alt-DEVEP). $Td_{i\%}$ stands for the temperature decomposition of i% weight loss of the copolymer.

Copolymer	$Td_{5\%}$ (°C)[a]	$Td_{10\%}$ (°C)[a]	Tg (°C)[b]
Poly(CTFE-*alt*-CEVE)	300	320	27
Poly(CTFE-*alt*-IEVE)	285	297	41
Poly(CTFE-*alt*-DEVEP)	268	302	3

a : determined by TGA analyses in dynamic mode at 10°C.min^{-1}.

b : determined by DSC analyses at 10°C.min^{-1}.

3 Realization and characterizations of Blend Membranes

The polymer obtained has a molecular weight around 20,000 g.mol^{-1}, this low molecular weight value is attributed to an exothermic effect observed during the radical copolymerization. This exothermic effect increases the concentration of radicals which leads to the initiation of new chains but also to the termination reaction as well as transfer reactions. Because of the low molecular weight, the copolymer shows poor mechanical properties and we also observe exfoliation phenomenon of the membrane in water. So, the use of this kind of polymer, in order to realize fuel cell, appears to be very limited. That is why it is necessary to develop a blend membrane strategy, in which we will use a fluoropolymer matrix, which shows high thermo-oxidative stability and good mechanical properties.

The use of a fluorinated polymer will increase the content of fluorine in the final material. A higher rate of fluorine should also allow a better separation of hydrophobic and hydrophilic parts.

3.1 Characterization of PVDF 31508®

The PVDF 31508® is a commercial copolymer composed by the difluorine vinilydene and the chlorotrifluoroethylene. It has a very high thermal stability, but also a high stability in acid medium. Furthermore, it has a very good mechanical resistance, with a break elongation of 475% and a break stress of 22MPa. The molecular weight of this copolymer is

about 95,000 g.mol^{-1} and has a polydispersity index of 2.33. In order to evaluate the thermal properties, the polymer is analyzed by TGA under a nitrogen atmosphere. The different characteristics of PVDF 31508® are summarized in Table 3.

Table 3 : Characteristics of PVDF 31508®

Mn (g.mol^{-1})[a]	95,000
Ip[a]	2.33
$Td_{10\%}$ (°C)[b]	440
Tg (°C)[c]	-30
Tf (°C)[c]	160

a : Determined by GPC calibrated with polystyrene
b : determined by TGA analyses in dynamic mode at 10°C.min^{-1}.
c : determined by DSC analyses at 10°C.min^{-1}.

3.2 Preparation of blend membranes

The membranes are prepared via the casting/evaporation process of polymers' solutions. For this, a precise amount of poly(CTFE-*alt*-DEVEP) phosphonated polymer is solubilized in dimethylsulfoxide (DMSO), then the poly(VDF-*co*-CTFE) is added to the solution at 50°C. Mass concentrations of polymers in DMSO vary between 20 and 25% with the aim of obtaining a solution with a viscosity suitable for the membrane casting. The solution is then subjected to two treatments with ultrasound: a first one in order to completely dissolve any remaining microgels and then a second one in order to eliminate air bubbles. Then, the solution is casted onto a glass plate at room temperature, using a hand-coater and a wedge whose size determines the thickness of the final membrane.

The first tests were carried out using the phosphonic acid polymer form. However, the results were not conclusive. Indeed, the heterogeneity of the membrane is observed (see Figure 64). That is why, it was decided to carry out the mixing of the two polymers using phosphonated polymer in the phosphonate form. Under these conditions, the membranes obtained after shaping are homogeneous (Figure 65).

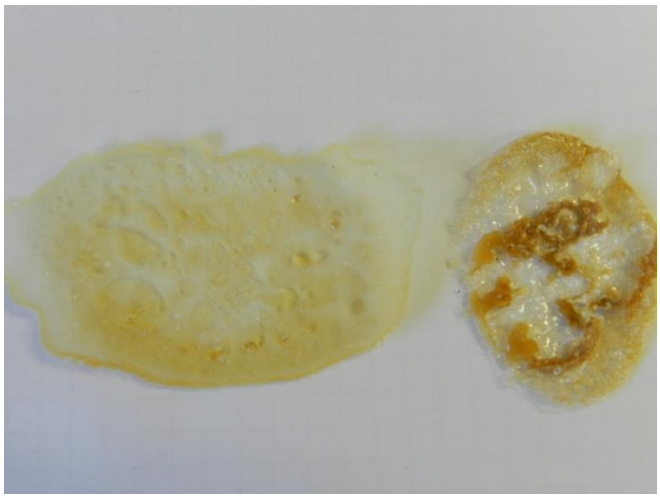

Figure 64 : Blend membrane PVDF31508®/Phosphonated polymer under phosphonic acid form

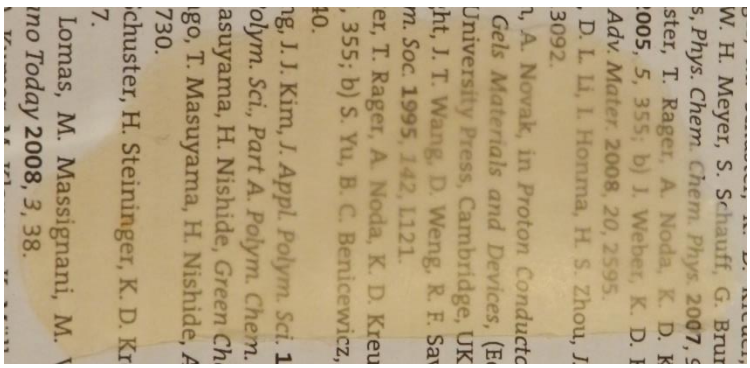

Figure 65 : Blend membrane PVDF31508®/Phosphonated polymer under phosphonate ester form

The cleavage of the phosphonate functions will be achieved by simple immersion of the membrane in hot hydrochloric acid for several days. Five membranes have been made by varying the proportion of PVDF 31508®.

The next part of this chapter is devoted to the preparation of a range of blend membranes, by using the above mentioned strategy. Then, their thermal, mechanical properties will be determined as well as their proton conductivities. This part is presented as a journal article entitled “A new PEMFC composed of a high fluorinated polymer blended with a fluorinated polymer containing phosphonic acid”, which was submitted to Journal of Power Sources.

A new PEMFC composed of a high fluorinated polymer blended with a fluorinated polymer containing phosphonic acid.

Etienne Labalme[1], Julien Souquet[2], Ghislain David[1], Pierrick Buvat[2], Janick Bigarre[2]

[1]Equipe Ingénierie et Architecture Macromoléculaires, Institut Charles Gerhardt UMR CNRS 5253, Ecole Nationale Supérieure de Chimie de Montpellier, 8 rue de l'Ecole Normale, 34296 Montpellier Cedex 5, France

[2]CEA, DAM, Le Ripault, F-37260 Monts, France

Abstract:

In order to enhance the thermo-chemical and mechanical properties of the proton exchange membrane (PEM), a series of five blend membranes made from poly(vinylidene fluoride-co-chlorotrifluoroethylene) (poly(VDF-co-CTFE)) with a fluorinated copolymer containing phosphonic acid was realized. The mechanical properties of these blend membranes were assessed by dynamic mechanical analysis (DMA). In order to determine the influence of fluorinated copolymer on the blend membrane morphology, a SAXS study was performed. The presence of the fluorine atoms from poly(VDF-co-CTFE) allows to obtain membranes with a better structuration, but also to enhance the oxidative stability in the presence of radicals. The best result obtained show a proton conductivity of 40mS.cm^{-1} at 80°C under fully hydrated conditions.

4 Introduction

During these last years, many research works have been carried out on the new technology development in order to use fuel cell as a new energy source. One of the main subjects of research was the amelioration of the proton exchange membrane which is the

heart of the fuel cell. Nowadays, the must used membranes are perfluorosulfonic polymers (Nafion®, Aquavion®…), which allow to reach the best performances in moderate range of temperature between 25 and 80°C and high level of hydration with a relative humidity more than 50% RH.

Nevertheless, in the automotive sector, fuel cell specifications were defined to be used nominally at 120°C with 30% RH and low pressure. Under these conditions, perfluorosulfonic membrane performances fall drastically due to lost of water. This implies the necessity to develop membranes with novel protogenic groups able to give proton conduction in low hydration condition at 120°C. In these conditions, membranes bearing phosphonic acid groups seem to be a good potential candidate [11, 12].

Indeed, the proton conductivity of phosphonic acid polyelectrolytes was better than sulfonated polymer at elevated temperatures and in a dry state. This higher proton conductivity demonstrates the amphoteric character of the acid phosphonic groups associated to a proton transport by a Gröthuss mechanism [13]. Furthermore, phosphonic acid-functionalized polyelectrolytes permit to obtain material with low water swelling, which improve the mechanical stability during cycle of use.

Then, during this last years different works were carried out on the synthesis of different polyarylphosphonic acid functionalized [10, 14-18] or polystyrene derivative carrying phosphonic acid groups [19, 20].

Among the required characteristics of the PEMFC membrane, mechanical and thermal properties become an important criterion because during fuel cell operation, membranes suffer from important mechanical deformations due to swelling cycles. Furthermore, a good chemical resistance is also required to be used in an acid aqueous solution and in the presence of radicals which were formed during the fuel cell operation. Despite interesting electrochemical performances, the use of the polymer membrane can be highly limited from low mechanical properties. In order to increase the performance of material, a blend of polymers can be used. The aim of this strategy consists to combine polymers which possess complementary properties. Finally, judicious choice of polymers make possible to obtain a material possessing all the properties required for the intended application. Fluorinated polymers are commonly used to perform blend membranes, because these polymers show

very high mechanical, chemical and thermal properties. So, it seems promising to perform membranes comprising both a polymer bearing protogenic groups, allowing the proton transport, and a fluorinated polymer, which improves the mechanical, thermal and chemical properties. The common fluorinated polymer used in the PEMFC domain is the poly(vinylidenefluoride) (PVDF) ($(CH_2\text{-}CF_2)_n$). Different grades of PVDF are commercialized and differ from the molar mass and the different chemical compositions. VDF can be also copolymerized with fluorinated monomers such as chlorotrifluoroethylene (CTFE) or hexafluoropropylene (HFP).

Previous work performed by our team [2-4] involved the synthesis of partially fluorinated copolymer bearing phosphonic acid groups. The polymer synthesis is a multistep pathway. In the first step, the radical polymerization of chlorotrifluoroethylene and 2-chloroethylvinylether was performed. The second step consists to perform the nucleophilic substitution of the chlorine atom by a iodine atom through the Finkelstein [6] reaction, thus allowing the phosphonation of polymer by the Michaelis-Arbuzov [7-9] reaction. Thanks to the acceptor/donor character of monomers used for the polymerization, the polymer obtained showed an alternated structure[21] between fluorinated and phosphonic acid units, which allows the presence of phosphonic acid groups distributed along the polymer. Interestingly, this polymer was used as PEMFC and showed a very good thermal stability (up to 200°C). Furthermore, when decreasing RH from 95 to 25%, the conductivity values decreased of only 1 order of magnitude, while the nafion® conductivity drops of about 3 orders of magnitude in the same range. Furthermore, an increase of the temperature (from 90 to 120°C) leads to an increase of the proton conductivity by twice in the same range of RH. This result indicates that water molecules and phosphonic acid hydrogen bonding are involved in the proton conduction mechanism. Finally, the proton conductivity increases by 3 orders of magnitude by increasing IEC (from 2.5 to 7 $meq.g^{-1}$) to reach 20 $mS.cm^{-1}$ at 25°C and 95% RH. It was concluded that the high IEC is the key factor to significantly change the water sorption and, as a consequence, to increase the proton conductivity. However, the molar mass of the polymer obtained was about 20,000 $g.mol^{-1}$, this implies that resulting membranes exhibit very poor mechanical properties, as they were very brittle. These low mechanical properties are greatly limiting their use in dry conditions, as well as decreasing life time of the membrane.

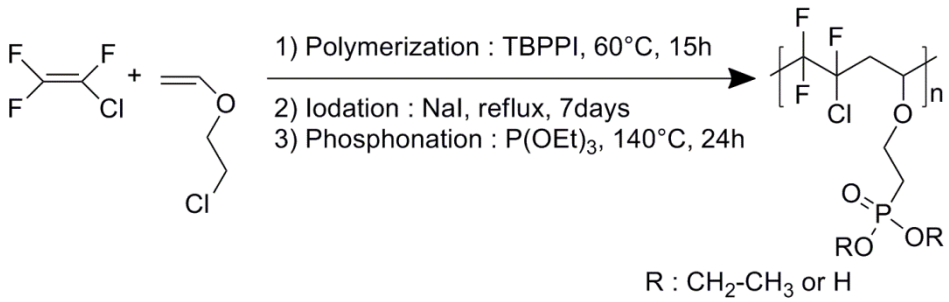

Figure 66 : Different steps of synthesis of poly(chlorotrifluoro ethylene-alt-Phosphonated-ethylvinylether) poly(CTFE-alt-DEVEP)

In order to optimize the performances of the phosphonated membrane, the present contribution reports on the realization of blend membranes composed by the phosphonated polymer exhibiting the highest IEC, i.e. poly(chlorotrifluoro ethylene-alt-Phosphonated-ethylvinylether) (poly(CTFE-*alt*-DEVEP)) with 47wt% of phosphonic groups and a low cost fluorinated polymer, i.e. poly(vinylidene fluoride-co-chlorotrifluoro ethylene) (poly(VDF-*co*-CTFE)). Several membranes have been elaborated with different contents of both polymers. Both thermal and mechanical properties were evaluated as a function of the polymers content. Then, membranes proton conductivities were studied as a function of temperature.

5 Experimental section

5.1 Materials

Polymers used for matrix were poly(vinylidene fluoride-*co*-chlorotrifluoro ethylene) and poly(chlorotrifluoro ethylene-*alt*-Phosphonated-ethylvinylether). Their structures were showed figure 3. The poly(VDF-*co*-CTFE) grade was Solef 31508 supplied by Solvay with Mn = 95,000 g.mol^{-1} (Mn/Mw = 2.33). The phosphonated polymer used was represented in figure 1. That was obtained by a radical polymerization of chlorotrifluoro ethylene and 2-chloro ethyl vinyl ether, followed by different steps of post-functionalization in order to obtain the polymer bearing phosphonated groups. Details of the syntheses can be found in the work of Tayouo et al.[2-5]. Dimethylsulfoxide (DMSO), hydrochloric acid (HCl), Sodium chloride (NaCl), Sodium hydroxide (NaOH) were purchased from Aldrich and used as received.

5.2 Synthetic procedure for blend membranes

A specific amount of poly(CTFE-*alt*-DEVEP) was dissolved in DMSO (20-25 wt%), then poly(VDF-*co*-CTFE) powder was added into the poly(CTEF-*alt*-DEVEP) solution, which was stirred several hours at 50°C. After the poly(VDF-*co*-CTFE) was fully dissolved, the solution was cast onto glass plate, and then dried at 60°C during 24 h.

To obtain the phosphonic acid groups, membranes were immerged in an HCl concentrated solution (12N) at 90°C during 3 days. After reaction, membranes were washed by deionized water, and then dried under vacuum at 80°C during one night. Different compositions of membranes were given in Table 4.

Table 4 Compositions of the different blend membranes

Sample	poly(VDF-*co*-CTFE) (wt%)	poly(CTFE-*alt*-DEVEP) (wt%)
M-0	100	0
M-20	80	20
M-35	65	35
M-50	50	50
M-65	35	65
M-80	20	80
M-100	0	100

5.3 Thermal analysis

The thermal stability of the different blend membranes was evaluated from thermogravimetric analysis (TGA) on a Q50 analyzer from TA Instruments. The data were collected from 25 to 600°C. The samples were analyzed both under a nitrogen atmosphere at a heating rate of 20°C.min^{-1}. Differential scanning calorimetry (DSC) measurements were carried out using a Perkin-Elmer Pyris 1 apparatus. Scans were recorded at a heating/cooling

rate of 20°C min^{-1} from -100 to 150°C. A second scan was required for the assessment of the Tg, defined as the inflection point in the heat capacity jump.

5.4 Ion exchange capacity

The ion exchange capacity (IEC) of the different blend membranes was determined from back titration. The sample were immersed and stirred in an aqueous solution of NaOH (0.1N, 2.5mL) and NaCl (2N, 50mL). This solution was back titrated with 0.01N HCl aqueous solution. The IEC value (meq.g^{-1}) of the blend membranes was calculated using the equation 1, where V_{eq} is the volume of 0.01 HCl aqueous solutions for the volumetric titration, [OH^-] the OH^- concentration of the initial aqueous solution and m_d the dry weight of the membrane.

$$IEC(meq.g^{-1}) = \frac{[OH^-]*V_{eq}}{m_d} \quad (1)$$

5.5 Water uptake and swelling measurements

Water uptake was assessed from the wet and dry states of the materials according to the following protocol: the membranes were immersed in distilled water for 24 hours and then removed. The membranes were wiped with a tissue paper, and then both the mass and thickness of the blend membranes were determined in these wet conditions. The membranes were dried at 70-80°C for 72 h to determine the dry weight and the dry film thickness. The water uptake was determined by the following equation:

$$\text{Water uptake } (\%) = \frac{m_w - m_d}{m_d} * 100 \quad (2)$$

Where, m_w is the wet mass of the blend membranes, and the swelling of the membranes was determined by the following equation:

$$Swelling\ (\%) = \frac{t_w - t_d}{t_d} * 100 \quad (3)$$

Where t_w and t_d are the wet and dry thickness of the blend membranes, respectively.

5.6 Oxidative stability

For the measurement of oxidative stability, a membrane was immersed in a Fenton's solution containing 3% H_2O_2 and 4 ppm Fe^{2+} at 68°C[22]. After stirring for a determined time, the membrane was washed with water and dried under vacuum at 80°C, and the weight loss % was measured.

5.7 Mechanical properties

Dynamic-mechanical analysis (DMA) was conducted with a METRAVIB DMA 25. Uniaxial stretching of samples were performed while heating at a rate of 2°C/min from -100 to 150°C, keeping frequency at 1 Hz (viscoelastic region) and a constant deformation rates. The glass transition temperature was obtained from tanδ determination. It has been shown that tanδ maximum relates much better to the value obtained by DSC[23]. Furthermore, the mechanical behavior was studied versus the RH range between 0 and 80% and in the temperature range between 25 and 70°C.

5.8 Small angle X-ray scattering

SAXS measurements were done on the fully hydrated sample. We worked in a transmission configuration. X-ray scattering patterns were obtained by plotting the scattered intensity as a function of the wave vector q (nm^{-1}).

5.9 Proton conductivity

The proton conductivity was evaluated by electrochemical impedance spectroscopy (EIS) using MATERIALS MATES 7260 dielectric analyzer with high and low frequencies

compensations in order to take into account cables and connections effects. The temperature and humidity were controlled by FUMATEC MK3 device with three heating areas. The FUMATEC cell was composed by two parallel wires electrodes of platinum separated by 10mm.

Before conductivity measurements, membranes were previously stored 24 hours in deionised water at room temperature. Measurements were carried out in wet state membranes (5 x 20 mm). The proton conductivity was measured between 20 and 80°C with sample completely immerged in water. Impedance data were gathered over the frequency range of 10^{-1} – 10^{7} Hz at voltage amplitude of 100 mV and were analyzed with the MATERIALS MATES software. A typical impedance diagram measured with the EIS cell is presented in Figure 67. The proton conductivity (σ) was calculated following the equation:

$$\sigma = \frac{d}{e \times L \times R}$$

Where d is the distance between the two electrodes

e is the thickness of the wet membrane

L is the larger of the wet membrane

R is the diameter of the half-circle in the impedance diagram Z', -Z" (Figure 67)

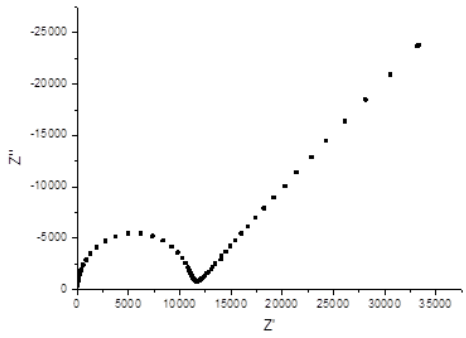

Figure 67 : Example of impedance diagram recorder with the EIS cell in order to calculate the proton conductivity of membrane.

6 Results and discussion

The aim of this work is to improve the mechanical properties of membranes having a real potential for fuel cell application. In order to determine the influence of the

incorporation of the fluoropolymer on the membranes structure, and the effect on the proton conductivities, the membranes with poly(VDF-*co*-CTFE) rates varying from 0 to 80% were studied. Firstly the poly(VDF-*co*-CTFE) and the poly(CTFE-*alt*-DEVEP) were mixed where the phosphonated groups were under the acid forms. However this blend membrane showed a visual phase separation. Finally poly(CTFE-*alt*-DEVEP) was added under ester form making possible to obtain homogeneous blend membranes. After acid treatment to HCl, there stayed homogenous. In order to improve the affinity between both polymers, we used a commercial fluorinated copolymer which possess the same monomer that the phosphonated polymer, the CTFE.

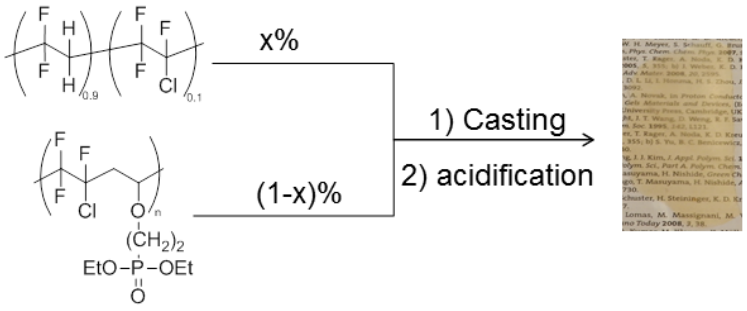

Figure 68 : Schematic representation of procedure to obtain blend membrane composed of both poly(VDF-co-CTFE) and poly(CTFE-alt-DEVEP).

6.1 **Thermal analysis**

The thermal stability of different blend membranes was evaluated by TGA analysis, the result were showed Figure 69 and Figure 70. To better understand the thermal degradation curves of blend membranes, the first analyses were performed on the M-0 and M-100 membranes (i.e. 100% poly(VDF-*co*-CTFE) and 100% poly(CTFE-*alt*-DEVEP), respectively) (Figure 69). Both thermograms show only one weight loss. Hence, degradation of phosphonated membrane (M-100) starts at 200°C, corresponding to about 70% of weight loss, which may be ascribed to the splitting of C-P bond (Binding energy = 259.41kJ.mol^{-1})[24], followed by the degradation of backbone[2] from the partially fluorinated copolymer bearing phosphonate moieties. Concerning the fluorinated membrane (M-0), the main degradation ranges from 400°C to 500°C, corresponding to about 80% of weight loss, also

attributed to the backbone degradation. These two main degradations were also observed for all the thermograms of blend membranes (Figure 70). Furthermore, from these thermograms, the membrane composition can be determined. Indeed, at 400°C, the weight loss corresponds to the phosphonated polymer degradation, thus allowing the real membrane composition determination. The temperatures corresponding to 5% ($Td_{5\%}$) and 10% ($Td_{10\%}$) weight loss are given in Table 5. For all blend membranes, $Td_{5\%}$ and $Td_{10\%}$ were higher than 270°C and 290°C, respectively and consequently these blend membranes can be used as PEM. Isotherms at 140°C would definitively assess the good thermal stability of these fluorinated copolymers. Hence, TGA thermograms were recorded at 140°C under air during 60 h for the M-50 and M-80 membranes (i.e. composed with 50 and 80%wt of phosphonic polymer). Only 5% of degradation was observed for both blend membranes, ascribed to the loss of water molecules due to the formation of anhydride bonds between phosphonic acid groups[25]. All these results demonstrate the good thermal stability of these membranes for a temperature range from 25 to 250°C.

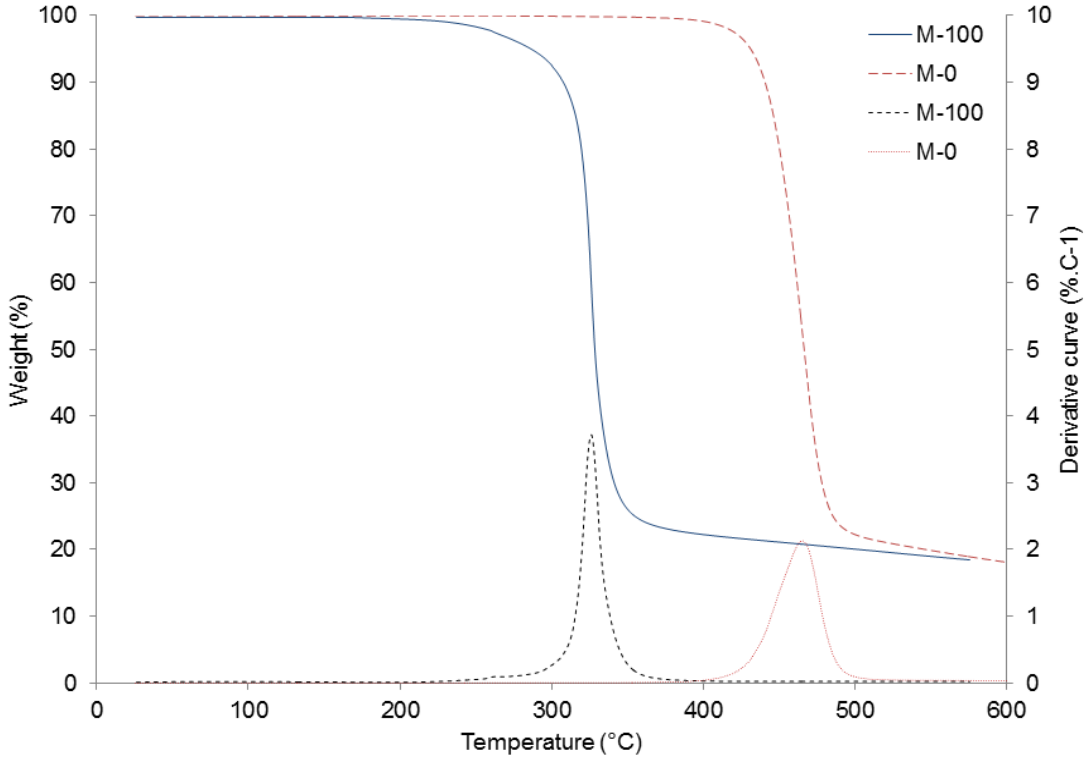

Figure 69 : TGA curves of the M-0 and M-100 membranes under nitrogen at 20°C.min^{-1}

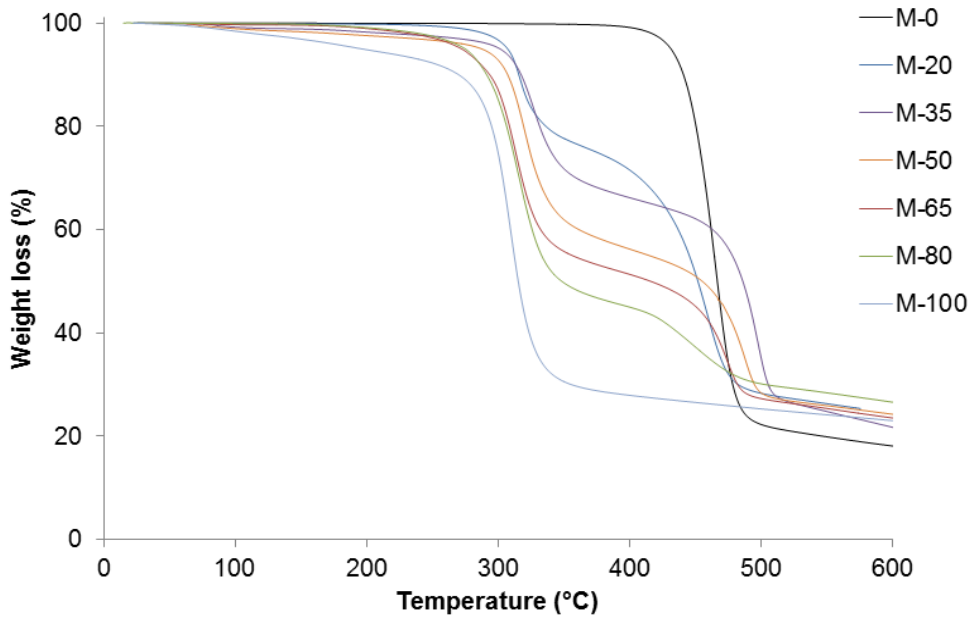

Figure 70 : TGA curves of blend membranes under nitrogen at 20°C.min-1

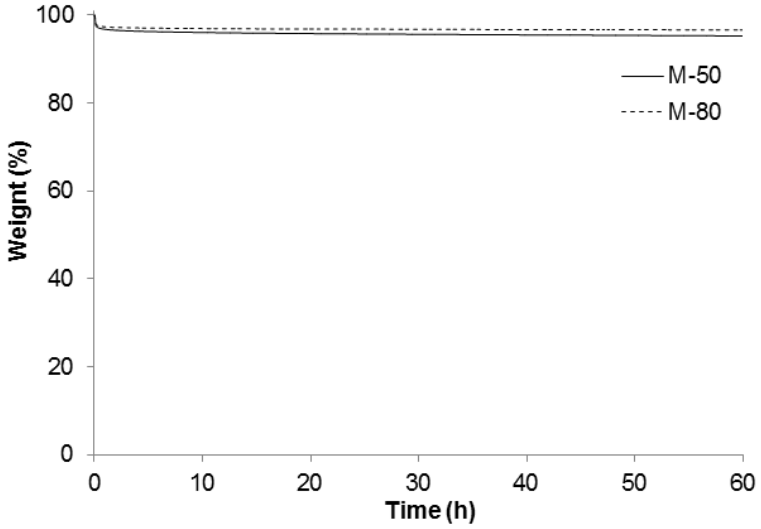

Figure 71 : Isotherm curves of the M-50 and M-80 membranes under air at 140°C

The Fenton test was performed for each blend membrane and their stability was then assessed. The blend membranes were tested with respect to their oxidative stability using the Fenton test. Figure 72 gives the TGA curves for the M-65 membrane before and

after the Fenton test and clearly shows the same TGA curves. Thus the blend membranes are not degraded by the oxidative treatment.

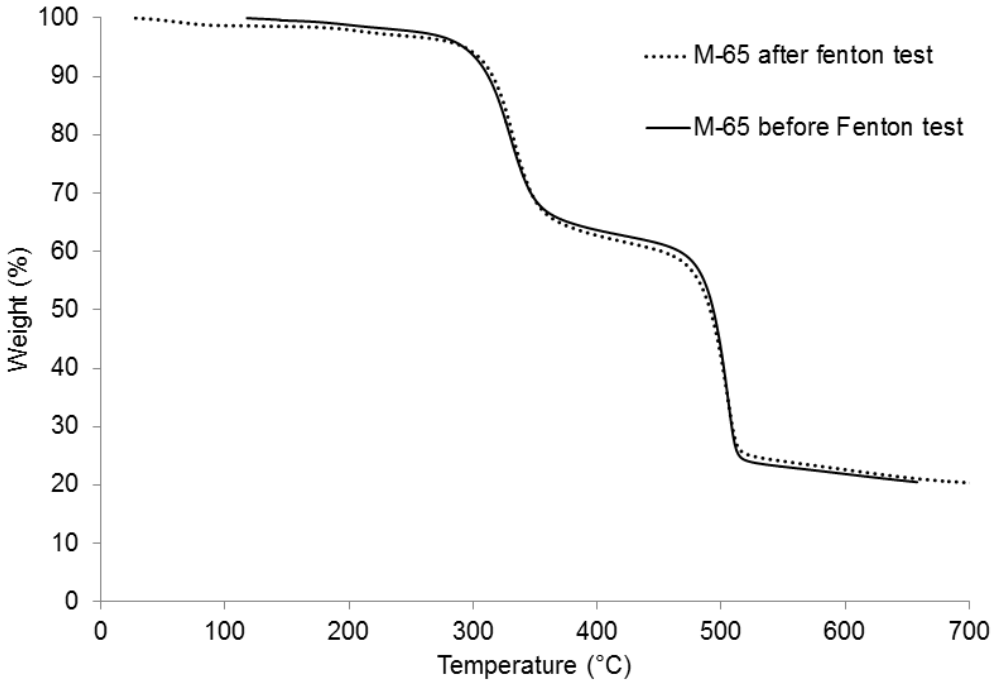

Figure 72 : TGA curves of M-65 membrane before (-) and after (•) the Fenton test.

Glass transition temperatures (Tg) of blend membranes were determined from differential scanning calorimetry (DSC), the results are listed in Table 5. First, Tg of poly(VDF-*co*-CTFE) (Tg_1) and poly(CTFE-*alt*-DEVEP) (Tg_2) were determined, the values are -30°C and 70°C, respectively. For a polymer blend, the glass transition value is governed by the Fox-Flory equation.

$$\frac{1}{T_g} = \frac{w_1}{Tg_1} + \frac{w_2}{Tg_2} \qquad (3)$$

Where Tg, Tg_1 Tg_2 are the glass transition temperature of polymer blend, poly(VDF-*co*-CTFE) and poly(CTFE-*alt*-DEVEP) in K respectively, and w_1 and w_2 are weight fractions of poly(VDF-*co*-CTFE) and poly(CTFE-*alt*-DEVEP) respectively.

The theoretical Tg are given in Table 5. An increase of poly(VDF-*co*-CTFE) content in the membrane composition should lead to a decrease of the theoretical Tg membranes. The values are ranged from -15 to 44°C for a poly(VDF-*co*-CTFE) rate varying from 80 to 20wt%. However, DSC analysis of blend membranes shows very different results. Indeed, from the DSC curves, only one Tg can be observed for all membranes, ascribed to the phosphonated polymer. Indeed, Tg of poly(VDF-*co*-CTFE) isn't measurable by DSC (Tg_1 given in table from data supplier). Furthermore, these values are higher than that of the M-100 membrane (membrane performed with the phosphonated polymer only) and Tg values increase with the poly(VDF-*co*-CTFE) rate. To conclude, we didn't observe an average Tg, but just an increase of the Tg_2 of all membranes proportionally with the poly(VDF-*co*-CTFE) rate. The evolution of Tg_2 is due to the presence of hydrogen bonding between the phosphonic groups. Indeed, poly(VDF-*co*-CTFE) is a high hydrophobic polymer, so during the polymer mixture, in order to minimize the hydrophobic/hydrophilic interaction, phosphonic acid groups would become closer. This phenomenon induces stronger hydrogen bonding, resulting in an increase of the Tg_2.

Generally, when two polymers are mixed, the intrinsic properties as the cristalinity are directly impacted. The poly(VDF-*co*-CTFE) is a crystalline polymer, so during the cooling thermograms of blend membranes the phenomena of crystallization can be observed. In order to determine the affinity between both polymers, the variation on the crystallization endotherm can be observed by analyzing the cooling thermograms. Figure 73 shows the evolution of the crystallization temperature (T_c) of poly(VDF-*co*-CTFE) for different blend membranes. The increase of phosphonated polymer content in the blend membranes composition leads to an increase of T_c. This increase is due to the presence of interactions, primarily hydrogen bonding, between the fluorinated polymer and the phosphonated polymer. Thus, although the difference of character hydrophilic/hydrophobic of the both polymer results in a segregation phenomenon of the acid phosphonic groups, interaction between both polymers exists. These interactions indicate the partially miscibility of polymer.

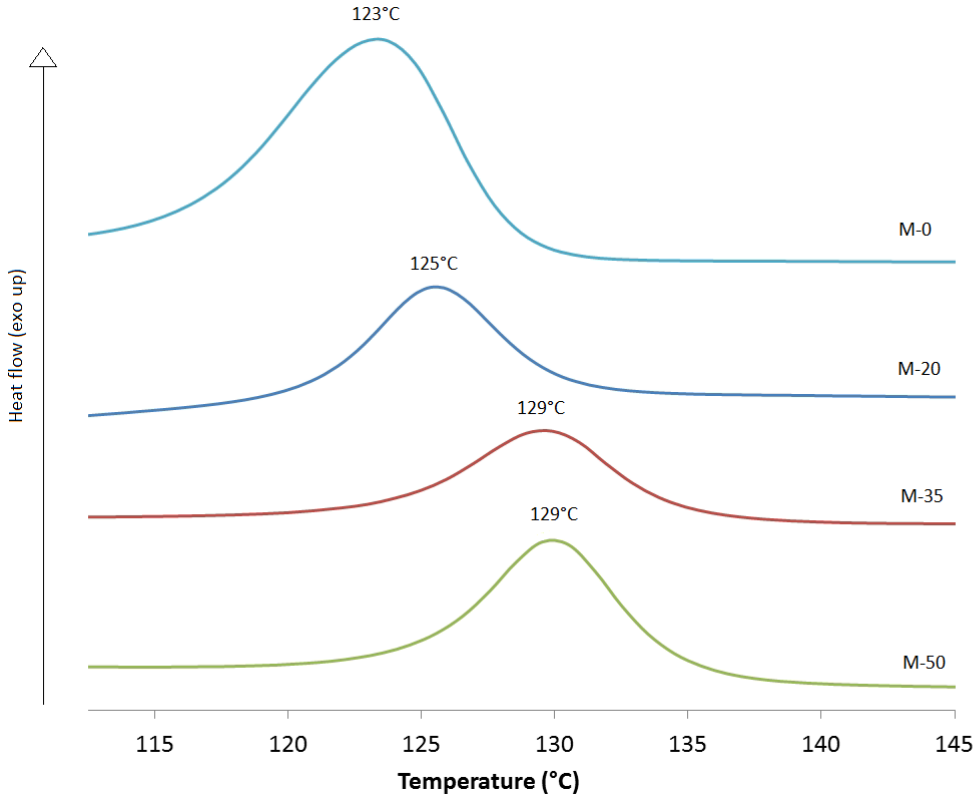

Figure 73 : The crystallization temperature (Tc) of the blend membranes.

Table 5 Temperature of 5 and 10% of weight loss and Tg of different blend membranes.

Sample	Theoretical rate of phosphonated polymer (%)	Experimental rate of phosphonated polymer (%)	$Td_{5\%}$ (°C)	$Td_{10\%}$ (°C)	$Tg_{theoretical}$ [a] (°C)	Tg_1 (°C)	Tg_2 (°C)
M-0	0	0	430	440	-	-30[b]	nd
M-20	20	19	307	315	-15	nd	112
M-35	35	36	301	317	-3	nd	102
M-50	50	50	287	306	11	nd	103
M-65	65	66	272	293	27	nd	93
M-80	80	81	274	291	44	nd	82
M-100	100	100	196	270	-	nd	70

a: calculated by the Fox-Flory equation; b: data supplier

6.2 SAXS analyses

In order to obtain more insight on the copolymers organization during the casting, SAXS analyses have been realized. These analyses allowed to determine their morphology and structure at the mesoscopic scale[26]. Indeed, adding a high fluorinated polymer in the membrane may impact the polymer organization, whereas the presence of hydrophilic domains in the membrane facilitates the proton transport. The hydrophilic domains are characterized by the formation of ionic clusters. For example in the Nafion®, this presence of ionic cluster allows the formation of water network, which ensure the proton transport. Figure 74 shows the SAXS profiles of M-100, M-65 and M-20 membranes (100, 65 and 20w% of poly(CTFE-*alt*-DEVEP), respectively). In first, several peaks for the large angle scattering ($q>1.10^1$ nm^{-1}) can be seen. These peaks represent the crystallinity of poly(VDF-*co*-CTFE). From the low angle region, the presence of a maximum scattering was fund for all the membranes, characterizing the presence of an ionomer peak, implying ionic clusters formed by the phosphonic acid groups. From this maximum scattering, the distance (center-center) separating the ionic clusters can be evaluated by the following equation:

$$d = \frac{2\pi}{q} \qquad (6)$$

Where, d is the distance (center-center) between clusters (nm) and q the scatter vector (nm^{-1}).

From Figure 74, a large angle scattering shift for the maximum scattering was observed when the rate of poly(VDF-*co*-CTFE) increases in the membrane composition. So, as q was inversely proportional to *d*, the distance between ionic clusters decreases. Indeed, concerning the M-100 membrane, *d* was equal to 8 nm, whereas for the M-65 and M-20 membranes, *d* was equal to 3.5 and 2.8 nm, respectively. This decrease of the distance is ascribed to the hydrophobic/hydrophilic balance between the poly(VDF-*co*-CTFE) and the phosphonic acid polymers, respectively. Indeed, phosphonic groups were closed to each other, in order to limit the interaction between hydrophilic part (phosphonic groups) and hydrophobic part (fluorinated polymer). The results obtained from SAXS analyses confirm the primary conclusions drawn from DSC analyses.

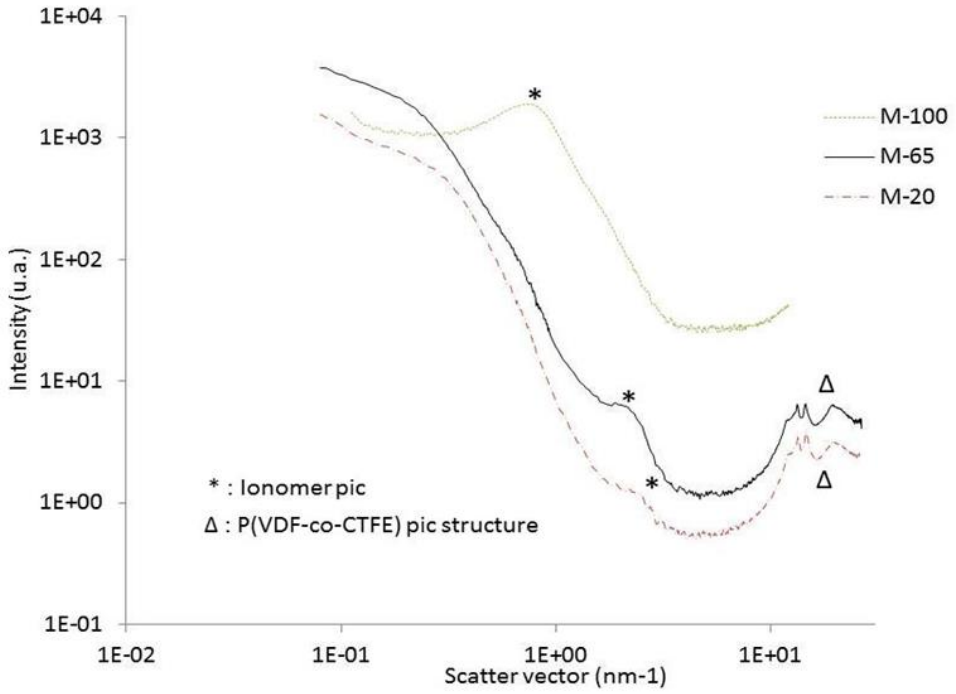

Figure 74 : The SAXS profiles of M-100 membrane and M-65, M-20 blends membranes in fully hydrated state

6.3 **Mechanical properties**

The different blend membranes were analyzed by DMA, at different temperatures and relative humidity (RH). The mechanical behavior of membranes was measured on temperature ranging from -100 to 150°C. Before studying the mechanical behavior of blend membranes, the DMA measurements of M-0 and M-100 membranes were performed. The M-0 membrane shows very good mechanical properties. Indeed, on the temperature range, storage modulus of poly(VDF-*co*-CTFE) is ranged between 10^8 and 10^9 Pa. This loss of one order of magnitude is observed when the temperature was superior at the Tg_1. On the other hand, the DMA analyses the M-100 membrane is impossible, since the membrane is too brittle.

The mechanical properties of M-0, M-20, M35, M-50, M-65 membranes were then assessed, and the results were showed in the Table. For the M-80 membrane (i.e. composed with 80% of phosphonic polymer), membrane is also very brittle to. In order to improve the

mechanical properties of the phosphonated membranes, the minimum ratio of poly(VDF-*co*-CTFE) is 35%.

The mechanical properties of the M-50 membrane are representative of the mechanical behavior for all blend membranes. An example of DMA curve is given in figure 10, where the temperature dependence of the storage modulus (E') and tanδ are plotted. The presence of two peaks on tanδ curve was observed, one around -40°C and the other one at around 100°C. The existence of these two peaks indicates the presence of two Tgs, the one of poly(VDF-*co*-CTFE) at -40°C and the one of poly(CTFE-*alt*-DEVEP) at 100°C. At around -30°C, a small change in the storage modulus at low temperature is observed because the rigidity of phosphonated polymer dominates the mechanical behavior. Then, around 100°C, there is a sharp decrease of the storage modulus (about one order of magnitude). Indeed, when the temperature is above the Tg of the phosphonated polymer, the rigidity of the membrane decreases and the mechanical behavior is then provided from the fluorinated polymer. This result illustrates the partially miscible blend membranes behavior, as previously observed from both SAXS and DSC. Nevertheless, the mechanical properties of blend membranes were highly improved compared to the phosphonic membrane M-100. Indeed, the storage modulus values remain high in the whole temperature range.

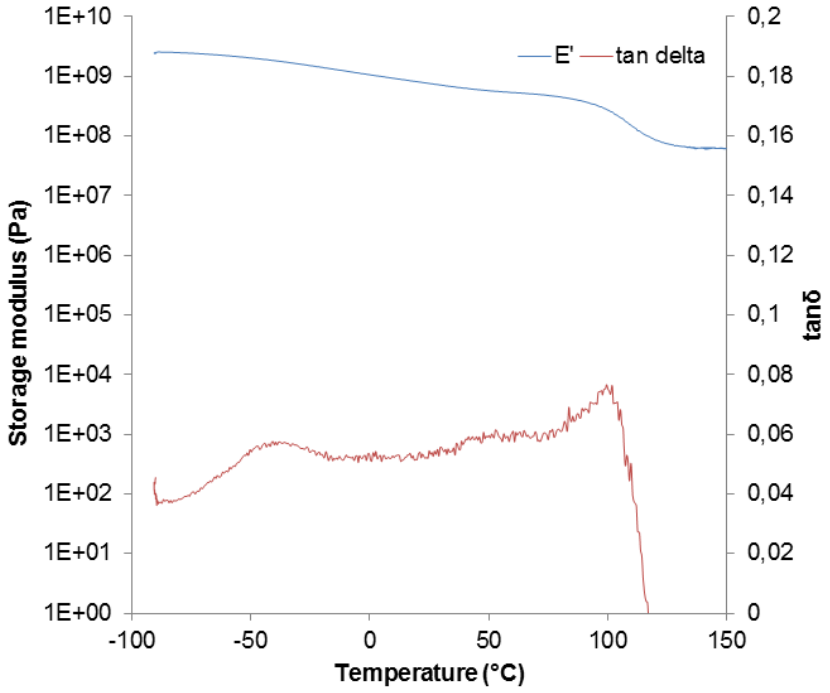

Figure 75 : Temperature dependence of storage modulus and tan delta of M-50 membrane

During the operating fuel cell, the relative humidity (RH) is a very important parameter. RH impacts the electrochemistry performance of the PEMFC since the water molecules play a crucial role in the proton conduction mechanism. Indeed, during the increasing of RH, the membranes swell, and this swelling impacts the mechanical properties of the membrane. Thus, the study of the evolution of mechanical behavior of the membranes with the variation of RH and temperature will provide an interesting insight. DMA analyses were realized under nitrogen flow with controlled water content. This analysis allows to sweep the whole range of RH (from 0 to 100%) and temperatures ranging from 25 to 70°C. The M-50 membrane's results obtained at room temperature were showed in Figure 76.

A low variation for the storage modulus of about one order of magnitude on the whole RH range was observed. Even so, from 70% of RH, storage modulus variation is a little bit more important, due to a higher swelling. Indeed, water content only impacts the mechanical properties of poly(CTFE-*alt*-DEVEP), and this polymer poorly contributes to the mechanical behavior of the membrane's.

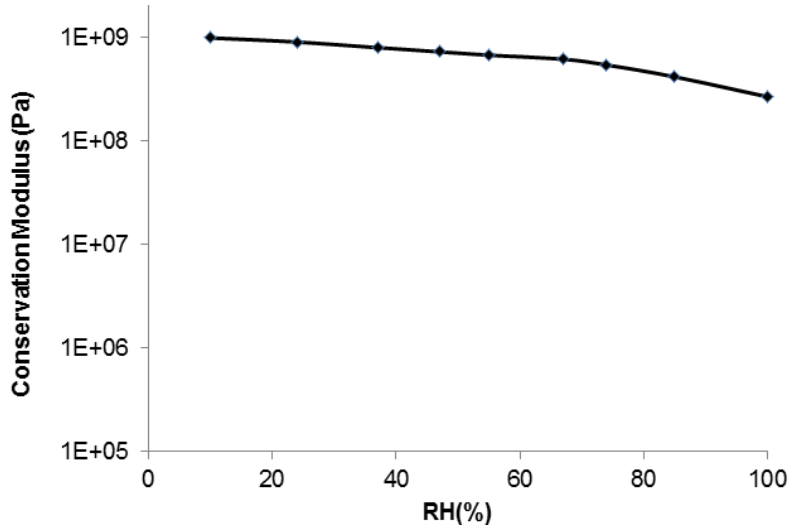

Figure 76 : Storage modulus evolution with RH variation for the M-50 membrane.

The membrane elongation was assessed for all the blend membranes. A typical result obtained for M-50 membrane was showed in

Figure *77*. A stress higher than 2.5 10^7 Pa applied on the membrane implied the membrane breaking. This traction force applied matches an elongation of 3%. All the membranes elongation was in the same order, and this, even for the membrane possessing a high poly(VDF-*co*-CTFE) rate, since the elongation of the membrane is limited by the phosphonated polymer.

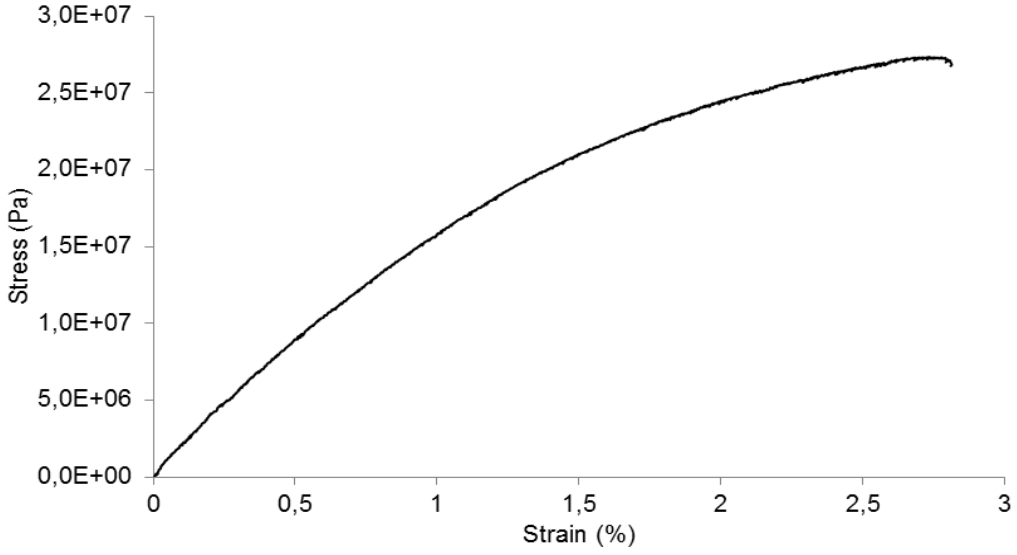

Figure 77 : Typical nominal stress-strain curve for M-50 membrane at room temperature

The value of the storage modulus of different membranes determined in function of temperature and RH are listed in Table 6. A similar evolution of the storage modulus was observed. Namely, a reduction of about two orders of magnitude on the whole temperature range, and about one order of magnitude on the whole RH range can be see. To conclude the mechanical study, the four membranes possess the mechanical properties required for use in PEMFC.

Table 6 : Storage Modulus of the blend membranes at different temperature and RH

	Storage modulus (MPa)			Storage modulus (MPa)		
	-100°C	25°C	140°C	10%	50%	100%
M-20	4350	556	37	1400	1200	900
M-35	3600	410	27	1000	734	270
M-50	2600	762	61	410	310	140
M-65	6440	1300	84	520	210	32

*Determined at variable Temperature and a Ambient RH

**Determined at 25°C and variable RH

6.4 Water uptake and IEC of blend membranes

The IEC values of different blend membranes were determined from titration method, the results are given in Table 7. The IEC_{exp} values were compared to the IEC_{theo} values calculated from the following equation:

$$IEC_{theo} = \%(PVDF - co - CTFE) * IEC_{M-100} \qquad (7)$$

Where, $IEC_{M\text{-}100}$ was calculated form ^{1}H NMR considering two acidities of phosphonic groups [2].

IEC_{exp} values were very close to that of the IEC_{theo} one. This result allows to conclude on two points: Ionics clusters formed by the phosphonic groups in the fluorinated matrix were totally free and the two acidities of phosphonic groups were available for proton transport. So, IEC_{exp} values increase with the poly(CTFE-*alt*-DEVEP) content in the blend membranes. Concerning the water uptake values, they are proportional to the phosphonic polymer rate. These results confirmed the freedom of the phosphonic acid groups. Hydration number of different membranes was equal to 5. In comparison with the number

of water molecules required to realize a perfect hydration sphere around the phosphonic groups[27] (i.e. about 7), this values was a little bit low, but, enough to form ionic clusters.

Table 7 : IECexp, IECtheo, water uptake and hydration number of the blend membranes

Sample	IEC_{theo} ($meq.g^{-1}$)	IEC_{exp} ($meq.g^{-1}$)	Water uptake (%)	λ
M-0	nd	Nd	0	nd
M-20	1.4	1.1	9	4.5
M-35	2.45	2.1	21	5.5
M-50	3.5	3.2	28	4.9
M-65	4.55	4.6	37	4.4
M-80	5.6	5.6	55	5.6
M-100	7	7	65	5.2

6.5 **Proton Conductivity**

The performance of a membrane for PEMFC is closely dependent to the proton conductivity which directly influences the ohmic losses and finally the power densities. Proton conductivity measurements of M-80, M-65, M-50 membranes were performed from 20 to 80 °C in water immersed conditions in order to characterize fully hydrated membrane properties. These results were compared with those obtained for the M-100 membrane. Figure 78 gives an example of the evolution of proton conductivity as a function of temperature and time for the M-50 membrane.

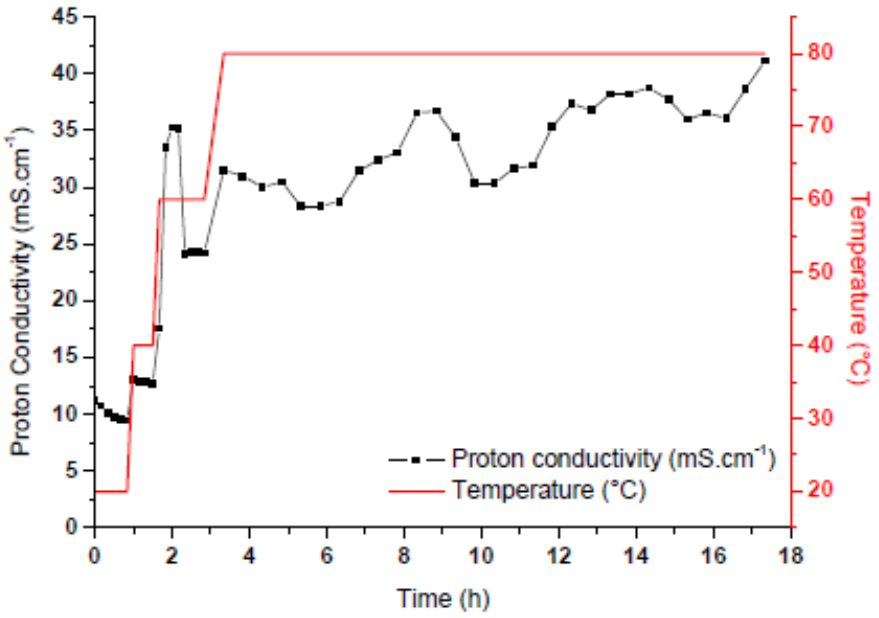

Figure 78 : Example of the evolution of Proton conductivity in liquid water versus time for various temperatures for the M-50 membrane

At 20°C, proton conductivity is around 11 mS.cm^{-1} during the beginning of measurements. However it quickly decreases to reach 9 mS.cm^{-1} after 1 hour. This behavior should be due to mechanical relaxation between sample and electrodes caused by long temperature stabilization at 20°C. At 40°C, the conductivity is more stable and reaches 13 mS.cm^{-1} after 45 min. At 60°C, the variations are much more complex since the conductivity strongly increases until 35 mS.cm^{-1}. Nevertheless, it decreases after 50 minutes and stabilizes at 24 mS.cm^{-1}. In order to follow the conductivity variation during a long time at 80°C, spectra was recorded every 30 minutes over the night. As we can see, proton conductivity is not stable and varies between 25 and 36 mS.cm^{-1} during a 4 to 6 hours period. This behavior can't be explained by the temperature stabilization of water which is very constant (regulated at 0.1°C). The average tendency is a slow increasing of conductivity. Considering the significant duration of the measurements at 80°C (~20 h), it is interesting to note that no significant elution of the phosphonated polymer occurred and no loss of mechanical properties were observed as it was the case for M-100 membrane. These novel properties are presumably due to the poly(VDF-*co*-CTFE) matrix.

Figure 79 gives the average proton conductivity versus temperature for the M-100, M-80, M-65 and M-50 membranes.

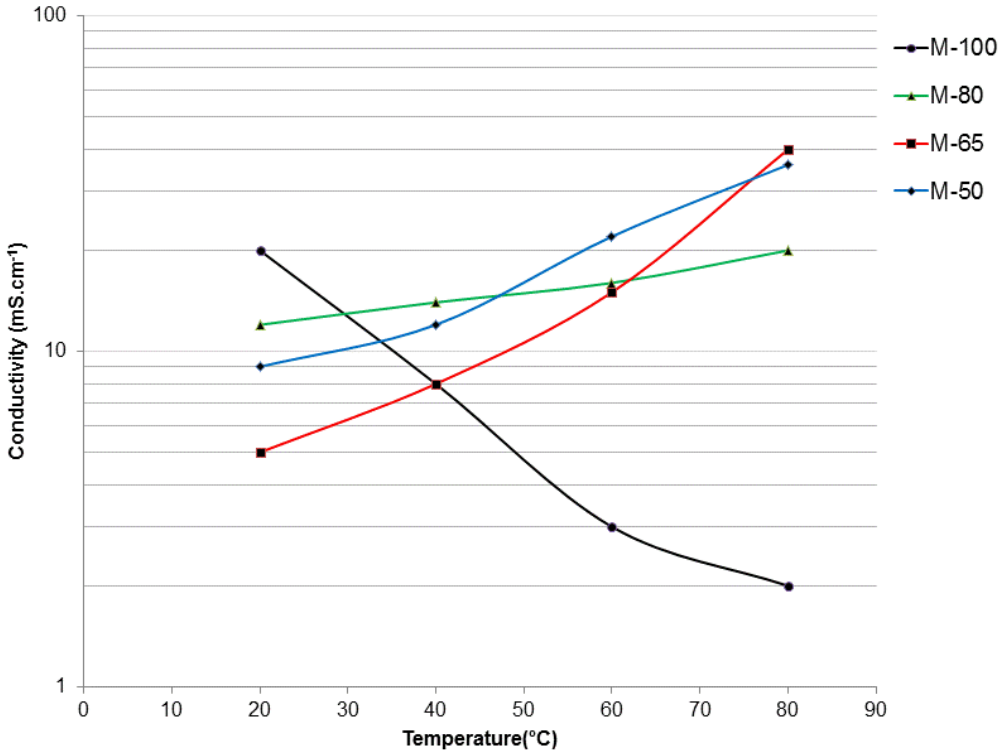

Figure 79 : Average Conductivity versus temperature in immersed conditions for the M-100, M-80, M-65 and M-50 membranes

Firstly, the evolution of the proton conductivity versus temperature is very different between the M-100 membrane and the M-80, M-65 and M-50 blend membranes. Indeed, concerning the M-100 membrane, a decrease of the proton conductivity versus temperature is observed. At 20°C, proton conductivity is around 20 $mS.cm^{-1}$ and at 80°C is around 2 $mS.cm^{-1}$. In the previous works [2, 3], a diminution of the swelling was demonstrated when the temperature increases, which may explain this behaviour. Concerning the blend membranes, an increase of the proton conductivity versus temperature was observed. In this case, the increase of the proton conductivity can be connected to a better structuration of the membranes. Indeed, a decrease of the inter-cluster distance was observed when the poly(VDF-*co*-CTFE) was added to the membrane composition (Figure 74). At 80°C, the best

results, obtained for the M-65 and M-50 membranes, are around 40mS.cm^{-1}. Though these membranes do not possess the highest IEC values, the better structuration allows to facilitate the transport of the protons through the membrane.

To summarise, the conductivity in water increased with temperature. These results may be attributed to the better mobility of both water molecules and phosphonic acid polymer chains. It finally proves the easy accessibility of acid sites.

6.6 Fuel cell performance

The fuel cell performance of the membrane which possesses the best proton conductivity has been realized. The realization of this test allows to confirm the gas impermeability of the blend membrane. This part presents the result obtained for the M-50 membrane. Indeed, this membrane possesses the best proton conductivity at low and medium temperature.

One of the major problems of the new membrane carrying phosphonic groups, during the fuel cell performance test is the poor affinity between the electrodes and the membrane. Indeed, the electrodes were soaked with Nafion® which possesses sulfonic acid groups, and this difference of acid groups involves this low affinity. So, in order to solve this problem, the membrane can be soaked with the same copolymer used to perform the membrane[28]. To determine the impact of the membrane/electrode affinity on the fuel cell performance, the tests were realized with one electrode soaked with Nafion® and one soaked with poly(VTFE-*alt*-VEPA). The results obtained at 25°C were showed in Figure 80.

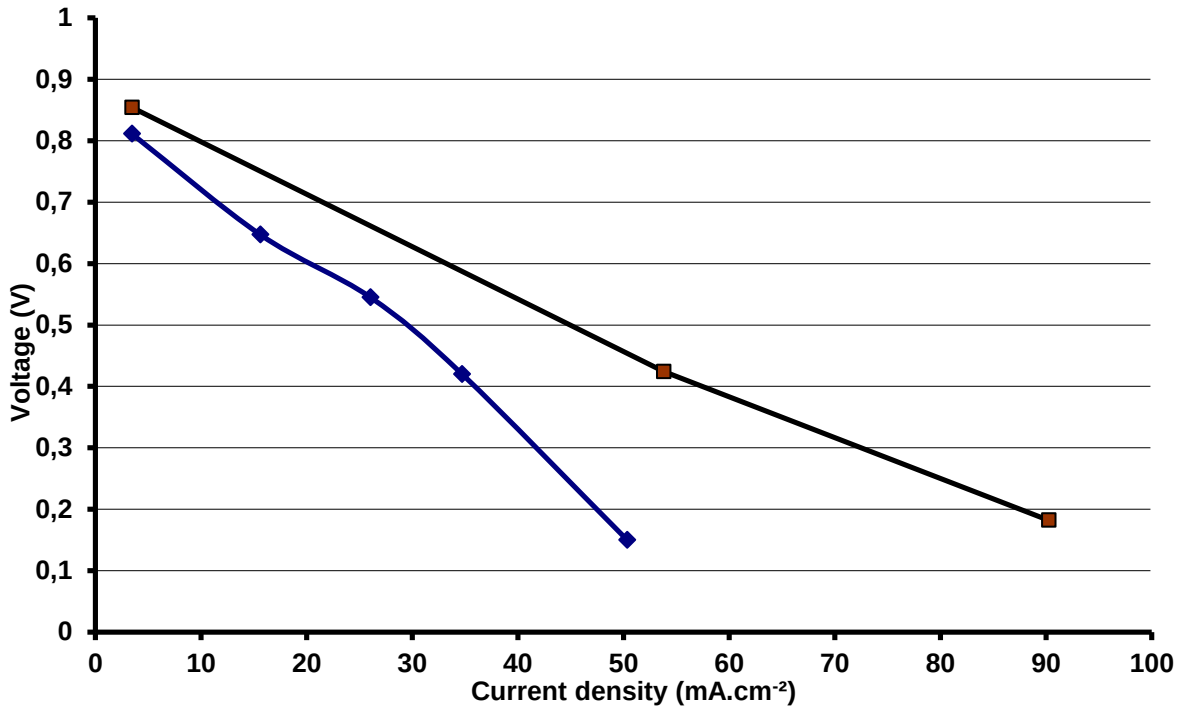

Figure 80 : Hydrogen-air fuel cell performance of M-50 with Nafion® based electrode (♦) and poly(CTFE-alt-VEPA) based electrode (■) at 25°C

From Figure 80 discrepancies between fuel cell performance of M-50 with Nafion® based electrode (♦) and poly(CTFE-*alt*-VEPA) based electrode (■) can be observed. The first difference concerns the value of the Open Current Voltage (OCV). For the test with the poly(CTFE-*alt*-VEPA) based electrode, the OCV value is slightly higher, due to a decrease in various surges during the activation of the fuel cell. The big difference concerns the capacity of the system to deliver a current density. Indeed with the poly(CTFE-*alt*-VEPA) based electrode, at 0.2V the current density is equal to 90 $mA.cm^{-2}$ while with Nafion® based electrode at 0.2V the current density is equal to 50 $mA.cm^{-2}$.

Although these results are very low to consider a Fuel Cell application, these results show the importance of the membrane/electrode affinity. To the next fuel cell performance test of the new membranes, the use of this poly(CTFE-*alt*-VEPA) based electrode will be interesting.

7 Conclusion

New polymer electrolyte membrane have been prepared composed of polymer blend of poly(VDF-*co*-CTFE) and poly(CTFE-*alt*-DEVEP) containing phosphonic acid groups. These blend membranes exhibit high thermal and oxidative stability and good mechanical properties. The decrease of the inter-cluster distance in the blend membranes allows the proton transport. Thus, in comparison with the M-100 membrane, the conductivity of the blend membranes is in the same order of magnitude, whereas the IEC of the blend membranes are twice lower. Proton conductivity (40 $mS.m^{-1}$ at 80°C), thermal stability (measured at 140°C), thickness (around 30 micrometers) and good mechanical properties of M-50 and M-65 membranes allow to use these materials as membrane for PEMFC. The fuel cell performance shows the importance of the membrane/electrode affinity

However, the miscibility of the two polymers remains partial. So in order to increase the miscibility of the two polymers we can add in the membrane preparation, a compatibilizer polymer which posses a hydrophobic part and a hydrophilic part. Consequently, a better miscibility can improve the microstructure of blend polymer and induce higher proton conductivity.

One of the main issues for both this chapter and for the MemFOS project was the increase of the mechanical properties of the M-100 membrane. With a simple technique consisting in realizing a mixture of copolymers we have obtained a series of membranes which possess sufficient mechanical properties to ensure the barrier role in the heart of the membrane.

The price of the proton exchange membrane is also a crucial point in the industrial development of the fuel cell technologies. This technique allows to make low cost membranes. Indeed, both fluorinated and phosphonated copolymers are less expensive than Nafion®, according to their syntheses.

However, during the synthesis of the membrane and in particular during the acidification protocol, we observe coloration of the acid solution. This degradation of the phosphonated copolymer implies a loss of phosphonic acid group. So, an increase of the acid

stability for the phosphonated polymer can allow an increase of proton conductivity, and so the fuel cell performance. The crosslinking of the phosphonated polymer should increase the acid stability. Furthermore, the cross-linking of the phosphonated copolymer during the membrane casting will enhance the compatibility of both copolymers. This strategy will be discussed in chapters III and IV.

8 Experimental part

8.1 Materials

Chlorotrifluoroethylene (CTFE, 1,1,1,3,3,-pentafluorobutane (solkane®) and the PVDF 31508 were kindly provided by Solvay S.A. Le *tert*-butyl peroxipivalate (TBPPI) 75% purity was purchased from Azko Nobel®. 2-chloroethyl vinyl ether (CEVE), carbonate potassium, methanol, diethylique ether, sodium iodide, acetone, triethyle phosphite, bromotrimethylsilane, dichloromethane were purchased from Aldrich. All reactants were used without further purification except for the solvents (solkane, acetone and dichloromethane), which were distillate prior to use.

8.2 Copolymerization of CTFE with CEVE: poly(CTFE-*alt*-CEVE)

As CTFE is a gas, the reactions were carried out in a Hastelloy (HC276) autoclave Parr system equipped with a manometer, a rupture disk (3000 psi), inlet and outlet valves, and a magnetic stirrer. Prior to reaction, the auto-clave was pressurized with 30 bar (i.e., 430 psi) of nitrogen to check for eventual leaks. The autoclave was then conditioned for the reaction with several nitrogen/vacuum cycles (10^{-2}mbar) to remove any traces of oxygen. The liquid phase was first introduced via a funnel, and then the gases were inserted by double weighing (i.e. the difference of weight before and after filling the autoclave with the gas). Then, the autoclave was placed in a mantle heated with a vigorous mechanical stirring. Both heating and stir-ring were monitored by a controller. After an initial in-crease of the internal pressure due to the increasing temperature, the pressure dropped by consumption of the gaseous monomer to produce a polymer in the liquid phase. After the reaction was complete, the autoclave was cooled to room temperature and then degassed. After distillation of the solvent, the copolymers were precipitated from cold methanol. The product was dried under vacuum (10^{-2} mbar) at 70°C until constant weight.

As an example, 150 mL de solkane® as the solvent, TBPPI 1.00 g (5.75 mmol) as the initiator, K_2CO_3 0.79 g (5.72 mmol) (to prevent the cationic homopolymerization of CEVE),

CEVE 20 g (187.71 mmol) and CTFE 25 g (214.74 mmol) were introduced in the 300mL autoclave. The reaction was allowed to proceed at 75°C for 12h, showing a drop of pressure as CTFE was reacting. After purification, the copolymer, obtained as a pal yellow solid. It was then dried in a vacuum oven (10^{-2} mbar) at 50°C until constant weight. The mass yield was 75%.

Structure:

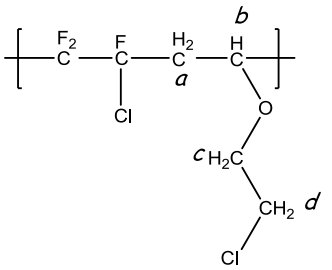

Mass yield: 75%

Glass transition temperature (Tg): 29°C

Number average molecular mass (M_n) ≈19,000 $g.mol^{-1}$

Mass average molecular mass (M_w) ≈57,000 $g.mol^{-1}$

Polydispersity indices: 3

^1H NMR (400MHz, 297K, $CDCl_3$, ppm) δ: 4.4 to 4.9 (m, 1H, H_b); 3.95 (m, 2H, H_c); 3.6 (m 2H, H_d); 2.3 to 3.2 (m, 2H, H_a)

^{19}F NMR {^1H} (377 MHz, 297K, $CDCl_3$, ppm) δ: -108 to -123 (m, 3F)

8.3 Synthesis of the copolymer poly(CTFE-*alt*-IEVE): Finkelstein Reaction

One equivalent of the copolymer was dissolved in dry acetone in a single-neck round bottom flask equipped with a magnetic stirrer and a condenser. Then, 3 equivalent of sodium iodide were introduced in the flask (relative to the chlorine atom of the vinyl ether copolymer). The reaction was allowed to reflux for 7 days. After reaction and upon cooling

to room temperature, the produced salts (sodium chloride and sodium iodide) were filtered off. The, polymer was precipitated from methanol and dried under vacuum et 50°C for 4 h to produce a pale yellow solid. The product was obtained in high mass yield (>85%).

As an example, in a 100mL single-neck round bottom flask equipped with a magnetic stirrer and a condenser, poly(CTFE-*alt*-CEVE) 30g (129.40 mmol de chlorine), 3 equivalents of NaI 57.80 g (388.15 mmol) and acetone 350 mL were introduced. After the copolymer was dissolved, the reaction was allowed to reflux for 7 days. After filtration and distillation of solvent, the polymer was precipitated in the methanol. The, polymer was precipitated from methanol and dried under vacuum et 50°C for 4 h to produce a pale yellow solid.The poly(CTFE-*alt*-IEVE) was obtained in high substitution rate (>90%) and in a high mass yield (>85%).

Structure :

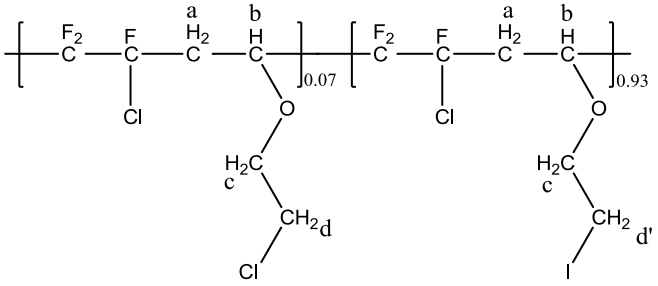

Mass yield: 85%

Iodation rate: 93%

Glass transition temperature (Tg): 33°C

Number average molecular mass (M_n) ≈ 18,000 g.mol^{-1}

Mass average molecular mass (M_w) ≈ 57,000 g.mol^{-1}

Polydispersity indices (Ip): 3.15

^{1}H NMR (400MHz, 297K, $CDCl_3$, ppm) δ: 4.3 to 4.8 (m, 1H, H_b); 3.95 (m, 2H, H_c); 3.6 (m 2H, H_d); 3.15 (m, 2H, $H_{d'}$); 2.3 to 3.1 (m, 2H, H_a)

8.4 Direct phosphonation of the halogenated copolymer: Michaelis-Arbuzov reaction

One equivalent of the poly(CTFE-*alt*-IEVE) was dissolved in triethyl phosphite in a single-neck round bottom flask equipped with a magnetic stirrer and a condenser. The reaction was allowed to 130°C for 24 h. After reaction and upon cooling to room temperature, the side product (triethyl phosphite and diethyl phosphite) were removed by vacuum distillation (60°C/5mbar and 90°C/5mbar, respectively). The remaining viscous solution was diluted in 50mL of acetone and then precipitated in distilled water. The dark red polymer was obtained after drying under vacuum at 90°C for 12h. The product was obtained in a high mass yield (>90%).

As an example, in a 250 mL single-neck round bottom flask equipped with a magnetic stirrer and a condenser, poly(CTFE-*alt*-IEVE) 20g and triethyl phosphite 100 mL were introduced. After the copolymer was dissolved, the reaction was allowed to 135°C for 24h. After the vacuum distillation of triethyl phosphite (60°C/5mbar) then the diethyl phosphite (90°C/5mbar), the remaining viscous solution was diluted in 50mL of acetone and then precipitated in 2,000 mL distilled water. After filtration the phosphonated polymer (poly(CTFE-*alt*-DEVEP) was obtained after drying under vacuum at 90°C for 12h. The product was obtained in a high mass yield (>90%).

Structure:

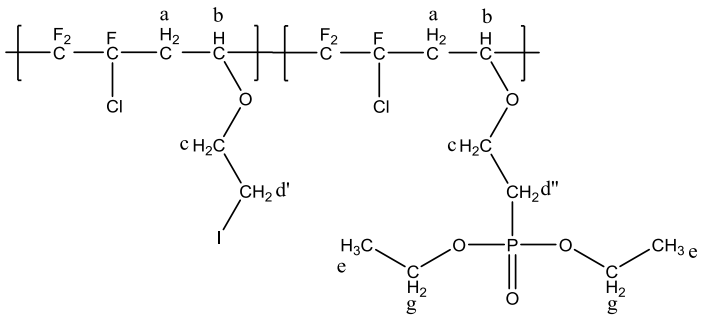

Mass yield: 92%

Phosphonation rate: 93%

Glass transition temperature (Tg): 3°C

^{1}H RMN (400MHz, 297K, $CDCl_3$, ppm) δ: 4.3 to 4.8 (m, 1H, H_b) 4.1 (m, 4H, H_g); 3.95 (m, 2H, H_c); 3.2 (m, 2H, $H_{d'}$); 2.3 to 3.1 (m, 2H, H_a), 2.12 (m, 2H, $H_{d''}$); 1.3 (t, 6H, H_e)

^{31}P NMR {^{1}H} (160MHz, 297K, $CDCl_3$, ppm) δ: 27 (s, 1P)

8.5 Hydrolysis of phosphonated groups

One equivalent of poly(CTFE-*alt*-DEVEP) was dissolved in anhydrous dichloromethane under an argon atmosphere in a 250 mL three-neck round-bottom flask equipped with a condenser, a magnetic stirrer. Then, 2.2 equivalent of bromotrimethylsilane $BrSi(CH_3)_3$ was added in a drop wise manner, and the mixture was stirred at 40°C for 6 h. After the reaction, solvent and volatile residues were evaporated (40°C/30 mbar). The alcoholysis of the silylated intermediate was performed by adding an excess of methanol. The mixture was stirred at 30°C for 4 h, and the solvent was evaporated. The remaining solution was precipitated in distilled water. The dark brown polymer poly(CTFE-*alt*-VEPA) was quantitatively obtained (mass yield >95%) after drying under vacuum at 90°C for 12 h.

AS an example, in a 250 mL three-neck round-bottom flask equipped with a condenser, a magnetic stirrer, 15 poly(CTFE-*alt*-DEVEP) was dissolved in 50 mL of anhydrous dichloromethane under an argon atmosphere. Then, 2.2 equivalent of bromotrimethylsilane $BrSi(CH_3)_3$ (8 mL, 52.6 mmol) was added in a drop wise manner, and the mixture was stirred at 40°C for 6 h. After the reaction, solvent and volatile residues were evaporated (40°C/30 mbar). The alcoholysis of the silylated intermediate was performed by adding an excess of methanol (100mL). The mixture was stirred at 30°C for 4 h, and the solvent was evaporated. The remaining solution was precipitated in distilled water. The dark brown polymer poly(CTFE-*alt*-VEPA) was quantitatively obtained (mass yield >95%) after drying under vacuum at 90°C for 12 h.

Structure:

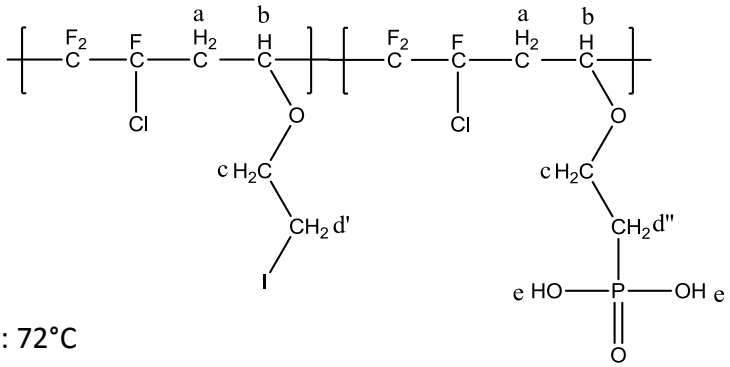

Mass yield: 91%

Glass transition temperature (Tg): 72°C

^{1}H RMN (400MHz, 297K, $CDCl_3$, ppm) δ: 7.55 (m, 1H, H_e), 4.3 to 4.8 (m, 1H, H_b); 3.95 (m, 2H, H_c); 3.2 (m, 2H, $H_{d'}$); 2.3 to 3.1 (m, 2H, H_a), 2.12 (m, 2H, $H_{d''}$).

^{31}P NMR {^{1}H} (160MHz, 297K, $CDCl_3$, ppm) δ: 21.3 (s, 1P)

9 References

1. Carnevale, D.; Wormald, P.; Ameduri, B.; Tayouo, R.; Ashbrook, S. E., Multinuclear Magnetic Resonance and DFT Studies of the Poly(chlorotrifluoroethylene-alt-ethyl vinyl ether) Copolymers. *Macromolecules* **2009,** *42* (15), 5652-5659.
2. Tayouo, R.; David, G.; Ameduri, B.; Roziere, J.; Roualdes, S., New Fluorinated Polymers Bearing Pendant Phosphonic Acid Groups. Proton Conducting Membranes for Fuel Cell. *Macromolecules (Washington, DC, U. S.)* **2010,** *43* (Copyright (C) 2013 American Chemical Society (ACS). All Rights Reserved.), 5269-5276.
3. Tayouo, R.; David, G.; Ameduri, B., New fluorinated polymers bearing pendant phosphonic groups for fuel cell membranes: Part 1 synthesis and characterizations of the fluorinated polymeric backbone. *Eur. Polym. J.* **2010,** *46* (Copyright (C) 2013 American Chemical Society (ACS). All Rights Reserved.), 1111-1118.
4. Tayouo, R.; David, G.; Ameduri, B.; Roualdes, S.; Galiano, H.; Bigarre, J. Copolymers comprising phosphonates and/or phosphonic acid groups useful for fuel-cell membrane constituents. WO2011048076A1, 2011.
5. Tayouo, R.; David, G.; Ameduri, B.; Roualdes, S.; Galiano, H.; Bigarre, J. Copolymers comprising phosphonates and/or phosphonic acid groups useful for fuel-cell membrane constituents. FR2951729A1, 2011.
6. Valade, D.; Boschet, F. d. r.; Améduri, B., Synthesis and Modification of Alternating Copolymers Based on Vinyl Ethers, Chlorotrifluoroethylene, and Hexafluoropropylene†. *Macromolecules* **2009,** *42* (20), 7689-7700.
7. Michaelis A.; Kahne, R., *Chem. Ber.* **1898,** *31*, 1048.
8. Arbuzov, A. E., *J. Russ. Phys. Chem. Soc.* **1906,** *38*, 687.
9. Arbuzov, A. E., *Chem. Zentr.* **1906,** *II*, 1639.
10. Parvole, J.; Jannasch, P., Poly(arylene ether sulfone)s with phosphonic acid and bis(phosphonic acid) on short alkyl side chains for proton-exchange membranes. *Journal of Materials Chemistry* **2008,** *18* (45), 5547-5556.
11. Schuster, M.; Rager, T.; Noda, A.; Kreuer, K. D.; Maier, J., About the Choice of the Protogenic Group in PEM Separator Materials for Intermediate Temperature, Low Humidity Operation: A Critical Comparison of Sulfonic Acid, Phosphonic Acid and Imidazole Functionalized Model Compounds. *Fuel Cells* **2005,** *5* (3), 355-365.
12. Paddison, S. J.; Kreuer, K. D.; Maier, J., About the choice of the protogenic group in polymer electrolyte membranes: Ab initio modelling of sulfonic acid, phosphonic acid, and imidazole functionalized alkanes. *Physical chemistry chemical physics : PCCP* **2006,** *8* (39), 4530-42.
13. Parvole, J.; Jannasch, P., Poly(arylene ether sulfone)s with phosphonic acid and bis(phosphonic acid) on short alkyl side chains for proton-exchange membranes. *J. Mater. Chem.* **2008,** *18* (Copyright (C) 2013 American Chemical Society (ACS). All Rights Reserved.), 5547-5556.
14. Abouzari-Lotf, E.; Ghassemi, H.; Shockravi, A.; Zawodzinski, T.; Schiraldi, D., Phosphonated poly(arylene ether)s as potential high temperature proton conducting materials. *Polymer* **2011,** *52* (21), 4709-4717.
15. Abu-Thabit, N. Y.; Ali, S. A.; Javaid Zaidi, S. M., New highly phosphonated polysulfone membranes for PEM fuel cells. *Journal of Membrane Science* **2010,** *360* (1–2), 26-33.

16. Bock, T.; Möhwald, H.; Mülhaupt, R., Arylphosphonic Acid-Functionalized Polyelectrolytes as Fuel Cell Membrane Material. *Macromolecular Chemistry and Physics* **2007,** *208* (13), 1324-1340.
17. Liu, B.; Robertson, G. P.; Guiver, M. D.; Shi, Z.; Navessin, T.; Holdcroft, S., Fluorinated poly(aryl ether) containing a 4-bromophenyl pendant group and its phosphonated derivative. *Macromol. Rapid Commun.* **2006,** *27* (Copyright (C) 2012 American Chemical Society (ACS). All Rights Reserved.), 1411-1417.
18. Papadimitriou, K. D.; Andreopoulou, A. K.; Kallitsis, J. K., Phosphonated fully aromatic polyethers for PEMFCs applications. *Journal of Polymer Science Part A: Polymer Chemistry* **2010,** *48* (13), 2817-2827.
19. Wu, Q.; Weiss, R. A., Synthesis and characterization of poly (styrene-co-vinyl phosphonate) ionomers. *Journal of Polymer Science Part B: Polymer Physics* **2004,** *42* (19), 3628-3641.
20. Tamura, Y.; Sheng, L.; Nakazawa, S.; Higashihara, T.; Ueda, M., Polymer electrolyte membranes based on polystyrenes with phosphonic acid via long alkyl side chains. *Journal of Polymer Science Part A: Polymer Chemistry* **2012,** *50* (20), 4334-4340.
21. Boutevin, B.; Cersosimo, F.; Youssef, B., Studies of the alternating copolymerization of vinyl ethers with chlorotrifluoroethylene. *Macromolecules* **1992,** *25* (11), 2842-2846.
22. Rozière, J.; Jones, D. J., NON-FLUORINATED POLYMER MATERIALS FOR PROTON EXCHANGE MEMBRANE FUEL CELLS. *Annual Review of Materials Research* **2003,** *33* (1), 503-555.
23. Felisberti, M.-I.; de Lucca Freitas, L. L.; Stadler, R., Mechanical relaxation in miscible polymer systems: the glass transition regime in poly(vinylmethylether) (PVME)-cross-polystyrene (PS) semi-interpenetrating networks. *Polymer* **1990,** *31* (8), 1441-1448.
24. Huggins, M. L., Bond Energies and Polarities1. *Journal of the American Chemical Society* **1953,** *75* (17), 4123-4126.
25. Nagarajan, R.; Tripathy, S.; Kumar, J.; Bruno, F. F.; Samuelson, L., An Enzymatically Synthesized Conducting Molecular Complex of Polyaniline and Poly(vinylphosphonic acid). *Macromolecules* **2000,** *33* (26), 9542-9547.
26. Gebel, G.; Diat, O., Neutron and X-ray Scattering: Suitable Tools for Studying Ionomer Membranes. *Fuel Cells* **2005,** *5* (2), 261-276.
27. Pereira, R. P.; Felisberti, M. I.; Rocco, A. M., Intermolecular interactions and formation of the hydration sphere in phosphonic acid model systems as an approach to the description of vinyl phosphonic acid based polymers. *Polymer* **2006,** *47* (4), 1414-1422.
28. Harrison, W. L.; Hickner, M. A.; Kim, Y. S.; McGrath, J. E., Poly(arylene ether sulfone) copolymers and related systems from disulfonated monomer building blocks: synthesis, characterization, and performance - a topical review. *Fuel Cells (Weinheim, Ger.)* **2005,** *5* (Copyright (C) 2013 American Chemical Society (ACS). All Rights Reserved.), 201-212.

CHAPTER III

SYNTHESIS AND CHARACTERIZATIONS OF CROSSLINKABLE TERPOLYMER POLY(CTFE-*alt*-VE)

Butyl vinyl ether mesylé (BVEMs)

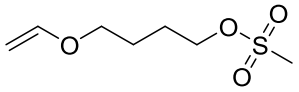

Butyl vinyl ether tosylé (BVETs)

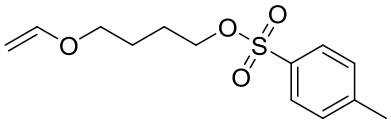

Chloro Tri Fluoro Ethylene (CTFE)

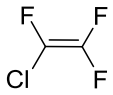

poly(CTFE-*alt*-VEPA)

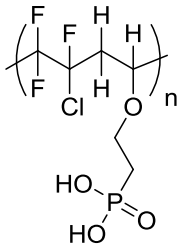

poly[(CTFE-*alt*-EVE)$_{0.9}$-*co*-(CTFE-*alt*-BVEMs)$_{0.1}$]

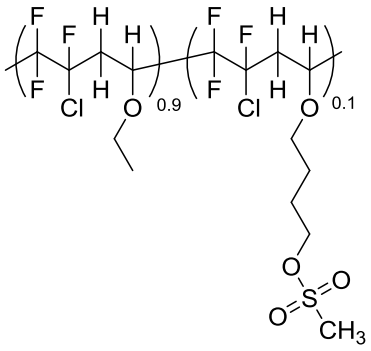

poly[(CTFE-*alt*-EVE)$_{0.9}$-*co*-(CTFE-*alt*-BVETs)$_{0.1}$]

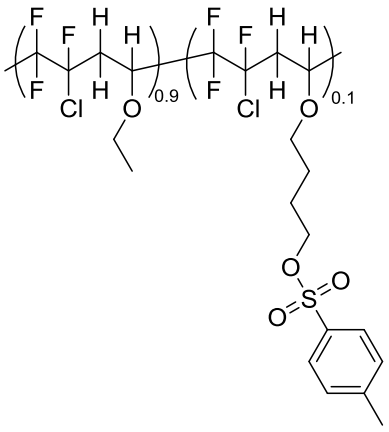

1 Introduction

In the general introduction, we pointed out the mechanical weakness of the membrane casted from poly(CTFE-*alt*-VEPA), namely very low mechanical properties and high values of water uptake (around 70%) involving exfoliation phenomena. These exfoliation phenomena imply a membrane deterioration. To solve these problems we described in the bibliographic part (Chapter I) different methods to improve the properties of a material. The first technique presented concerned the casting of membrane from the blend technique. It was developed in Chapter II, and allowed us to obtain membranes having mechanical properties required for the use of these membranes as PEMFC. However, poly(VDF-*co*-CTFE) and poly(CTFE-*alt*-VEPA) remain partially miscible. Moreover, during the acidification step, a slight coloration of the acid solution can be observed, due to poly(CTFE-*alt*-VEPA) degradation. In the bibliographic part, we presented different methods of chemical crosslinking and their impact on the physico-chemical properties of a material. Crosslinking of poly(CTFE-*alt*-VEPA) during the casting of the blend membrane is expected to overcome the problem of partial miscibility but also stability problems during the acidification step of the membrane. In the literature (see Chapter I), we found only few examples for cross-linking either fluoro-copolymer or phosphonated copolymer. Thus it appears very interesting to develop a technique for cross-linking fluoro-phosphonated copolymer. For the sake of simplicity of implementation, this technique should be done without adding catalyst or initiator. In addition, although many methods of crosslinking exist, it seems interesting to develop a new technique for polymer crosslinking by simple heat treatment. Prior to crosslinking fluoro-phosphonated copolymer, it is necessary to study the crosslinking reaction by the synthesis of a model fluoro-copolymer. To do this, in the first part of this chapter we will focus on the synthesis and physicochemical characterization of a model fluoro-copolymer (without any phosphonic acid group) to validate the method. Since the crosslinking reaction implies the production of an insoluble material, we will also perform a molecular study to try to determine the mechanism of the crosslinking reaction.

2 Bibliographic study of the crosslinking reaction

The conditions of PEMFC are quite extreme, high concentration of acid, high temperature, presence of radicals. It is thus necessary to perform the crosslinking through formation of strong covalent bonding that will able the membrane to resist to this hostile environment. In this framework, the formation of ether bonds between the polymer chains appears to realize all these requirements. In order to form ether bonds, several reactions occur. We can cite for example the use of catalysts such as chloride zinc[1] to achieve ether bond from two alcohol groups, or palladium on coal[2] that will allow the formation of ether bond between an alcohol group and a ketone group. However, in order to achieve lower cost PEMFC, the use of catalyst is not favorable. The formation of ether bond can also be made from the Williamson reaction based on the use of alkali metals. However, the objective of this work is to develop a strategy to achieve crosslinking through thermal activation without addition of catalyst or initiator.

For this purpose, the use of the coupling reaction between the sulfonate group ($R\text{-}SO_2\text{-}OR$) and alcohol should meet this goal. To better understand the reactivity of these groups, we will firstly describe the reactivity of sulfonate groups. Different existing mechanisms from the sulfonate groups are illustrated in Figure 81. The sulfonate groups are very good leaving group commonly used for the protection of alcohol functions. They can be easily substituted by a nucleophilic attack (Figure 81 a). In basic medium, two types of mechanisms can coexist:

-the formation of allyl functions through a elimination reaction due to the attack of a base in beta position of mesylate groups (Figure 81 b) ;

-the formation of an alkoxide ion due to the elimination of a proton of the alkyl (or aryl) function carried out by the sulfur atom. This mechanism will also lead, in the case of mesylate group, to the formation of a sulfene group (Figure 81 c). It should be noted that this type of mechanism is thermally favored.

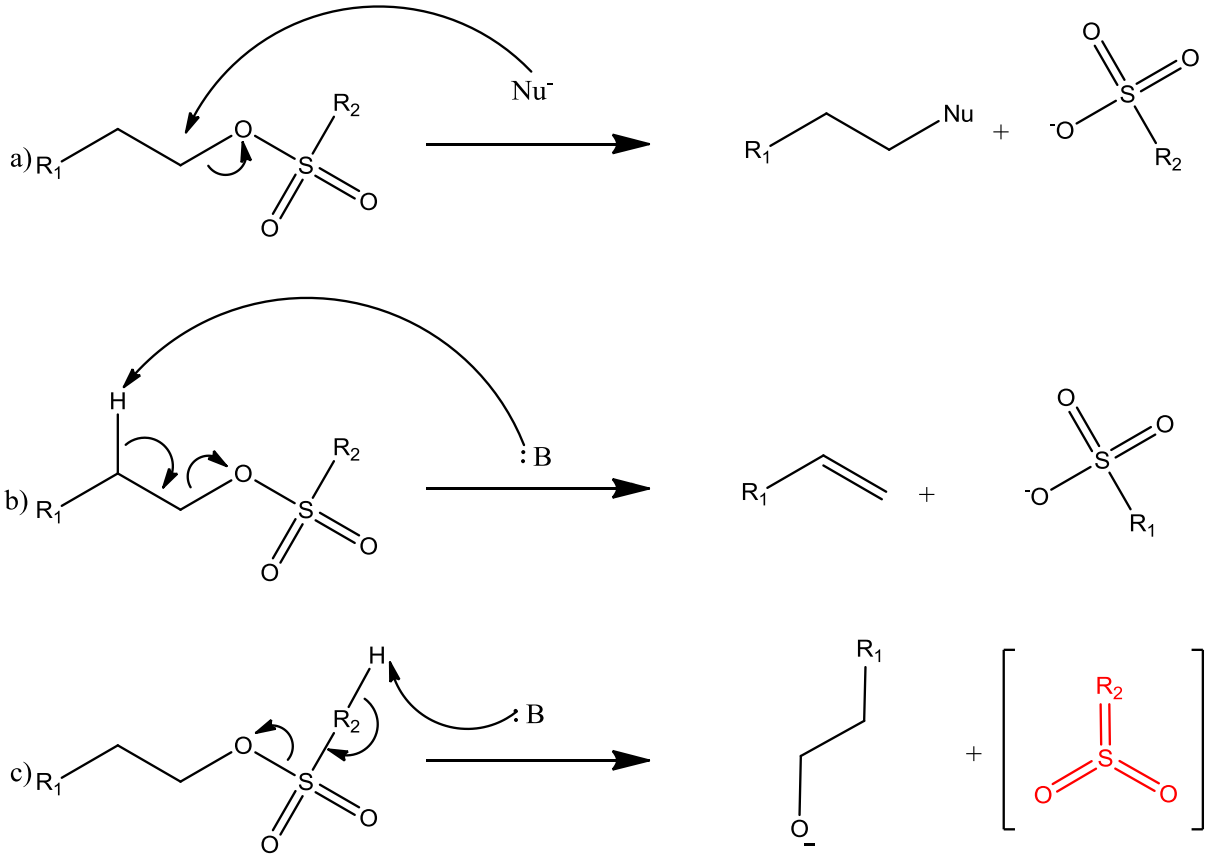

With R_1 : alkyl
R_2 : alkyl, aryl

Figure 81 : Reactivity mechanism sulphonate group

The alkoxide ion formed (nucleophile), will allow the nucleophilic substitution of the sulfonate group through the mechanism shown in Figure 81a, and thus lead to the formation of ether bonds. This kind of reaction was used by Neal W. co[3] for the synthesis of aryl ethers via the sulfonate groups. The mechanism of this reaction is shown in Figure 82.

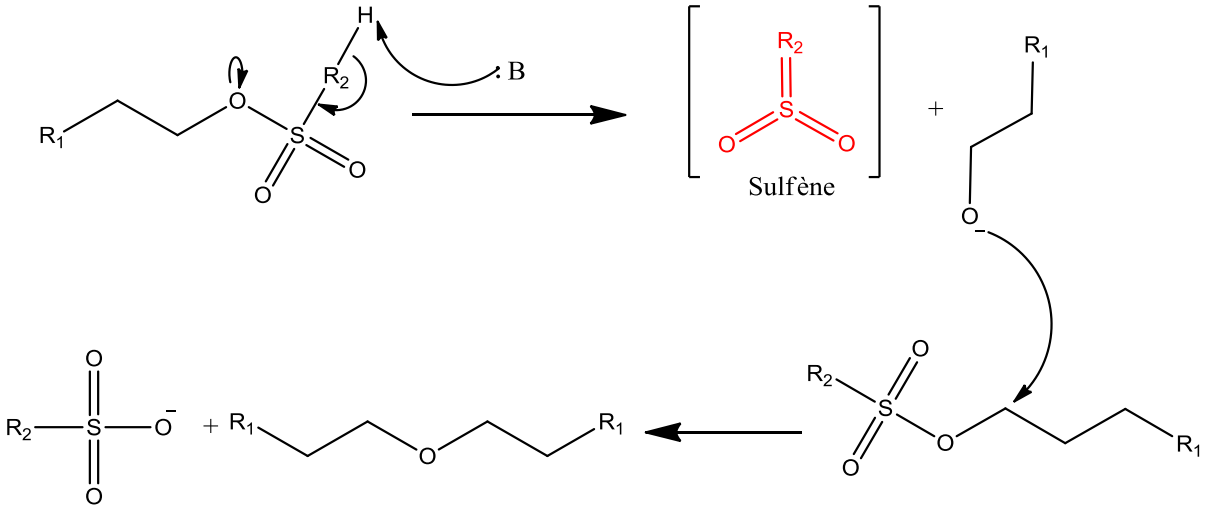

Figure 82 : Synthesis of ether bond from the sulfonate groups[3]

3 Synthesis and crosslinking of model terpolymer

To demonstrate the validity of the cross-linking strategy described above, a macroscopic study was conducted. For this, several model copolymers were synthesized. In order to achieve the crosslinking of poly(CTFE-*alt*-VEPA) which, is obtained from the polymerization of CTFE and a vinyl ether (see chapter II), the model copolymers synthesized must have the same structure. The monomer carrying the reactive function is derived from the functionalization of vinyl ether. The model study will be conducted without phosphonated group on the terpolymer. Indeed, the presence of this group could influence the crosslinking mechanism. To limit the amount of monomer carrying the reactive function, the synthesis will be carried out from a mixture of CTFE, ethyl vinyl ether (EVE) and vinyl ether functionalized in the proportions 50% / 45% / 5% respectively.

In order to determine the influence of the group R_2 (see Figure 82 on the cross-linking mechanism, two vinyl ethers carrying the reactive function were synthesized; butyl vinyl ether mesylated (BVEMs) and butyl vinyl ether tosylated (BVETs). After the synthesis of terpolymer, physicochemical characterizations will be conducted to evaluate the contribution of the crosslinking reaction on the physicochemical properties of the final material.

3.1 **Synthesis of monomers carrying the reactive function.**

The objective of this chapter is to achieve the crosslinking of a model copolymer obtained from the radical copolymerization of CTFE with either BVEMs or BVETs vinyl ethers in order to then apply this technique to poly(CTFE-*alt*-VEPA) (see chapter IV). Thus, for the synthesis of the model terpolymers, it is necessary to first synthesize the vinyl ether monomers carrying the sulfonated group. The synthesis of these monomers will be performed via a nucleophilic substitution reaction between 4-hydroxy butyl vinyl ether and the alkyl or aryl sulfonyl chloride (Figure 83). This reaction is commonly used in order to achieve the protection of the alcohol groups. The presence of four carbon atoms between the oxygen atoms should allow easy access for the sulfonate group (i.e. low steric effect). The nucleophilic substitution reaction was performed by using as reagent methanesulfonyl chloride (mesyl chloride) and p-toluene-sulfonyl chloride (tosyl chloride). The reaction is illustrated Figure 83.

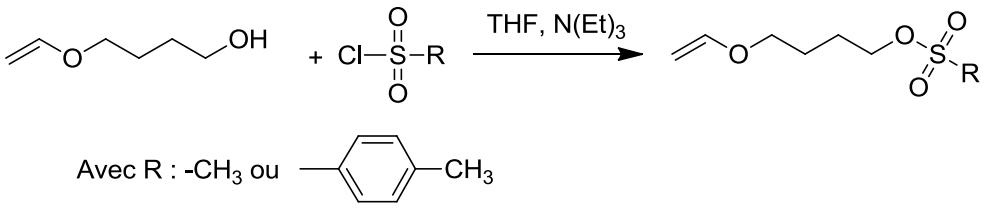

Figure 83 : Synthesis of BVEMs and BVETs

Depending on the reagent used for performing the nucleophilic substitution of the 4-hydroxy butyl vinyl ether, the experimental conditions are different. Indeed, mesyl chloride is much less stable and thus much more reactive than the tosyl chloride. Therefore, if the tosyl chloride is used, the reaction is realized at 50°C for 24 hours. But, if the mesyl chloride is used, the reaction is performed at a temperature between 5 and 10°C for only 2 hours. In both cases, the syntheses lead to functionalized vinyl ether with high conversion rates to 90% (calculated from the ^{1}H NMR of the crude product).

At the end of the reaction, the triethylamine salt is filtered. Then the THF was removed using a rotary evaporator. However, without prior precautions during the removal of THF, we

observe polymerization of vinyl ethers in the presence of acid traces. It is therefore necessary to add a base such as potassium carbonate (K_2CO_3) to stabilize the monomer before THF removal. . After liquid/liquid extraction to remove residual 4-hydroxy butyl vinyl ether, functionalized vinyl butyl ether is kept in the presence of K_2CO_3. The ^1H NMR spectra of butyl vinyl ether mesylated (BVEMs) and butyl vinyl ether tosylated (BVETs) are shown in Figure 84 and

Figure 85respectively.

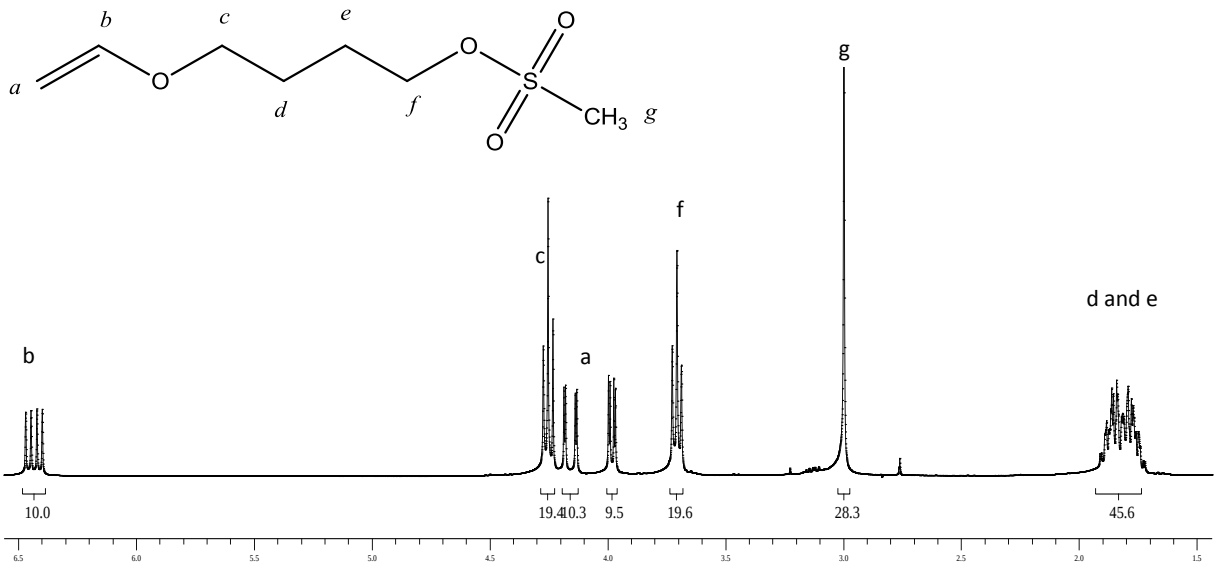

Figure 84 : ^1H NMR spectrum of BVEMs (realized in $CDCl_3$)

In Figure 84, after purification, the presence of the signal centered at 3ppm representative of the -CH_3 group (g) of the mesylate function can be observed. In addition, we observe a light shielding of the signal representative of the -C**H_2**- group (f) (from 3.8 to 3.7) in α position of the mesylate group due to the delocalization of the electron cloud of oxygen.

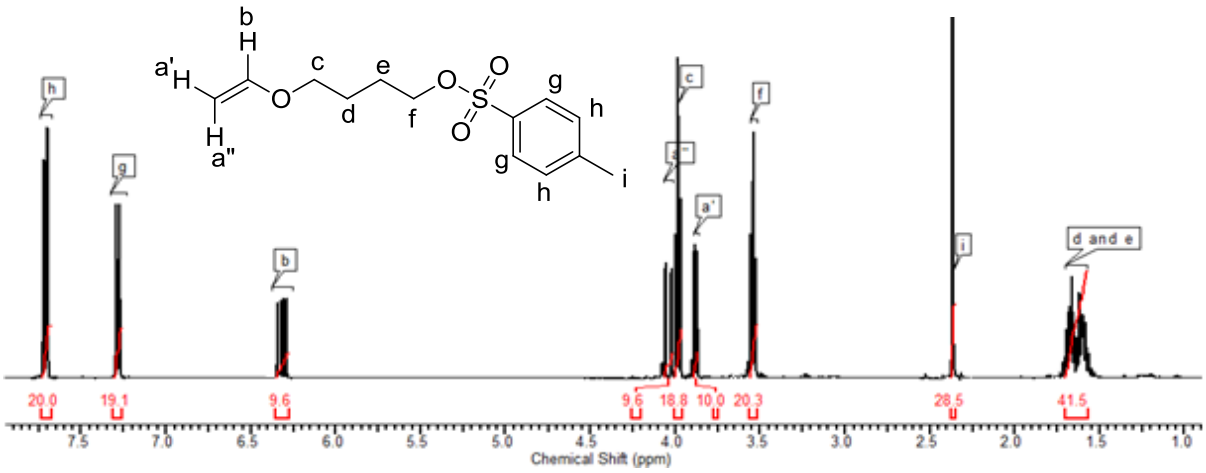

Figure 85 : ^{1}H NMR of BVETs (realized in $CDCl_3$)

In Figure 85, after purification, the presence of signals *h*, *g* and *i* of tosylate groups centered respectively at 7.8, 7.25 and 2.4 ppm can be observed. As for BVEMs, we observe a light shielding signal representative of the group -C**H**$_2$- (f) (from 3.8 to 3.6) in α position of the tosylate according to a delocalization of the electron cloud of oxygen.

3.2 **Synthesis of model terpolymer**

The copolymer synthesis is performed by radical terpolymerization between chlorotrifluoroethylene (CTFE), ethyl vinyl ether (EVE), and Butyl vinyl ether tosylate or mesylated (BVEMs or BVETs). The use of BVEMs and BVETs will allow us to determine whether the alkyl or aryl group influence the crosslinking reaction. As a reminder, the synthesized terpolymers are shown in Figure 86.

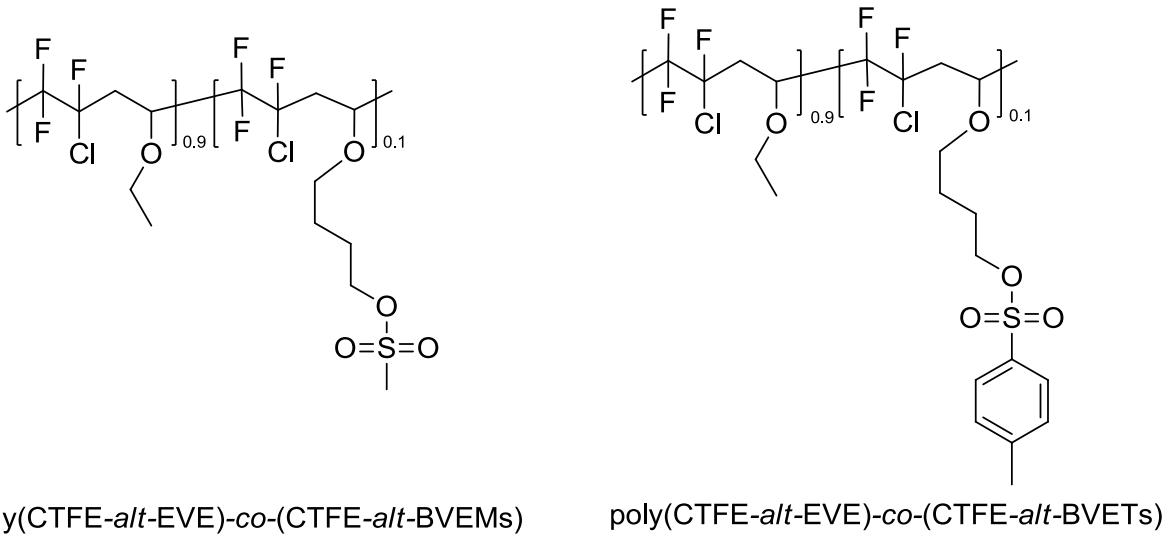

Figure 86 : Representation of the different model terpolymer synthesized.

The reaction is a radical copolymerization between the chlorotrifluoroethylene (CTFE), ethyl vinyl ether (EVE) and butyl vinyl ether functionalized (BVETs ou BVEMs) (Figure 87).). As the fluorinated monomers are gaseous, the polymerization are realized in an autoclave. The reaction was initiated by *tert*-butyl peroxypivilate (TBPPI) (1 mole % compared to the monomers) and carried out in 1,1,1,3,3-pentafluorobutane (solkane®) used as solvent, with the presence of potassium carbonate (3% molar compared to ethyl vinyl ether), to prevent the cationic homopolymerization of the vinyl ether . The reaction was performed at 75°C for 12h. The alternated terpolymers were obtained with a mass yield of 70% (Table 2).

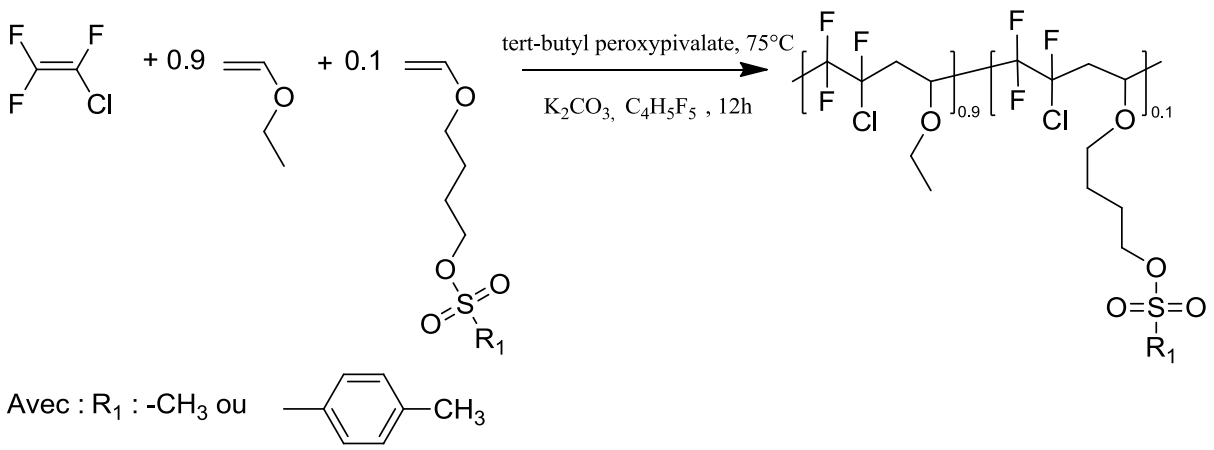

Figure 87 : Radical model terpolymerization

To confirm the expected structure, poly[(CTFE-*alt*-EVE)-*co*-(CTFE-*alt*-BVEMs)] was characterized by ^{1}H and ^{19}F NMR (Figure 88 and Figure 89)

Based on previous work carried out by our team[4-6], various significant signals, in ^{1}H NMR, of the methyl and methylene groups were clearly identified. Indeed, Figure 88, the presence of groups signals: -O-**CH_2**-CH_3(*c*) and -O-CH_2-**CH_3**(*d*) of EVE ; -O-**CH_2**-CH_2-CH_2-CH_2-O-S(O)$_2$-CH_3 (*e*), -O-CH_2-**CH_2**-**CH_2**-CH_2-O-S(O)$_2$-CH_3 (f, f'), -O-CH_2-CH_2-CH_2-**CH_2**-O-S(O)$_2$-CH_3(g); -O-CH_2-CH_2-CH_2-CH_2-O-S(O)$_2$-**CH_3**(h) respectively centered at 3.79, 1.21 ppm and at 3.79, 1.71, 1.84, 4.25 and 3.02 ppm can be observed. The light-shielded signals of the –CH_2- and -CH-OR, due to the presence of halogenated groups around, confirm the complete conversion of the vinyl ethers in the final terpolymer.

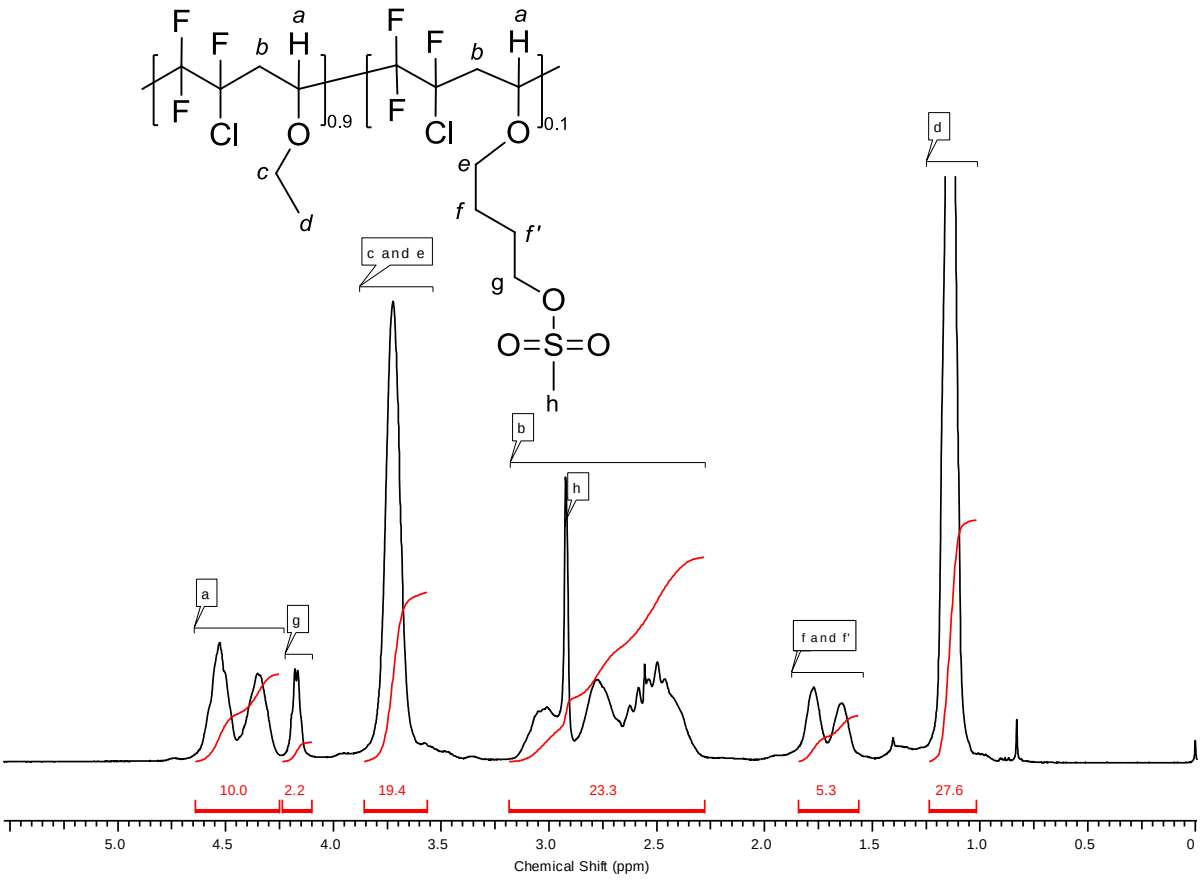

Figure 88 : ^{1}H NMR spectrum of poly(CTFE-alt-EVE)$_{0.9}$-co-(CTFE-alt-BVEMs)$_{0.1}$

The ^{19}F NMR (Figure 89) spectrum of terpolymer is similar with the results obtained in the literature[4-6]. Indeed, we can observe the presence of the four signals significant of

the fluorine atom of the main polymer chain. Concerning the -C**F**$_2$- groups, the large signals range between -108 to -112, -115 to -119, and -120.7 to -123ppm and for the -C**F**Cl- the signal is centered at -120ppm.

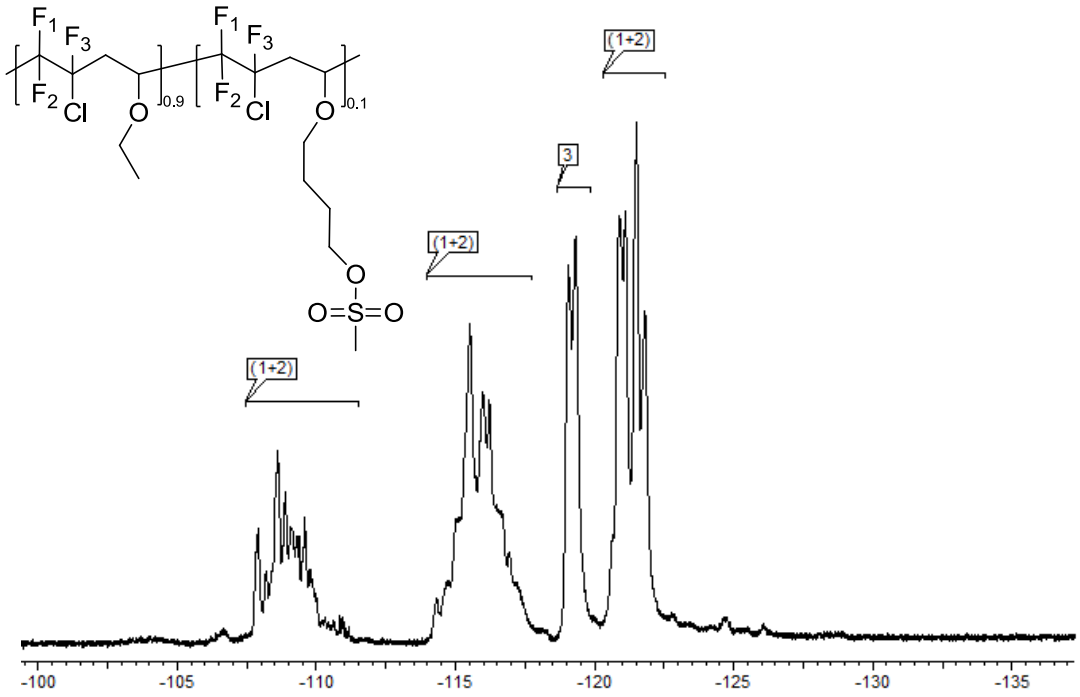

Figure 89 : ^{19}F NMR Spectrum of poly[(CTFE-alt EVE)$_{0.9}$-co-(CTFE-alt-BVEMs)$_{0.1}$] in $CDCl_3$

To confirm the expected structure, poly[(CTFE-*alt*-EVE)-*co*-(CTFE-*alt*-BVETs)] was characterized by ^{1}H and ^{19}F NMR (Figure 90 and Figure 91 respectively).

From the Figure 90, the presence of groups signal : -O-**CH$_2$**-CH$_3$(*c*) and -O-CH$_2$-**CH$_3$**(*d*) of EVE ; -O-**CH$_2$**-CH$_2$-CH$_2$-CH$_2$-O-S(O)$_2$-C- (*e*), -O-CH$_2$-**CH$_2$**-**CH$_2$**-CH$_2$-O-S(O)$_2$-CH$_3$ (f, f'), -O-CH$_2$-CH$_2$-CH$_2$-**CH$_2$**-O-S(O)$_2$-CH$_3$(g) respectively centered at 3.79, 1.21 ppm and at 3.79, 1.71, 1.84, and 4.25ppm can be observed. The presence of the aromatic groups signal centered at 2.4 (j), 7.34 (h) et 7.79 (i) can be also observed. The light-shielded signals of the –C**H$_2$**- and -C**H**-OR, due to the presence of halogenated groups around, confirm the complete conversion of the vinyl ethers in the final terpolymer.

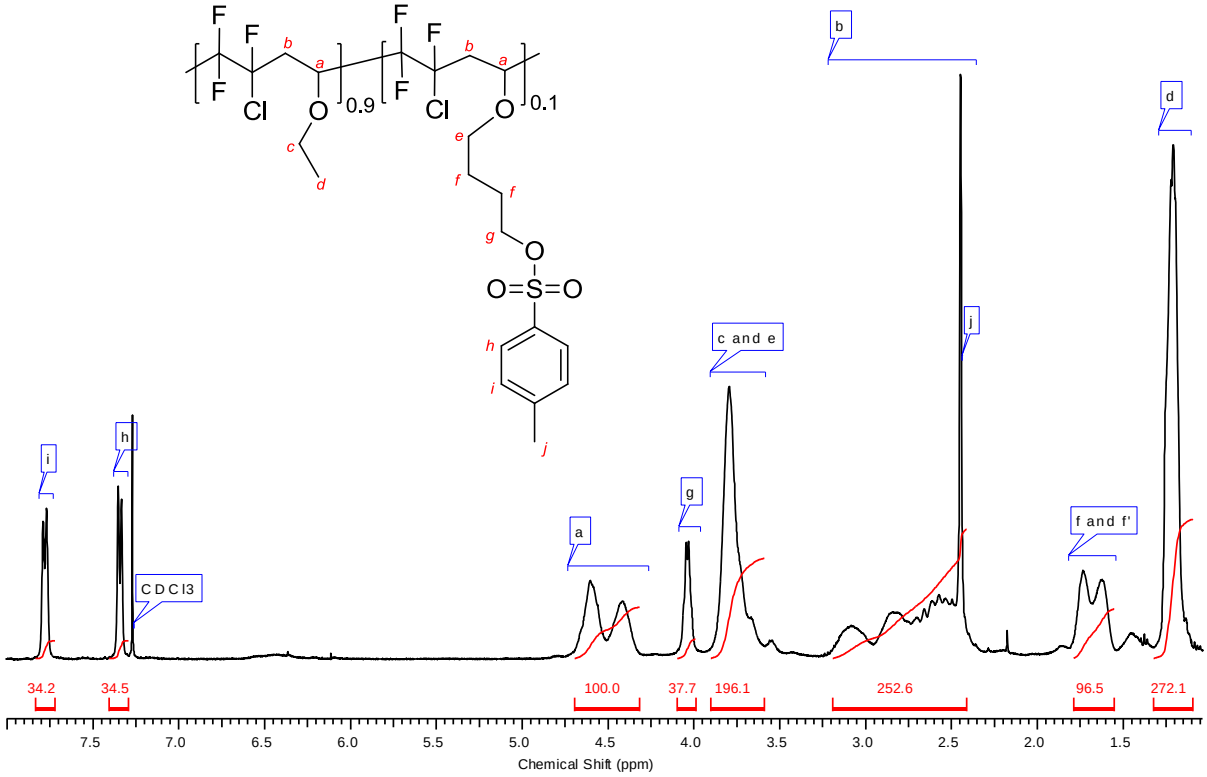

Figure 90 : ^{1}H NMR spectrum of poly[(CTFE-EVE)$_{0.9}$-(CTFE-BVETs)$_{0.1}$]

The ^{19}F NMR (Figure 91) spectrum of terpolymer is similar to that of poly[(CTFE-*alt*-EVE)-*co*-(CTFE-*alt*-BVEMs)]. Indeed, we can observe the presence of the four signals significant of the fluorine atom of the main polymer chain. Concerning the -C**F$_2$**- groups, the large signals range between -108 to -112, -115 to -119, and -120.7 to -123ppm and for the -C**F**Cl- the signal is centered at -120ppm.

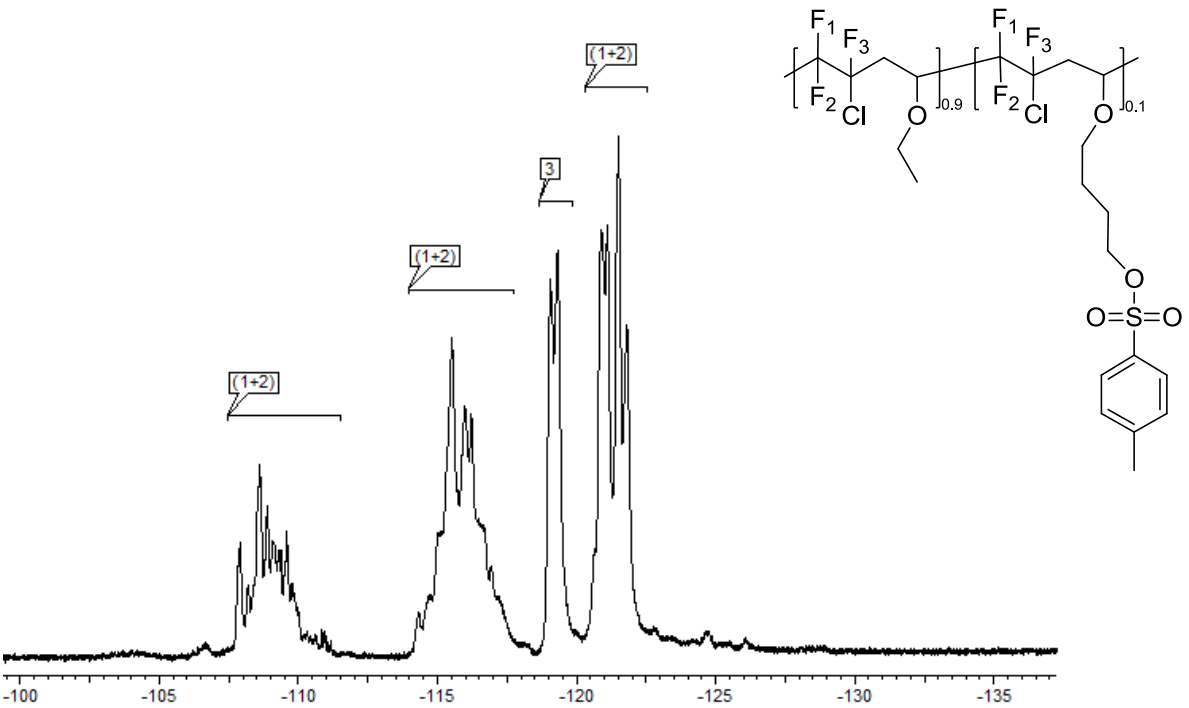

Figure 91 : ^{19}F NMR spectrum of poly[(CTFE-alt-EVE)$_{0.9}$-co-(CTFE-alt-BVEMs)$_{0.1}$] in $CDCl_3$

The terpolymer composition in vinyl ethers (EVE, BVEMs or BVETs) can be obtained by the integration of the –**CH**-OR signal (*a*) that appears between 4.34 to 4.73 ppm of the main chain and the –CH_2-**CH_2-CH_2**-CH_2-O-S(O)$_2$-CH_3 (*f* et *f'*) signal of BVEMs (or BVETs) showed between 1.65 to 1.95 ppm from the Equation 1.

$$\%BVEMs = \frac{\frac{\int_{1,65}^{1,95} f + f'}{4}}{\int_{1,65}^{1,95} f + f' + \int_{4,34}^{4,73} a}$$

Equation 1 : Determination of the BVEMs (or BVETs) incorporation in the terpolymer.

The results are listed in Table 8 and show a good agreement between the percentage of functionalized monomer introduced into the reaction mixture and the rate of incorporation in the terpolymer obtained, thanks to the opposite polarity to that of CTFE. The synthesis allows keeping the alternating nature of the polymer.

Table 8 : Terpolymer composition

Terpolymers	Initial molar proportion of monomers (%)			Incorporation rate of monomer in the terpolymer $(\%)_a$			Rdt (wt %)
	CTFE	EVE	$BVER_1$	CTFE	EVE	$BVER_1$[a]	
Poly[(CTFE-*alt*-EVE)$_{0.9}$-*co*-(CTFE-*alt*-BVEMs)$_{0.1}$]	50	45	5	50	46	4	72
Poly[(CTFE-*alt*-EVE)$_{0.9}$-*co*-(CTFE-*alt*-BVETs)$_{0.1}$]	50	45	5	50	44	6	71

a: determined by ^{1}H NMR

R1 : mesylate or tosylate

3.3 Crosslinking and characterizations of model terpolymers

3.3.1 *Crosslinking of terpolymers*

In order to achieve terpolymers crosslinking, membranes have been cast from these terpolymers. The membranes are prepared by the process of casting-evaporation of the polymer solution. For this, the terpolymers are dissolved in a solution of DMF. The concentration of the solution is about 30 wt%. To carry out the crosslinking reaction, the glass plate on which the membrane was cast is placed in a programmable oven. The heat treatment consists of two steps. In the first step, allowing solvent evaporation used for the casting, the temperature is set at 90°C for 12 h. The second heat treatment is performed to achieve the crosslinking reaction. We saw in the first part of this chapter (see 2.Bibligraphic study of the crosslinking reaction.), that the formation of the alkoxide ion is favored at high temperatures. In order to both avoid copolymer degradation and perform cross-linking reaction, the heat treatment temperature will be 150°C for 12h. After this heat treatment, applied for both terpolymers, the glass plate is immersed in distilled water for 24 hours in order to take off the membranes.

3.3.2 *Physico-chemical characterizations*

The physico-chemical characterizations of the membranes were performed before and after the heat treatment for the crosslinking reaction, i.e. 150°C. The comparisons of the different results obtained should allow us to confirm the success of the crosslinking reaction. Indeed, crosslinking reaction should cause an increase of the thermal resistance but also the glass transition temperature of the membranes. This is because of the densification of the polymer network. The densification of the network should also lead to membranes insolubility.

3.3.2.1 Thermal analysis of terpolymers

The analyses of each terpolymer model are presented separately. We first describe the thermal analysis of the poly[(CTFE-EVE)$_{0.9}$-(CTFE-BVEMs)$_{0.1}$] followed by the thermal analysis of poly[(CTFE-EVE)$_{0.9}$-(CTFE-BVETs)$_{0.1}$].

poly[(CTFE-alt-EVE)$_{0.9}$-co--(CTFE-alt-BVEMs)$_{0.1}$]

The thermal stability of the membrane has been assessed by Thermogravimetric analysis (TGA) before and after the crosslinking reaction. Figure 92 shows the thermogram obtained by TGA analyses of the membrane cast from the poly[(CTFE-*alt*-EVE)$_{0.9}$-co-(CTFE-*alt*-BVEMs)$_{0.1}$] before (-) and after (-) crosslinking. The derivative curves are also given.

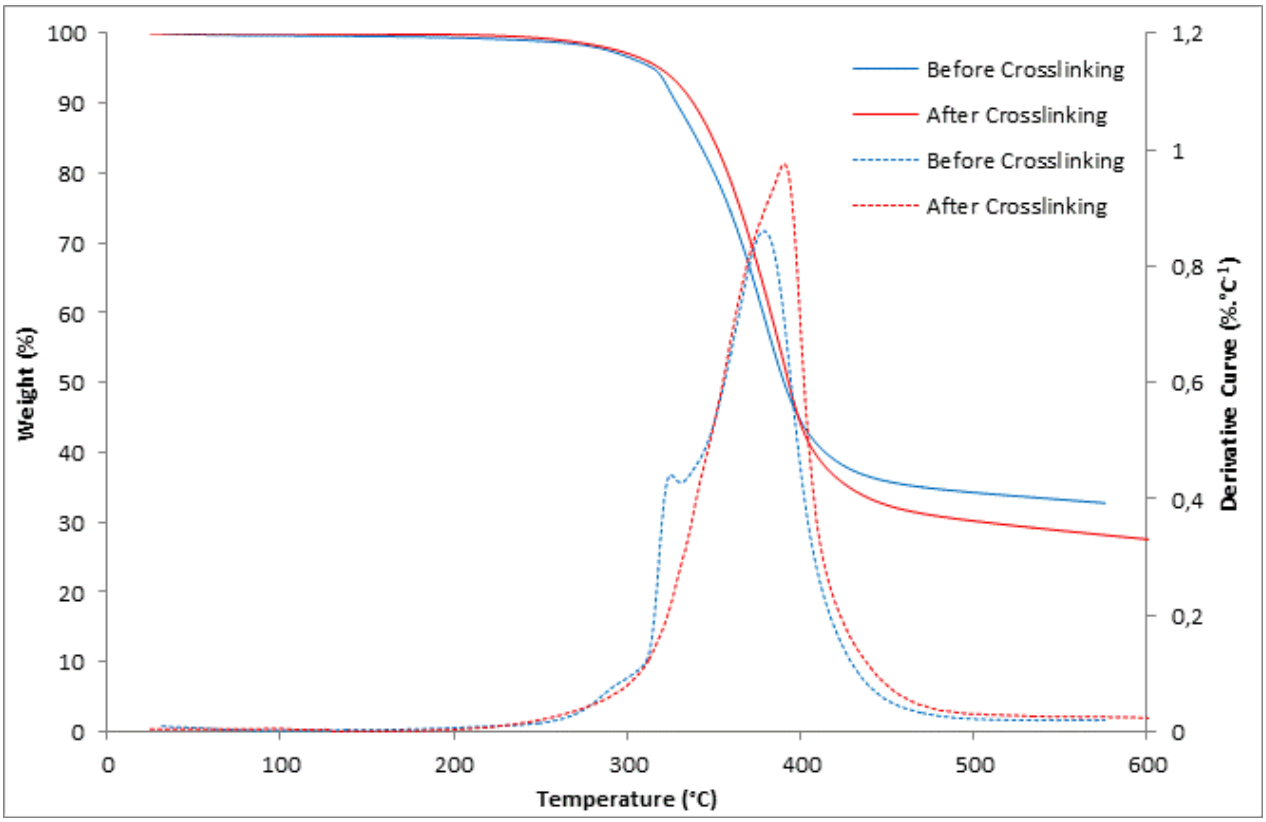

Figure 92 : TGA analyses of poly(CTFE-alt-EVE)$_{0.9}$-co-(CTFE-alt-BVEMs)$_{0.1}$

From the membrane before crosslinking, we see two main decompositions between 270 and 500°C. The first degradation occurs between 270 and 330°C. The bond energy (–O-S) of C-**O-S(O$_2$)-CH$_3$** groups is weaker than the bond energy (-O-C) of -C-**O-CH$_2$CH$_3$** groups, so we can attribute this weight loss to the breaking of the -O-S- bond of BVEMs units. Then from 350°C, the degradation of all pending polymer chains can be observed. From the membrane after crosslinking, only one main decomposition was observed ranging from 270 to 500°C, unlike the thermogram of the membrane before crosslinking. Indeed, between 270 and 330°C on the derivative curve, the peak attributed to the breaking of the -O-S-bond of BVEMs units is no longer observed. Thus, during the crosslinking reaction, it seems that all mesylate groups are consumed. We also note that the crosslinked membrane has a slightly higher thermal stability than the non-crosslinked membrane. This increase of the thermal stability resulted in a slight increase in temperature corresponding to 5% and 10% mass loss. These temperatures are listed in Table 9. Indeed, after crosslinking, the temperature

corresponding to 10% weight loss ($Td_{10\%}$) is 338°C, whereas for the non-crosslinked membrane, the $Td_{10\%}$ is 328°C.

poly[(CTFE-alt-EVE)$_{0.9}$-co-(CTFE-alt-BVETs)$_{0.1}$]

The thermal stability of the membrane has been determined by TGA before and after the crosslinking reaction. Figure 93 shows the thermogram obtained by TGA analyses of the membrane cast from the poly[(CTFE-*alt*-EVE)$_{0.9}$-*co*-(CTFE-*alt*-BVETs)$_{0.1}$] before (-) and after (-) crosslinking.

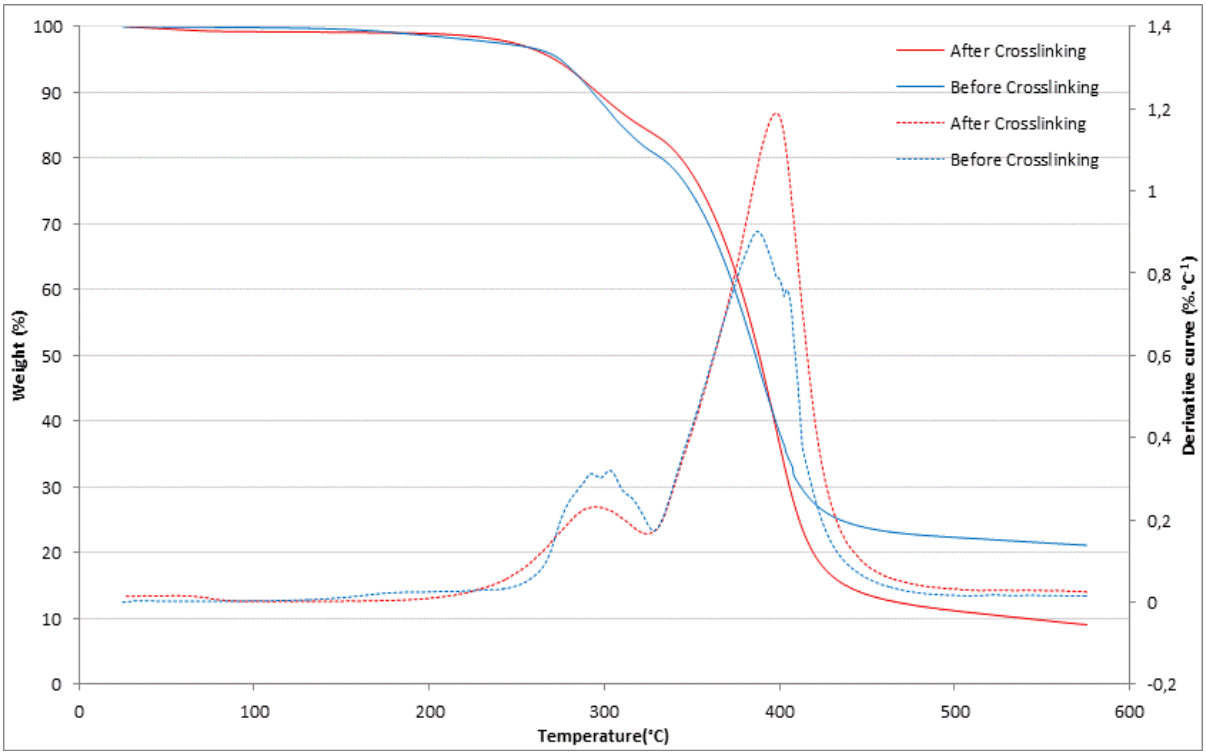

Figure 93 : TGA analyses of poly[(CTFE-alt-EVE)$_{0.9}$-co-(CTFE-alt-BVETs)$_{0.1}$]

From the membrane before crosslinking, we see two main decompositions between 240 and 500°C. A first degradation occurs between 240 and 330°C. The bond energy (–O-S) of C-**O-S(O_2)-C** groups is weaker than the bond energy (-O-C) of -C-**O-CH_2CH_3** groups, so we can attribute this weight loss to the breaking of the -O-S- bond of BVETs units. Then from 350°C, the polymer chains degradation can be observed. From the membrane after crosslinking, we still observe the presence of two decompositions between 240 and 500°C.

However, the weight loss corresponding to the first decomposition decreased. Indeed, before crosslinking it corresponded to around 17%, while after crosslinking it is 14%. So, during the crosslinking reaction, all tosylate groups are not consumed. We also note that the thermal resistance of the membrane is the same before and after crosslinking. These temperatures are listed in Table 9. Indeed, after crosslinking, the temperature corresponding to 10% weight loss ($Td1_{0\%}$) is 294°C, whereas for the non-crosslinked membrane, the $Td_{10\%}$ is 296°C.

Table 9 :Degradation temperatures and glass transition temperatures before and after crosslinking membranes obtained respectively by TGA under nitrogen at 10 ° C.min^{-1} and DSC at 20 ° C.min^{-1}.

Terpolymer	Step	**$Td_{5\%}$(°C)**	**$Td_{10\%}$(°C)**	**Tg_{exp}(°C)[a]**
poly(CTFE-*alt*-EVE)$_{0.9}$-*co*-(CTFE-*alt*-BVEMs)$_{0.1}$	**Before crosslinking**	314	328	10
	After crosslinking	319	338	90
poly(CTFE-*alt*-EVE)$_{0.9}$-*co*-(CTFE-*alt*-BVETs)$_{0.1}$	**Before crosslinking**	275	294	20
	After crosslinking	277	296	23

a : Uncertainty about the glass transition temperature determined by DSC : ±2°C

The glass transition temperatures of the terpolymers before and after crosslinking reaction were determined by DSC. The results obtained are illustrated in the Table 9. Concerning poly(CTFE-*alt*-EVE)$_{0.9}$-*co*-(CTFE-*alt*-BVEMs)$_{0.1}$Tg value is 10°C before crosslinking. But, after crosslinking, Tg values increases to reach 90°C. This increase of the glass transition temperature characterizes a significant polymer network rigidification due to the formation of inter-chain bridges during the second heat treatment at 150°C. Then, concerning poly(CTFE-*alt*-EVE)$_{0.9}$-*co*-(CTFE-*alt*-BVETs)$_{0.1}$ the difference of the Tg values before and after crosslinking is not significant. This result is in agreement with that obtained from TGA, where we showed that few tosylate groups reacted during the heat treatment. Thus the formation of inter chain bridges is not sufficient to obtain a polymer network rigidification.

3.3.2.2 Terpolymer solubility

The crosslinking reaction of the terpolymer will lead to a three-dimensional network due to the formation of inter-chain bonds. This will directly impact the solubility of the polymer in various organic solvents, even resulting in total insolubility of the polymer for a sufficient degree of crosslinking. Thus, in order to confirm the crosslinking of membranes, solubility tests were carried out in different solvents. The test consists of immersing the membrane in the solvent for a period of 72 hours with weak stirring. The tests were conducted at room temperature and at a temperature of 50 ° C. The results of solubility tests are summarized in Table 10.

Table 10 :Solubility tests at RT and 50°C of terpolymer before and after crosslinking .

T=RT (72h)				
Solvent	poly(CTFE-*alt*-EVE)$_{0.9}$-*co*-(CTFE-*alt*-BVEMs)$_{0.1}$		poly(CTFE-*alt*-EVE)$_{0.9}$-*co*-(CTFE-*alt*-BVETs)$_{0.1}$	
	Before Crosslinking	After crosslinking	Before Crosslinking	After crosslinking
Methanol	+	x	+	X
Acetone	+	x	+	X
MEK	+	x	+	X
THF	+	x	+	X
DMSO	+	x	+	X
DMF	+	x	+	X
T=50°C (72h)				
	poly(CTFE-*alt*-EVE)$_{0.9}$-*co*-(CTFE-*alt*-BVEMs)$_{0.1}$		poly(CTFE-*alt*-EVE)$_{0.9}$-*co*-(CTFE-*alt*-BVETs)$_{0.1}$	
Solvent	Before Crosslinking	After crosslinking	Before Crosslinking	After crosslinking
Methanol	+	x	+	x
Acetone	+	x	+	x
MEK	+	x	+	x

THF	+	x	+	x
DMSO	+	x	+	x
DMF	+	x	+	x

+ : soluble membrane

x : insoluble membrane

From Table 10, we note that the thermal treatment allows membranes to become totally insoluble in most organic solvents after crosslinking, this at room temperature but also at 50°C. For the poly(CTFE-*alt*-EVE)$_{0.9}$-*co*-(CTFE-*alt*-BVETs)$_{0.1}$, although all crosslinkable groups did not completely react, the membrane is still insoluble. The insolubility of the membranes, especially in the solvents used in the casting, confirm the success of the crosslinking reaction of the membrane during heat treatment as well as poly(CTFE-*alt*-EVE)$_{0.9}$-*co*-(CTFE-*alt*-BVETs)$_{0.1}$ where only a small amount of tosylate groups did react.

The results obtained from the solubility tests combined with those obtained from thermal analyzes clearly allow us to conclude the success of the crosslinking reaction. However, the use of mesylate groups in order to achieve crosslinking of the polymer appears more appropriate since the mesylate groups seem to be more reactive than tosylate ones. Synthesis of copolymer from the CTFE and vinyl ether bearing sulfonate groups leads to the production of crosslinked polymer by simple heat treatment. This crosslinking technique is limited by the thermal resistance of the copolymer which must be higher than 150°C.

It is now important to focus on the reaction but also on the mechanism by which the crosslinking reaction occurs.

3.4 **Study of the crosslinking reaction**

Fourier transform infrared spectroscopy (FTIR) analyses have been realized on the both terpolymers before and after the crosslinking reaction. This analysis will allow us to especially observe the evolution of the signals characterizing the presence of sulfonate groups before and after crosslinking. The results are illustrated Figure 94 and Figure 95 (for poly[(CTFE-*alt*-EVE)$_{0.9}$-*co*-(CTFE-*alt*-BVETs)$_{0.1}$] and poly[(CTFE-*alt*-EVE)$_{0.9}$-*co*-(CTFE-*alt*-

BVEMs)$_{0.1}$] respectively). From these figures, we note that both areas from 1800 to 2800 cm^{-1} and 3000-4000 cm^{-1} are superimposed. Therefore, the differences in peak intensities before and after crosslinking of the material are significant of a decrease or increase of the groups. By FTIR, the sulfonate groups are characterized by the presence of two bands around 1150 and 1350 cm^{-1}.

From Figure 94, the most intense peak around 1200 cm^{-1} corresponds to carbon-halogen bond (in our case, C-F and C-Cl). On tosylate groups, it is interesting to compare the evolution of the characteristic signals of aromatic groups. However, the signal of these groups appears between 800 and 1100 cm^{-1}, areas in which we also find alkanes signals. So we only focus on sulfonate groups signals. On these signals, we note a slight decrease in weak bands at 1350 and 1180 cm^{-1}. We also observe a slight increase of significant ether linkages band (-C-O-C-) around 1220 cm^{-1}. These results are in good agreement with those obtained from thermal analysis (TGA, DSC), that only a small amount of tosylate groups reacted during the crosslinking reaction.

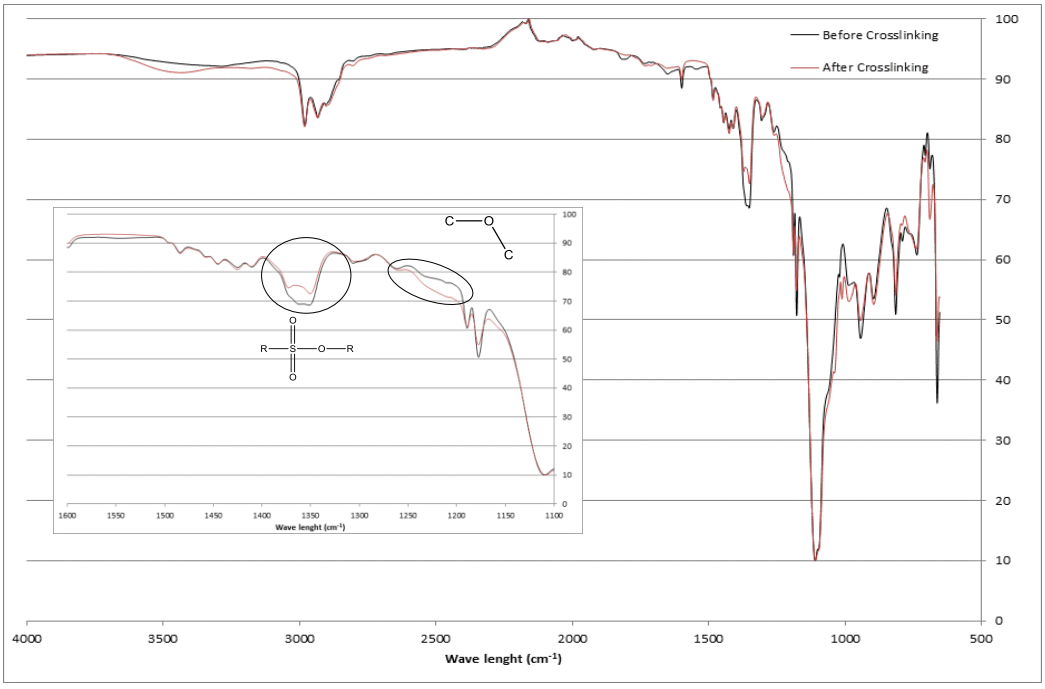

Figure 94 : FTIR spectrum of poly[(CTFE-alt-EVE)$_{0.9}$-co-(CTFE-alt-BVETs)$_{0.1}$] before and after crosslinking.

From Figure 95, as to poly[(CTFE-*alt*-EVE)$_{0.9}$-*co*-(CTFE-*alt*-BVETs)$_{0.1}$], the most intense peak at about 1200 cm^{-1} corresponds to the halogen-carbon bonds. Concerning the evolution of the characteristic band of sulfonate groups, although the TGA results show a total consumption of mesylate groups after heat treatment, we observe a slight decrease of the characteristic band. But, the band characteristic of ether bonds significantly increases. In the case of poly[(CTFE-*alt*-EVE)$_{0.9}$-*co*-(CTFE-*alt*-BVEMs)$_{0.1}$] cross-linking the emergence of a new band between 1700 and 1800 cm^{-1}, which is not present after poly [(CTFE-*alt*-EVE)$_{0.9}$-*co*-(CTFE-*alt*-BVETs)$_{0.1}$] crosslinking, can be observed. This band is characteristic of carbonyl bonds. In view of the required thermal crosslinking of the terpolymer after (>150°C), this band cannot be characteristic to the formation of ester or aldehyde group. This band corresponds to the formation of a ketone group during the crosslinking reaction. Further investigations are nevertheless necessary to fully understand this reaction.

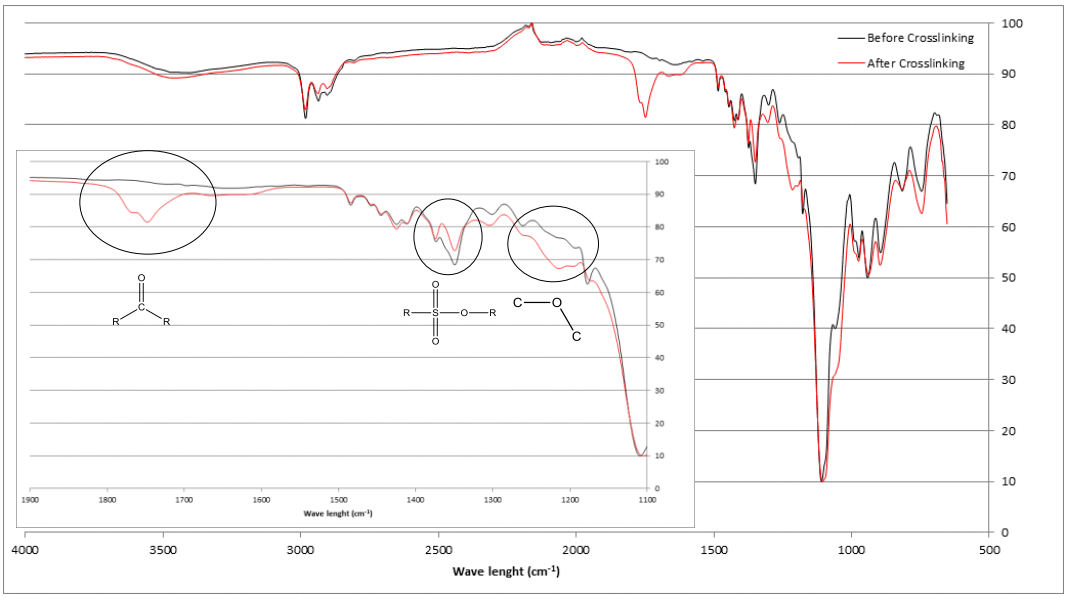

Figure 95 : FTIR spectrum of poly[(CTFE-alt-EVE)$_{0.9}$-co-(CTFE-alt-BVEMs)$_{0.1}$] before and after crosslinking.

The results obtained from FTIR analysis are only semi-quantitative, and enable confirming the reduction of sulfonate groups after the crosslinking reaction. The composition of the membranes cast from poly[(CTFE-*alt*-EVE)$_{0.9}$-*co*-(CTFE-*alt*-BVEMs)$_{0.1}$] was determined by elemental analysis. The results before and after crosslinking are listed in

Table 11. We can note that before crosslinking the calculated and experimental values are very close. These results agree with those obtained by ^{1}H NMR. The molar percentage of sulfur before and after crosslinking of the membrane is very important information. We observe that this percentage decreases to about 60%. This result confirms the FTIR observation. We also note that the molar percentage of oxygen increases after crosslinking, this result is contradictory. Indeed, the loss of a sulfonate group in the crosslinking reaction should lead to a decrease of oxygen levels. However, this oxygen percent increase may be attributed to the formation of ketone band observed on the FTIR spectrum (Figure 95).

Table 11: Elemental analyses theoretical and experimental in molar percent for the poly[(CTFE-alt-EVE)$_{0.9}$-co-(CTFE-alt-BVEMs)$_{0.1}$] before and after crosslinking

Element	Before crosslinking		After crosslinking	
	Theoretical values (% mol)	Experimental values (% mol)	Theoretical values (% mol)	Experimental values (% mol)
C	38.31	37.9	38.86	37.01
H	4.55	4.35	4.53	4.48
S	1.57	1.69	0.80	0.69
O	10.21	11.29	9.43	12.78

From these results we propose a structure obtained after the crosslinking reaction (Figure 96). The molar composition of this structure model was calculated and compared with experimental results.

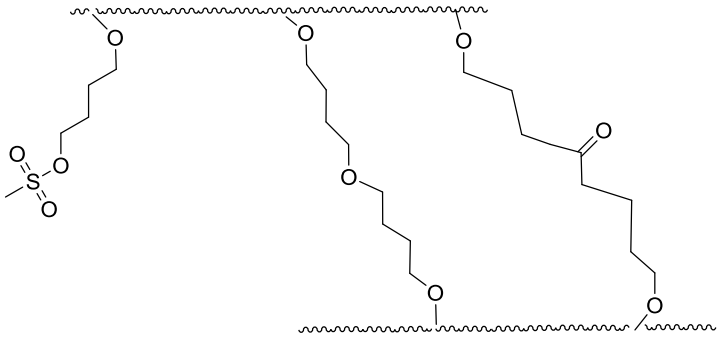

Figure 96 : Possible structure after reaction.

Based on the decrease in the percentage of sulfur atom and the sulphonate group-reactivity, the crosslinking reaction probably occurs via the formation of ether and ketone bonds. During the reaction, the denser polymer network thereby reduces the mobility of the groups. Thus, all groups cannot react (Figure 96) which justifies the fact that after crosslinking reaction there is still 40 mol% of sulfonate groups. However, the increase of the molar percentage of oxygen cannot be explained by this mechanism. In addition, we did not find any mechanism that could explain the formation of ketones groups. A model study from the coupling molecule with a mesylate or tosylate group will be carried out to obtain more insight about the reaction occurring during the crosslinking of the copolymer.

3.5 **Molecular study of the crosslinking reaction**

The macroscopic study did not clearly identify the mechanism of the crosslinking reaction. To determine the mechanism, different model molecules were synthesized. The crosslinking reaction is thermally activated, the difficulty of this study lies in the synthesis of molecules that possess high required thermal stability (about 150°C).

3.5.1 ***Synthesis of 1H,1H,2H,2H-Perfluoro-1-octyl 4-methylbenzenesulfonate***

The first model molecule synthesized is 1H,1H,2H,2H-Perfluoro-1-octyl 4-methylbenzenesulfonate. It was obtained by nucleophilic substitution reaction between the mesyle chloride and 1*H*,1*H*,2*H*,2*H*-Perfluoro-1-octanol according to the Figure 97.

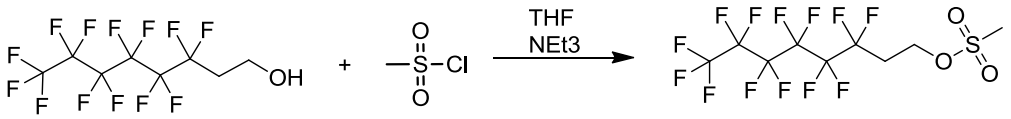

Figure 97 : synthesis of 1H,1H,2H,2H-Perfluoro-1-octyl 4-methylbenzenesulfonate

In order to neutralize the hydrochloric acid which is formed during the reaction, 1.1 equivalent of triethylamine (NEt_3) was added. After reaction, the triethylamine salt is removed by precipitation, and after filtration the solvent was removed. After several liquid/liquid extractions, a white product is obtained with a mass yield of 90%. The expected structure was confirmed by ^{1}H NMR.

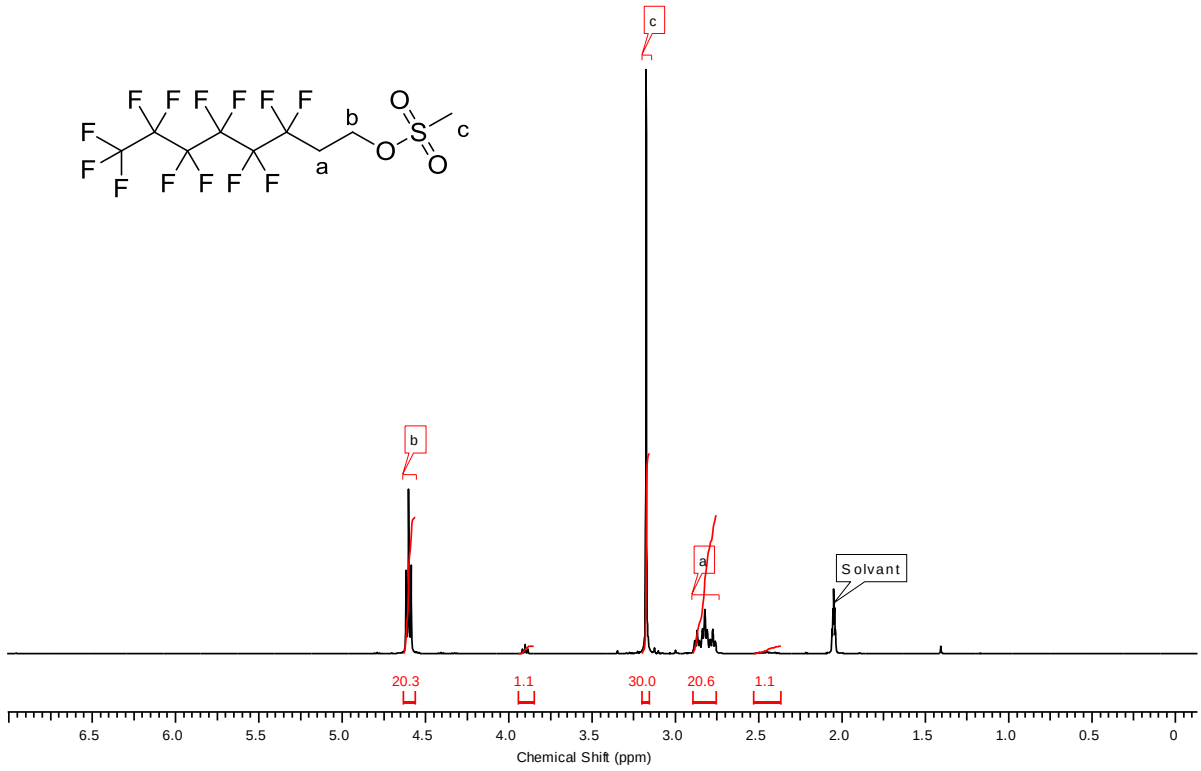

Figure 98 : ^{1}H NMR spectrum of 1H,1H,2H,2H-Perfluoro-1-octyl 4-methylbenzenesulfonate (realized in acetone d_6)

^{1}H NMR spectrum allows us to confirm the expected structure. Indeed, we observe a deshielding of -CH2- groups in alpha (3.9 to 4.6ppm) and beta (2.45 to 2.85 ppm) positions of oxygen compared to the starting molecule. This is due to the electron-withdrawing effect of the sulfur atom.

To perform the coupling reaction between the mesylate groups without catalyst or initiator, it is necessary to realize the reaction at high temperature. With the 1*H*,1*H*,2*H*,2*H*-Perfluoro-1-octyl 4-methylbenzenesulfonate, we are limited by the boiling temperature of the product (90°C). We therefore carried out the tests at 90°C for 12 hours. After reaction, the ^{1}H NMR characterization shows no change. The reaction temperature is not sufficient to

enable the reaction. It is therefore necessary to use a molecule having a higher boiling point and with an alcohol to achieve the functionalization

3.5.2 *Synthesis of pentyl-4-methylbenzenesulfonate*

The alcohols having at least 4 carbons show a high boiling point (about 140°C). We will use the pentan-1-ol as starting molecule. The synthesis of pentyl-4-methylbenzenesulfonate is a nucleophilic substitution reaction between the tosyl chloride and pentan-1-ol. The presence of triethylamine is necessary to neutralize the formation of HCl. The reaction scheme is shown in Figure 99.

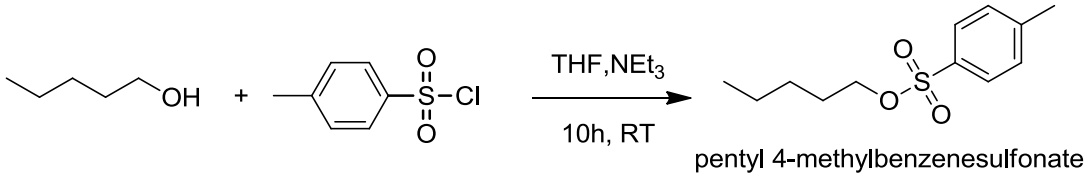

Figure 99 : Synthesis of pentyl-4-methylbenzenesulfonate.

Using tosyl chloride, the reaction kinetics is slower, in consequence the reaction is performed during 10h. This difference in kinetics is due to a better stability of tosyl chloride compared to to mesyl chloride. After reaction, the solution is filtered to remove the triethylamine salt formed. The expected structure was confirmed by ^{1}H NMR.

.

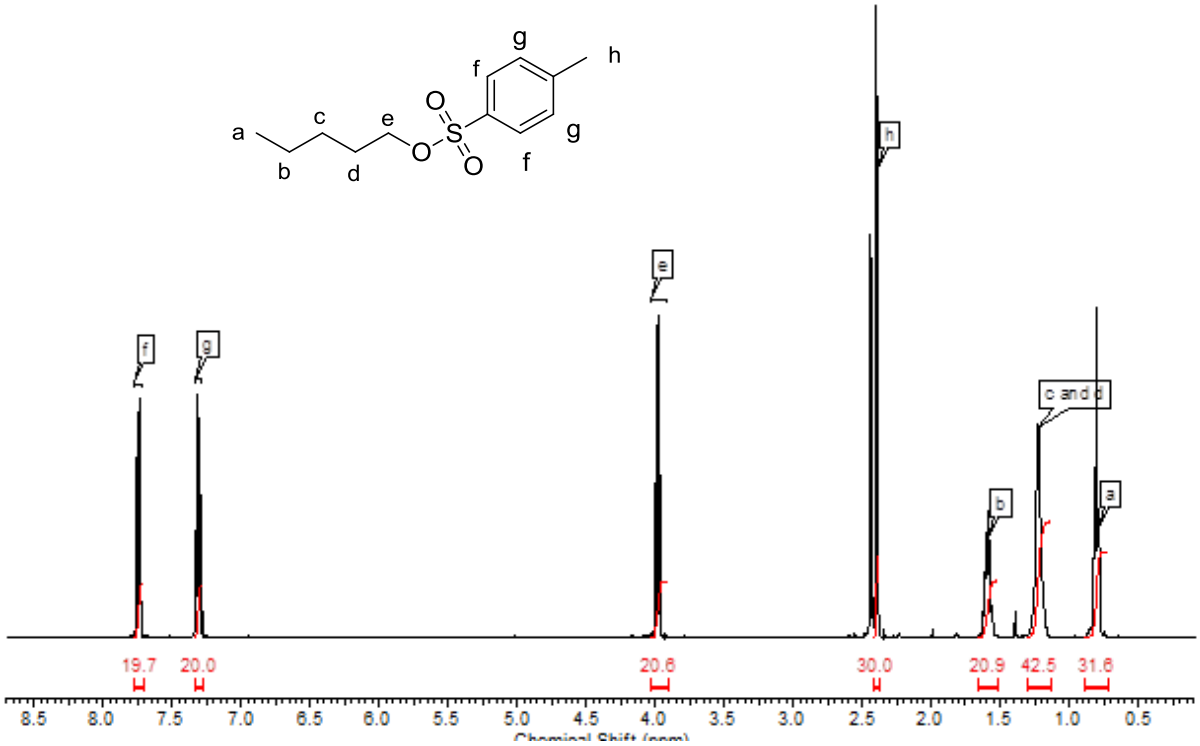

Figure 100 : 1H NMR spectrum of pentyl-4-methylbenzenesulfonate (realized in $CDCl_3$)

The ^{1}H NMR spectrum confirms the success of the reaction. The most significant effect is the deshielding of the signal representing the -CH_2-(e) group in alpha position of the oxygen atom (from 3.5 to 3.95ppm). We also observe a slight deshielding of significant signals from other groups of the alkane chain (CH_3-CH_2-CH_2-CH_2-CH_2-O-) (a, b, c and d). The deshielding of the signals is due to the delocalization of the electron cloud of the oxygen atom.

The tests performed with the coupling reaction of pentyl-4-methylbenzenesulfonate did not allow to assess the type of mechanism. Indeed, after several hours of reaction at 150°C, no change is observed in the ^{1}H NMR spectrum (Figure 101).

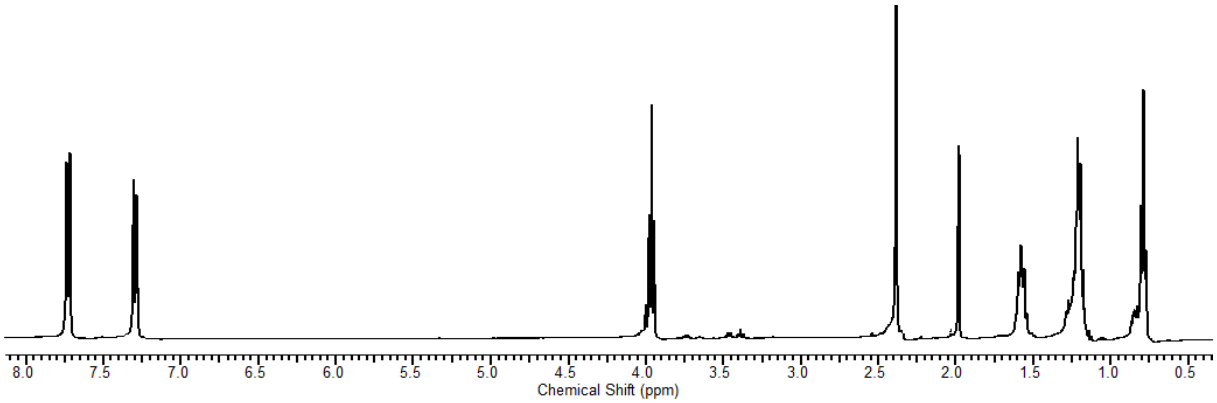

Figure 101 : ^{1}H NMR spectrum of pentyl-4-methylbenzenesulfonate after reaction (realized in $CDCl_3$)

4 Conclusion

The objective of this chapter was the implementation of a cross-linking technique of fluoropolymer by a simple heat treatment. The synthesis of terpolymer from CTFE, EVE and vinyl ether carrying sulfonate group led us to obtain crosslinked polymer. To do this, the membrane casting from these terpolymers undergoes a simple heat treatment (150°C, 12h) without any special conditions. We have seen that the use of mesylate group allows a better crosslinking of the polymer, due to greater reactivity of this group. However, although the low reactivity of tosylate groups does not allow for a high degree of crosslinking, it is still sufficient to obtain an insoluble material in various organic solvents. After heat treatment, analyzes of the membranes allowed to suggest a potential structure from the bonds formed during the crosslinking reaction. However, from the macroscopic study it is difficult to determine the exact mechanism for the crosslinking reaction. Molecular study did not allow us to determine the mechanism of the reaction. The reaction mechanism seems to be more complex than the simple formation of ether bonds. Thus, when terpolymers are crosslinked, the formation of radicals or some other highly reactive species occur from the sulfonate groups and cause a not easily identifiable reaction. To obtain more information solid carbon and proton NMR could be useful. Further new model compound can be synthesized with higher thermal stability. Indeed, we can use an alcohol with more carbon, as the octan-ol, or

even an aromatic compound as the benzyl alcohol. It is therefore important to mention that this work waspatented by CNRS and CEA.

5 Experimental part

5.1 Reagent

Chlorotrifluoroethylene (CTFE) and 1,1,1,3,3,-pentafluorobutane (solkane®) were kindly provided by Solvay S.A. 1*H*,1*H*,2*H*,2*H*-Perfluoro-1-octanol, pentan-1-ol, ethyl vinyle ether, hydroxyl butyl vinyl ether, mesyl chloride, tosyl chloride, triethylamine, tertrahydrofurane, acetone, le methanol, ethyle acetate, hexane, carbonate potassium were purchased from Sigma-Aldrich. *Tert*-butyl peroxipivalate (TBPPI) 75% purity was purchased from Azko Nobel®. All reactants were used without further purification except for the solkane, which were distillate prior to use.

5.2 1*H*,1*H*,2*H*,2*H*-Perfluoro-1-octyl 4-methylbenzenesulfonate

In a single-neck round bottom flask equipped with a magnetic stirrer, one equivalent of 1*H*,1*H*,2*H*,2*H*-Perfluoro-1-octanol and 1 equivalent of mesyl chloride were introduced in THF 1.1equivalent of triethylamine was also introduced in order to neutralize the formation of HCl. After 2h, the produced salts were filtered. After several liquid/liquid extractions, the product was obtained in high masse yield (90%).

As an example, in a 250mL single-neck round bottom flask equipped with a magnetic stirrer, one equivalent of 1*H*,1*H*,2*H*,2*H*-Perfluoro-1-octanol (10g, 27.5mmol), 1 equivalent of mesyl chloride were introduced (3.15g, 27.5mmol) and 1 equivalent of triethylamine (3.05g, 30.25mmol) were introduced in THF (50mL). After 2h, the produced salts were filtered. Two liqudi/liquid (water/ethyl acetate) extractions have been realized and the product was obtained in high masse yield (90%).

Structure:

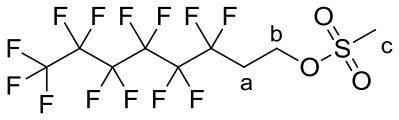

Mass yield: 90%

^{1}H NMR (400MHz, 297K, Acetoned$_6$, ppm) : 4.60 (t, 2H, H_b), 3.18 (s, 3H, H_c) and 2.82(tt, 2H, H_a).

5.3 **Tosylated pentanol**

In a single-neck round bottom flask equipped with a magnetic stirrer, one equivalent of pentanol and 1 equivalent of tosyl chloride were introduced in THF 1.1equivalent of triethylamine was also introduced in order to neutralize the formation of HCl. After 10h, the produced salts were filtered. After purification by flash chromatho, the product was obtained in high masse yield (86%).

As an example, in a 250mL single-neck round bottom flask equipped with a magnetic stirrer, one equivalent of pentanol (10g, 113.4mmol), 1 equivalent of tosyl chloride were introduced (21.6g, 113.4mmol) and 1 equivalent of triethylamine (12.6g, 124.7mmol) were introduced in THF (100mL). After 10h, the produced salts were filtered. After purification by flash chromatho, the product was obtained in high masse yield (86%).

Structure :

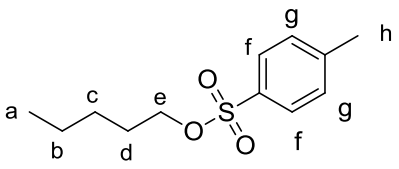

Mass yield: 86%

^{1}H NMR (400MHz, 297K, Acetoned$_6$, ppm) : 7.77 to 7.71 (dd, 2H, H_f), 7.34 to 7.28 (dd, 2H, H_g) 4.0 to 3.96 (td 2H H_e), 2.46 to 2.38 (d, 3H, H_h), 1.63 to 1.55(q, 2H, H_b), 1.28 to 1.17 (m, 4H, H_c et H_d) and 0.83 to 0.77 (td, 3H, H_a).

5.4 Butyl vinyl ether mesylated

In a single-neck round bottom flask equipped with a magnetic stirrer, one equivalent of hydroxide butyl vinyl ether and 1 equivalent of mesyl chloride were introduced in THF. 1.1equivalent of triethylamine was also introduced in order to neutralize the formation of HCl. After 2h, the produced salts were filtered. After several liquid/liquid extractions, the product was obtained in high masse yield (80%).

As an example, in a 250mL single-neck round bottom flask equipped with a magnetic stirrer, one equivalent hydroxide butyl vinyl ether (10g, 86.2 mmol), 1 equivalent of mesyl chloride were introduced (9.85g, 86.2mmol) and 1 equivalent of triethylamine (9.6g, 94.9mmol) were introduced in THF (100mL). After 2h, the produced salts were filtered. Two liqudi/liquid (water/ethyl acetate) extractions have been realized and the product was obtained in high masse yield (80%).

Structure :

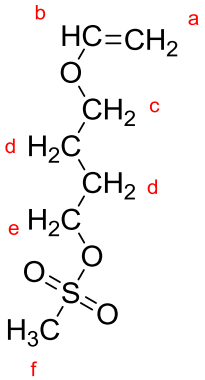

Mass yields : 80%

^{1}H NMR (400MHz, 297K, $CDCl_3$, ppm) : 6.37 to 6.35 (q, 1H, H_b), 4.17 to 4.14 (t, 2H, H_c), 4.09 to 4.05 (q, 1H, H_a), 3.9 to 3.87 (q, 1H, H_a), 3.63 to 3.60 (t, 2H, H_e), 2.91 (s, 3H, H_f), 1.8 to 1.64 (m, 4H, H_d)

5.5 Butyl vinyl ether tosylated

In a single-neck round bottom flask equipped with a magnetic stirrer, one equivalent of hydroxide butyl vinyl ether and 1 equivalent of tosyl chloride were introduced in THF. 1.1equivalent of triethylamine was also introduced in order to neutralize the formation of HCl. After 24h at 40°C, the produced salts were filtered. After several liquid/liquid extractions, the product was obtained in high masse yield (80%).

As an example, in a 250mL single-neck round bottom flask equipped with a magnetic stirrer, one equivalent hydroxide butyl vinyl ether (10g, 86.2 mmol), 1 equivalent of tosyl chloride were introduced (16.37g, 86.2mmol) and 1 equivalent of triethylamine (9.6g, 94.9mmol) were introduced in THF (100mL). After 24h at 40°C, the produced salts were filtered. Two liqudi/liquid (water/ethyl acetate) extractions have been realized and the product was obtained in high masse yield (80%).

Structure :

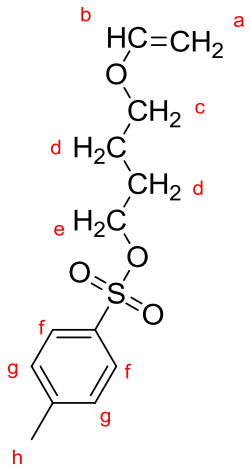

Mass yield : 75%

^{1}H NMR (400MHz, 297K, $CDCl_3$, ppm) : 7.73 to 7.68 (d, 2H, H_f), 7.31 to 7.26 (d, 2H, H_g), 6.35 to 6.29 (q, 1H, H_b), 4.07 to 4.02 (dd, 1H, H_a), 4.0.1to 3.96 (t, 2H, H_c), 3.89 to 3.86 (dd, 1H, H_a), 3.56 to 3.52 (t, 2H, H_e), 2.36 (s, 3H, H_h), 1.72 to 1.56 (m, 4H, H_d).

5.6 **Terpolymerisation**

As CTFE is a gas, the reactions were carried out in a Hastelloy (HC276) autoclave Parr system equipped with a manometer, a rupture disk (3000 psi), inlet and outlet valves, and a magnetic stirrer. Prior to reaction, the auto-clave was pressurized with 30 bar (i.e., 430 psi) of nitrogen to check for eventual leaks. The autoclave was then conditioned for the reaction with several nitrogen/vacuum cycles (10^{-2}mbar) to remove any traces of oxygen. The liquid phase was first introduced via a funnel, and then the gases were inserted by double weighing (i.e. the difference of weight before and after filling the autoclave with the gas). Then, the autoclave was placed in a mantle heated with a vigorous mechanical stirring. Both heating and stir-ring were monitored by a controller. After an initial in-crease of the internal pressure due to the increasing temperature, the pressure dropped by consumption of the gaseous monomer to produce a polymer in the liquid phase. After the reaction was complete, the autoclave was cooled to room temperature and then degassed. After distillation of the solvent, the terpolymers were precipitated from cold methanol. The product was dried under vacuum (10^{-2} mbar) at 70°C until constant weight.

As an example, 50 mL de solkane® as the solvent, TBPPI 0.8 g (4.6 mmol) as the initiator, K_2CO_3 0.36 g (2.57 mmol) (to prevent the cationic homopolymerization of EVE and BVEMs or BVETs), EVE 20 g (187.71 mmol), BVEMs () and CTFE 25 g (214.74 mmol) were introduced in the 300mL autoclave. The reaction was allowed to proceed at 75°C for 12h, showing a drop of pressure as CTFE was reacting. After purification, the copolymer, obtained as a pal yellow solid. It was then dried in a vacuum oven (10^{-2} mbar) at 50°C until constant weight. The mass yield was 75%.

5.6.1 *Poly[(CTFE-alt-EVE)-co-(CTFE-alt-BVEMs)]*

Structure :

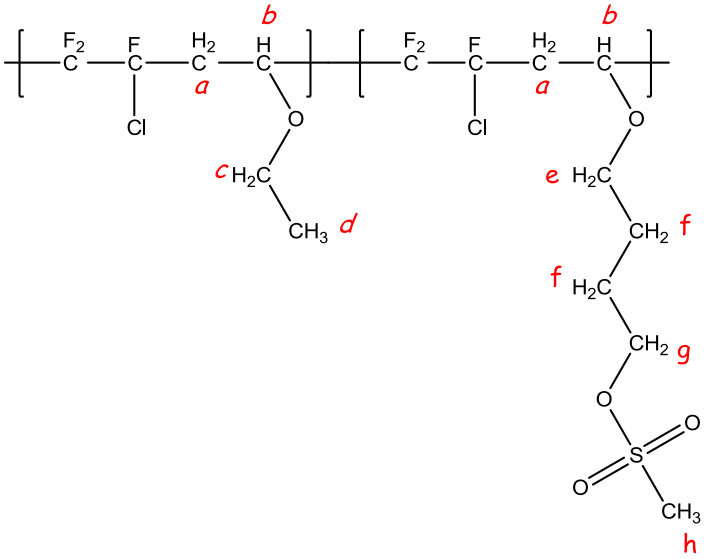

Mass yield: 70%

Glass transition temperature: 10°C

^{1}H NMR (400MHz, 297K, $CDCl_3$) δ : 4.70 to 4.32 (m, 1H, H_b), 4.29 to 4.20 (m, 2H, H_g), 3.89 to 3.67 (s, 4H, H_c and H_e), 3.22 to 2.37 (m, 2H, H_a), 2.99 (s, 3H, H_h) 1.92 to 1.63 (m, 4H, H_f), 1.28 to 1.12 (m, 3H, H_d).

^{19}F NMR {^{1}H} (400MHz, 297K, $CDCl_3$, ppm) δ : -108 at -123 (m, 3F)

5.6.2 ***Poly[(CTFE-alt-EVE)-co-(CTFE-alt-BVETs)]***

Structure :

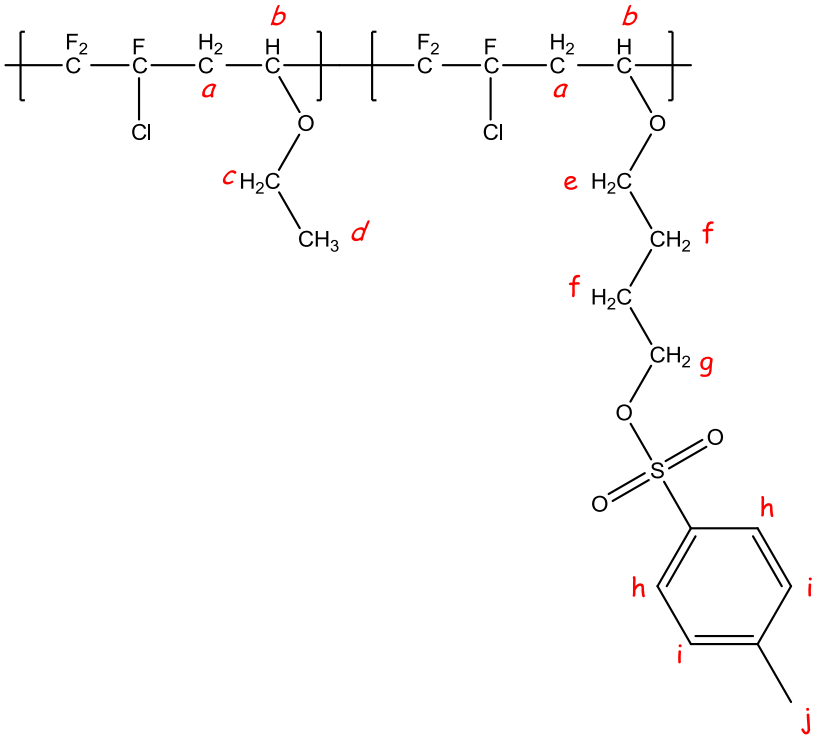

Mass yield: 68%

Glass transition temperature: 20°C

^{1}H NMR (400MHz, 297K, $CDCl_3$) δ : 7.81 to 7.75 (d, 2H, H_i), 7.38 to 7.31 (d, 2H, H_h), 4.70 to 4.32 (m, 1H, H_b), 4.29 to 4.20 (m, 2H, H_g), 3.89 to 3.67 (s, 4H, H_c and H_e), 3.22 to 2.37 (m, 2H, H_a), 2.45 (s, 3H, H_j) 1.92 to 1.63 (m, 4H, H_f), 1.28 to 1.12 (m, 3H, H_d).

^{19}F NMR {^{1}H} (400MHz, 297K, $CDCl_3$, ppm) δ : -108 at -123 (m, 3F)

6 References

1. Kim, S.; Chung, K. N.; Yang, S., Direct synthesis of ethers via zinc chloride-mediated etherification of alcohols in dichloroethane. *J. Org. Chem.* **1987,** *52* (Copyright (C) 2013 American Chemical Society (ACS). All Rights Reserved.), 3917-19.
2. Bethmont, V.; Fache, F.; Lemaire, M., An alternative catalytic method to the Williamson's synthesis of ethers. *Tetrahedron Lett.* **1995,** *36* (Copyright (C) 2013 American Chemical Society (ACS). All Rights Reserved.), 4235-6.
3. McGuigan, C.; Hinsinger, K.; Farleigh, L.; Pathirana, R. N.; Bugert, J. J., Novel Antiviral Activity of l-Dideoxy Bicyclic Nucleoside Analogues versus Vaccinia and Measles Viruses in Vitro. *Journal of Medicinal Chemistry* **2013,** *56* (3), 1311-1322.
4. Boutevin, B.; Cersosimo, F.; Youssef, B., Studies of the alternating copolymerization of vinyl ethers with chlorotrifluoroethylene. *Macromolecules* **1992,** *25* (11), 2842-2846.
5. Valade, D.; Boschet, F. d. r.; Améduri, B., Synthesis and Modification of Alternating Copolymers Based on Vinyl Ethers, Chlorotrifluoroethylene, and Hexafluoropropylene†. *Macromolecules* **2009,** *42* (20), 7689-7700.
6. Carnevale, D.; Wormald, P.; Ameduri, B.; Tayouo, R.; Ashbrook, S. E., Multinuclear Magnetic Resonance and DFT Studies of the Poly(chlorotrifluoroethylene-alt-ethyl vinyl ether) Copolymers. *Macromolecules* **2009,** *42* (15), 5652-5659.
7. Braun, D.; Hu, F., Polymers from non-homopolymerizable monomers by free radical processes. *Progress in Polymer Science* **2006,** *31* (3), 239-276.

CHAPTER IV

SYNTHESIS AND CHARACTERIZATIONS OF BLEND MEMBRANE OBTAINED FROM CROSSLINKABLE TERPOLYMER POLY(CHLOROTRIFLUOROETHYLENE-*ALT*-VINYL ETHERS) AND A COMMERCIAL FLUORINATED COPOLYMER

Butyl vinyl ether mesylé (BVEMs)

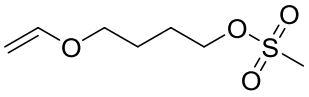

Di Ethyl Vinyl Ether Phosphonated (DEVEP)

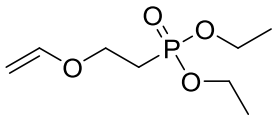

Vinyl Ether Phosphonic Acid (VEPA)

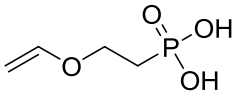

Chloro Tri Fluoro Ethylene (CTFE)

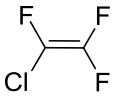

poly(CTFE-*alt*-VEPA)

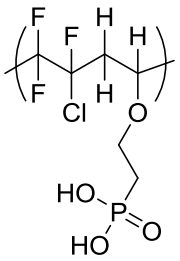

poly[(CTFE-*alt*-DEVEP)$_{1-x}$-*co*-(CTFE-*alt*-BVEMs)$_x$]

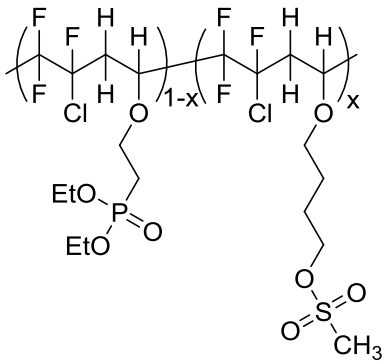

poly(VDF-co-CTFE)

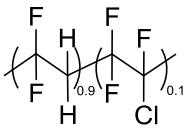

1 Introduction

The aim of the chapter II concerned the improvement of the mechanical properties of membrane obtained from the poly(CTFE-*alt*-VEPA). To do this, a commercial fluorinated copolymer, the poly(VDF-*co*-CTFE) which possesses excellent mechanical properties was added. Thus, from this technique a series of blend membranes have been realized. The obtained membranes show very good mechanical properties for a poly(VDF-*co*-CTFE) content higher than 20wt%. Nevertheless, during the acidification reaction of the phosphonate groups, membranes breakdown were observed. Indeed, the conditions of the acidification reaction are very hard: a hydrochloric acid solution concentered at 12N, a temperature at 90°C and during 3 days. Furthermore, the strong hydrophilic/hydrophobic balance between the two polymers resulted in only partial miscibility.

In order to use all the potential of these kinds of membranes, an improvement of two crucial points is required. In order to solve these problems, the most suitable method consists in crosslinking of the phosphonated copolymer. Indeed, one of the direct effects of the crosslinking reaction is the increase of the chemical stability, in particular in acid medium. In chapter III we have described a thermal crosslinking reaction from a terpolymer carrying sulfonated groups. This technique, based on the use of either tosylate or mesylate functional groups, allowed cross-linking the copolymer via inter-chain ether bonds. We showed that the incorporation of these functional groups requires the syntheses of vinyl ether monomers carrying these groups. Furthermore, the synthesis of vinyl ether containing mesylate group, i.e. BVEMs, was easier. Thus, in the following study, only BVEMs will be used as cross-linkable monomer since we showed that the cross-linking reaction proceeds similarly with the tosylate group. In chapter III we have performed the cross-linking reaction from model terpolymer, i.e. without any phosphonate group, to assess the cross-linking reaction. In this chapter, the cross-linking reaction with mesylate groups will be carried out in the presence of phosphonate groups. Thus, prior to cross-linking, the synthesis of terpolymer will be required, containing both mesylate and phosphonate units. The radical copolymerization will be performed through alternated copolymerization of CTFE with two vinyl ethers: BVEMs and diethyl vinyl ether phosphonate (DEVEP), which has also to be synthesized.

Densily grafted copolymer cross-linking generally undergoes loss of mechanical properties. This is the reason why the phosphonate terpolymer will be blended with poly(VDF-*co*-CTFE) and then cross-linked. Membranes will be casted after blending both copolymers and a thermal treatment of the membrane will allow cross-linking of the phosphonated terpolymer. A pseudo semi-interpenetrated network (semi-IPN) should be obtained by following this strategy. Finally, after cross-linking the membrane will be acidified in order to generate the phosphonic acid groups, required for proton conductivity.

This chapter will be divided in two parts; the first one will be focused on the syntheses of both DEVEP and to the terpolymer, which will be cross-linked in order to check the effect of phosphonated groups on the cross-linking reaction. The second part will be devoted to the formation and characterizations of pseudo semi-IPN membranes.

2 Synthesis of cross-linkable fluoro-phosphonate terpolymer

In chapter III, we illustrated the synthesis of poly(CTFE-*alt*-EVE)-*co*-(CTFE-*alt*-BVEMs) terpolymer that was able to cross-link from a simple thermal treatment through the mesylate functions. The next step is the synthesis of a terpolymer carrying both mesylate and phosphonate groups. In chapter II, we have performed the phosphonate functionalization of a fluorinated copolymer by the Arbusov reaction at 130°C. Nevertheless, in the presence of mesylate groups, a partial cross-linking reaction may occur at 130°C. Thus we have decided to first perform the synthesis of a new vinyl ether carrying phosphonate group (DEVEP), which then will be copolymerized with CTFE and BVEMs.

2.1 Synthesis of Di ethyl Vinyl Ether Phosphonate (DEVEP)

The synthesis of the vinyl ether monomer is realized by following the same synthetic pathway than that of the phosphonate functionalization of the fluorinated copolymer (see chapter II). The synthesis is thus performed in two steps: the first one corresponds to the nucleophile substitution of the chloride atom of 2-chloro ethyl vinyl ether (CEVE) by an iodide atom, i.e. Finkelstein reaction. In a second step, the Mickaelis-Arbusov reaction will be performed to incorporate the phosphonate group.

2.1.1 *Iodation of 2-chloro vinyl ether: Finkelstein reaction*

Finkelstein reaction is a SN_2 nucleophile reaction, characterized by a one-step exchange mechanism. Some works already performed the iodation of 2-chloro ethyl vinyl ether (CEVE)[1, 2] through the Finkelstein reaction, which proceeds in acetone during 3 days at 60°C in the presence of a large excess of sodium iodide (Figure 102).

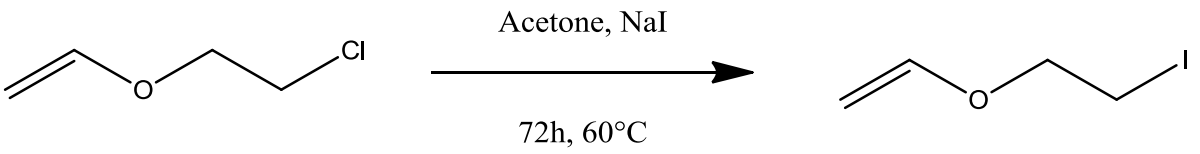

Figure 102 : Iodation of 2-chloro ethyl vinyl ether

After reaction, the excess of salt was eliminated by filtration, followed by acetone evaporation. The product was distilled under high vacuum (70°C/5.10^{-1}mbar) to extract residual CEVE. A colorless liquid was obtained with 50% mass yield. The monomer 2-Iodo-ethyl vinyl ether was characterized by ^{1}H NMR (Figure 103).

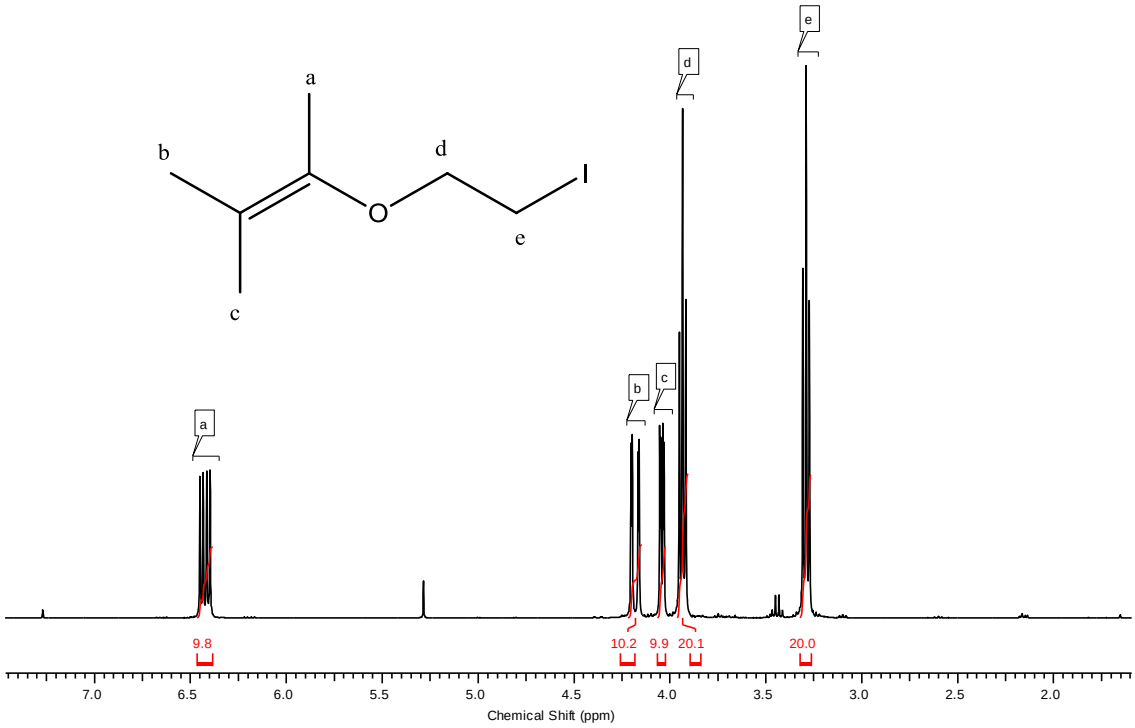

Figure 103 : ^{1}H NMR spectrum of 2-Iodo-ethyl vinyl ether (In $CDCl_3$)

From Figure 103, we note that the signal characteristic of -C**H_2**-I (e) was down-shifted, characterizing the modification of chloride atom to iodide atom.

2.1.2 ***Phosphonation of 2-iodo ethyl vinyl ether : Michaelis –Arbuzov reaction***

The direct phosphonation of 2-iodo ethyl vinyl ether was performed according to the nucleophilic substitution of the iodide atom by the phosphonate group. To carry out a quantitative reaction, triethyl phosphite was used as solvent (Figure 104).

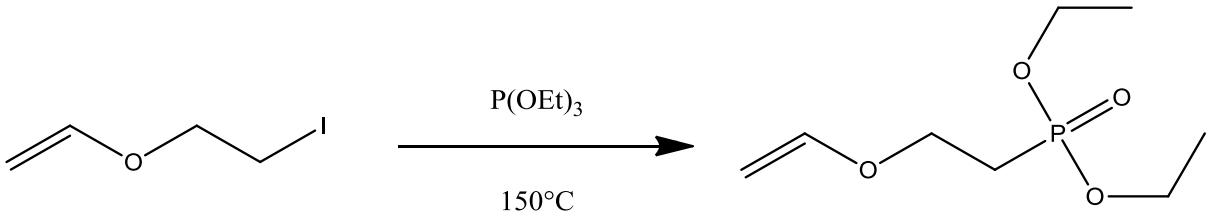

Figure 104 : Phosphonation of 2-iodo ethyl vinyl ether

After reaction, the excess of triethyl phosphite is suppressed from distillation under pressure (60°C/10^{-2}mbar), as well as the side products formed during the reaction (90°C/10^{-2}mbar). The purified DEVEP monomer is a yellow/orange liquid, obtained with a mass yield of 90% and characterized by means of both ^{1}H and ^{31}P NMR (Figure 105 and Figure 106).

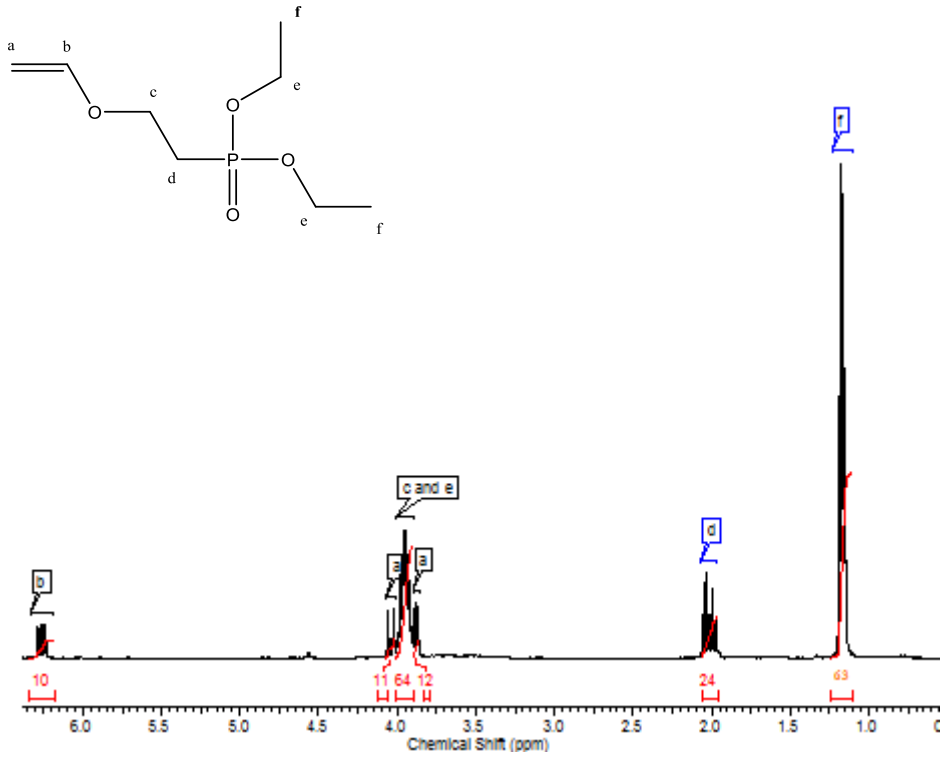

Figure 105 : ^{1}H NMR spectrum of DEVEP (in $CDCl_3$)

From Figure 105, we show the presence at 3.8 and 1.2 ppm the significant signal of P-O-C**H$_2$**-CH$_3$ (e) et P-O-CH$_2$-C**H$_3$** (f) groups. And, a deshielding of the signal significant the -C**H$_2$**-groups in alpha position of the oxygen can be observed.

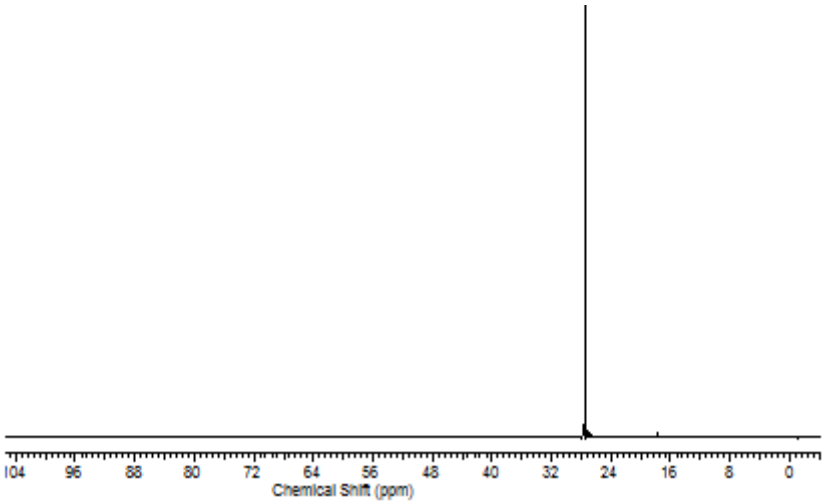

Figure 106 : ^{31}P NMR spectrum of DEVEP (in $CDCl_3$)

From Figure 106, only 1 peak is observed at 27ppm. This peak is significant of the phosphonated groups. The signal of other phosphonated product, as triethyl phosphite or other derivative product, are not observed.

2.2 Radical copolymerization of CTFE with vinyl ethers

The radical copolymerization of phosphonated monomers generally leads to low molecular weights polymers[3], which show poor thermal and chemical stability. The phosphonate polymer cross-linking should allow to perform polymers with better thermal and chemical stabilities. Prior to cross-linking, we have carried out the radical copolymerization of CTFE with two vinyl ethers: DEVEP and BVEMs (Figure 107). The reaction conditions are similar to those previously used for of poly[(CTFE-*alt*-EVE)-*co*-(CTFE-*alt*-BVEMs)], the synthesis of which being described in chapter III.

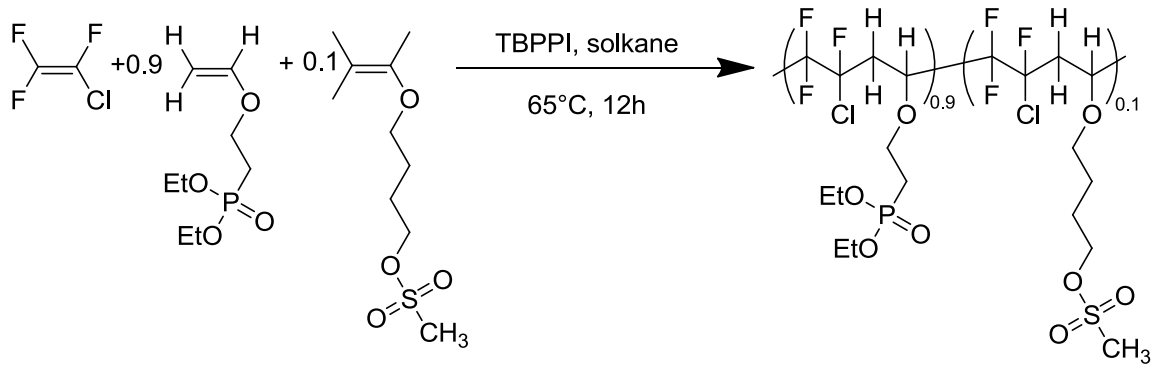

Figure 107 : Radical copolymerization of CTFE, diethyl vinyl ether phosphonate (DEVEP) and BVEMs

The radical copolymerization was initiated with *tert*-butyl peroxypivilate (TBPPI) (1mol %) in 1, 1, 1, 3, 3-pentafluorobutane (solkane) at 75°C, in the presence of potassium carbonate (3mol % of vinyl ether monomers) during 12h. The molar ratios of both DEVEP and BVEMs are 45% and 5%, respectively. These monomer contents will allow to incorporate sufficient amount of phosphonate units to gain high IEC. Furthermore, a 5mol % of BVEMs should be enough to both characterize the mesylate incorporation into the copolymer by means of NMR but also to efficiently cross-link the copolymer. The terpolymer was synthesized with 65% mass yield and characterized by steric exclusion chromatography as well as ^{1}H, ^{31}P and ^{19}F NMR analysis.

2.3 **NMR study of the terpolymer structure**

On the basis of fundamental study realized on the copolymer poly(CTFE-*alt*-EVE)[4-6]and the former works realized in our laboratory, the different resonance signal of methylene and methyl groups in ^{1}H NMR spectroscopy namely : -O-C**H**$_2$-CH_2-P(OEt)$_3$(c),-O-CH_2-C**H**$_2$-P(OEt)$_3$(d), -P-O-C**H**$_2$-CH_3(e) et -P-O-CH_2-C**H**$_3$(f) of DEVEP; -O-C**H**$_2$-CH_2-CH_2-CH_2-SO_3CH_3 (g), -O-CH_2-C**H**$_2$-CH_2-CH_2-SO_3CH_3(h), O-CH_2-CH_2-CH_2-C**H**$_2$-SO_3CH_3 (i)-O-CH_2-CH_2-CH_2-CH_2-SO_3-C**H**$_3$(j) of BVEMs; have been clearly identified and are respectively centered at 4.23, 2.12, 3.96, 1.3, 3.78, 1.69, 1.82, 4.08, 2.99 ppm (Figure 108). Moreover, the ^{1}H NMR spectroscopy (Figure 108) allows to determine the vinyl ether composition of poly[(CTFE-*alt*-

DEVEP)-*co*-(CTFE-*alt*-BVEMs)] (Equation 2). The total conversion of vinyl ethers monomers in the final polymer is confirmed by the slight shielding of the signals -C**H**-OR (a) and –C**H$_2$**- (b) of the vinyl ethers functions caused by the presence of the halogenated groups around.

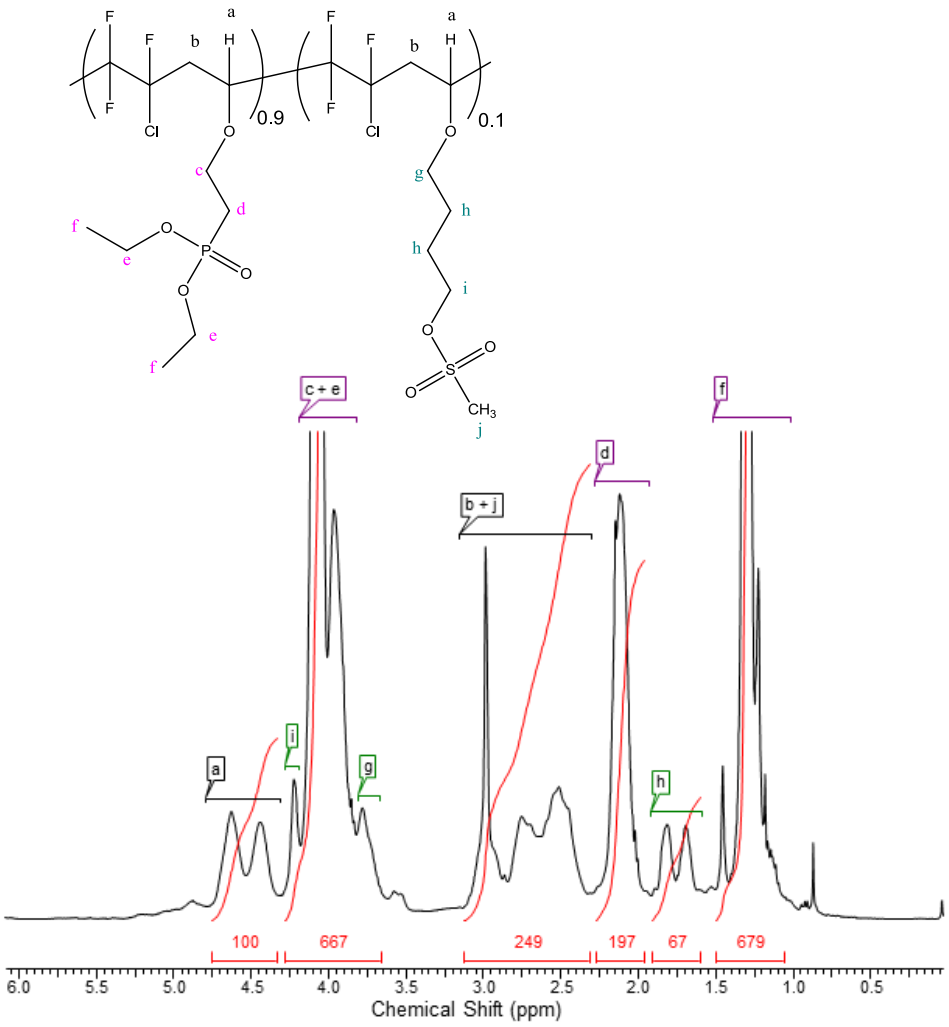

Figure 108 : ^{1}H NMR spectrum of poly[(CTFE-alt-DEVEP)-co-(CTFE-alt-BVEMs)] (realized in $CDCl_3$)

The DEVEP and BVEMs composition of terpolymer poly[(CTFE-*alt*-DEVEP)-*co*-(CTFE-*alt*-BVEMs)] (Figure 108), can be obtained by the signals integration of the -O-CH_2-**CH_2**-**CH_2**-CH_2-S- (h) groups of BVEMs showed between 1.60 and 1.90 ppm and that of –CH-OR group (a) showed between 4.35 and 4.75ppm of the main chain via the Equation 2.

$$\%BVEMs = \frac{\frac{\int_{1,60}^{1,90} h}{4}}{\int_{1,60}^{1,90} h + \int_{4,35}^{4,75} a}$$

Equation 2: Determination of the BVEMs incorporation in the terpolymer synthesis.

The incorporation rate of both DEVEP and BVEMs correspond to the proportions of monomers initially introduced. By achieving the comparison with other protons of BVEMs (g, i, and j), we also find a percentage of 7 mol %. So we have a good correlation between the percentage of BVEMs introduced into the reaction mixture and incorporated into the polymer, thanks to the opposite polarity of CTFE. The synthesis allows to keep the alternating nature of the copolymer.

The ^{31}P NMR spectrum of terpolymers is showed Figure 109. The presence of one signal centered at 27ppm characterizing diethyl phosphonate groups of the terpolymers can be observed. Indeed, concerning the DEVEP, the signal characterizing the diethyl phosphonate groups is centered at 30ppm.

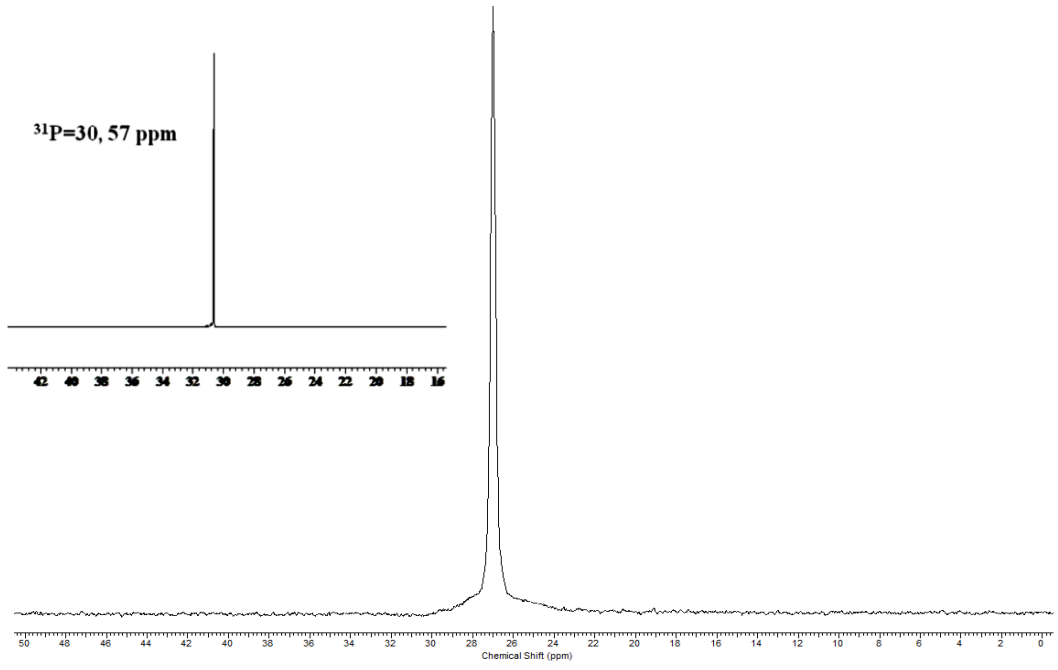

Figure 109 : ^{31}P NMR spectrum of terpolymer poly[(CTFE-alt-DEVEP)$_{0.9}$-co-(CTFE-alt-BVEMs)$_{0.1}$] (realized in $CDCl_3$). The inlet represents the 31P NMR of the DEVEP monomers.

The ^{19}F NMR (Figure 110) spectrum of terpolymer is similar with the results obtained in the literature [4-6]. Indeed, we can observe the presence of the four signals significant of the fluorine atom of the main polymer chain. Concerning the -C**F**$_2$- groups, the large signals range between -108 to -112, -115 to -119, and -120.7 to -123ppm and for the -C**F**Cl- the signal is centered at -120ppm.

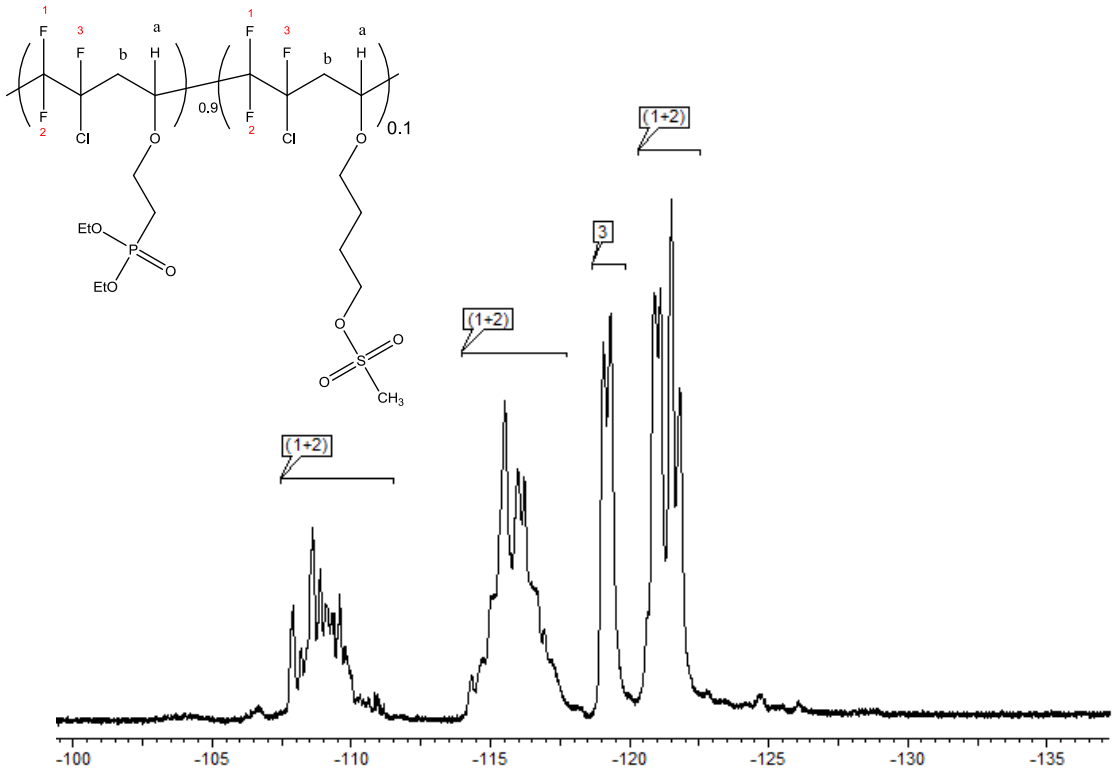

Figure 110 : ^{19}F NMR spectrum of terpolymer poly[(CTFE-*alt*-DEVEP)$_{0.9}$-*co*-(CTFE-*alt*-BVEMs)$_{0.1}$] (realized in $CDCl_3$)

2.4 Steric exclusion chromatography (SEC) of the terpolymer

The molecular weight of the terpolymer was determined by SEC, with polystyrene standarts (Mn ranging from 580 to 840000 g.mol^{-1}) and compared to that of poly(CTFE-*alt*-VEPA) (cf Table 12and Figure 111).

Table 12 : Molecular weight values of both the terpolymer and poly(CTFE-alt-VEPA)

Polymères	M_n (g.mol^{-1})	M_w (g.mol^{-1})	Ip
poly[(CTFE-*alt*-DEVEP)$_{0.9}$-*co*-(CTFE-*alt*-BVEMs)$_{0.1}$]	7300	19000	2.6
Poly(CTFE-*alt*-VEPA)	25000	70000	2.8

The molecular weight value of poly(CTFE-*alt*-VEPA) was limited due to the transfer reaction occurring from the vinyl ether during the radical copolymerization of CTFE with CEVE. Furthermore, the transfer reactions were enhanced by the exothermic character of the copolymerization (see chapter II). On the case of poly[(CTFE-*alt*-DEVEP)$_{0.9}$-*co*-(CTFE-*alt*-BVEMs)$_{0.1}$], the molecular weight is even lower, about 7300 g/mol. This seems to show that the transfer reactions occurring during the radical copolymerization are increased by the presence of the phosphonate vinyl ether monomer. Nevertheless, blending poly[(CTFE-*alt*-DEVEP)$_{0.9}$-*co*-(CTFE-*alt*-BVEMs)$_{0.1}$] with poly(VDF-*co*-CTFE) followed by its cross-linking reaction should allow us to obtain a membrane with the specific properties for fuel cell applications.

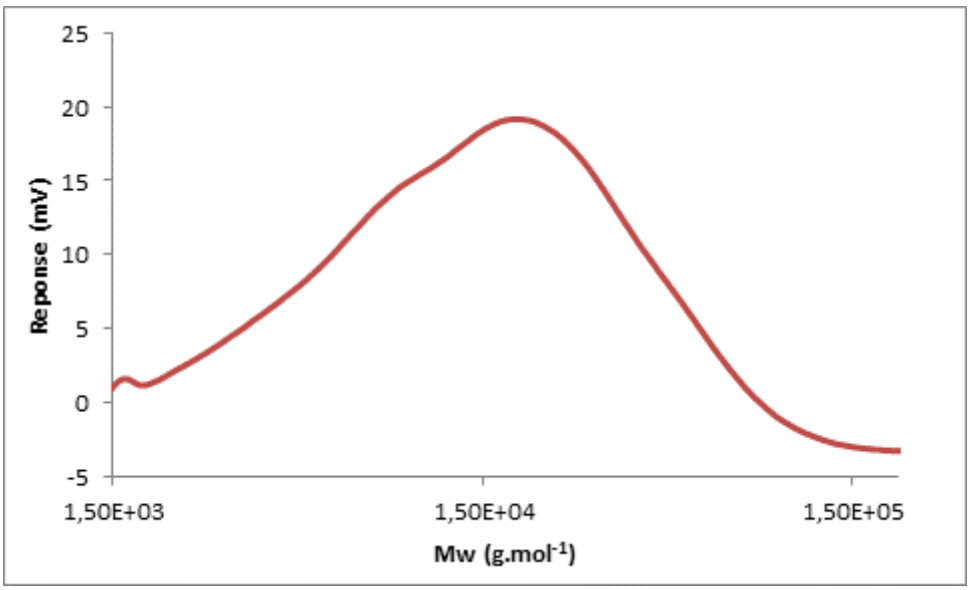

Figure 111 : SEC trace of terpolymer poly[(CTFE-alt-DEVEP)$_{0.9}$-co-(CTFE-alt-BVEMs)$_{0.1}$]

2.5 **Thermal analysis of the terpolymer**

The thermal behavior of the terpolymer poly[(CTFE-*alt*-DEVEP)$_{0.9}$-*co*-(CTFE-*alt*-BVEMs)$_{0.1}$] was evaluated by thermo-gravimetric analysis (TGA) in Figure 112.

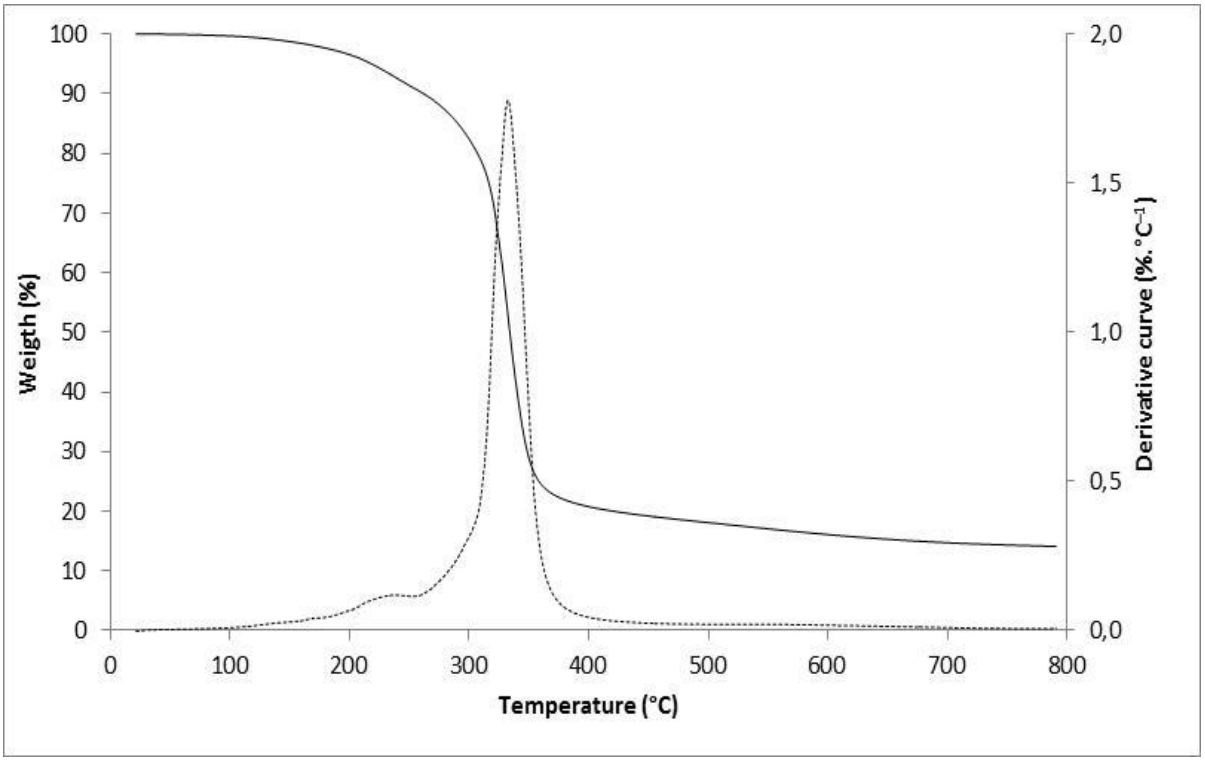

Figure 112 : Thermogram of poly[(CTFE-alt-DEVEP)$_{0.9}$-co-(CTFE-alt-BVEMs)$_{0.1}$] by using dynamic mode under nitrogen at 20°C.min^{-1}

From Figure 112, some solvent traces (about 3%) are observed at low temperature. Then, two main degradations are showed. The first one occurs from 200 to 260°C and can be attributed to mesylate group's degradation. Indeed, in comparison, on the thermogram of poly(CTFE-*alt*-DEVEP) the loss weight from 200 to 260°C was not observed. This degradation corresponds to approximately 5% of weight loss, as the content of BVEMs into the copolymer. The second one occurs from 270 to 400°C and is related to the degradation of the main chain as well as to the phosphonate functions. In chapter II, we showed that poly(CTFE-*alt*-VEPA) having phosphonate groups only showed one degradation from 250 to 400°C.

Tables 13 gathers the decomposition temperatures corresponding to 5 and 10% weight loss, and are equal to 218 and 261 °C, respectively.

Table 13 : Degradation temperatures at 5 and 10% weight loss of the terpolymer obtained from TGA in dynamic mode at 20°C.min^{-1} and glass transition temperature obtained from DSC at 20°C.min^{-1}.

Polymère	$Td_{5\%}$ (°C)	$Td_{10\%}$ (°C)	Tg (°C)
poly[(CTFE-*alt*-DEVEP)$_{0.9}$-*co*-(CTFE-*alt*-BVEMs)$_{0.1}$]	218	261	-8

For comparison, the Tg of poly [(CTFE-*alt*-EVE)$_{0.9}$-*co*-(CTFE-*alt*-BVEMs)$_{0.1}$] is 10°C, so the incorporation of phosphonated monomer instead of EVE during the synthesis of the terpolymer leads to a decrease in Tg. This decrease of the Tg is due to the volume of the phosphonates group which results in a spacing the polymer chains. This volume effect is also reflected in the incorporation of the mesylate group. In fact, the Tg of poly (CTFE-alt-EVE) is 18°C.

2.6 Synthesis and characterization of the membrane

2.6.1 *Cross-linking and acidification of the copolymer*

As previously mentioned, the synthetic strategy to obtain the membrane is as follows:

-Synthesis of the copolymer

-Casting of the copolymer blended with poly(VDF-*co*-CTFE)

-Thermal cross-linking and acidification

In chapter III, we showed that the cross-linking reaction of both tosyle and mesyle groups efficiently occurred at 150°C. It is now necessary to perform the cross-linking reaction in the presence of the phosphonate group. Thus we have decided to first carry out

the cross-linking reaction followed by the acidification of the terpolymer without blending with poly(VDF-*co*-CTFE). The synthetic strategy is showed in Figure 113.

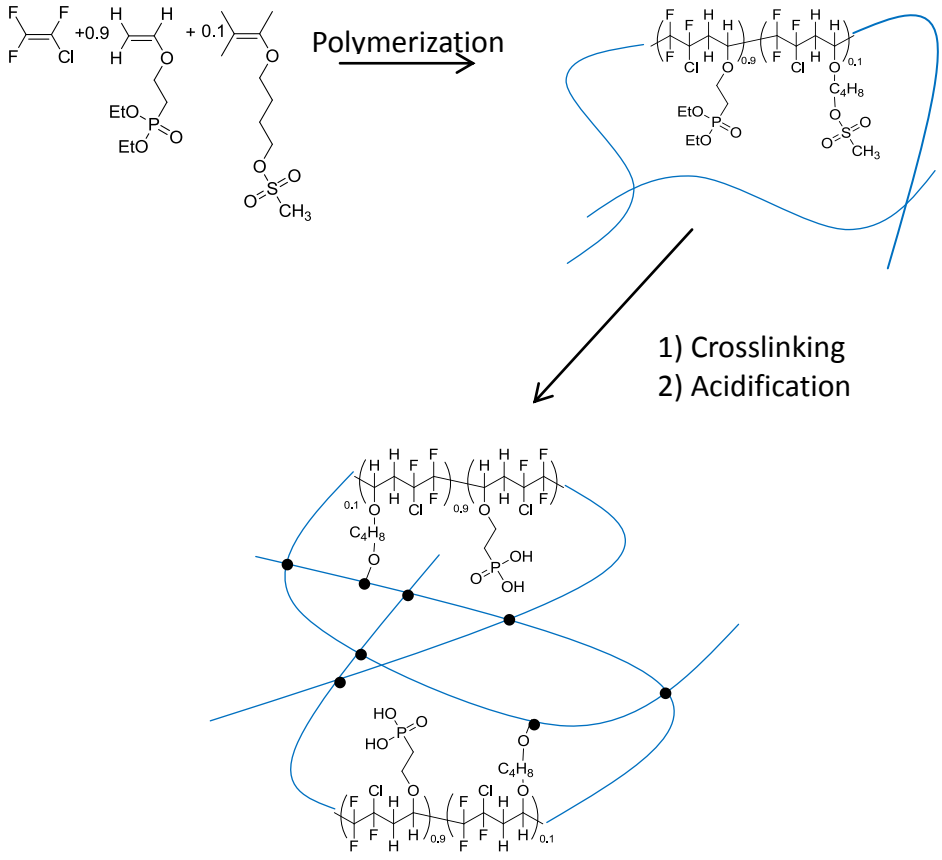

Figure 113 : Synthetic strategy to obtain a membrane from du poly[(CTFE-alt-DEVEP)-co-(CTFE-alt-BVEMs)]

A precise amount of poly[(CTFE-*alt*-DEVEP)$_{0.9}$-*co*-(CTFE-*alt*-BVEMs)$_{0.1}$] is solubilized in DMF to obtain a concentration ranging from 30 to 50 wt%. The membrane is then casted in an oven at 120°C during one night in order to evaporate the solvent and the temperature is then increased to 150°C to perform the cross-linking reaction. Once the membrane was cross-linked acidification is carried out in HCl solution 12N at 90°C during 3 days. We noticed that no coloration of the acidic solution was observed, which shows that the cross-linking affords a better stability of the resulting membrane towards acidic medium.

2.6.2 *Thermal analyses*

The thermal analyses were done on the membrane obtained from poly[(CTFE-*alt*-DEVEP)$_{0.9}$-*co*-(CTFE-*alt*-BVEMs)$_{0.1}$] after cross-linking and acidification. The results were compared to that obtained before cross-linking and acidification. They are given in

Figure 114 and Table 14. We first remark that from the thermogram of the membrane obtained after cross-linking and acidification the weight loss attributed to mesylate groups (Figure 114) is not observed anymore. Furthermore, the cross-linking reaction enables to obtain a high content of residue up to 600°C. At 700°C, the content of residue for the membrane, i.e. after cross-linking and acidification, is also about 26%, whereas the content of residue for the copolymer was less than 16%. The membrane shows a very good thermal behavior, with a 5% weight loss temperature of about 262°C. The membrane was then analyzed by DSC and a glass transition temperature of 110°C was obtained. This value allows to confirm the efficiency of the acidification process, since the T_g value of the poly[(CTFE-*alt*-DEVEP)$_{0.9}$-*co*-(CTFE-*alt*-BVEMs)$_{0.1}$] was about -8°C. Moreover, the T_g value of the membrane is higher than that of poly(CTFE-*alt*-VEPA), i.e. about 75°C, this difference can be attributed to the network formation from cross-linking reaction.

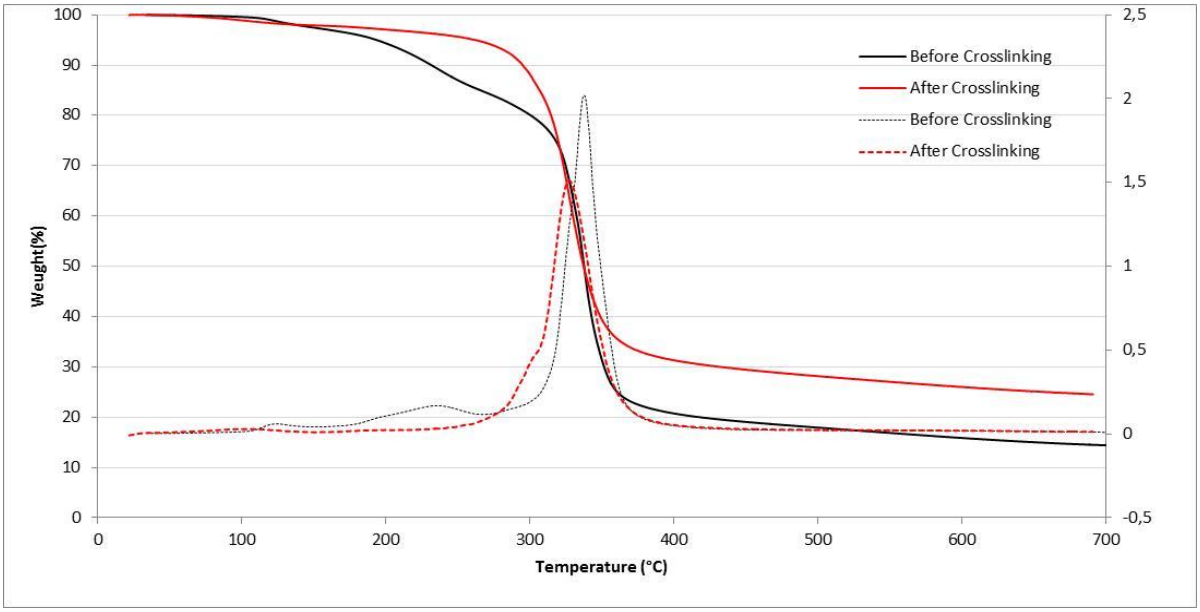

Figure 114 : thermograms of the terpolymer poly[(CTFE-alt-DEVEP)$_{0.9}$-co-(CTFE-alt-BVEMs)$_{0.1}$]and of the membrane (after cross-linking and acidification of the terpolymer) recorded under nitrogen at 20°C.min^{-1}

Table 14 : Degradation temperatures at 5 and 10% weight loss of the terpolymer and of the membrane obtained from TGA in dynamic mode at 20°C.min^{-1} and glass transition temperature obtained from DSC at 15°C.min^{-1}.

	$Td_{5\%}$ (°C)	**$Td_{10\%}$ (°C)**	**Tg (°C)**
poly[(CTFE-*alt*-DEVEP)$_{0.9}$-*co*-(CTFE-*alt*-BVEMs)$_{0.1}$]	218	261	-8
membrane	262	294	110

2.6.3 ***Mechanical properties:***

After cross-linking reaction and acidification of the copolymer, the resulting membrane show very poor mechanical properties. Indeed, in the dry state the membrane cannot be manipulated and can easily be broken. As a reminder, the membrane obtained

from poly(CTFE-*alt*-VEPA) also showed low mechanical properties, attributed to the low molecular weight value of the copolymer. The cross-linking reaction does not allow to increase the mechanical properties since it undergoes creation of inter-chain bridges and thus network formation. As mentioned in chapter I, the network formation generally leads to a loss of the mechanical properties of the membrane, even if the swelling rate is better controlled by the network formation. Then, in the following part of this chapter the membranes will be obtained by blending the terpolymer with poly(VDF-*co*-CTFE), followed by cross-linking and acidification. Pseudo semi-IPN membranes should then be obtained.

2.7 **Conclusion**

The synthesis of terpolymer poly[(CTFE-*alt*-DEVEP)$_{0.9}$-*co*-(CTFE-*alt*-BVEMs)$_{0.1}$] was performed by radical copolymerization of CTFE with both DEVEP and BVEMs. DEVEP was first synthesized in order to avoid post-functionalization of the copolymer, carried out at high temperature where partial cross-linking may occur. One of the main objectives of MemFOS project was the synthesis of a cross-linkable fluoro-phosphonate copolymer in order to control the swelling rate of poly(CTFE-*alt*-VEPA), which led to membrane destructuration. We demonstrated in the first part of this chapter as well as in chapter III that cross-linking reaction was efficient at high temperature by using mesylate groups even in the presence of phosphonate groups. Thus this cross-linking technique and the results associated were patented by the CEA and CNRS.

The cross-linking reaction of poly[(CTFE-*alt*-DEVEP)$_{0.9}$-*co*-(CTFE-*alt*-BVEMs)$_{0.1}$] allowed to overcome to main issues:

-During the acidification step no damage of the cross-linked membrane was observed, whereas in chapter II we showed that acidification of the composite membranes led to degradation.

-We also showed in chapter II that in aqueous solution exfoliation phenomenon of the membrane was observed, thus leading to a decrease of the membrane properties. In the

case of cross-linked membranes, no exfoliation phenomenon was observed. Furthermore, the cross-linked polymer remains insoluble in most of common solvents.

Nevertheless, the membrane obtained from poly[(CTFE-*alt*-DEVEP)$_{0.9}$-*co*-(CTFE-*alt*-BVEMs)$_{0.1}$] show very poor mechanical properties. Thus, the next part of the chapter concerns the synthesis of pseudo semi-IPN membranes obtained by blending poly[(CTFE-*alt*-DEVEP)$_{0.9}$-*co*-(CTFE-*alt*-BVEMs)$_{0.1}$] with poly(VDF-*co*-CTFE) followed by cross-linking and acidification of the resulting membranes.

3 Syntheses and Properties of pseudo « semi-IPN » membranes obtained from poly[(CTFE-*alt*-DEVEP)-*co*-(CTFE-*alt*-BVEMs)]

According to IUPAC, interpenetrating networks (IPN) of polymers are defined as " polymeric materials containing networks, or more exactly partially interlaced polymers at a molecular scale, without any covalent bonds between them and can only be separated by breakdown of chemical bonds from both networks. A mixture of two pre-formed polymeric networks is not considered as IPN" [7]. A semi-IPN is also defined, according to IUPAC, as "A polymer comprising one or more networks and one or more linear or branched polymer(s) characterized by the penetration on a molecular scale of at least one of the networks by at least some of the linear or branched macromolecules". Semi-IPNs are different than IPN in the way that linear or branched polymers can be separated from the polymeric network without breaking any covalent bonds [7]. Both IPN and semi-IPN materials, the miscibility between the polymers is generally forced, but the polymers miscible during long-term, whereas in the case of blend polymers separation occurs with time. The development of IPNs and semi-IPNs has started in the sixties for wide range of applications such as biomedical applications [8-10], adhesives [11-13], or as solid electrolytes[14-16]. In recent years, they have been also used for the development of fuel cell membranes, and especially semi-IPNs have been used to perform PEMFC or DMFC. Chikh and co[17] have recently

reviewed these works. For instance, semi-IPNs have been used to enhance the performances of the Nafion®membrane[18-21], such as permeability towards methanol.

In the case of PEMFC, the synthesis of semi-IPN should allow to solve problems such as:

-the elution of the polymer during the fuel cell operation should be avoided

-the swelling rate of the membrane should be more easily controlled

It is to be noted that, to our knowledge, no study has so far described the synthesis of semi-IPN membranes from polymers containing phosphonic acid groups.

First of all, the synthetic strategy employed in this work does not exactly affords semi-IPN, according to the IUPAC definition. Indeed, interlacement of polymers has to be done by polymerization of a monomer into a cross-linked polymer. In our case, interlacement is performed from two linear polymers, then cross-linking of one polymer occurs, ending to a linear polymer, i.e. poly(VDF-*co*-CTFE), interlaced into a cross-linked polymer, i.e. poly[(CTFE-*alt*-DEVEP)-*co*-(CTFE-*alt*-BVEMs)]. Since it does not exactly correspond to the IUPAC definition of semi-IPN, we have decided to name our membranes pseudo semi-IPN.

3.1 Syntheses and acidification of membranes

In order to study the effect of the cross-link density onto physico-chemical properties of the membranes, we have synthesized fluorophosphonate terpolymer with a BVEMs content of 5, 10 and 20 mol%. The molar content of BVEMs, DEVEP and CTFE is ascribed in Table 15 for each terpolymer. The synthesis of the three terpolymers is similar to that of poly[(CTFE-*alt*-DEVEP)$_{0.9}$-*co*-(CTFE-*alt*-BVEMs)$_{0.1}$] described in section 2.2.

Table 15 : terpolymers composition

Terpolymers	Initial molar ratio of monomers (%)			Molar ratio of monomers into the terpolymer (%)[a]		
	CTFE	DEVEP	BVEMs	CTFE	DEVEP	BVEMs
Poly[(CTFE-*alt*-DEVEP)$_{0.95}$-*co*-(CTFE-*alt*-BVEMs)$_{0.05}$]	50	45	5	50	43	7
Poly[(CTFE-*alt*-DEVEP)$_{0.90}$-*co*-(CTFE-*alt*-BVEMs)$_{0.10}$]	50	40	10	50	39	11
Poly[(CTFE-*alt*-DEVEP)$_{0.80}$-*co*-(CTFE-*alt*-BVEMs)$_{0.20}$]	50	30	20	50	31	19

a : calculated by ^{1}H NMR

The synthetic strategy to prepare the pseudo semi-IPN membranes is illustrated in Figure 115.

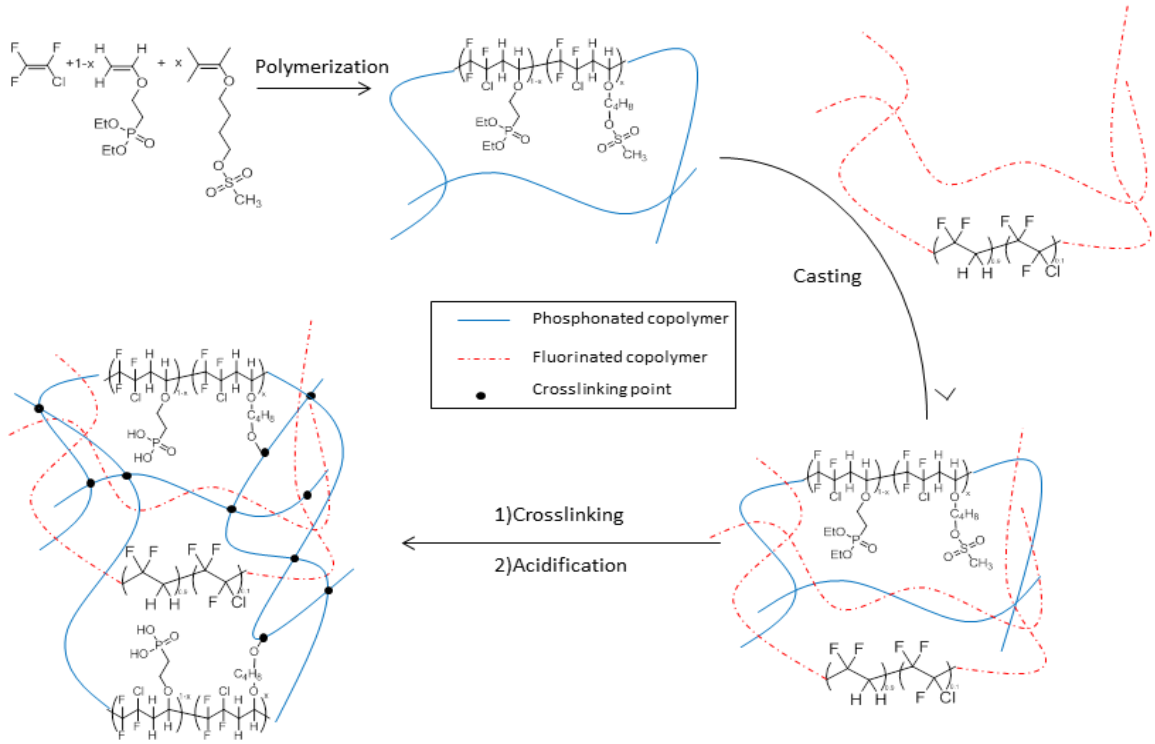

Figure 115 : Schematic representation of procedure to obtain pseudo semi-IPN membrane comprising crosslinked poly[(CTFE-alt-DEVEP)-co-(CTFE-alt-BVEMs)] and poly(VDF-co-CTFE).

The membranes were prepared from film casting of a polymeric solution. First, the fluorophosphonate terpolymer was solubilized in DMSO at 45°C during 4h, then poly(VDF-co-CTFE) was added to the solution, which was heated at 45°C under mechanical stirring during 16h. The polymeric solution was degased from two successive ultra-sonic treatments in order to avoid air bubbles into the solution. The polymer concentration is ranging from 20 to 50 wt% to obtain a solution allowing good casting (according to its viscosity). The solution was casted with a hand-coater on a glass plate and put in an oven at 80°C during 24h to afford solvent evaporation. Then, the temperature was increased to 150°C in order to perform the cross-linking reaction. The membranes were removed from the glass plate in distilled water and showed a thickness comprised between 30 to 60 µm. Cleavage of the ester groups from the phosphonate was then performed in 12N HCl solution at 90°C during 3 days. Once again, no coloration was observed during the acidification process, which proves that cross-linking allows the polymer stabilization. Once the acidification step was accomplished, the membranes were rinsed in distilled water several times until pH remains neutral. From the three synthesized terpolymers, a range of membranes was synthesized by varying the content of poly(VDF-co-CTFE). The membranes have been noted M_x-Y, where x is the molar content of BVEMs into the copolymer and Y is the mass content of poly[(CTFE-*alt*-DEVEP)-*co*-(CTFE-*alt*-BVEMs)]. For instance M_5-80 was obtained from 80w% of poly[(CTFE-*alt*-DEVEP)-*co*-(CTFE-*alt*-BVEMs)], which contains 5 mol% of BVEMs. The different membranes synthesized for this study are gathered in Table 16.

Table 16 : Composition of the different pseudo semi-IPN membranes

Membranes	Rate of BVEMs (mol %)	Rate of fluorophosphonate terpolymer (wt%)	Rate of Poly(VDF-co-CTFE) (wt%)	% mol of phosphonic acid
M_5-80	5	80	20	38
M_5-60	5	60	40	28.5
M_5-50	5	50	50	23.75
M_5-30	5	30	70	14.25
M_{10}-80	10	80	20	36
M_{10}-60	10	60	40	27
M_{10}-50	10	50	50	22.5
M_{10}-30	10	30	70	13.5
M_{20}-80	20	80	20	32
M_{20}-60	20	60	40	24
M_{20}-50	20	50	50	20
M_{20}-30	20	30	70	12

The minimum rate of fluorophosphonate terpolymer was 30 wt% in order to get sufficient values of IECs into the pseudo semi-IPN membranes. Moreover, the minimum rate of poly(VDF-co-CTFE) was assessed to 20 wt% to afford sufficient mechanical properties for fuel cell applications.

3.2 Thermal properties of the membranes

The thermal properties of the different membranes were assessed before and after acidification, especially to control if the glass transition temperature was raised after acidification of the membranes. The T_5, T_{10} and Tg values for all membranes are gathered in Table 17. First of all, the thermal stability for membranes obtained before and after acidification reaction was analyzed by means of TGA. Figure 116 shows the thermal stability for the membranes having 5% of cross-linking agent BVEMs. We can see that for each M_5

membrane the thermal stability is increased after acidification, since the O-Et groups of the phosphonate are replaced by OH groups. Furthermore, the higher the poly(VDF-co-CTFE) content into the membrane, the better the thermal stability, i.e. from M_5-30 to M_5-60 the thermal stability decreases.

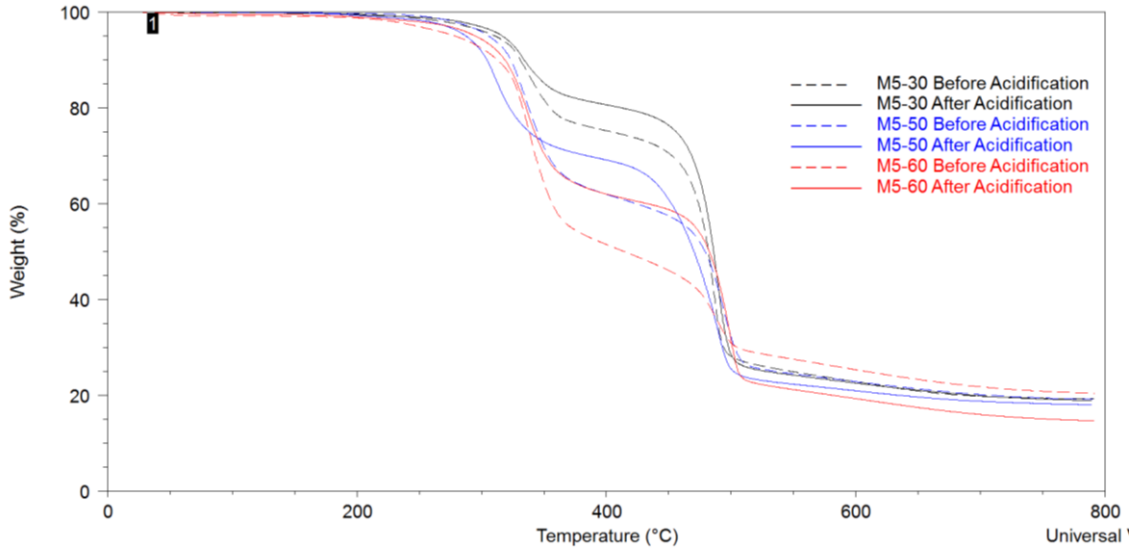

Figure 116 : Thermogram obtained from TGA in dynamic mode at 20°C.min^{-1} before and after acidification for M_5 membranes (i.e. having 5mol% of BVEMs)

The thermal behavior of the membranes is correlated to both the content of cross-linking agent BVEMs and to the content of fluorophosphonate terpolymer. Figure 117 gives the thermal stability of the membranes obtained from the phosphonate terpolymers having 20 mol% of BVEMs. In chapter II we showed that the blend membranes, without cross-linking agent, were characterized by two main degradations:

-the first one occurred from 200 to 400 °C, corresponding to pendant groups of the phosphonate polymer

-the second one occurring from 400 to 800 °C is the degradation of both poly(VDF-co-CTFE) and of poly(CTFE-*alt*-VEPA) main chain.

In Figure 117 we show the evolution of the weight loss with the membrane composition. Indeed, as already mentioned, the higher the flurophosphonate terpolymer

content, the higher the first thermal degradation, i.e. from 200 to 400 °C. We note also that both 5 and 10% weight loss temperatures are higher than 190 and 300 °C, respectively.

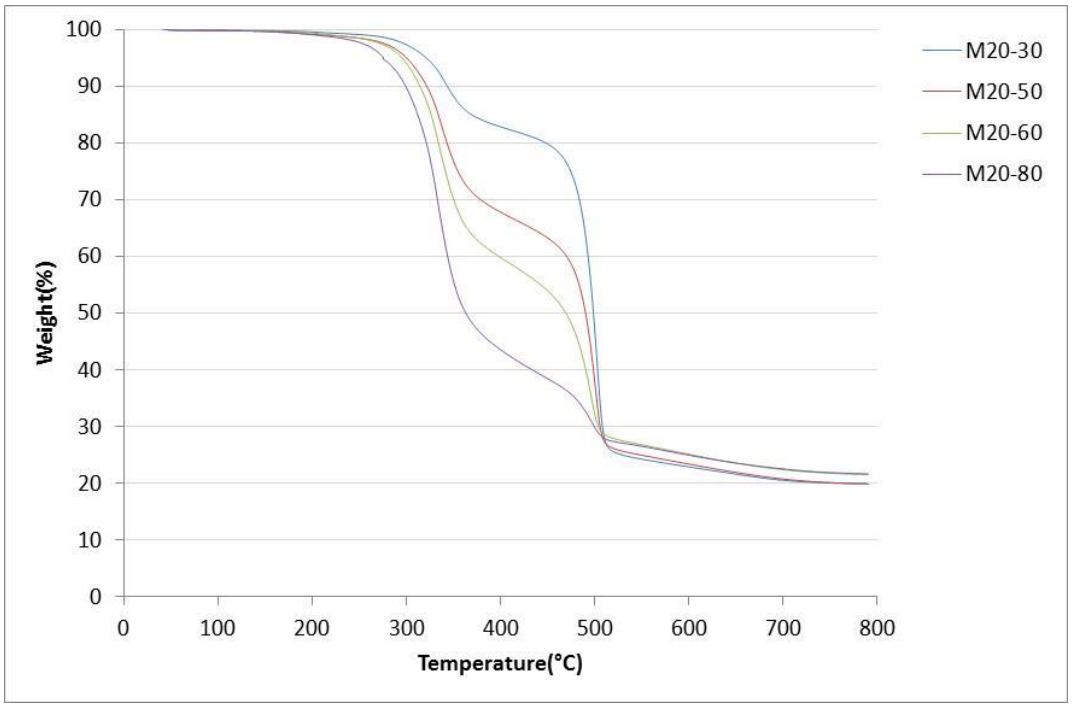

Figure 117 : Thermograms obtained from TGA in dynamic mode at 20°C.min^{-1} of membranes M_{20}-30, M_{20}-50, M_{20}-60 and M_{20}-80.

Figure 17 gathers the thermal stability for membranes containing the same amount of fluorophosphonate terpolymer, i.e. 50 w%, but with different contents of cross-linking agent BVEMs. The thermal stability slightly increases with the cross-linking density, but an increase from 5 to 20mol% of BVEMs affords only a gain of about 10°C for the thermal stability.

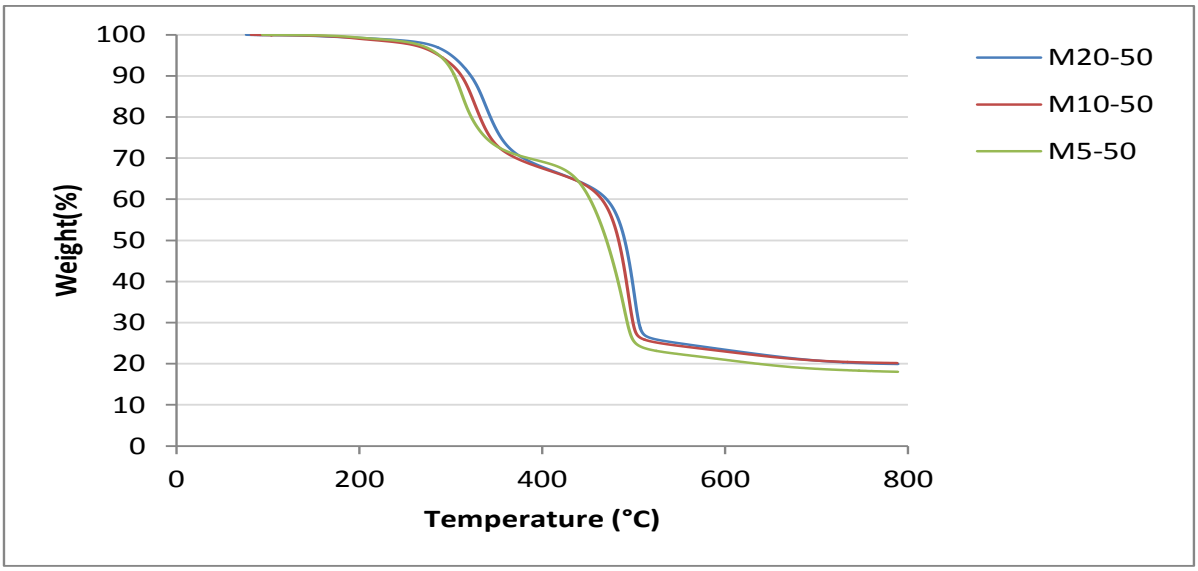

Figure 118 : Thermograms obtained from TGA in dynamic mode at 20°C.min^{-1} of membranes M_5-50, M_{10}-50 and M_{20}-50.

Table 17 : Degradation temperatures at 5 and 10% weight loss of the membranes obtained from TGA in dynamic mode at 20°C.min^{-1} and glass transition temperature obtained from DSC at 15°C.min^{-1}.

Membranes	$Td_{5\%}$(°C)		$Td_{10\%}$(°C)		Tg(°C)	
	Before acidification	After acidification	Before acidification	After acidification	Before acidification	After acidification
M_5-80	292	285	316	310	11	92
M_5-60	293	295	318	318	10.5	95.5
M_5-50	305	287	323	304	12	108
M_5-30	310	316	331	333	-5	85.8
M_{10}-80	280	283	306	308	31	92.5
M_{10}-60	302	286	320	311	54	98
M_{10}-50	304	288	324	313	55	105
M_{10}-30	307	310	331	330	1	101.4
M_{20}-80	300	284	312	305	54	92
M_{20}-60	310	295	327	314	90	98
M_{20}-50	313	300	325	322	80	115
M_{20}-30	322	311	339	334	76	90.8

The glass transition temperature was determined by DSC with ±2°C

The glass transition temperatures were determined for each membrane before and after acidification. The T_g values clearly increase for all membranes after acidification reaction, which proves that the phosphonic acid groups undergo hydrogen bonding between them. Thus more energy is then required to go from the rubbe to the glassy state. In Figure 119 we have plotted the evolution of the T_g values vs the content of fluorophosphonate terpolymer for the membranes M_5, M_{10} and M_{20} after acidification.

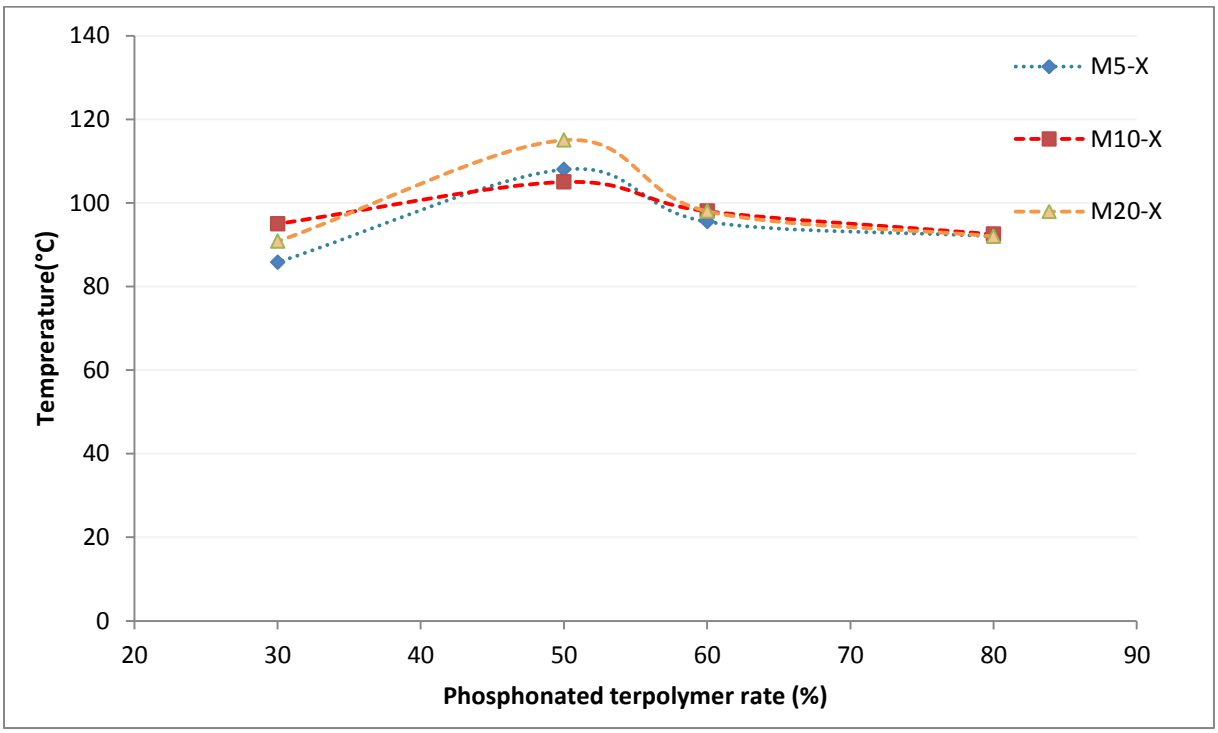

Figure 119 : Evolution of Tg vs the content of flurophosphonate terpolymer for the membranes M_5, M_{10} and M_{20} after acidification

For membranes M_5, M_{10} and M_{20} T_g values increase with a decrease of fluorophosphonate terpolymer content until reaching a maximum for 50% of terpolymer, below this content the T_g values slightly decrease. The increase of poly(VDF-co-CTFE) content in the membranes probably allows the phosphonic acid groups been closer to each other and then an increase of hydrogen bonding (see chapter II). But when the content of fluorophosphonate terpolymer becomes too low, i.e. 30 wt%, this effect is no more predominant and thus the T_g values decrease. Finally, from Table 17 we can note that the content of cross-linking agent does not really impact the T_g values of the membranes.

3.3 Evaluation of the water uptake and swelling of the membranes

Water uptake of the membranes is a key parameter for the electro-chemical performances of the PEMFC as well as for the mechanical properties. Indeed, water is essential for the proton transport through a vehicular mechanism. Even if membranes made from fluorophosphonate polymers aim to be used at high temperature (from 90 to 130°C) and at low relative humidity (< 50%), these membranes have to show sufficient water uptake to undergo proton transport at low temperature and high RH as well. Nevertheless, too high water uptake will therefore lead to a sharp decrease of the mechanical properties of the membrane during the fuel cell operation. We have determined the water uptake for all the membranes at room temperature and at 100% RH from the mass difference between the dry and the hydrated states (Equation 2), as described in chapter II. The results are gathered in Figure 120.

$$wu(\%) = \frac{m_h - m_d}{m_d} \times 100$$

With m_d been the mass of the membrane at the dry state and m_h the mass of the membrane at the hydrated state.

Equation 3 : Water uptake calculation

The experimental water uptakes (WU) were compared to the theoretical ones, calculated from the WU of poly(CTFE-*alt*-VEPA) been about 65% at 100% RH and room temperature. Figure 120 represents the evolution of experimental and theoretical WUs for the M_5, M_{10} and M_{20} membranes *vs* the content of fluorophosphonate terpolymer. Concerning first the M_5 membranes, both experimental and theoretical WU values are very close, which means that all the phosphonic acid groups can be easily accessible in the membrane. But, when the membranes are more densely cross-linked, i.e. M_{10} and M_{20} membranes, the accessibility to the phosphonic acid groups remains limited; this is the reason why we note a discrepancy between the experimental and theoretical WU values for M_{10} and M_{20} membranes. We can remark that both M_{10}-80 and M_{10}-60 show Wu of about

20%, which should be enough for reaching good proton conductivity. For M_{20}-X membranes, the WU remains lower than 10%, which seems to be detrimental for the proton conductivity.

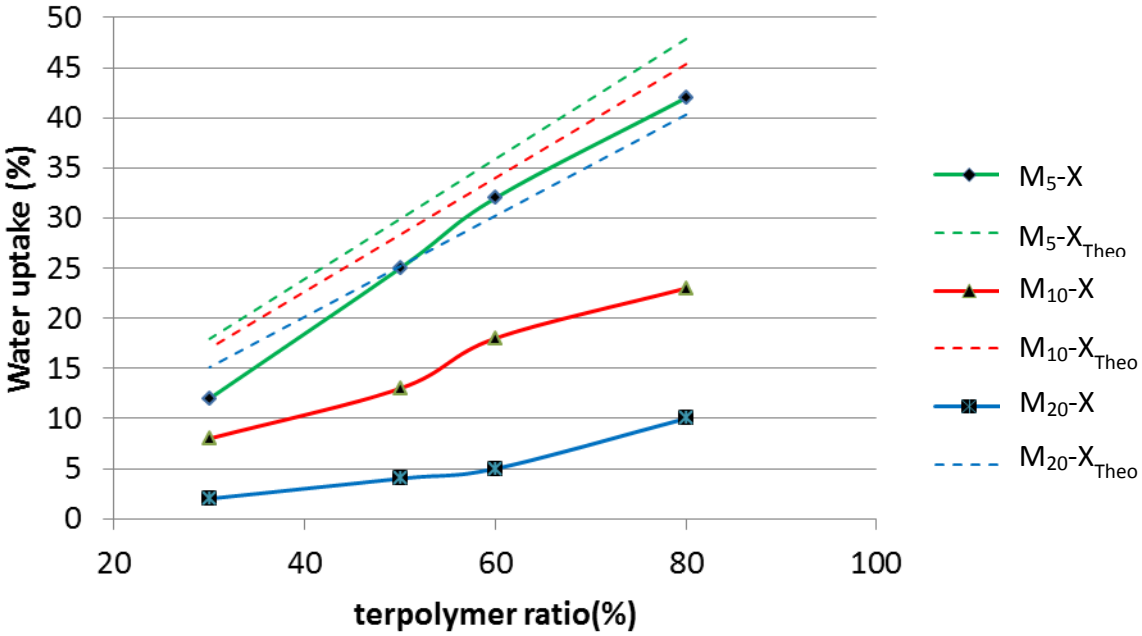

Figure 120 : Evolution of the water uptake vs the content of fluorophosphonate terpolymer for the M_5-X, M_{10}-X and M_{20}-X membranes.

The swelling rate of the membranes is also an important parameter to take into account for PEMFC use. The swelling is characterized by an increase of the membrane thickness due to water uptake. During the fuel cell operation, cycles of swelling/no swelling of the membrane are observed. If the membrane swelling is too high, a loss of the mechanical properties occurs during these cycles. Thus, we have assessed the swelling rate for each membrane by putting first the membrane in deionized water and then the thickness of the membrane was measured at both the hydrated (l_h)and dry (l_d)states. The swelling rate is then obtained, according to the following equation:

$$sw(\%) = \frac{l_h - l_d}{l_d} \times 100$$

Equation 4 : Calculation of the swelling rate

Figure 121 shows the evolution of the swelling rate for the M_5-X, M_{10}-x and M_{20}-x membranes *vs* the content of fluorophosphonate terpolymer.

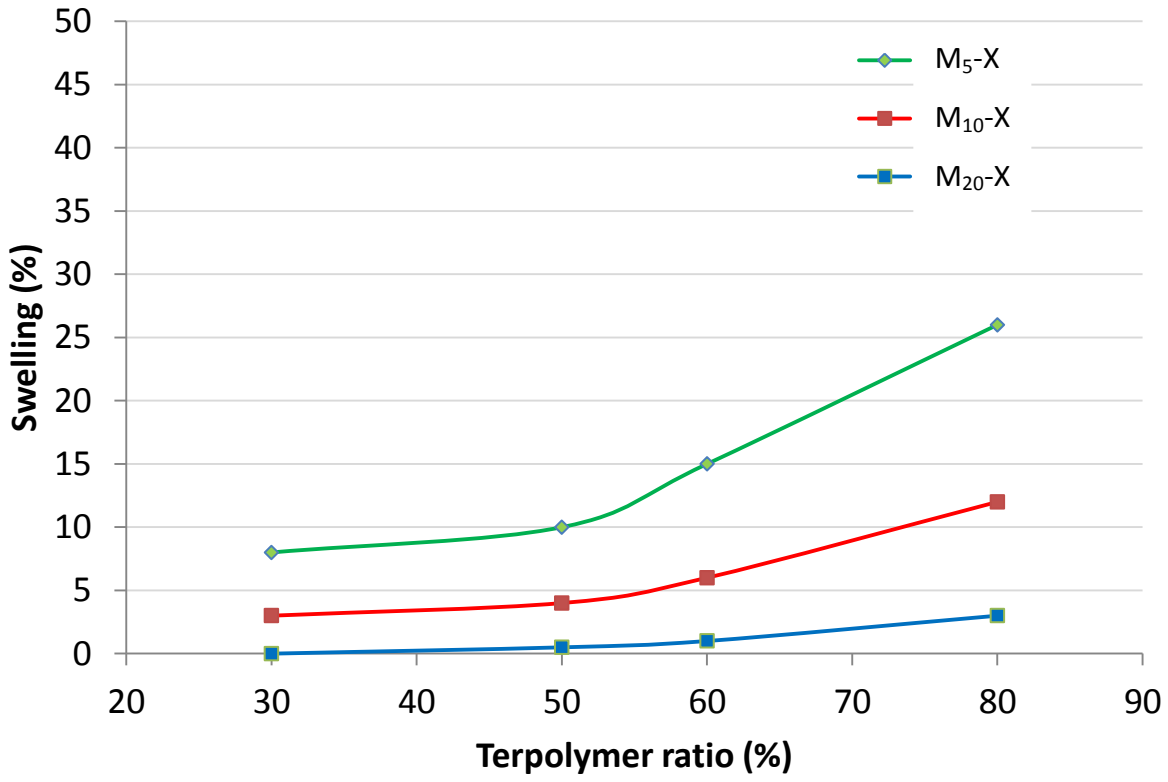

Figure 121 : Evolution of the swelling rate (%) vs the content of fluorophosphonate terpolymer for the M_5, M_{10} and M_{20} membranes.

We can observe that the swelling rate of the M_{20} membranes is very low, which can be connected to the low water uptake for these membranes. Furthermore, even for a lower content of BVEMS, lower cross-linking rate, the swelling rate remains lower than 30%. The cross-linking reaction of the terpolymer in the membrane leads to a network stiffness, which limits the polymer expansion due to the water uptake. The swelling rates showed in Figure 121 are nevertheless acceptable and in the same order than that of Nafion112®[22]. Thus,

we except that the swelling cycles during the fuel cell operation should not lead to a loss of the mechanical properties of the membranes.

3.4 Evaluation of the Ionic Exchange Capacity (IEC)

Both theoretical and experimental ionic exchange capacities (IECs) have been determined for all the membranes. The IEC_{theo} was calculated by using the IEC of poly(CTFE-*alt*-VEPA) equal to 7 meq.g^{-1}. For each fluorophosphonate terpolymer, the IEC_{theo} was calculated according to Equation 4:

$$IEC_{théo} = (7\ \times (1 - \tau_{CL})) \times \tau_{ter}$$

Equation 5 : Calculation of IEC_{theo}. τ_{CL} is the content of cross-linking agent BVEMs into the terpolymer ; τ_{ter} is the content of terpolymer in the membrane

Since poly(CTFE-*alt*-VEPA) shows an alternated structure, the IEC is rather high. Thus the IEC_{theo} values in the case of pseudo semi-IPN membranes are expected to be high. The values are gathered in Table 18 and range from 5.32 for M_5-80 membrane to 1.68 for M_{20}-30 membrane. The IEC_{exp} was also determined from titration of phosphonic acid groups contained in the membrane, according to equation 5:

$$IEC_{exp}(meq.g^{-1}) = \frac{[HO^-] \times V}{m_d}$$

Equation 6 : Calculation of IEC_{exp}, where $[HO^-]$ is the HO^- (mol.L^{-1}) concentration in the exchange solution, V the exchange volume (mL) and m_d the mass of the dry sample.

Table 18 : Theoretical and experimental IEC for all membranes obtained from the IEC of the poly(CTFE-alt-VEPA) (7 meq.g^{-1})and by acido-basic titration.

Acronym	IEC_{theo} (meq.g^{-1})	IEC_{exp} (meq.g^{-1})
M_5-80	5.32	2.1
M_5-60	3.99	0.44
M_5-50	3.15	0.8
M_5-30	2	0.4
M_{10}-80	5.04	1
M_{10}-60	3.78	0.3
M_{10}-50	3.15	0.4
M_{10}-30	1.89	0.52
M_{20}-80	4.48	0.9
M_{20}-60	3.36	0.5
M_{20}-50	2.8	0.8
M_{20}-30	1.68	0.9

We can see in the Table 18 that the IEC_{exp} values are much lower than the IEC_{theo} values. As a reminder, the principle of this method is based on the transformation of phosphonics acid of the membranes in a sodium phosphonate groups according to the reaction shown in Figure 122

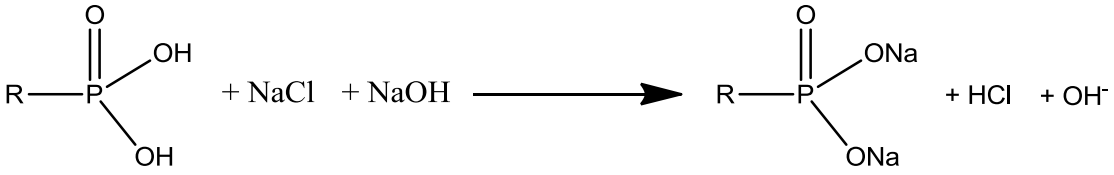

Figure 122 : Transformation of phosphonics acid in a sodium phosphonate groups

In order to realize the transformation of the phosphonic acid functions in a phosphonate groups, it is necessary that the Na^+ cation can migrate through the membrane. However, the membrane crosslinking results an increase of the density of the polymer network, therefore the accessibility of phosphonic acid groups is much reduced. Indeed, we have already observed in determining the water uptake, the values for membranes M_{10}-X

and M_{20}-X are well below than the theoretical values, so that the phosphonic acid groups are much less accessible. On the other hand, the experimental M_5-X water uptake values are the same order of magnitude than the theoretical values. But, the IEC_{exp} values concerning the M_5-X membranes are even so much lower than the IEC_{theo}. In this case, the polymer network densification allow the migration of water molecule to create the hydration sphere around the phosphonic groups, but for the Na^+ cation, the access of the phosphonic acid groups is more difficult in particular when you consider the solvation effect. However, the proton being much smaller than the cation Na^+, transport through the membrane should be achievable. The measurement of the membranes proton conductivity allows us to confirm this hypothesis.

3.5 Study of the oxidative stability: Fenton's Test

During the fuel cell use, oxygen can be present at the cathode. Indeed, some gas permeability may occur towards the membrane. Thus, via a parasite reaction with 2 electrons (Figure 123), H_2O_2 in a very little quantity can be formed.

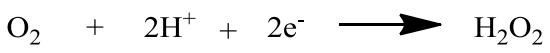

Figure 123 : Reaction of the H_2O_2 formation via a parasite reaction with 2 electrons.

In order to test the membrane resistance to the radicals, Fenton's test are recommended by DOE (Department Of Energy). To do this, membrane are immersed in a hydrogen peroxide solution in presence of transition metal[23], generally Fe^{2+}. The metallic cations present in the Fenton's solution catalyze the hydrogen peroxide degradation in a hydroxyl radical. These radicals are responsible for membrane degradation. In the presence of Fenton's reagent, the membranes are exposed to more severe conditions than in the stack (where hydrogen peroxide is formed in small quantities) to accelerate the degradation reactions.

To perform the Fenton's test, the membranes are immersed in a solution of concentrated hydrogen peroxide 30 wt% with a few ppm of Fe^{2+}. The reaction is realized at room temperature for 60 hours. A second test was performed by immersing the membrane

in the same solution but at the temperature of 80 ° C for 60 hours. The membranes resistances to radicals were determined by TGA in dynamic mode by comparing the results before and after Fenton's test. The most significant results obtained for membranes M_5-60, M_{10}-30 and M_{20}-60 are presented Figure 124.

(a) M_5-60

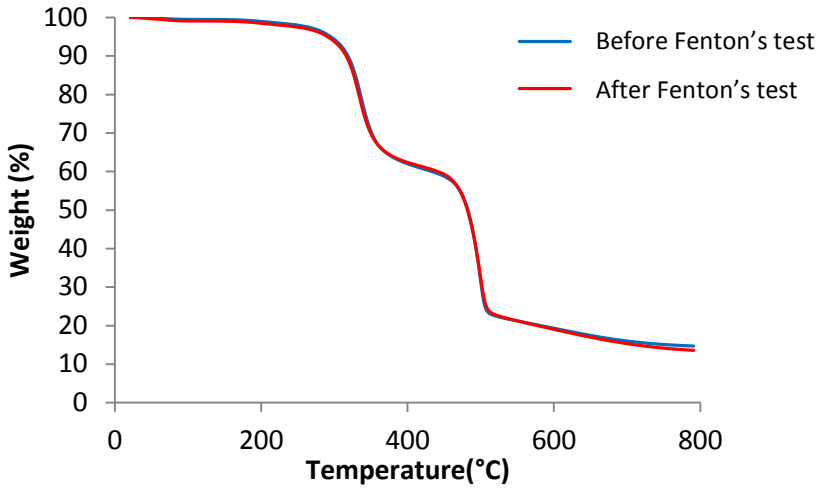

(*b*) M_{10}-30

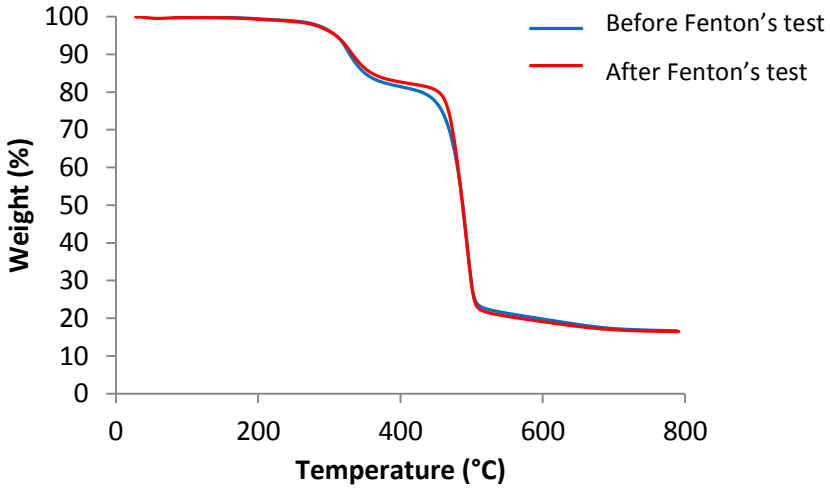

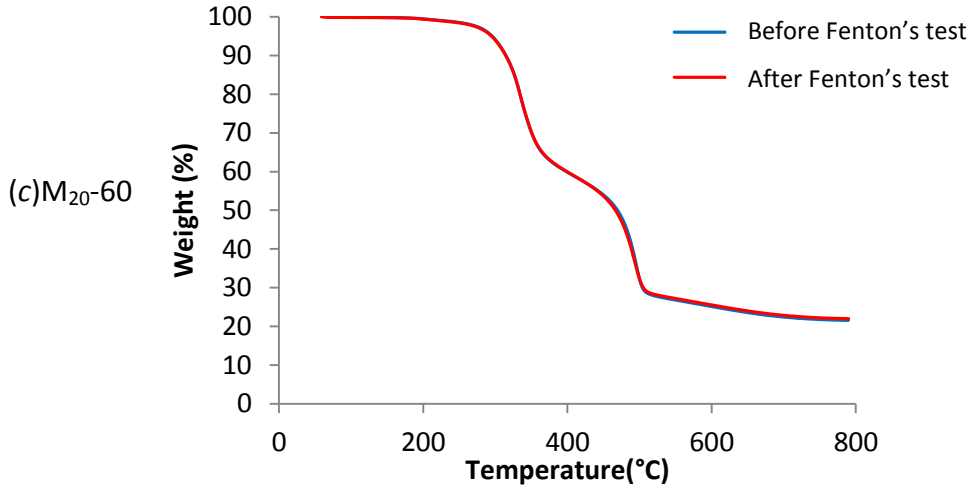

Figure 124 : TGA before and after the Fenton's test at 30% and RT for the M_5-60 (a), M_{10}-30(b) et M_{20}-60(c) membranes performed under N_2 at 20°C.min^{-1}

From the Figure 124 we clearly see that the thermograms before and after reaction are clearly the same. So, during the Fenton's test, no phosphonic acid groups have been degraded. This therefore reflects the radicals resilience of membranes under these conditions. For comparison, the result obtained for the M65 blend membrane (see chapter II) under the same conditions is shown in Figure 125. In the case of blend membranes, we observe a good stability to radicals only for a concentration of 3 wt% hydrogen peroxide. For a concentration of 30 wt%, we observe a sharp decrease in mass loss between 200 and 400°C, so that the chains carrying phosphonic acid groups are no present on the polymer after the test. So, membranes cast from crosslinkable terpolymer thus greatly increased radicals resilience.

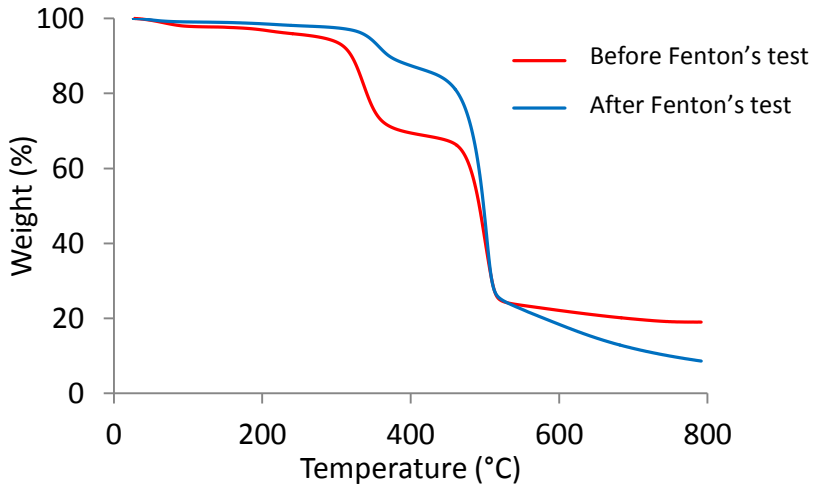

Figure 125: TGA before and after Fenton's test at 30% and RT of M-65 blend membrane under N_2 at 20°C.min^{-1} (cf Chapter II)

The Figure 126 shows the result obtained from the Fenton's test performed at 80°C for the M_5-30 membrane. We clearly see that the test conditions are much drastic for this type of membrane.

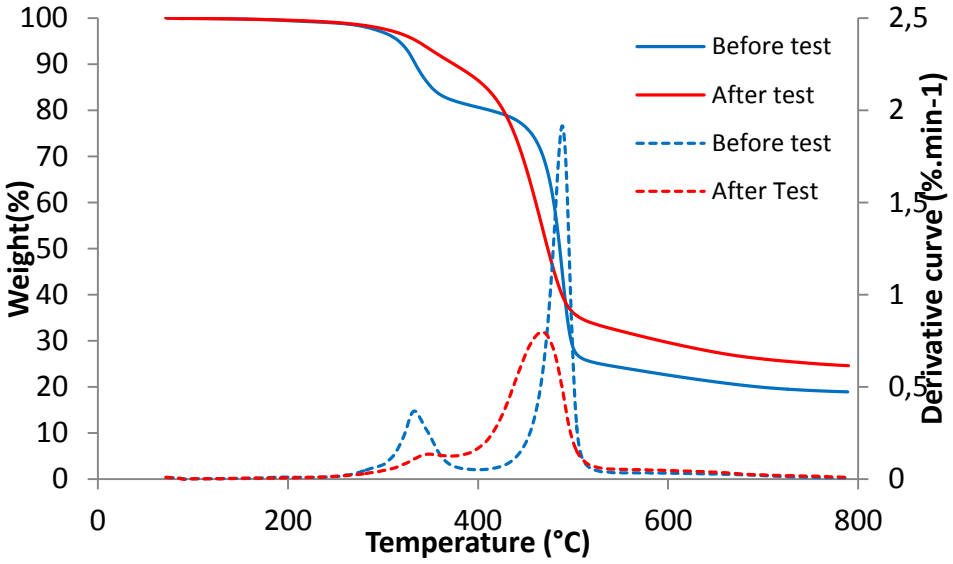

Figure 126 : TGA before and after Fenton's test at 30% and 80°C of M_5-30 membrane under N_2 at 20°C.min^{-1}.

Indeed, several phenomena are observable from the thermogram shown in Figure 126. First, we observe a sharp decrease in mass loss between 200 and 400°C. Before the Fenton's

test, mass loss recorded for a temperature of 400°C was 19.5%, after the test the mass loss is 13%. This difference in weight losses can be identified by the degradation of phosphonic acid groups. The assignment of the mass loss can be confirmed by comparing the percentage of residue at the end of analysis. Before the test the percentage of residue at 800°C is 19% while after the test is 25%, so we find again a difference of about 6%. Indeed, phosphonic acid groups were not present after Fenton's test, the rate of residue is then higher after test. Then, we observe a change in the second degradation occurring before the test, from 430°C while after the test it starts before 400°C. The second mass loss is mainly attributed to the degradation of poly(VDF-*co*-CTFE). This change in thermal behavior certainly reflects a change in the chemical structure of the copolymer. This change in structure may be due to depolymerization reactions as in the case of Nafion®[23].

3.6 **Mechanical properties**

As a reminder, one of the main drawbacks for membranes obtained from poly(CTFE-*alt*-VEPA) lay on their very low mechanical properties, especially at very low RH which led to obtaining extremely brittle membranes. The synthesis of crosslinked terpolymer allowed us to obtain membranes, but their mechanical properties were not sufficient for use as PEMFC. Indeed, the rigidity caused by crosslinking reaction causes extreme fragility. The addition of fluorinated polymer such as poly(VDF-*co*-CTFE), which has excellent mechanical properties has allowed to obtain materials with the required mechanical properties. Before to realize the mechanical study of different membranes, it appears interesting to look at the mechanical properties of poly(VDF-*co*-CTFE). For this, a membrane cast from poly(VDF-*co*-CTFE) was analyzed by dynamic mechanical analysis (DMA). The result is shown in Figure 127.

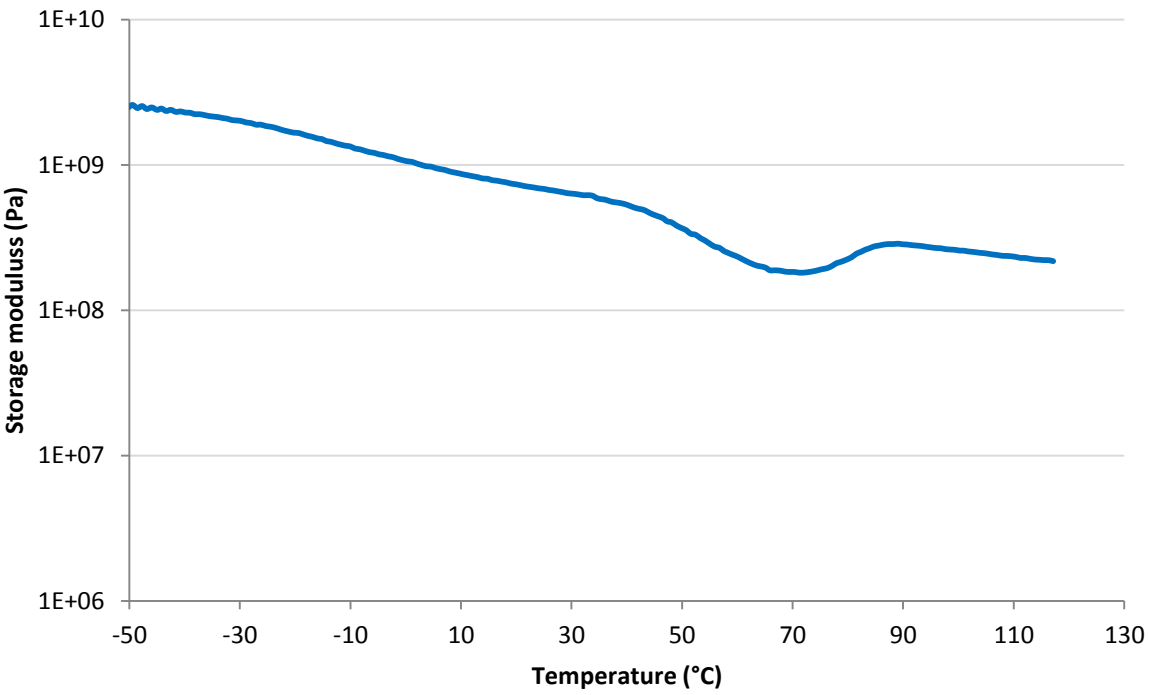

Figure 127 : Conservation modulus versus temperature realized at 1Hz and 2°C.min^{-1}.

Figure 127 shows the variation of storage modulus (E') for a temperature ranging from -50 to 120°C. We observe that the storage modulus of the membrane cast only from poly(VDF-*co*-CTFE) is high throughout the temperature range studied. Indeed, it is 2.6*10^{9} Pa at a temperature of -50°C, and then declined steadily to 1.8*10^{8} Pa at a temperature of 120°C. Around 70°C, we observe a slight decrease followed by an increase of the storage modulus. This variation of the modulus corresponds to a change of crystallographic state of poly(VDF-*co*-CTFE). Although the Tg of the polymer is -30 ° C (determined by DSC), we do not see a drastic drop in the storage modulus, this is due to the semi-crystalline nature of poly(VDF-*co*-CTFE). This semi-crystalline character will bring stability throughout the temperature range used.

To assess the contribution of poly(VDF-*co*-CTFE) on the mechanical properties of pseudo semi-IPN membranes, it would be interesting to realize the determination of the mechanical properties concerning the membrane cast only from the crosslinked terpolymers (having 5, 10 and 20% of crosslinkable monomer). However, the fragility of the membranes obtained does not allow the achievement of measurements. We therefore directly present the results obtained for the different semi-IPN membranes.

Analyzes were performed at a frequency of 1 Hertz, applying a static force of 10 N and with a temperature increase of 2°C.min^{-1}. Two parameters may vary during the analysis: temperature and relative humidity of the measuring chamber. However, when we perform the tests by varying the temperature, it is impossible to control the chamber humidity of the measurement, since it varies during the measurement. For temperatures close to room temperature, the RH will correspond to ambient RH. For temperatures higher than 70°C, giving a value of relative humidity is impossible since the chamber is not sealed.

Figure 128 shows the conservation modulus evolution for the M_{10}-30, M_{10}-50, M_{10}-60 and M_{10}-80 for a temperature range from 25 to 150°C. Concerning the low temperature (<0°C) (cf Table 19), the mechanical behavior is the same that the M0 membrane (cast only from poly(VDF-*co*-CTFE)). Indeed, we find the same values of storage modulus (2.5*10^{9}Pa). Then, the storage modulus gradually decreases with temperature. From 80°C, we observed that the storage modulus starts to decrease more significantly, reaching a plateau of 5*10^{7}Pa. This drop in the storage modulus is due to the change of state of the phosphonated polymer which has a Tg of about 100°C. Indeed, for T>Tg, the storage modulus of an amorphous polymer drops drastically, reaching several decades. In our case, the drop of the storage modulus is limited by the presence of poly(VDF-*co*-CTFE) which possesses a storage modulus about 2*10^{8}Pa at this temperature. However, we note that there are slight differences with the rate of phosphonated polymer. Indeed, for the membrane M_{10}-80, which has the highest rate of phosphonated polymer, the storage modulus is slightly higher, especially for temperatures above 50°C. However for T> Tg (Tg of phosphonated copolymer), M_{10}-80 membrane shows the lowest modulus values. In contrast, for the M_{10}-30 membrane, which has the lowest rate of phosphonated copolymer, for T<Tg, it has the lowest storage modulus and for the T>Tg, it has the higher modulus values. From the observation of the curve of tanδ, we can determine a mechanical glass transition temperature. This mechanical Tg corresponds to the maximum of the curve, they are all listed in Table 19. Overall, the Tg determined by DMA are higher than those determined by DSC. However, for the membrane M_{10}-30, the influence of the phosphonated copolymer on the mechanical properties is too low in order to perform the determination of Tg by DMA.

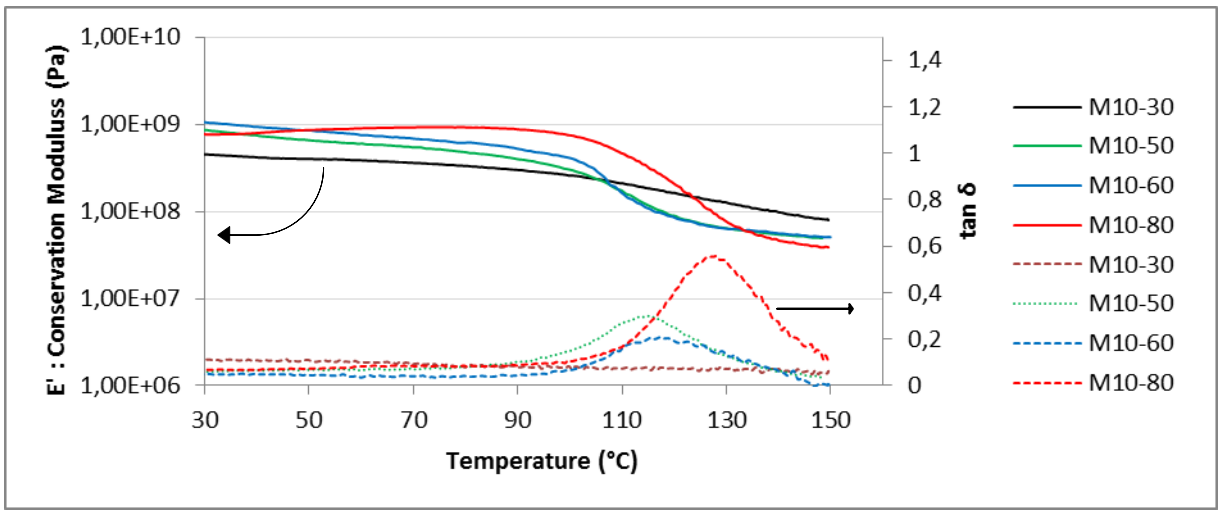

Figure 128 : Conservation modulus (-) and tanδ (---) evolution versus temperature for the M_{10}-X membranes

Table 19 : Conservation modulus of M_{10}-X membranes compared to the M0 membrane (100% poly(VDF-co-CTFE))

Membrane	Conservation modulus (Pa)			Tg(°C)[1]	Tg(°C)[2]
	-50°C	25°C	150°C		
M_{10}-80	$2.6*10^9$	$8.6*10^8$	$4*10^7$	92.5	95
M_{10}-60	$2.4*10^9$	$8.5*10^8$	$5*10^7$	98	100
M_{10}-50	$2.3*10^9$	$6.5*10^8$	$5*10^7$	105	102
M_{10}-30	$2.2*10^9$	$4*10^8$	$8*10^7$	101.4	nd
M0	$2.2*10^9$	$3.5*10^8$	$2*10^8$	nd	nd

[1] : Determined by DSC ; [2] : Determined by DMA

The results obtained for the different membranes of the category M_{10}-X are listed in Table 19 and compared with the results obtained for M0 membrane (100% poly(VDF-*co*-CTFE)). We can see that the higher the rate of poly(VDF-*co*-CTFE) in the composition of the membrane, the higher the values of storage modulus. In addition we can see that the Tg obtained by DSC are similar to that determined from the DMA analysis.

The results obtained for the different membranes M_5-X, M_{10}-X and M_{20}-X are shown in Figure 129.

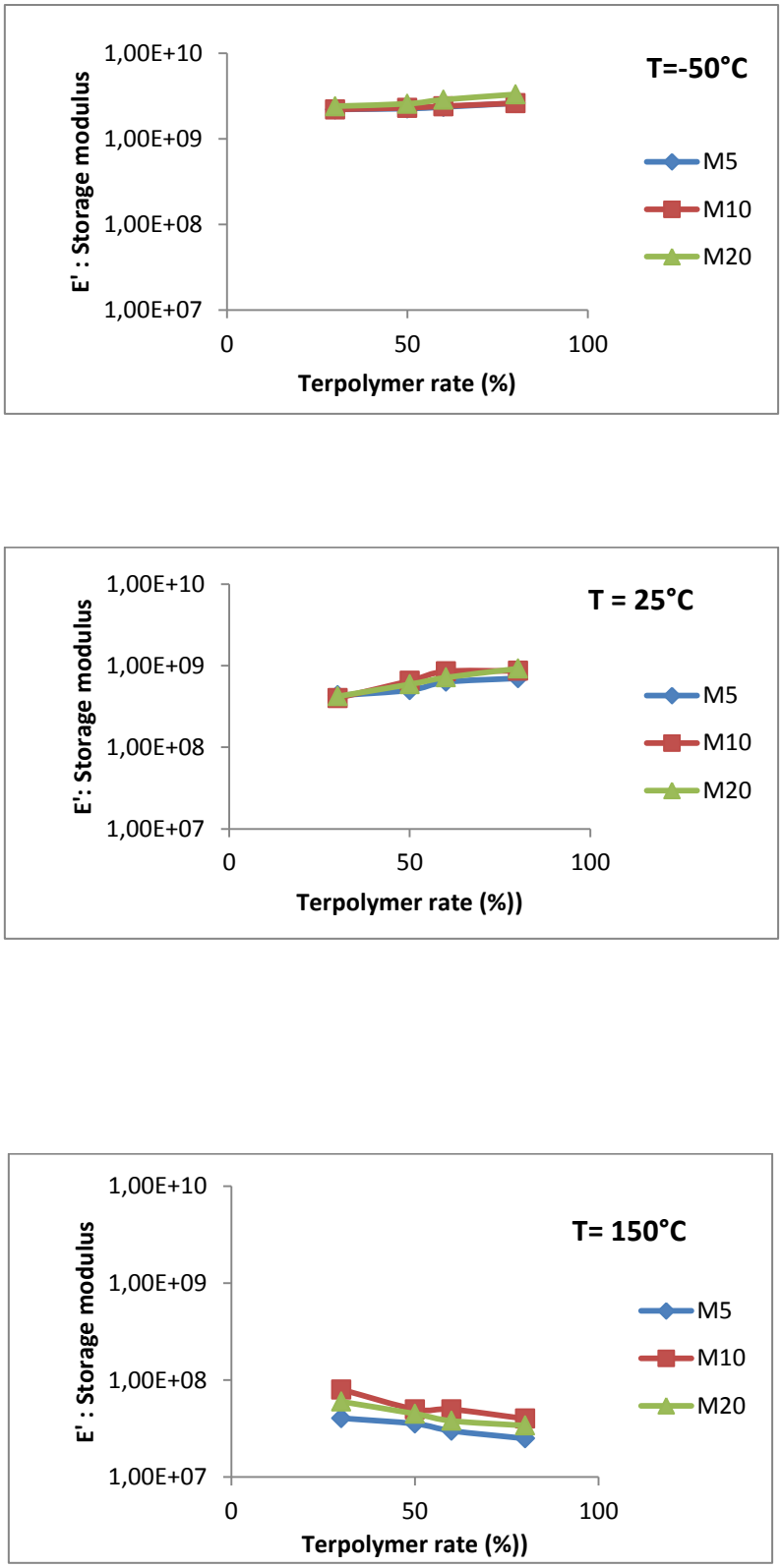

Figure 129 : Storage modulus evolution versus the content of phosphonate terpolymer at 50, 25 and 150°C for the M_5-X, M_{10}-X and M_{20}-X membranes.

Figure 129 shows the value of the storage modulus for all membranes (the M_5-X, M_{10}-X and M_{20}-X) at three temperatures, namely :

- -50°C: temperature below the poly(VDF-*co*-CTFE) Tg.
- 25°C: at room temperature, between the poly(VDF-*co*-CTFE) Tg and the phosphonated copolymer Tg.
- 150°C: temperature higher than the Tg of the two copolymers.

From the Figure 129 we can observe for a temperature of -50°C, that the composition of membranes has little influence on the values of storage modulus. For this temperature, the mechanical properties were dominated by the poly(CTFE-*co*-VDF). However, at temperatures above the Tg of poly(VDF-*co*-CTFE) some variations are observed. For a temperature of 25°C, the membranes with the highest rate of phosphonated terpolymer (M_5-80, M_{10}-80 and M_{20}-80) possess the highest storage modulus. This behavior is due to the rigidity of the phosphonated copolymer when the temperature is below its Tg. And for a temperature of 150°C, we observe the opposite behavior, ie, the lowest storage modulus correspond to membranes having the highest rate of phosphonated copolymer.

In order to analyze the behavior of the membrane in humid condition, the DMA analysis can be realized with a regulation of the HR during the measure. To do this, the measuring chamber is crossed by the flow of neutral gas (nitrogen or argon) more or less charged with water molecule. Thus, we can observe the mechanical behavior for RH ranging from 0 to about 80% and a temperature of 30°C. The results are listed in Table 20. The membranes used are very thin (about 40µm), so it is necessary that the membranes have a significant capacity of water uptake to see an influence of RH on the mechanical behavior. Tests conducted on the M_{20}-X and M_{10}-X membranes were not conclusive, due to too low amount of water recovery and swelling (see Figure 120 and Figure 121). The most interesting results were obtained for the M_5-X membranes, thanks to their high values of water uptake and swelling (see Figure 120 and Figure 121). The results obtained are presented in Table 20.

Table 20: Storage modulus evolution (in Pa) versus RH for the M_5-X membrane at RT.

RH	M_5-80	M_5-60	M_5-50	M_5-30
0%	$8.1*10^8$	$7.2*10^8$	$6*10^8$	$6.4*10^8$
35%	$7.1*10^8$	6.410^8	$5.2*10^8$	$3*10^8$
70%	$6.3*10^8$	$5.1*10^8$	$4.3*10^8$	$1.6*10^8$

The Table 20 shows the values obtained at 0, 35 and 80% of relative humidity for membranes M_5-80, M_5-60, M_5-30, M_5-50. From this table, two trends are distinguishable. Indeed, when the HR is low, we can observe that a high rate of phosphonated terpolymer implies a high storage modulus. Indeed, when we reduce the RH the phosphonated terpolymer becomes more rigid, so the storage modulus is higher and the mechanical behavior is dominated by the phosphonated terpolymer. However, at high RH, the effect is reversed. Indeed, the mechanical behavior of the membrane is then dominated by the poly(VDF-*co*-CTFE), and we find the same trend in the temperature study, i.e. a high rate of poly(VDF-*co*-CTFE) leads to a lower storage modulus. We can nevertheless conclude that, in the operating cycles of the fuel cell, the mechanical properties of membranes remain high and ensure their role as a gas barrier between two electrodes.

4 Proton Conductivity

The performance of a membrane for PEMFC is closely dependent to the proton conductivity, which directly influences the ohmic losses and finally the power densities. Proton conductivity measurements of M_5-80, M_{10}-80, M_{20}-80 membranes were performed from 20 to 90 °C in water immersed conditions in order to characterize fully hydrated membrane properties (Figure 130). These results were compared with those obtained for the M-100 membrane (cast only from phosphonate terpolymer). These membranes have been chosen because they show the best results. Indeed, these membranes possess the higher phosphonated terpolymer rate.

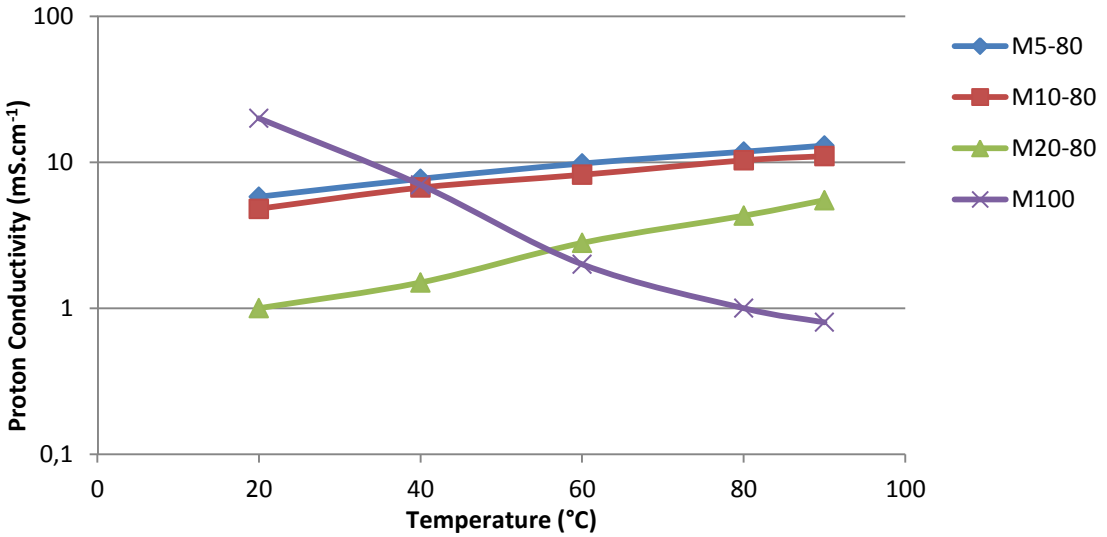

Figure 130 : Average Conductivity versus temperature in immersed conditions for the M100, M_5-80, M_{10}-80 and M_{20}-80 membranes

Firstly, the evolution of the proton conductivity versus temperature is very different between the M-100 membrane and the M_5-80, M_{10}-80 and M_{20}-80 membranes as in the case of the blend membranes showed in chapter II. Indeed, concerning the M-100 membrane, a decrease of the proton conductivity versus temperature is observed. At 20°C, proton conductivity is around 20 $mS.cm^{-1}$ and at 80°C is around 2 $mS.cm^{-1}$. In the previous works [2, 3], a diminution of the swelling was demonstrated when the temperature increases, which may explain this behaviour. Concerning the crosslinked membranes, an increase of the proton conductivity versus temperature was observed. In this case, the increase of the proton conductivity can be connected to a better structuration of the membranes. However, the performances of the crosslinked membranes are lower than that of blend membranes. Indeed, the mobility of phosphonic groups was decreased by the crosslinking reaction. So, the macroscopic organisation of the crosslinked membrane is not the same that the blend membrane. This diminution of the proton conductivity can also be attributed to the decrease of the phosphonic acid accessibility, due to the higher crosslinking rate.

5 Conclusion

New polymer electrolyte membranes have been realized from a pseudo semi-IPN strategy between a crosslinkable fluoro-phosphonated copolymer and a commercially available fluorinated copolymer. In the chapter III, we have described a new crosslinking method of fluorinated copolymer. This method can also be applied to the fluorinated copolymer carrying phosphonated groups. These membranes exhibit the same thermal and mechanical properties than the blend membrane presented in Chapter II. But thanks to the crosslinking reaction, the oxidative stability was improved. Thus, in comparison with the M-100 membrane (with only the poly(CTFE-*alt*-VEPA), the conductivity of the blend membranes is in the same order of magnitude, whereas the IEC of the blend membranes are twice lower.

However, the proton conductivity of the pseudo semi IPN membrane is twice lower than the blend membrane. Indeed, the crosslinking reaction increases the densification of the polymer network, so the accessibility of the phosphonic acid groups is decreased. But, in other hand, the stability of the crosslinkable membrane versus acid is enhanced. Indeed, during the acidification step, no coloration of the acid solution is observed. As reminder, during the acidification of the blend membrane, a coloration of the acid solution was observed. So, this better stability implies a better reproducibility of the result during proton conductivity tests.

To conclude, with these kinds of membranes, the main goals of the MemFOS project are achieved. Indeed, from the poly(CTFE-*alt*-VEPA), membranes with high thermal, oxidative and mechanical properties have been realized. Furthermore, these membranes possess reasonable proton conductivity.

In order to enhance the proton conductivity of these membranes, it could be interesting to perform the synthesis of the terpolymer with only 2 or 3 percent of crosslinkable monomer in the composition of the poly[(CTFE-*alt*-DEVEP)-*co*-(CTFE-*alt*-BVEMs)], in order to increase the access of the phosphonic acid group.

6 Experimental part

6.1 Materials

Chlorotrifluoroethylene (CTFE) and 1,1,1,3,3,-pentafluorobutane (solkane®) were kindly provided by Solvay S.A. The poly(VDF-*co*-CTFE) grade was Solef 31508 supplied by Solvay. 2-chloro ethyl vinyl ether, sodium iodide, triethyl phosphite, acetone, le methanol, carbonate potassium were purchased from Sigma-Aldrich. *Tert*-butyl peroxipivalate (TBPPI) 75% purity was purchased from Azko Nobel®. All reactants were used without further purification except for the solkane, which were distillated prior to use.

6.2 Iodo ethyl vinyl ether

In a single-neck round bottom flask equipped with a magnetic stirrer and a condenser, one equivalent of 2-chloro ethyl vinyl ether, 1.5 equivalents of sodium iodide and acetone were introduced. The reaction was allowed to reflux for 3 days. After reaction and uppon to room temperature, the produced salts (sodium chloride and sodium iodide) were filtered off. After removal of the solvent, the crude reaction was washed several times with diethyl ether. The 2-iodo vinyl ether was purified by a distillation under reduce pressure.

As an example, in a 250 mL single-neck round bottom flask equipped with a magnetic stirrer and a condenser, 2-chloro ethyl vinyl ether (20g, 188mmol), sodium iodide (22.2g, 282mmol) and acetone (100mL) were introduced. The reaction was allowed to reflux for 3 days. After reaction and upon to room temperature, the produced salts (sodium chloride and sodium iodide) were filtered off. After removal of the solvent, the crude reaction was washed several times with diethyl ether (200mL). The 2-iodo vinyl ether was purified by a distillation under reduce pressure (70°C/10^{-2} mbar. The product (incolor liquid) was obtained with a mass yield of 40%.

Structure:

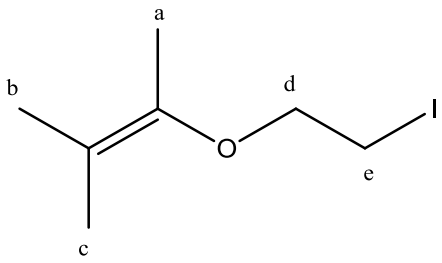

^{1}H NMR (400MHz, 297 K, CDCl3, ppm) δ: 6.39 to 6.46 (q, 1H, H_a), 4.15 to 4.21 (dd, 1H, H_b), 4.02 to 4.06 (dd 1H, H_c), 3.90 to 3.97 (t, 2H, H_d), 3.26 to 3.31 (t, 2H, H_e).

6.3 **DiEthyl Vinyl Ether Phosphonated**

In a single-neck round bottom flask equipped with a magnetic stirrer and a condenser, one equivalent of 2-iodo ethyl vinyl ether and a large excess of triethyl phosphite were introduced. The reaction was allowed to 160°C for 1 hour. After reaction and upon to room temperature, the crud product was distilled under reduce pressure.

As an example, in a 100mL single-neck round bottom flask equipped with a magnetic stirrer and a condenser, 2-iodo ethyl vinyl ether (12g, 60.6mmol) and a large excess of triethyl phosphite (50mL) were introduced. The reaction was allowed to 160°C for 1 hour. After the vacuum distillation of triethyl phosphite (60°C/5mbar) then the diethyl phosphite (90°C/5mbar), Di ethyl vinyl ether phosphonated was obtained with a mass yield of 70%.

Structure:

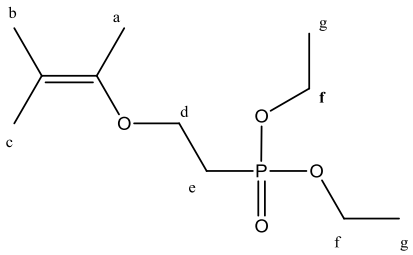

RMN ^{1}H (400MHz, 297 K, CDCl3, ppm) δ : 6.39 à 6.46 (q, 1H, H_a), 4.15 à 4.21 (dd, 1H, H_b), 4.02 à 4.06 (dd 1H, H_c), 4.02 à 4.10 (m, 4H, H_f), 3.90 à 3.97 (t, 2H, H_d), 2.1 à 2.3 (m, 2H, H_e), 1.3 à 1.5 (m, 6H, H_g).

RMN ^{31}P $\{^{1}H\}$: (160MHz, 297K, CDCl3, ppm) δ : 30.57 (s, 1P)

6.4 Synthesis of terpolymer poly[(CTFE-*alt*-DEVEP)-*co*-(CTFE-*alt*-BVEMs)]

As CTFE is a gas, the reactions were carried out in a Hastelloy (HC276) autoclave Parr system equipped with a manometer, a rupture disk (3000 psi), inlet and outlet valves, and a magnetic stirrer. Prior to reaction, the auto-clave was pressurized with 30 bar (i.e., 430 psi) of nitrogen to check for eventual leaks. The autoclave was then conditioned for the reaction with several nitrogen/vacuum cycles (10^{-2}mbar) to remove any traces of oxygen. The liquid phase was first introduced via a funnel, and then the gases were inserted by double weighing (i.e. the difference of weight before and after filling the autoclave with the gas). Then, the autoclave was placed in a mantle heated with a vigorous mechanical stirring. Both heating and stir-ring were monitored by a controller. After an initial in-crease of the internal pressure due to the increasing temperature, the pressure dropped by consumption of the gaseous monomer to produce a polymer in the liquid phase. After the reaction was complete, the autoclave was cooled to room temperature and then degassed. After distillation of the solvent, the copolymers were precipitated from cold methanol. The product was dried under vacuum (10^{-2} mbar) at 70°C until constant weight.

As an example, 50 mL de solkane® as the solvent, TBPPI (0.8 g, 4.6 mmol) as the initiator, K_2CO_3 (0.36g, 2.57 mmol) (to prevent the cationic homopolymerization of vinyl ether), DEVEP (14.3g, 68.7 mmol), BVEMs (3.33g, 17.2mmol) and CTFE (10g, 85.8 mmol) were introduced in the 100mL autoclave. The reaction was allowed to proceed at 75°C for 12h, showing a drop of pressure as CTFE was reacting. After purification, the copolymer, obtained as a pal yellow solid. It was then dried in a vacuum oven (10^{-2} mbar) at 50°C until constant weight. The mass yield was 72%.

Structure :

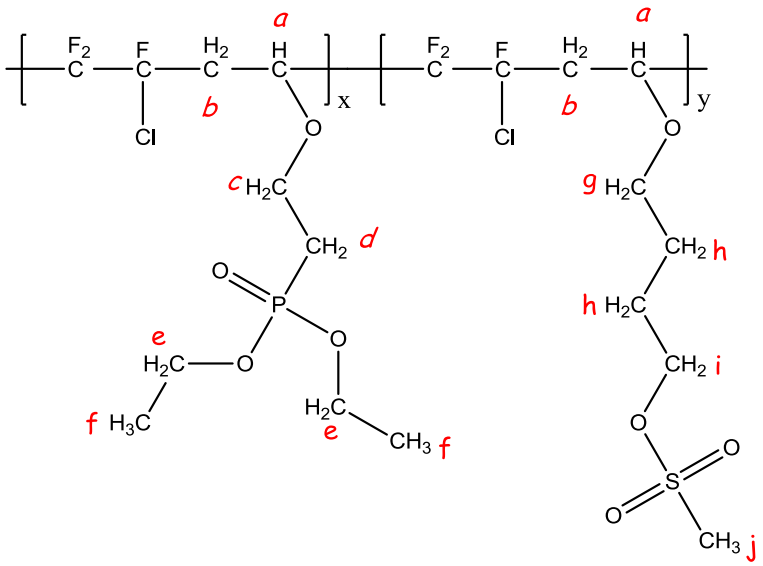

Mass yield :72%

Température de transition vitreuse :

^{1}H RMN (400MHz, 297K, $CDCl_3$) δ : 4.74 to 4.3 (m, 1H, H_a), 4.23(m, 2H,H_i), 4.08(m, 4H, H_e), 3.96(m, 2H, H_c), 3.78(m, 2H, H_g), 2.99 (m, 3H, H_j), 2.84 to 2.35 (m, 2H, H_b), 2.12(m, 2H, H_d), de 1.84 to 1.66 (m, 4H, H_h), 1.30 (m, 6H, H_f).

^{19}F RMN {^{1}H} (400MHz, 297K, $CDCl_3$, ppm) δ : -108 to -123 (m, 3F)

^{31}P RMN {^{1}H} (400MHz, 297K, $CDCl_3$, ppm) δ : 27 (s, 1P)

6.5 Cast, crosslinking and acidification of membrane

A specific amount of poly[(CTFE-*alt*-DEVEP)-co-(CTFE-alt-BVER)] was dissolved in DMSO (30 wt%), then poly(VDF-*co*-CTFE) powder was added into the poly[(CTFE-*alt*-DEVEP)-co-(CTFE-*alt*-BVER)] solution, which was stirred several hours at 50°C. After the poly(VDF-*co*-CTFE) was fully dissolved, the solution was cast onto glass plate, and then dried at 100°C during 24h. To obtain the crosslinked membranes, they are dried at 150°C during 15h.

To obtain the phosphonic acid groups, membranes were immerged in an HCl concentrated solution (12N) at 90°C during 3 days. After reaction, membranes were washed by deionized water, and then dried under vacuum at 80°C during one night.

7 References

1. Lee, J.-Y.; Park, E.-J., Synthesis of novel polyurethanes containing dioxybenzylidenecyanoacetate, as non-linear optical chromophores and their properties. *Polymer International* **2002,** *51* (3), 228-232.
2. Lee, J.-Y.; Lee, W.-J.; Rhee, B. K.; Min, H. S., Synthesis of novel poly(vinyl ether)s containing the oxybenzylidenemalononitrile group as a nonlinear optical chromophore, and their electro-optic properties. *Polymer International* **2004,** *53* (2), 169-175.
3. Negrell-Guirao, C.; Boutevin, B.; David, G.; Fruchier, A.; Sonnier, R.; Lopez-Cuesta, J.-M., Synthesis of polyphosphorinanes Part II. Preparation, characterization and thermal properties of novel flame retardants. *Polym. Chem.* **2011,** *2* (Copyright (C) 2013 American Chemical Society (ACS). All Rights Reserved.), 236-243.
4. Boutevin, B.; Cersosimo, F.; Youssef, B., Studies of the alternating copolymerization of vinyl ethers with chlorotrifluoroethylene. *Macromolecules* **1992,** *25* (11), 2842-2846.
5. Carnevale, D.; Wormald, P.; Ameduri, B.; Tayouo, R.; Ashbrook, S. E., Multinuclear Magnetic Resonance and DFT Studies of the Poly(chlorotrifluoroethylene-alt-ethyl vinyl ether) Copolymers. *Macromolecules* **2009,** *42* (15), 5652-5659.
6. Valade, D.; Boschet, F. d. r.; Améduri, B., Synthesis and Modification of Alternating Copolymers Based on Vinyl Ethers, Chlorotrifluoroethylene, and Hexafluoropropylene†. *Macromolecules* **2009,** *42* (20), 7689-7700.
7. Jenkins, A. D.; Kratochvil, P.; Stepto, R. F. T.; Suter, U. W., Glossary of basic terms in polymer science. *Pure Appl. Chem.* **1996,** *68* (Copyright (C) 2013 American Chemical Society (ACS). All Rights Reserved.), 2287-2311.
8. Chen, S.-C.; Wu, Y.-C.; Mi, F.-L.; Lin, Y.-H.; Yu, L.-C.; Sung, H.-W., A novel pH-sensitive hydrogel composed of N,O-carboxymethyl chitosan and alginate cross-linked by genipin for protein drug delivery. *J. Controlled Release* **2004,** *96* (Copyright (C) 2013 American Chemical Society (ACS). All Rights Reserved.), 285-300.
9. Patel, V. R.; Amiji, M. M., Preparation and characterization of freeze-dried chitosan-poly(ethylene oxide) hydrogels for site-specific antibiotic delivery in the stomach. *Pharm. Res.* **1996,** *13* (Copyright (C) 2013 American Chemical Society (ACS). All Rights Reserved.), 588-93.
10. Risbud, M. V.; Hardikar, A. A.; Bhat, S. V.; Bhonde, R. R., pH-sensitive freeze-dried chitosan-polyvinylpyrrolidone hydrogels as controlled release system for antibiotic delivery. *J. Controlled Release* **2000,** *68* (Copyright (C) 2013 American Chemical Society (ACS). All Rights Reserved.), 23-30.
11. Joo, H.-S.; Do, H.-S.; Park, Y.-J.; Kim, H.-J., Adhesion performance of UV-cured semi-IPN structure acrylic pressure sensitive adhesives. *J. Adhes. Sci. Technol.* **2006,** *20* (Copyright (C) 2013 American Chemical Society (ACS). All Rights Reserved.), 1573-1594.
12. Park, Y.-J.; Lim, D.-H.; Kim, H.-J.; Joo, H.-S.; Do, H.-S., Curing behavior and adhesion performance of UV-curable styrene-isoprene-styrene-based pressure-sensitive adhesives. *J. Adhes. Sci. Technol.* **2008,** *22* (Copyright (C) 2013 American Chemical Society (ACS). All Rights Reserved.), 1401-1423.
13. Pascal, T.; Mercier, R.; Sillion, B., New semi-interpenetrating polymeric networks from linear polyimides and thermosetting bismaleimides: 2. Mechanical and thermal properties of the blends. *Polymer* **1990,** *31* (Copyright (C) 2013 American Chemical Society (ACS). All Rights Reserved.), 78-83.
14. Lan, Z.; Wu, J.; Lin, J.; Huang, M.; Yin, S.; Sato, T., Influence of molecular weight of PEG on the property of polymer gel electrolyte and performance of quasi-solid-state dye-sensitized solar cells. *Electrochim. Acta* **2007,** *52* (Copyright (C) 2013 American Chemical Society (ACS). All Rights Reserved.), 6673-6678.
15. Li, P. J.; Wu, J. H.; Huang, M. L.; Hao, S. C.; Lan, Z.; Li, Q.; Kang, S., The application of P(MMA-co-MAA)/PEG polyblend gel electrolyte in quasi-solid state dye-sensitized solar cell at higher temperature. *Electrochim. Acta* **2007,** *53* (Copyright (C) 2013 American Chemical Society (ACS). All Rights Reserved.), 903-908.

16. Wu, J.; Lan, Z.; Lin, J.; Huang, M.; Hao, S.; Fang, L., Influence of solvent on the poly (acrylic acid)-oligo-(ethylene glycol) polymer gel electrolyte and the performance of quasi-solid-state dye-sensitized solar cells. *Electrochim. Acta* **2007,** *52* (Copyright (C) 2013 American Chemical Society (ACS). All Rights Reserved.), 7128-7135.
17. Chikh, L.; Delhorbe, V.; Fichet, O., (Semi-)Interpenetrating polymer networks as fuel cell membranes. *Journal of Membrane Science* **2011,** *368* (1–2), 1-17.
18. Cho, K.-Y.; Jung, H.-Y.; Shin, S.-S.; Choi, N.-S.; Sung, S.-J.; Park, J.-K.; Choi, J.-H.; Park, K.-W.; Sung, Y.-E., Proton conducting semi-IPN based on Nafion and crosslinked poly(AMPS) for direct methanol fuel cell. *Electrochim. Acta* **2004,** *50* (Copyright (C) 2013 American Chemical Society (ACS). All Rights Reserved.), 589-593.
19. Guan, Y.; Pu, H.; Pan, H.; Chang, Z.; Jin, M., Proton conducting membranes based on semi-interpenetrating polymer network of Nafion and polybenzimidazole. *Polymer* **2010,** *51* (Copyright (C) 2013 American Chemical Society (ACS). All Rights Reserved.), 5473-5481.
20. Kundu, P. P.; Kim, B. T.; Ahn, J. E.; Han, H. S.; Shul, Y. G., Formation and evaluation of semi-IPN of Nafion 117 membrane for direct methanol fuel cell. *J. Power Sources* **2007,** *171* (Copyright (C) 2013 American Chemical Society (ACS). All Rights Reserved.), 86-91.
21. Matsuguchi, M.; Takahashi, H., Methanol permeability and proton conductivity of a semi-interpenetrating polymer networks (IPNs) membrane composed of Nafion and cross-linked DVB. *J. Membr. Sci.* **2006,** *281* (Copyright (C) 2013 American Chemical Society (ACS). All Rights Reserved.), 707-715.
22. Gebel, G.; Aldebert, P.; Pineri, M., Swelling study of perfluorosulphonated ionomer membranes. *Polymer* **1993,** *34* (2), 333-339.
23. Curtin, D. E.; Lousenberg, R. D.; Henry, T. J.; Tangeman, P. C.; Tisack, M. E., Advanced materials for improved PEMFC performance and life. *Journal of Power Sources* **2004,** *131* (1–2), 41-48.

CHAPTER V

SYNTHESIS AND CHARACTERIZATIONS OF BLOCK COPOLYMER CARRYING PHOSPHONIC ACID GROUPS

PentaFluoroStyrene (PFS)

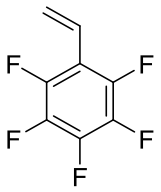

4-vinyl benzyl chloride (VBC)

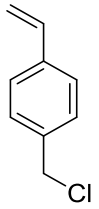

DiEthylVinylBenzyllPhosphonate (DEVBP)

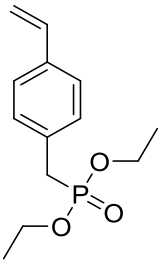

2-cyanopropan-2-yl undecyl carbonotrithioate

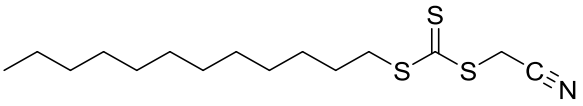

poly(DEVBP-b-PFS)

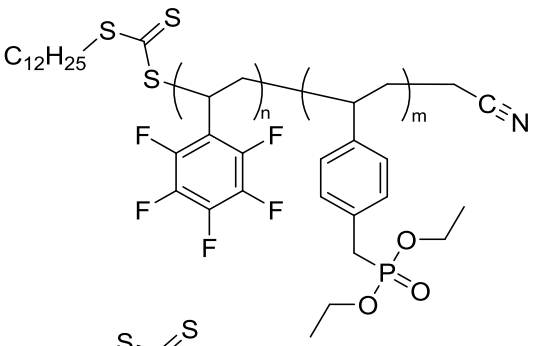

poly(VBPA-b-PFS)

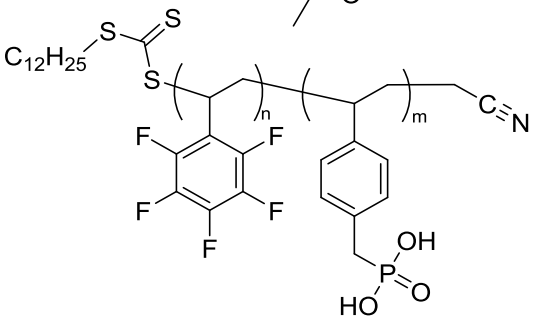

1 Introduction

In chapter I of this manuscript we showed the effect of the polymer structuration on the physic-chemical properties of the PEMFC. Indeed, the structuration generally leads to a percolation network, which then will facilitate the proton transport and thus increase the electrochemical performances of the fuel cell. To obtain a structuration of the membrane, the (co)polymer must show a controlled architecture, such as block or graft copolymers. In this chapter, we will only focus on the synthesis of block copolymer. We also showed in chapter I that the membrane structuration was the consequence of the balance between the hydrophobic/hydrophilic character of both blocks. We have decided to synthesize block copolymers with one block been a fluorinated one for its hydrophobic character and the second block carrying phosphonic acid moieties, which will be the hydrophilic part of the block copolymer. It is to mention that, to our knowledge, such block copolymer was never developed so far. In the literature, only few examples deal with the synthesis of block copolymers with one block carrying phosphonic acid units. For instance, Jannasch and co[1] performed the synthesis of poly(styrene-b-vinyl phosphonic acid) by anionic polymerization. To obtain block copolymers with one block been fluorinated and the second one been phosphonic acid type, a synthetic strategy based on the use of controlled radical polymerization (CRP) will be chosen. CRP techniques can be divided into two categories:

-Reversible termination such as Nitroxyde Mediated Polymerization (NMP)[2], or Atom Transfer Radical Polymerization (ATRP)[3].

-Reversible transfer such as Reversible Addition Fragmentation Transfer (RAFT/MADIX)[4] or Iodide Transfer Polymerization (ITP)[5].

The synthesis of phosphonate polymers from CRP generally leads to low molecular weights (Mw) polymers with high polydispersity index (PDI) values. For instance, Destarac and co[6] carried out the MADIX of vinyl phosphonic acid (VPA) and obtained poly(VPA) of low Mw of about 6000 $g.mol^{-1}$ with PDI of about 1.4. Few examples also deal with the ATRP of diethyl vinyl benzyl phosphonate (DEVBP) monomer[7, 8] (Figure 131), which proceeded with a good control.

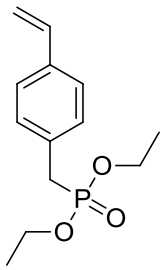

Figure 131 : Structure of Di Ethyl Vinyl Benzyl Phosphonate (DEVBP)

RAFT of phosphonate monomers seems to be most efficient technique in term of control of molecular weight and PDI. Indeed, Ribaut and co[9] realized the RAFT of Di Ethyl Vinyl Benzyl Phosphonate (DEVBP) with a fluorinated acrylate monomer, leading to a gradient copolymer containing about 20 mol% of DEVBP. Thus, the synthesis of block copolymer can be investigated by RAFT of DEVBP. The second block will then be obtained by RAFT of a fluorinated monomer, i.e. the pentafluorostyrene (Figure 132).

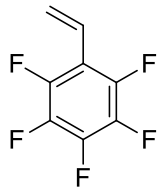

Figure 132 : Structure of PentaFluoroStyrene (PFS)

RAFT polymerization of PFS was already described in the literature [10, 11], where different block copolymers were synthesized such as 4-hydroxystyrene or 4-vinylpyridine or methacrylate monomers. In each case, the RAFT polymerization of PFS was carried out as the second block, i.e. from macro-RAFT obtained from the first block, due to the high reactivity of PFS compared to others monomers. Thus, in this chapter we have decided to perform first the RAFT polymerization of DEVBP, followed by the RAFT polymerization of PFS from the first DEVBP block. Furthermore, Canniccioni et al.[12] showed that the synthesis of block copolymers was more efficient when the first block was phosphonate type, in the case of methacrylate monomers. We except also that DEVBP is less reactive than PFS in RAFT polymerization. As mentioned above, this study is probably the first one focusing on the synthesis of diblock copolymers with one block been phosphonic acid type, and the second

one been fluorinated type. This chapter will be a model study on the synthesis of such diblock copolymers, with low targeted molecular weights, in order to show the efficiency of this synthetic strategy. The development of membranes from such copolymers will be one of the main perspectives of this work.

2 Synthesis and characterizations of poly(DEVBP-b-PFS) block copolymers

Poly(DEVBP-b-PFS) block copolymer will be performed by RAFT polymerization of DEVBP followed by PFS. PFS is commercially available monomers unlike DEVBP, which needs to be synthesized first.

2.1 Synthesis of DEVBP monomer

The synthesis of DiEthyl Vinyl Benzyl Phosphonate (DEVBP) monomer can be performed from two different synthetic pathways. The first one consists into the Michaelis-Arbuzov reaction of 4-Vinylbenzyl chloride (VBC) [13] (Figure 133). The second one consists into the nucleophilic substitution of VBC by using the salt of diethylphosphite [14] (Figure 134).

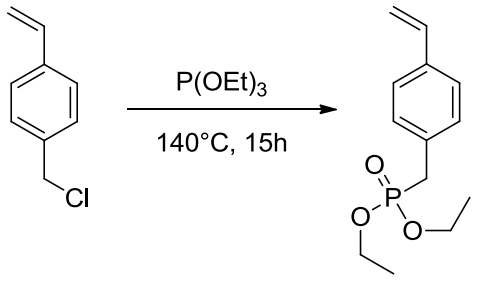

Figure 133 : Phosphonation of VBC via the Michaelis-Arbuzov reaction.

Concerning the first method, the synthesis is performed at 135 °C, temperature at which the monomer may polymerize. We have decided to use the second method, using soft conditions. The first step is the formation of the salt of sodium diethylphosphite and is performed in THF at 0 °C. The second step consists in adding VBC drop by drop into the solution in the presence of sodium iodide, which favors the nucleophilic substitution.

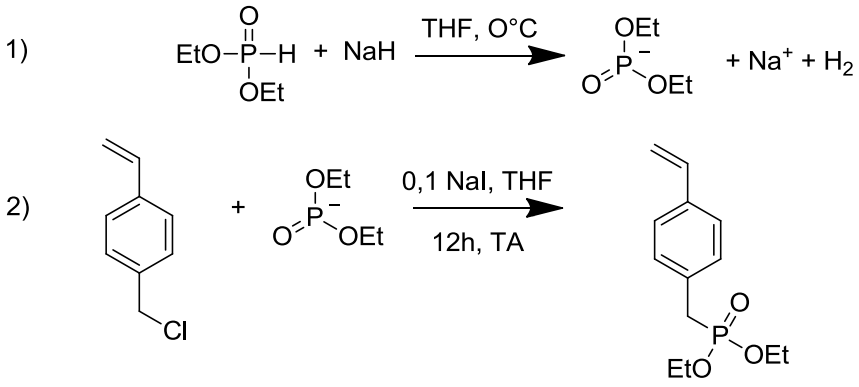

Figure 134 : Synthesis of DEVBP

After reaction, the solvent is eliminated and the crude product is purified from chromatography in an ethyl acetate/hexane mixture (1/100). The clear yellow product was obtained with 95 % mass yield and was characterized by ^{1}H and ^{31}P NMR (Figure 135 and Figure 136, respectively).

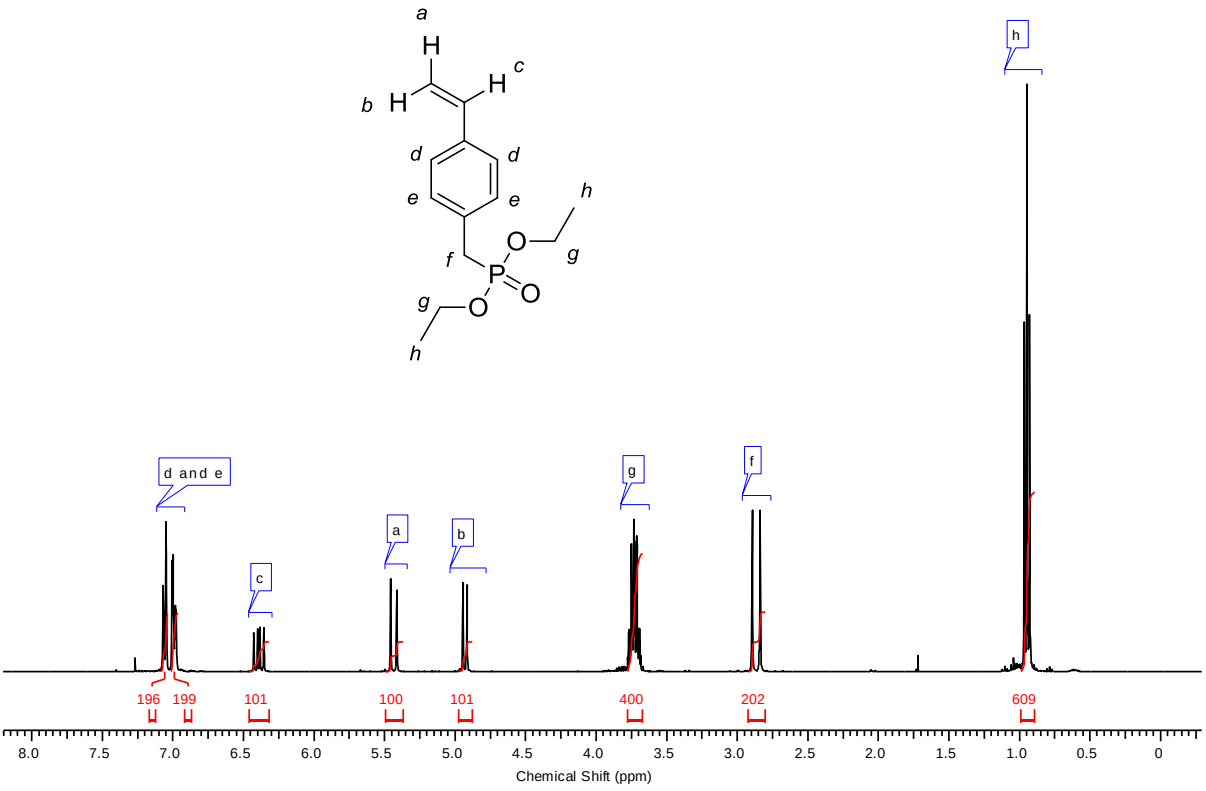

Figure 135 : ^{1}H NMR spectrum of DEVBP (realized in $CDCl_3$)

From Figure 135, the signal characterizing the -C**H**$_2$- (*f*) in alpha-position of the phosphonate group was clearly identified and allows to confirm the expected structure. From Figure 136, a single peak was observed from the phosphonate group situated at 26ppm. The excess of diethylphosphite was totally eliminated during the purification step.

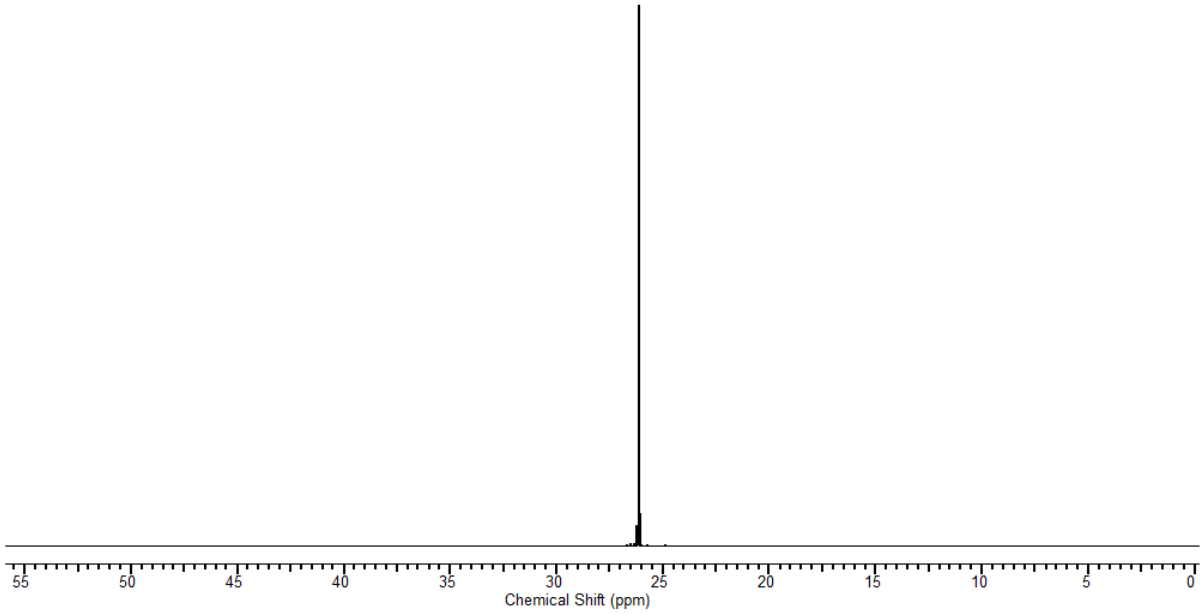

Figure 136 : ^{31}P NMR spectrum of DEVBP (realized in $CDCl_3$)

2.2 Synthesis and characterizations of poly(DEVBP) by RAFT

RAFT polymerization is based on reversible transfer by addition-fragmentation and by using a thiocarbonylthio (R-S-(C=S)-Z) compound, also named Chain Transfer Agent (CTA). The mechanism of RAFT, shown in Figure 137, comprises five steps:

-The first step corresponds to conventional initiation and propagation through a radical process;

-The second one corresponds to reversible addition of the propagating radical onto the thiocarbonylthio group of the CTA, enabling the formation of tertiary intermediary radical. This radical can undergo fragmentation and create either a new growing chain or a new $R^{\bullet}$ radical ;

-The third step corresponds to the $R^{\bullet}$ radical addition onto the monomer to form a new growing chain;

-The fourth step corresponds to the addition-fragmentation equilibrium. This step is crucial to afford polymers with low PDIs. Indeed, since the CTA is totally consumed, the

transfer occurs onto the thiocarbonylthio end-chain from the macro-chain transfer agent, thus allowing equilibrium between dormant and active species. This equilibrium implies that all the growing chains grow simultaneously, which allows a good control of the polymerization.

-The fifth step corresponds to undesirable termination reaction (recombination or disproportionation). In RAFT, the low content of radical initiator allows to avoid the termination reactions since the content of growing chains remains low. Thus, most of the chains are terminated by a thiocarbonylthio group, been reactivable for the polymerization of a second monomer, leading to block copolymer.

Initiation

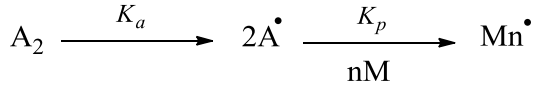

Reversible chain transfer

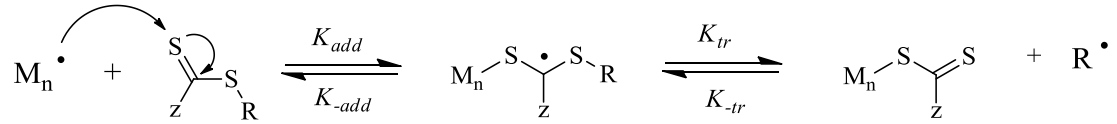

Reinitiation

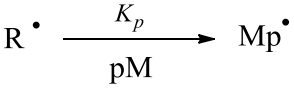

Chain equilibration

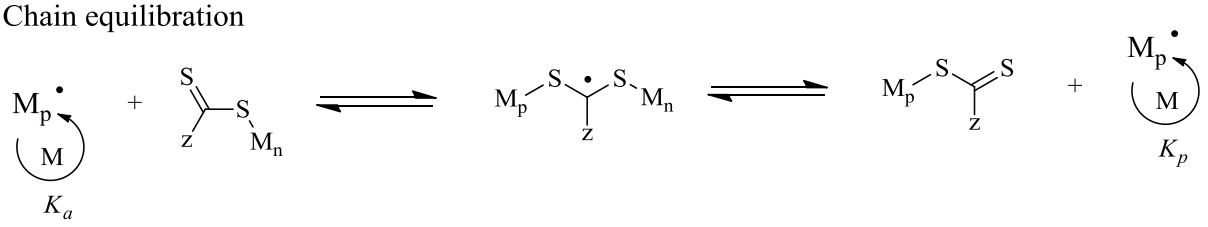

Termination

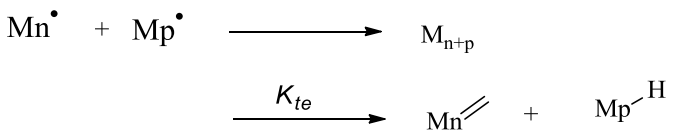

Figure 137 : Mechanism of RAFT polymerization

The synthesis of the first block is obtained by RAFT of DEVBP. We have chosen commercially available cyanomethyl dodecyl trithiocarbonate (cf Figure 138) as CTA, which is commonly used for the RAFT polymerization of styrenic monomers [15].

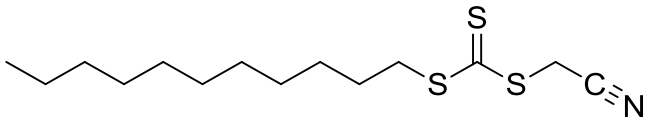

Figure 138 : Structure of CTA : cyanomethyl dodecyl trithiocarbonate

The ratio[CTA]/[AIBN] used is 5/1, and the polymerization is performed in trifluorotoluene in order to avoid transfer reactions to the solvent. As mentioned above, this polymerization is a model study and in consequence we have decided to perform low molecular weights of poly(DEVBP), which can be more easily characterized. The targeted Mw is 6000 $g.mol^{-1}$, and the conversion rate will be stopped to 70% to avoid any termination, which would lead to a loss of the living character of the polymerization. The reaction scheme of the polymerization is illustrated in Figure 139 and the reaction conditions gathered in Table 21.

Table 21 : polymerization conditions for the synthesis of the macro-CTA poly(DEVBP)

	DEVBP (mmol)	**CTA (mmol)**	**AIBN (mmol)**	**Reaction time(h)**	**Conv. %[a]**	**Mn_{th} ($g.mol^{-1}$)[b]**
Poly(DEVBP)	11.8	0.35	0.07	15	70	6400

a: Determined by ^1H NMR of the raw product

b: $M_{n,th}=conv.m_{DEVBP}/n_{CTA} + Mn_{CTA}$

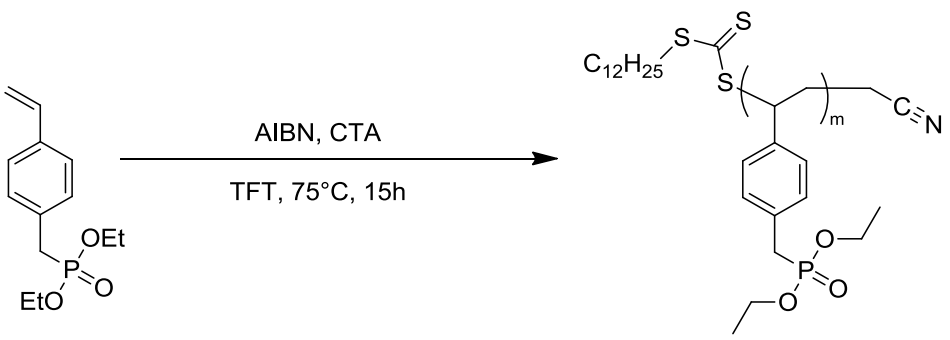

Figure 139 : RAFT polymerization of the DEVBP

After purification, the poly(DEVBP) was characterized from ^{1}H and ^{31}P NMR (cf Figure 140 and Figure 141) as well as from GPC (cf Figure 142).

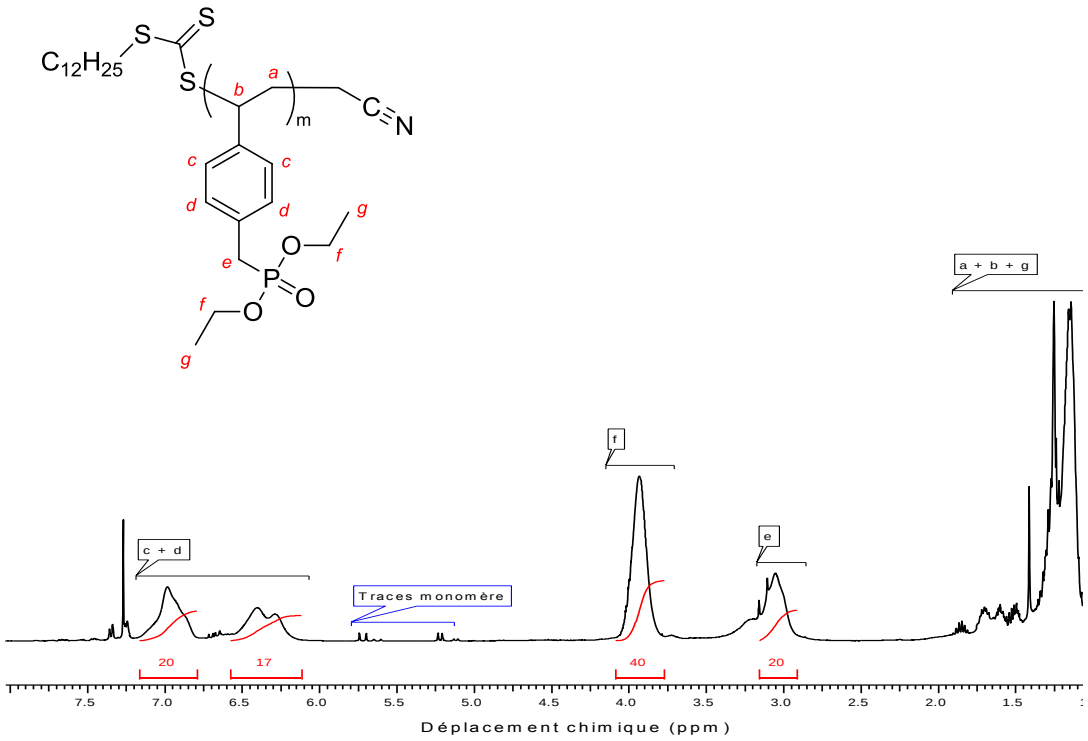

Figure 140 : ^{1}H NMR spectrum of poly(DEVBP)

From ^{1}H NMR (Figure 140) large signals are observed at 3.1 and 3.8 ppm and characterized -**CH_2**-P(d) and -O-**CH_2**-CH_3(f), respectively. The signals of the aromatic protons (c and d) are also observed at 6.3 and 6.9 ppm. From 1 to 2 ppm we can note signals characterizing the protons of the main chain (a and b) as well as the CH_2-**CH_3** protons. The 1H NMR does not allow to prove the presence of the chain-end protons. Only -**CH_2**- situated in alpha-position of the trithiocarbonate is observed but its signal is overlapped into the signal of protons *e*. The signals of the $C_{12}H_{25}$ end-group are also situated between 1 and 2 ppm, which then do not allow to assess the degree of polymerization by ^{1}H NMR. Finally, we can note some traces (about 7%) of residual monomer despite several precipitations in hexane.

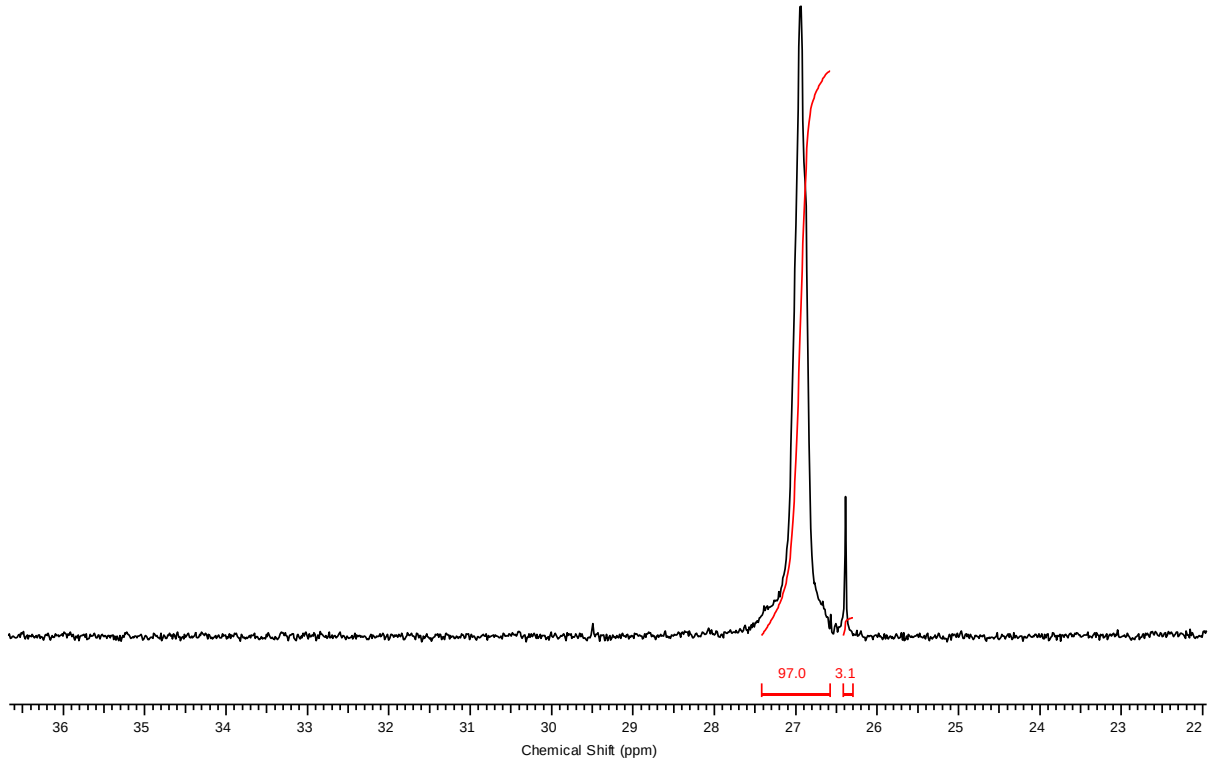

Figure 141 : ^{31}P NMR spectrum of poly(DEVBP)

Figure 141 shows the ^{31}P NMR of poly(DEVBP). Compared to the signal of DEVBP monomer, the signal of poly(DEVBP) is up-shifted from 26 to 30 ppm. Residual monomer is also observed, as already mentioned from spectrum of ^{1}H NMR. Poly(DEVBP) was also characterized by GPC. Figure 142 shows the GPC trace of poly(DEVBP)and the polystyrene standards allow to evaluate Mw of 5800 $g.mol^{-1}$ with a polydispersity index PDI of 1.3 (Table 2). The experimental Mw is in good agreement with the theoretical one, which proves the controlled character of the polymerization, confirmed by the low value of the PDI.

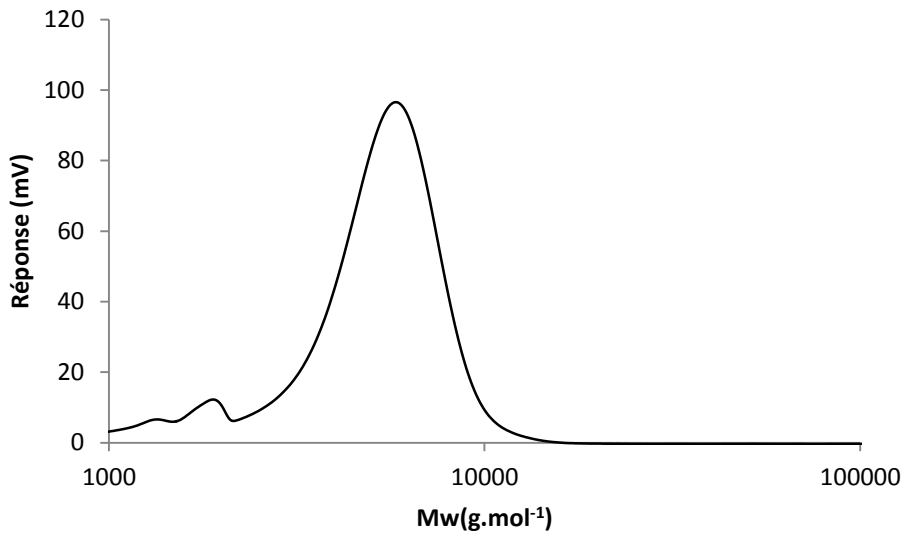

Figure 142 : GPC trace of poly(DEVBP) obtained by RAFT

Table 22 : Molar mass, PDI and thermal characteristics of poly(DEVBP).

	Conversion rate[a]	Mn^{b} ($g.mol^{-1}$)	$Mn_{theo}{}^{c}$ ($g.mol^{-1}$)	PDI^{b}	$Td_{5\%}{}^{d}$ (°C)	$Td_{10\%}{}^{d}$ (°C)	Tg^{e} (°C)
Poly(DEVBP)	70%	5800	6400	1.3	300	325	40

a: Calculated from ^{1}H NMR
b : Determined by GPC
c : $M_{n,th}=conv.m_{DEVBP}/n_{CTA} + Mn_{CTA}$
d: determined by TGA
e: determined by DSC

The thermal behavior of poly(DEVBP) was assessed from both TGA and DSC (Figure 143 and Table 22). From Figure 143, two main degradations are clearly observed. The first one occurs from 280 to 305°C and corresponds to approximately 20% weight loss. From date of chapters II and IV we can definitively attribute this weight loss to the phosphonate groups degradation. The second one, ranging from 450 to 520 °C, corresponds to the main chain degradation comprising the aromatic groups. The 5 and 10% decomposition temperatures are 300 and 325°C, respectively, whereas the glass transition temperature was equal to 40 °C.

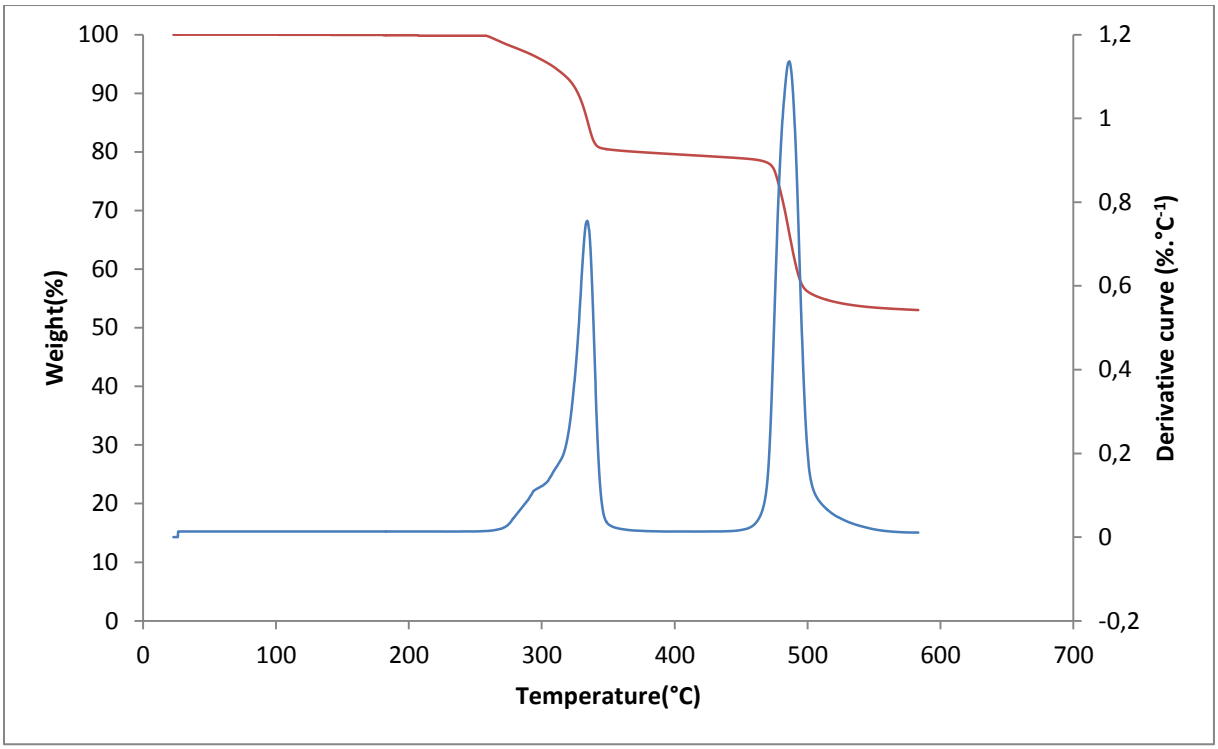

Figure 143 : Thermogram of poly(DEVBP) obtained from TGA in dynamic mode under nitrogen at 10°C.min^{-1}

2.3 Synthesis of poly(DEVBP-b-PFS)

The synthesis of poly(DEVBP-b-PFS) is performed by RAFT polymerization of PFS with poly(DEVBP) as macro-chain transfer agent. Some authors already carried out the RAFT polymerization of PFS from a macro CTA, such as methacrylate type, and demonstrated the living character of the polymerization [10, 11]. The living character of the polymerization also depends upon the reaction conditions such as the ratio between the macro CTA and AIBN or the temperature (> to 70°C). The reaction scheme and reaction conditions are gathered in Figure 144 and Table 3. The resulting block copolymer was analyzed by ^{1}H, ^{19}F and ^{31}P NMR, and by GPC (Figure 145, Figure 146, Figure 147 and Figure 149).

Table 23 : Polymerization conditions for the synthesis of the poly(DEVBP-b-PFS) block copolymer

	PFS(mmol)	Macro-CTA(mmol)	AIBN (mmol)	Reaction time (h)	Conv.%[a]	$M_{n,th}$ ($g.mol^{-1}$)[b]
Poly(DEVBP-b-PFS)	15.4	0.35	0.07	15	70	12000

a: Determined by ^{1}H NMR of the raw product

b : $M_{n,th}=conv.m_{DEVBP}/n_{Macro\text{-}CTA} + Mn_{CTA}$

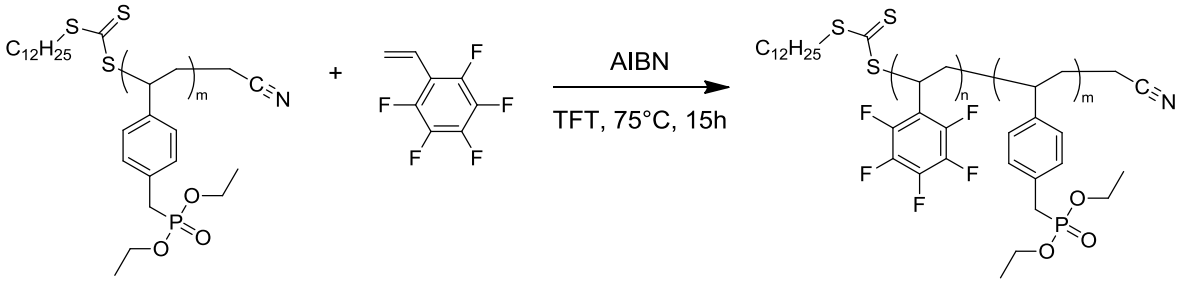

Figure 144 : Synthesis of poly(DEVBP-b-PFS) block copolymer

Figure 145 shows the ^{1}H NMR of poly(DEVBP-b-PFS), where we can note the signal of -**CH**-**CH_2**- (a and b) of the main chain for the fluorinated block centered at 2.7, 2.4 and 2.2 ppm, respectively. The signals of the phosphonate block are also clearly visible. From this spectrum, we can calculate the content of PFS to DEVBP into the copolymer (Equation 7), by using the signals of a and b protons of the fluorinated block as well as the signal of C**H_2**-(g) of the phosphonate block. So, the PFS block represents 60%.

$$\%poly(PFS) = \frac{\frac{\int_{1.7}^{2.1} b}{2}}{\frac{\int_{1.7}^{2.1} b}{2} + \frac{\int_{2.8}^{3.1} g}{2}}$$

Equation 7 : Calculation of the PFS content into poly(DEVBP-b-PFS)

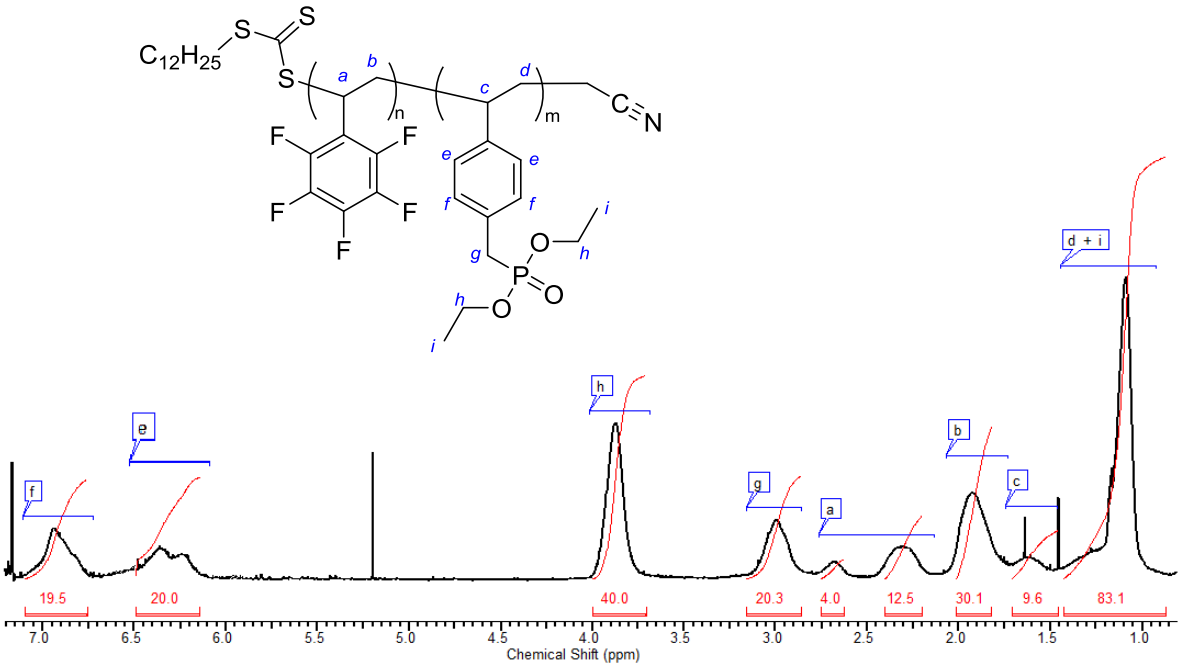

Figure 145 : ^{1}H NMR spectrum of poly(DEVBP-b-PFS)

Figure 146 shows ^{19}F NMR of poly(DEVBP-*b*-PFS), from which the conversion rate of PFS can be determined. Indeed, the polymerization of PFS leads to larger peaks of fluorinated atoms situated in ortho (F_1), metha (F_2) and para (F_3) of the aromatic ring. Concerning F_3, its signal is down-shifted after polymerization. The signal of the monomer is a triplet centered at -156 ppm and the signal of the polymer is a large peak centered at -154 ppm. From both signals we can calculate the PFS conversion, according to Equation 8 :

$$Conversion\ rate = \frac{\int_{-156.3}^{-156.1} F'_3}{\int_{-156.3}^{-156.1} F'_3 + \int_{-154.8}^{-153.6} F_1}$$

Equation 8 : Calculation of the PFS conversion rate during the RAFT polymerization from poly(DEVBP)

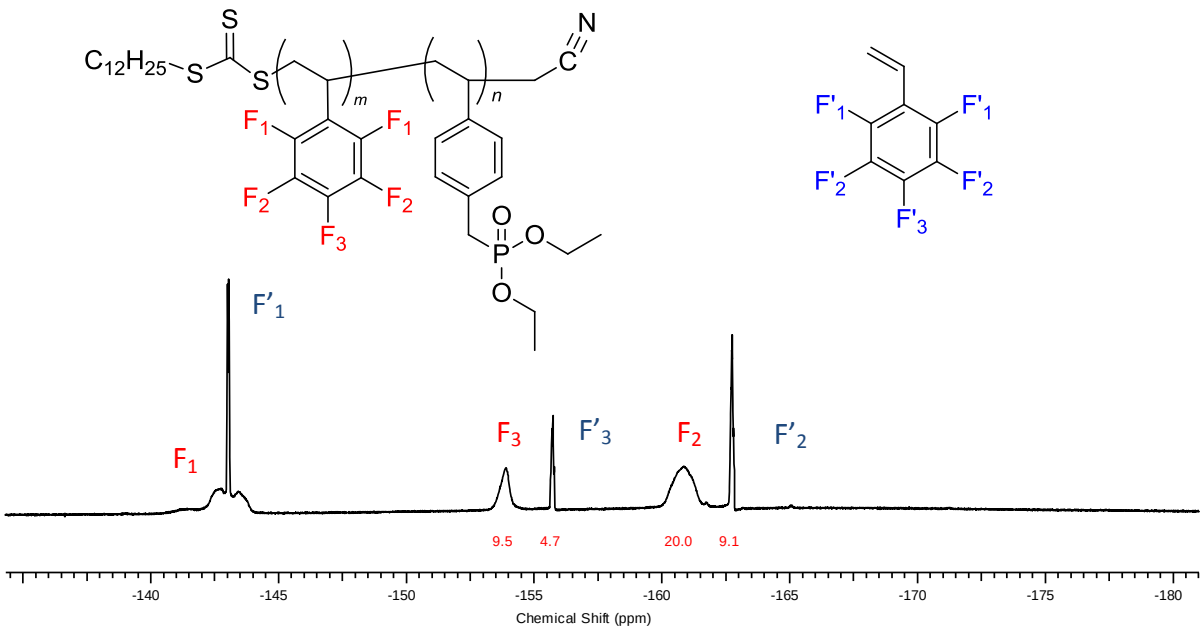

Figure 146 : ^{19}F NMR spectrum of poly(DEVBP-b-PFS)

From Figure 147, we observe the presence of a single peak from the phosphonate units. Thus, during the purification process of the diblock copolymer, the residual DEVBP monomer was extracted.

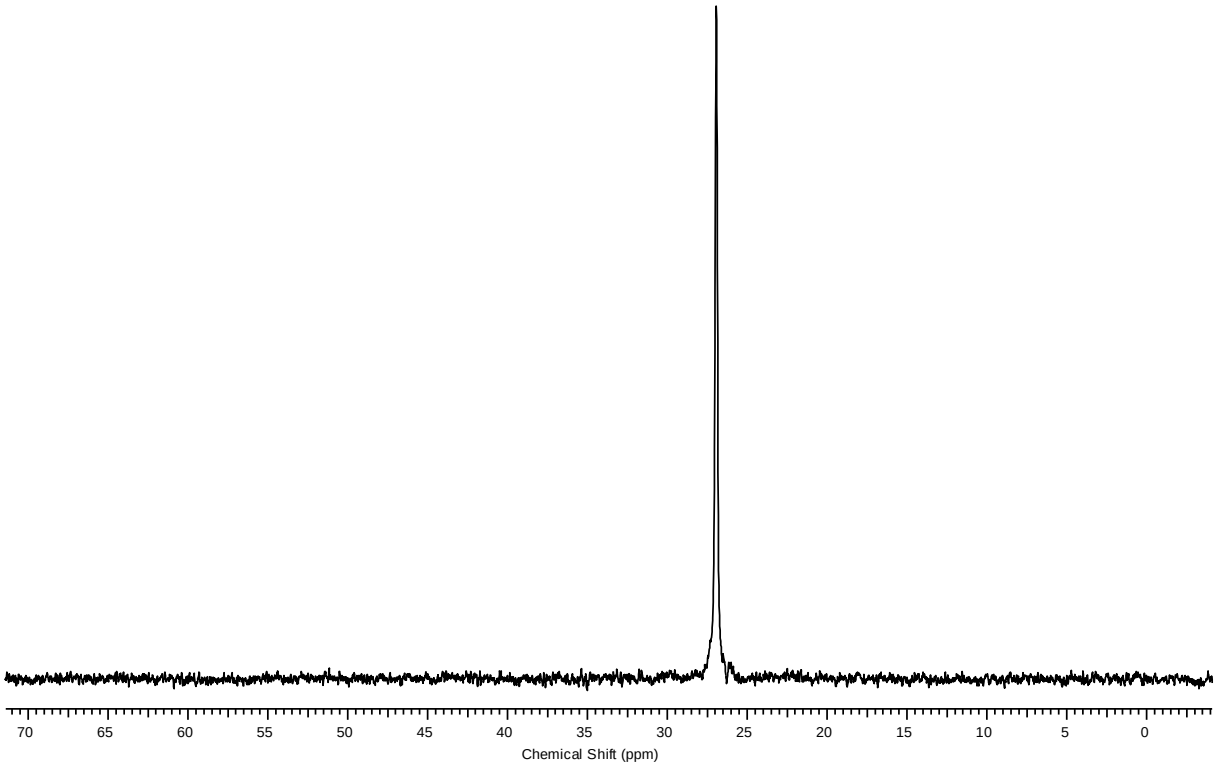

Figure 147 : ^{31}P NMR spectrum of poly(DEVBP-b-PFS)

The resulting block copolymer was characterized by GPC Figure 148 and the GPC trace of poly(DEVBP) was also added. After polymerization of PFS, the peak of poly(DEVBP) has totally disappeared and a single peak characterizes the diblock copolymer in the higher molecular weight region. The diblock copolymer shows Mw value of 11,000g.mol^{-1}, which proves the living character of the PFS RAFT polymerization (Table 4).

Table 24 Molar mass and PDI of poly(DEVBP-b-PFS)

Mn Macro-CTA (g.mol^{-1})^{a}	**Mn block copolymer (g.mol^{-1})^{a}**	**Mn_{theo} (g.mol^{-1})^{b}**	**PDI^{a}**
5800	11000	12000	1.6

a : Determined by GPC

b : $M_{n,th}=conv.m_{DEVBP}/n_{Macro\text{-}CTA} + Mn_{CTA}$

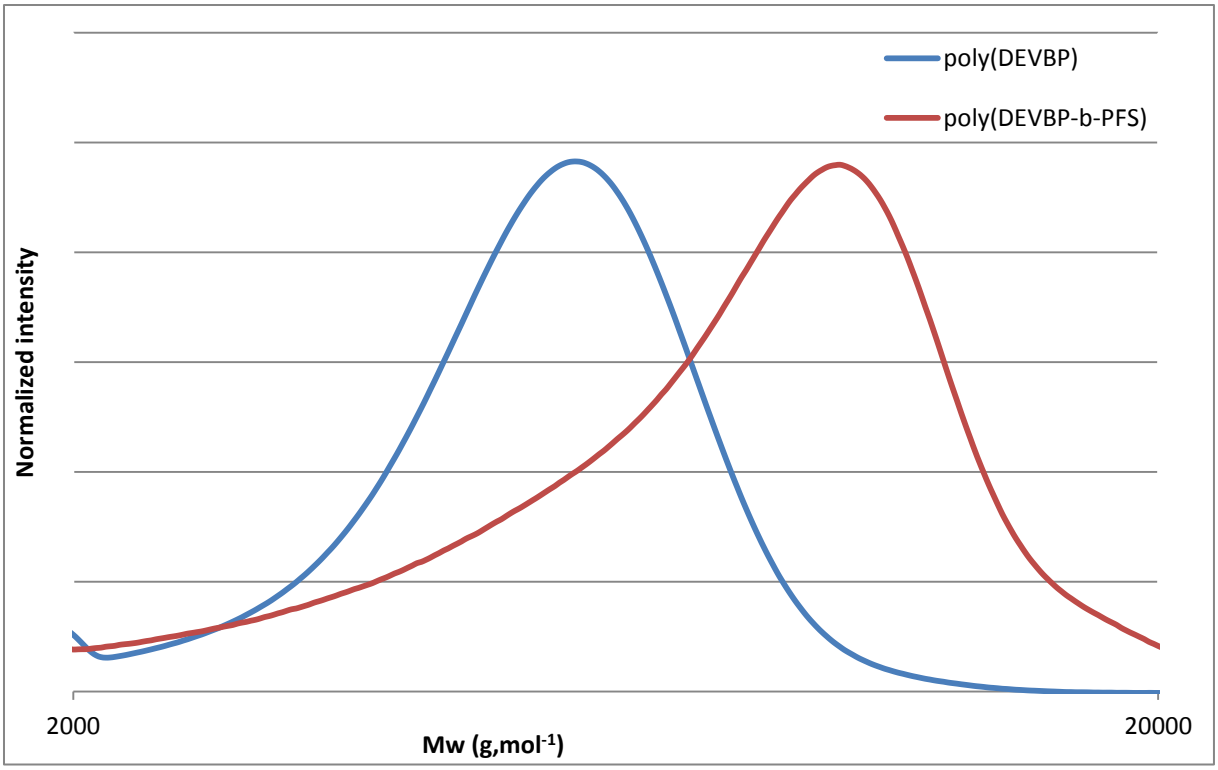

Figure 148 : SEC traces of the poly(DEVBP) and the poly(DEVBP-b-PFS)

The last synthetic step consists into the cleavage of the phosphonate moieties into phosphonic acid units. The reaction was performed by silylation, according to Figure 149.

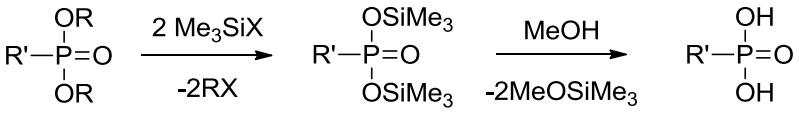

Figure 149 : Silylation reaction of phosphonate group

Unfortunately, after hydrolysis of the silane groups, the diblock copolymer carrying phosphonic acid groups is no more soluble in any solvents due to the strong amphiphilic character of the copolymer. We have then decided to use the strategy developed in chapters II and IV, where acidification was performed after membrane casting in HCl solution.

3 Membrane characterizations

3.1 Membrane casting

The membrane was casted from poly(DEVBP-*b*-PFS) diblock copolymer carrying phosphonate groups. To this aim, a precise amount of copolymer is solubilized in DMF to obtain a 50wt% concentration. The membrane was placed in an oven at 90°C during one night. As expected, the resulting membrane shows very poor mechanical properties due to the low molecular weight of the block copolymer. Acidification was carried out in 12N HCl solution at 90 °C during 3 days. The handling of the membrane remains complicated due to the poor mechanical properties. Nevertheless, this membrane will be characterized as a model membrane in order to assess a possible structuration from the diblock copolymer.

3.2 Thermal analyses

The thermal analyses were performed onto the membrane before and after acidification by TGA and DSC (Figure 151 and Table 25). From Figure 151 we note a clear difference between the thermograms recorded before and after acidification of the membrane. Indeed, before acidification the membrane shows a 5% weight loss temperature of about 313 °C, whereas this temperature drops to 180 °C after acidification. This weight loss is due to the loss of water molecules, which are produced by anhydride bonding between phosphonic acid groups. This reaction can be either intra-or inter-molecular, leading to the loss of one water molecule [16, 17]. The schematic representation of the chemical bonds is given in Figure 150.

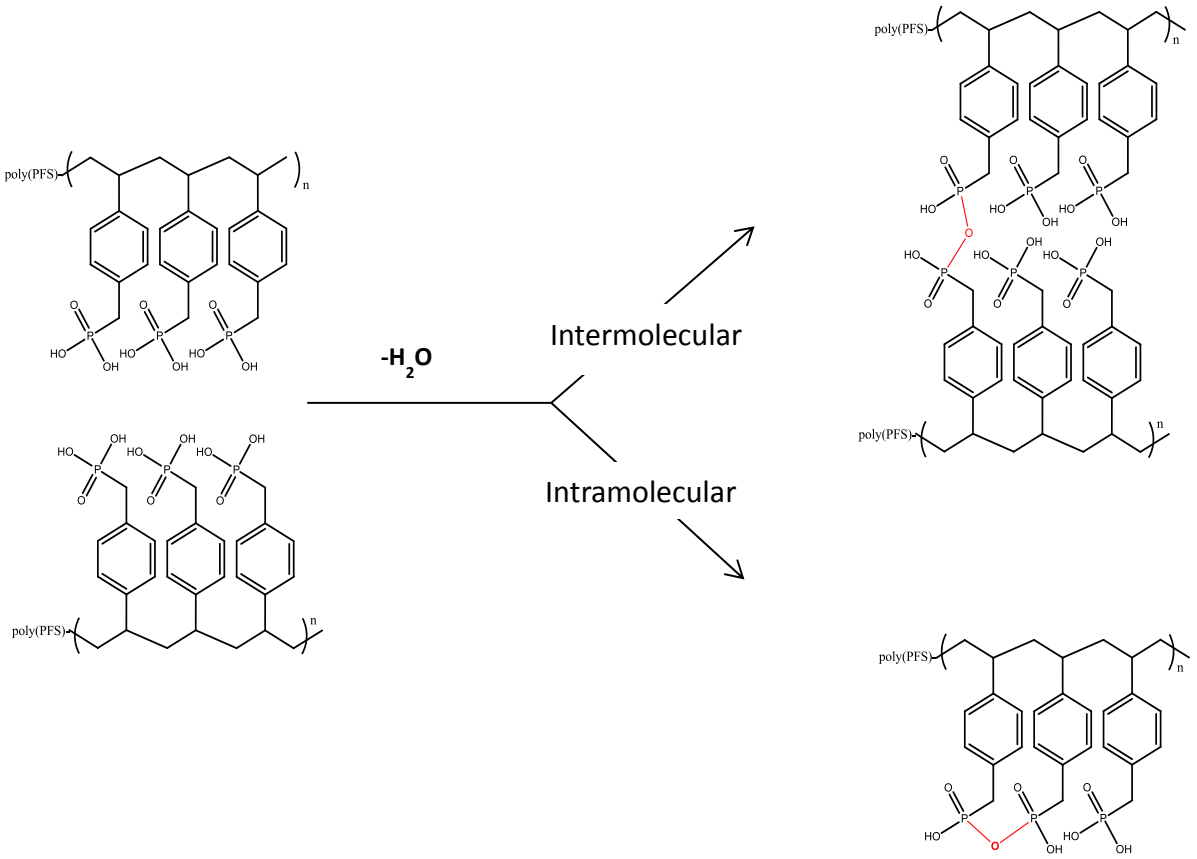

Figure 150 : Formation of anhydride bonds between the phosphonic groups by intra and inter molecular reactions

We can also remark that the difference of the thermal stability before and after acidification was less pronounced for both the blend and pseudo semi-IPN membranes (chapters II and IV). Indeed, these membranes were obtained from alternated copolymers where the distance between phosphonic acid groups is higher than that of poly(VBPA-b-PFS). This also shows that intra-molecular reactions between phosphonic acid groups seem to be predominant. From Figure 151 we also observe a degradation step at 300 °C for both membranes, which correspond to the degradation of the phosphonate/phosphonic acid moieties. This degradation is less pronounced with phosphonic acid groups due to the stabilization of the anhydride bonds. The anhydride bonds are also characterized by a high content of residue above 500 °C. Finally the main degradation is observed from 400 to 550°C, corresponding to the aromatic rings of the main chain.

Table 25 : Temperature correponding to 5 et 10% weight loss from TGA in dynamic mode at 10°C.min^{-1} and glass transition temperatures for each block determined from DSC.

	$Td_{5\%}$(°C)	$Td_{10\%}$(°C)	Tg_1 (°C)	Tg_2 (°C)
Poly(DEVBP-b-PFS)	313	342	40	90
Poly(VBPA-b-PFS)	180	284	160	110

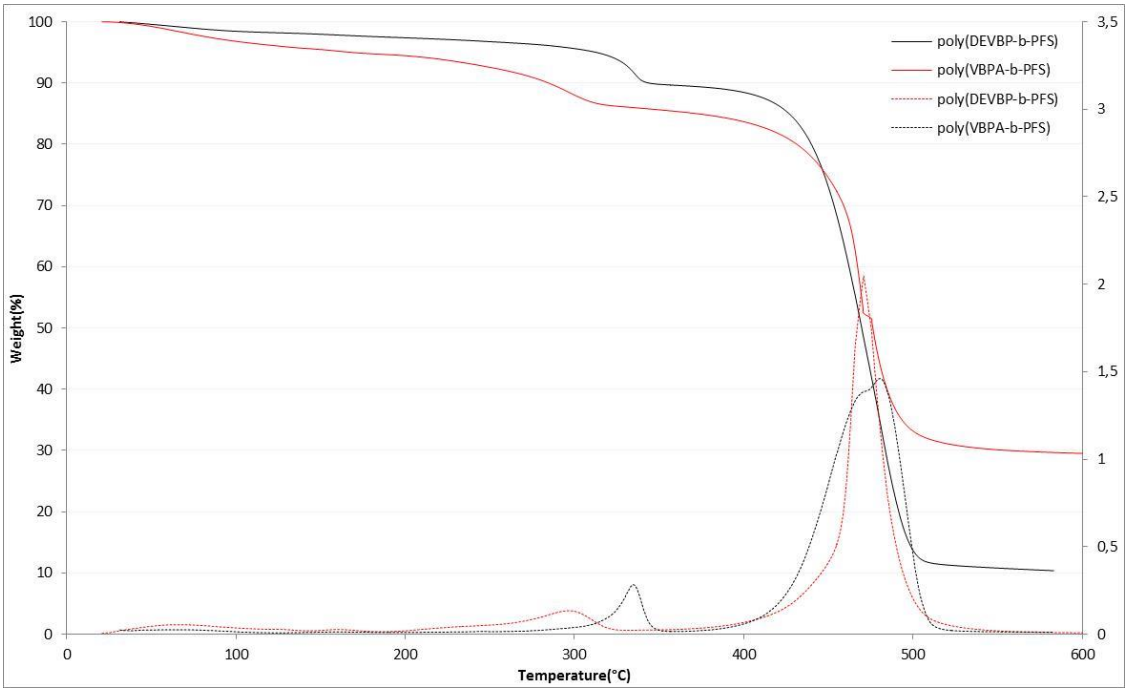

Figure 151 : Thermogram in dynamic mode recorded under nitrogen at 10°C.min-1 of membrane obtained from poly(DEVBP-b-PFS) before and after acidification

Figure 152 shows the DSC traces obtained at 10°C.min^{-1} for the membrane before and after acidification, where two T_g are observed. Tg_1 corresponds to the Tg of the phosphonate block and Tg_2 corresponds to the Tg of the fluorinated block. First of all, the DSC allows to confirm the cleavage of the phosphonate moieties. We previously showed (Chapters II and IV) that acidification reaction led to an increase of the T_g value. For the membrane obtained from poly(DEVBP-b-PFS) the T_g value is 40 °C (Table 5), and after membrane acidification the T_g value increases to about 170 °C. The T_g of the fluorinated block (Tg_2) is also influenced by the acidification step of the membrane since the value increases after acidification. Thus, the presence of two T_g allows to induce phase segregation

between the fluorinated and the phosphonic acid parts, due to their respective hydrophobic/hydrophilic opposite characters.

Figure 152 : DSC curves obtained at 10°C.min-1 for the membrane obtained from poly(DEVBP-b-PFS) before and after acidification

3.3 **Physico-chemical characterizations**

Determination of the Ionic Exchange Capacity (IEC)

The determination of the experimental IEC requires titration of the membranes under mechanical stirring, which leads to destruction of the membrane obtained from poly(DEVBP-*b*-PFS) after acidification. We calculate for this membrane the theoretical IEC instead, by using the molar ratio of each block.

$$IEC_{th} = \frac{\%VBPA * 1000 * n}{\%VBPA * M_1 * \%PFS * M_2}$$

Equation 9 : Determination of the IEC_{th}, with n the acidity number, M_1 molar mass of VBPA and M_2 molar mass of PFS

The theoretical IEC was calculated about 5 meq.g^{-1} by considering two acidities from phosphonic acid groups.

Atomic Force Microscopy (AFM) Observations

Block copolymer morphology was investigated by analyzing surface of membrane using atomic force microscopy (AFM). Figure 153 shows the analyses obtained by the tapping mode AFM. In order to determine the effect of the temperature on the membrane morphologies, AFM observations have been realized on membranes which annealed at different temperature:

-100°C: temperature which is lower than the Tg of the two blocks of the copolymer poly(VBPA-*b*-PFS) (Figure 153 A);

-130°C: temperature between Tg_1 et Tg_2. (Figure 153 B);

-160°C: higher temperature (or equal) than the two Tg (Figure 153 C);

-190°C: higher temperature than the two Tg, resulting in a slight degradation of the polymer (Figure 153 D).

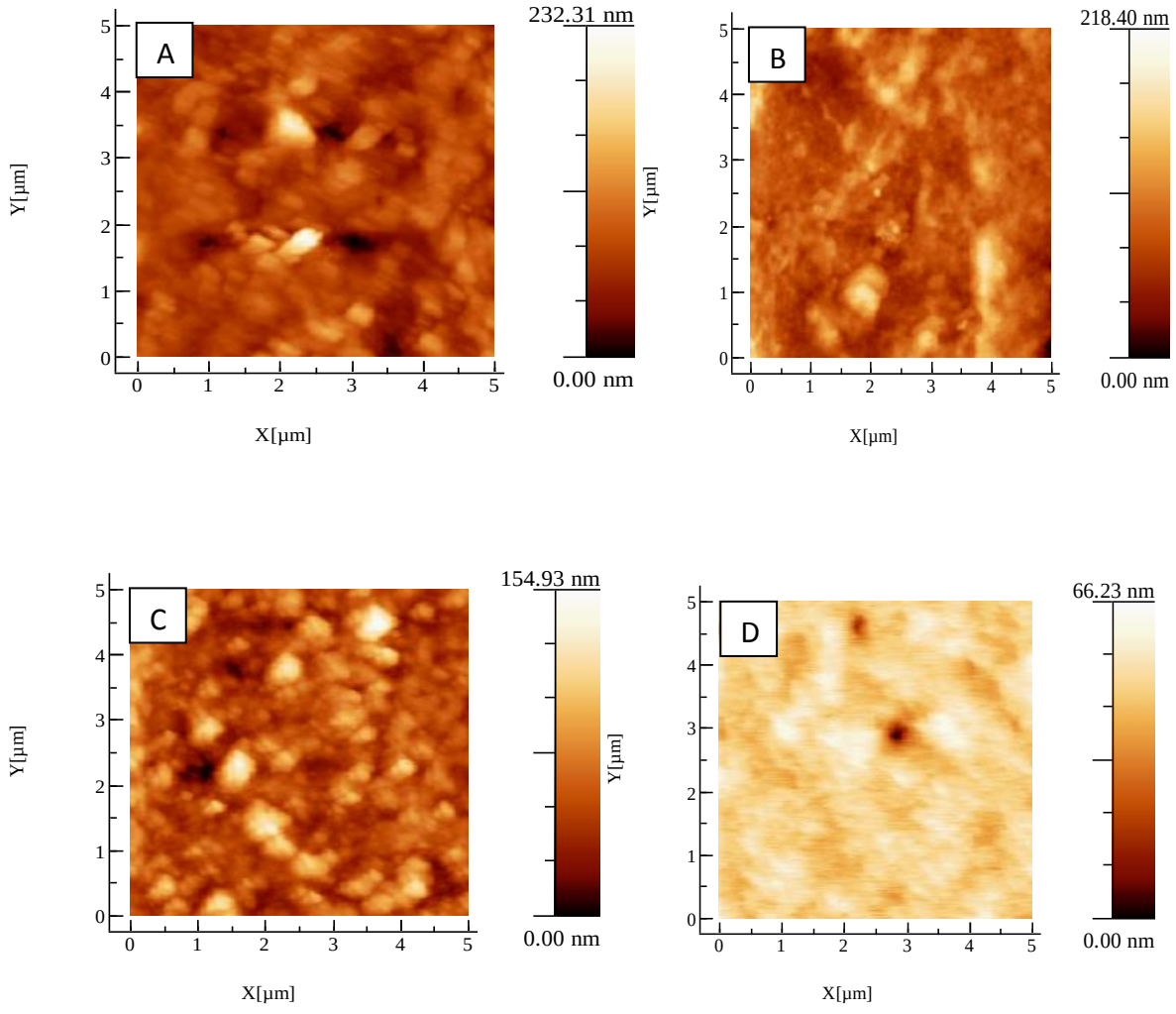

Figure 153 : AFM observation. A) Dry block copolymer, B) block copolymer annealing at 100°C, C) block copolymer annealing at 150°C, D) block copolymer annealing at 190°C

From the Figure 153, the effect of the temperature on the surface morphology can be determined. Indeed, the increase of the annealing temperature causes a change in surface roughness. Figure 153 shows a very low contrast. This low contrast means that the rough patch of the membrane surface is very low. However, when the annealing temperature was increased to 130°C then 160° ° (Figure 153 B et Figure 153 C), an increase of the contrast was observed. So when the annealing temperature is higher than the Tgs of block polymer, the structuration of the membrane is better. Indeed, the membrane is cast whereas the phosphonated groups are under the ester form. So as the difference between the hydrophobic/hydrophilic characters was not very high, the phase segregation is very weak. The acidification of the phosphonated groups increases the difference of the hydrophobic/hydrophilic characters of each block. But the mobility is weak, so the AFM observation shows a high degree of phase mixing (Figure 153 A). However, when the annealing temperature is higher than the Tgs the copolymer mobility is enhanced. Thus, a phase separation can be observed. But an annealing temperature around 190°C implies a deterioration of the membrane structuration. Indeed, the degradation of the block copolymer starts.

These observations have allowed to demonstrate that when membranes' acidification was realized after the casting, it is necessary to apply an annealing treatment higher than the Tgs in order to permit the membrane structuration. The difference of hydrophobic/hydrophilic character between the fluorinated part and the phosphonated part respectively, allows to obtain a phase segregation in the materials. This structuration should allow to increase the proton conductivity of the membrane. However, to confirm these results, the structure of the material must also be present at the heart of the material. To do this, we will make observations using transmission electron microscopy.

4 Conclusion

The RAFT polymerization technique has allowed to synthesize a model block copolymer having a hydrophilic block bearing phosphonic acid group and a hydrophobic block bearing fluorine atoms. The different characterizations realized during the synthesis of the block copolymer have allowed to demonstrate the feasibility of the RAFT polymerization of

phosphonated styrene with a conservation of the living character of this type of technique. Indeed, the synthesis of the second block was achieved by carrying out the polymerization of PFS from the macro-CTA synthesized. The DSC analyzes and AFM observations have put forward phase segregation within the material due to the difference in hydrophobic/hydrophilic character of the two blocks. To confirm this structure, it is necessary to continue the microscopic investigation using TEM observation. This kind of analysis should allow us to observe the internal structure of the material by making cuts.

In this model study, the molecular weight of the synthesized copolymer is too low to consider their use as PEMFC. Future work will therefore be devoted to the production of copolymer having a higher molecular weight. The difficulty of the work is to realize a high molecular weight for the phosphonated block with a conservation of the living character to allow the synthesis of the second block. Indeed, we saw in the introduction to this chapter that the CRP of phosphonated monomers is not easy. That is why, during the polymerization of DEVBP, incorporating small amount of styrene monomer could be used to obtain higher molecular weight while maintaining control and the living character of the CRP.

Moreover, this kind of block copolymer can be used as compatibilizer. Indeed, we saw in Chapter II that the compatibility of the polymers during the cast of blend membrane is very important. Thus, the use of block copolymer having a hydrophobic block with fluorinated and a hydrophilic block carrying protogenic phosphonic acid group could be very interesting.

5 Experimental part

5.1 Materials

Sodium hydride, diethylphosphite, 4-vinylbenzyl chloride, pentafluorostyrene sodium iodide, tetrahydrofuran, ethyl acetate, trifluorotoluene, were purchased from Aldrich. All reactants were used wiyhout purification except fot the THF, which was dried prior to use.

5.2 DiEthyl Vinyl Benzyl Phosphonate (DEVBP)

In a two-neck round bottom flask equipped with a magnetic stirrer, sodium hydride (NaH) was suspended in THF at 0°C. Then diéthylphosphite was added drop wise. The mixture was allowed to come to RT and then transferred by cannula to a solution of 4-Vinylbenzyl chloride and sodium iodide (NaI) in THF. The solution turned from pale yellow to orange. The mixture was stirred overnight. Salts were precipitated by the addition of ethyl acetate, and the mixture was filtered through celite. Volatiles were removed, and the residue was purified by flash chromatography. The product was isolated as a pale yellow oil (18g, 94%).

As an example, in a 250 mL, two-neck round bottom flask equipped with a magnetic stirrer, NaH (50% in grease, 3.26g, 81.5mmol) was suspended in THF (85mL) at 0°C. Then diéthylphosphite (12.65mL, 81.5mmol) was added drop wise. The mixture was allowed to come to RT, and then transferred by cannula to a solution of 4-Vinylbenzyl chloride (12.5g, 81.5mmol) and NaI (1.22g, 8.15mmol) in THF (85 mL). The solution turned from pale yellow to orange. The mixture was stirred overnight. Salts were precipitated by the addition of ethyl acetate, and the mixture was filtered through celite. Volatiles were removed, and the residue was purified by flash chromatography (hexane/ethyl acetate: 1/100).

Structure:

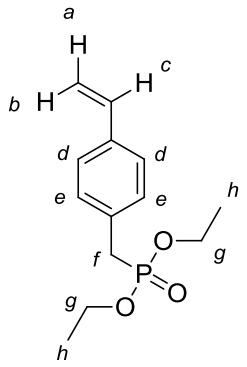

Mass yield : 94%

^{1}H NMR (400MHz, 297K, $CDCl_3$, ppm) δ: 7.06 (d, 2H, H_e), 6.99 (dd, 2H, H_d), 6.39 (dd, 1H, H_c), 5.43, d, 1H, H_a), 4.93 (d, 1H, H_b), 3.73 (m, 4H, H_g), 2.86 (d, 2H, H_f), 0.95 (t, 6H, H_h).

5.3 **poly(Diethylvinylbenzylphosphonate) (poly(DEVBP))**

In a two-neck round bottom flask equipped with a magnetic stirrer, DEVBP, CTA, AIBN and TFT were introduced under an inert atmosphere. Then, the reaction was allowed to 75°C. After 15h, the mixture was allowed to come to RT. The gel formed was dissolved with a minimum CH_2Cl_2 and precipitated in a big volume of hexane. The operation is repeated twice. The isolated product was dried under vacuum at 60°C 12h. The orange product was obtained with a mass yield of 56%.

As an example, 1 equivalent of DEVBP (3g, 14.4 mmol), 0.025 equivalent of CTA (0.10g, 0.35 mmol), 0.005 equivalent of AIBN (0.011g, 0.07mmol) and TFT (5 mL) were introduced in a two-neck round bottom flask of 25mL equipped with a magnetic stirrer under an inert atmosphere. Then, the reaction was allowed to 75°C. After 15h, the mixture was allowed to come to RT. The gel formed was dissolved with a minimum CH_2Cl_2 (around 10mL) and precipitated in a big volume of hexane (around 500mL). The operation is repeated twice. The isolated product was dried under vacuum at 60°C 12h. The orange product was obtained with a mass yield of 56%.

Structure:

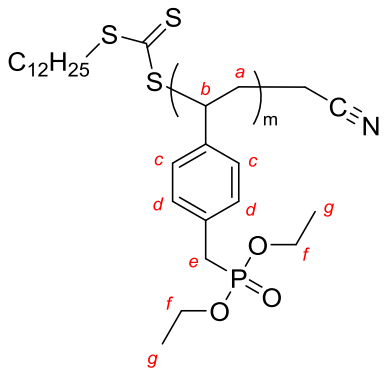

Mass yield: 56%

Glass transition temperature (Tg): 40°C

Number average molecular mass (M_n) ≈ 5,800 g.mol^{-1}

Mass average molecular mass (M_w)≈ 7,540 g.mol^{-1}

Polydispersity indices (Ip): 1.3

^{1}H NMR (400MHz, 297K, $CDCl_3$, ppm) δ: 6.7 to 7.2 (m, 2H, H_c); 6.2 to 6.5 (m, 2H, H_d); 3.85 (m 4H, H_f); 2.8 to 3.2 (m, 2H, H_e), 1.3 to 1.8 (m, 3H, H_a and H_b), 1.15 (m, 6H, H_g)

^{31}P NMR {^{1}H} (160MHz, 297K, $CDCl_3$, ppm) δ: 27 (s, 1P)

5.4 poly(Diethylvinylbenzylphosphonate-*bloc*-pentafluorostyrene) poly(DEVBP-*b*-PFS)

In a two-neck round bottom flask equipped with a magnetic stirrer, PFS, macro-CTA, AIBN and TFT were introduced under an inert atmosphere. Then, the reaction was allowed to 75°C. After 15h, the mixture was allowed to come to RT. The gel formed was dissolved with a minimum CH_2Cl_2 and precipitated in a big volume of hexane. The operation is repeated twice. The isolated product was dried under vacuum at 60°C 12h. The orange product was obtained with a mass yield of 58%.

As an example, 1 equivalent of PFS (3g, 15.4 mmol), 0.023 equivalent of macro-CTA (2.03g, 035 mmol), 0.005 equivalent of AIBN (0.011g, 0.07mmol) and TFT (5 mL) were introduced in a two-neck round bottom flask of 25mL equipped with a magnetic stirrer

under an inert atmosphere. Then, the reaction was allowed to 75°C. After 15h, the mixture was allowed to come to RT. The gel formed was dissolved with a minimum CH_2Cl_2 (around 10mL) and precipitated in a big volume of hexane (around 500mL). The operation is repeated twice. The isolated product was dried under vacuum at 60°C 12h. The orange product was obtained with a mass yield of 58%.

Structure:

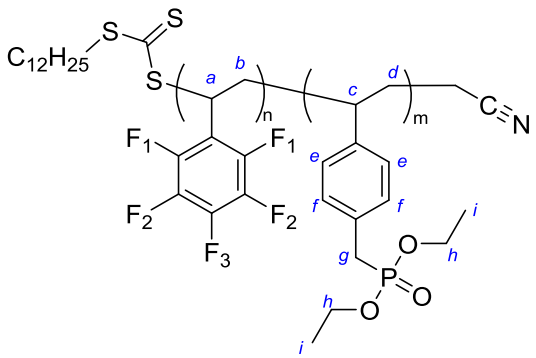

Mass yield: 58%

Glass transition temperature of phosphonated block (Tg_1): 40°C

Glass transition temperature of fluorinated block (Tg_2): 90°C

Number average molecular mass (M_n) ≈ 11,000 $g.mol^{-1}$

Mass average molecular mass (M_w) ≈ 17.600 $g.mol^{-1}$

Polydispersity indices (Ip): 1.6

^1H NMR (400MHz, 297K, $CDCl_3$, ppm) δ: 6.7 to 7.2 (m, 2H, H_e); 6.2 to 6.5 (m, 2H, Hf); 3.85 (m 4H, H_h); 2.8 to 3.2 (m, 2H, H_e), 2.70 and 2.25 (m, 1H, H_a), 1.85 (m, 2H, H_b), 1.65 (m, H, H_c), 1.15 to 1.3 (m, 8H, H_i and H_j)

^{31}P NMR {^1H} (160MHz, 297K, $CDCl_3$, ppm) δ: 27 (s, 1P)

^{19}F NMR {^1H} (377 MHz, 297K, $CDCl_3$, ppm) δ: -142 to -144 (m, 2F, F_1), -154 (m, 1F, F_3), -161 (m, 2F, F_2).

6 Casting and acidification of membrane.

A specific amount of poly(DEVBP-*b*-*PFS*) was dissolved in DMF (30 wt%), the solution was stirred several hours at 50°C. After the poly(VDF-*co*-CTFE) was fully dissolved, the solution was cast onto glass plate, and then dried at 80°C during 24 h.

To obtain the phosphonic acid groups, membranes were immerged in an HCl concentrated solution (12N) at 90°C during 3 days. After reaction, membranes were washed by deionized water, and then dried under vacuum at 80°C during one night.

7 References

1. Perrin, R.; Elomaa, M.; Jannasch, P., Nanostructured Proton Conducting Polystyrene−Poly(vinylphosphonic acid) Block Copolymers Prepared via Sequential Anionic Polymerizations. *Macromolecules* **2009,** *42* (14), 5146-5154.
2. Sciannamea, V.; Jerome, R.; Detrembleur, C., In-Situ Nitroxide-Mediated Radical Polymerization (NMP) Processes: Their Understanding and Optimization. *Chemical Reviews* **2008,** *108* (3), 1104-1126.
3. Matyjaszewski, K.; Xia, J., Atom Transfer Radical Polymerization. *Chemical Reviews* **2001,** *101* (9), 2921-2990.
4. Perrier, S.; Takolpuckdee, P., Macromolecular design via reversible addition–fragmentation chain transfer (RAFT)/xanthates (MADIX) polymerization. *Journal of Polymer Science Part A: Polymer Chemistry* **2005,** *43* (22), 5347-5393.
5. Tonnar, J.; Pouget, E.; Lacroix-Desmazes, P.; Boutevin, B., Synthesis of poly(vinyl acetate)-b-poly(dimethylsiloxane)-b-poly(vinyl acetate) triblock copolymers by iodine transfer polymerization. *Eur. Polym. J.* **2008,** *44* (Copyright (C) 2013 American Chemical Society (ACS). All Rights Reserved.), 318-328.
6. Destarac, M.; Van, G. E.; Dupuis, P.; Vila, X., MADIX polymerization of vinyl phosphonates. *Polym. Prepr. (Am. Chem. Soc., Div. Polym. Chem.)* **2008,** *49* (Copyright (C) 2013 American Chemical Society (ACS). All Rights Reserved.), 173-174.
7. Markova, D.; Kumar, A.; Klapper, M.; Müllen, K., Phosphonic acid-containing homo-, AB and BAB block copolymers via ATRP designed for fuel cell applications. *Polymer* **2009,** *50* (15), 3411-3421.
8. Kumar, A.; Pisula, W.; Markova, D.; Klapper, M.; Müllen, K., Proton-Conducting Poly(phenylene oxide)–Poly(vinyl benzyl phosphonic acid) Block Copolymers via Atom Transfer Radical Polymerization. *Macromolecular Chemistry and Physics* **2012,** *213* (5), 489-499.
9. Ribaut, T.; Lacroix-Desmazes, P.; Fournel, B.; Sarrade, S., Synthesis of gradient copolymers with complexing groups by RAFT polymerization and their solubility in supercritical CO2. *Journal of Polymer Science Part A: Polymer Chemistry* **2009,** *47* (20), 5448-5460.
10. Gudipati, C. S.; Tan, M. B. H.; Hussain, H.; Liu, Y.; He, C.; Davis, T. P., Synthesis of Poly(glycidyl methacrylate)-block-Poly(pentafluorostyrene) by RAFT: Precursor to Novel Amphiphilic Poly(glyceryl methacrylate)-block-Poly(pentafluorostyrene). *Macromolecular Rapid Communications* **2008,** *29* (23), 1902-1907.
11. Riedel, M.; Stadermann, J.; Komber, H.; Simon, F.; Voit, B., Synthesis, post-modification and self-assembled thin films of pentafluorostyrene containing block copolymers. *European Polymer Journal* **2011,** *47* (4), 675-684.
12. Canniccioni, B.; Monge, S.; David, G.; Robin, J.-J., RAFT polymerization of dimethyl(methacryloyloxy)methyl phosphonate and its phosphonic acid derivative: a new opportunity for phosphorus-based materials. *Polym. Chem.* **2013,** *4* (Copyright (C) 2013 American Chemical Society (ACS). All Rights Reserved.), 3676-3685.
13. Boutevin, B.; Hamoui, B.; Parisi, J.-P.; Améduri, B., Homopolymerization and copolymerization of salt formed from a new diethyl styrenic phosphonate monomer. *European Polymer Journal* **1996,** *32* (2), 159-163.

14. Frantz, R.; Durand, J.-O.; Carré, F.; Lanneau, G. F.; Bideau, J. L.; Alonso, B.; Massiot, D., Synthesis and Solid-State NMR Studies of P-Vinylbenzylphosphonic Acid. *Chemistry – A European Journal* **2003,** *9* (3), 770-775.
15. Moad, G.; Rizzardo, E.; Thang, S. H., Living radical polymerization by the RAFT process-A first update. *Aust. J. Chem.* **2006,** *59* (Copyright (C) 2013 American Chemical Society (ACS). All Rights Reserved.), 669-692.
16. David, G.; Boyer, C.; Tayouo, R.; Seabrook, S.; Ameduri, B.; Boutevin, B.; Woodward, G.; Destarac, M., A Process for Polymerizing Vinyl Phosphonic Acid with C6F13I Perfluoroalkyl Iodide Chain-Transfer Agent. *Macromolecular Chemistry and Physics* **2008,** *209* (1), 75-83.
17. Kaltbeitzel, A.; Schauff, S.; Steininger, H.; Bingöl, B.; Brunklaus, G.; Meyer, W. H.; Spiess, H. W., Water sorption of poly(vinylphosphonic acid) and its influence on proton conductivity. *Solid State Ionics* **2007,** *178* (7–10), 469-474.

General conclusion

And

Prospective

1 General Conclusion

The previous work realized in the laboratory about the synthesis of new fluorinated copolymer carrying phosphonic acid groups allowed to obtain a new polyelectrolyte membrane from the poly(CTFE-*alt*-VEPA). The performances of this new membrane were rather interesting since a high thermal and chemical stability were obtained, as well as reasonable values of proton conductivity. However, this membrane possesses very weak mechanical properties. Based on these results the "Agence National de la Recherche" has financed the MemFOS project, which aims at developing new fluorinated copolymer carrying phosphonic groups from the initial poly(CTFE-*alt*-VEPA). The membranes obtained from these copolymers will need to possess high mechanical properties and a controlled swelling. Different strategies have been used to achieve this objective.

In the chapter II, new polymer electrolyte membranes have been prepared from a blend strategy of poly(VDF-*co*-CTFE) and poly(CTFE-*alt*-DEVEP) containing phosphonic acid groups. These blend membranes exhibit the same thermal stability than the M-100 (i.e. cast only from the poly(CTFE-*alt*-VEPA)). However, the oxidative stability and the mechanical properties of the blend membranes are better. The decrease of the inter-cluster distance in the blend membranes allows to facilitate the proton transport. Thus, in comparison with the M-100 membrane, the conductivity of the blend membranes is in the same order of magnitude, whereas the IEC of the blend membranes are twice lower. Proton conductivity (40 $mS.m^{-1}$ at 80°C), thermal stability (measured at 140°C), thickness (around 30 micrometers) and good mechanical properties of M-50 and M-65 membranes allowed to use these materials as membranes for PEMFC. The fuel cell performance shows the importance of the membrane/electrode affinity. However, the miscibility of the two polymers remains partial and during the synthesis of the membrane and in particular during the acidification protocol, we observe coloration of the acid solution. This degradation of the phosphonated copolymer implies a loss of phosphonic acid groups. So, in order to increase of the acid stability for the phosphonated polymer, which can allow an increase of proton conductivity, a crosslinking strategy was then employed.

To perform the crosslinking of the fluoro-phosphonated copolymer, it seemed interesting to use a new crosslinking technique. To this aim models terpolymers were synthesized, which allowed the implementation of a cross-linking technique by a simple heat treatment (150°C, 12h). The synthesis of terpolymer from chlorotrifluoroethylene (CTFE), ethyl vinyl ether (EVE) and vinyl ether carrying sulfonate group led us to obtain chemically cross-linked polymer. The different characterizations realized confirmed the crosslinking reaction efficiency of the terpolymers. We have also showed that the sulfonate groups had an influence on the crosslinking reaction. In order to realize the crosslinking of the fluoro-phosphonated terpolymer, we showed that mesylate groups were better cross-linkable groups than the tosylate ones. The kind of chemical bond formed during the crosslinking reaction seems to be ether bonds (and cetone bonds in the case of the use of mesylate groups). However, the mechanism is not clearly identified yet.

So, from this new cross-linkable technique, new polymer electrolyte membranes have been realized from a pseudo semi-IPN strategy between a cross-linkable fluoro-phosphonated copolymer and a commercially available fluorinated copolymer. This new method can also easily be applied to the fluorinated copolymer carrying phosphonated groups. These membranes exhibit similar thermal and mechanical properties than the blend membranes presented in Chapter II. But thanks to the crosslinking reaction, the oxidative stability was really enhanced compared to the blend membranes. Thus, in comparison with the M-100 membrane (with only the poly(CTFE-*alt*-VEPA)), the conductivity of the membranes is in the same order of magnitude, whereas the IEC of the blend membranes are twice lower. In other hand, the stability of the crosslinkable membrane in the acid medium is enhanced, and this better stability implies a better reproducibility of the result during proton conductivity tests.

To conclude, with these kinds of membranes, the main goals of the MemFOS project are achieved. Indeed, from the poly(CTFE-*alt*-VEPA), membrane with high thermal, oxidative and mechanical properties have been realized. Furthermore, these membranes possess reasonable proton conductivity. Thus, all these works led to the redaction of two articles and one Patent.

Another aim of the MemFOS project concerned the elaboration structured fluoro-phosphonated copolymer. To do this, a RAFT strategy has been envisaged. The Controlled Radical Polymerization (CRP) of phosphonated monomer is a real challenge. The RAFT polymerization technique has allowed to synthesize a model block copolymer having a hydrophilic block bearing phosphonic acid group and a hydrophobic block bearing fluorine atoms. The different characterizations realized during the synthesis of the block copolymer have allowed to demonstrate the feasibility of the RAFT polymerization of phosphonated styrene with a conservation of the living character of this type o f technique. The DSC analyzes and AFM observations have put forward phase segregation within the material due to the difference of hydrophobic/hydrophilic character of the two blocks. Thus, the strategy to obtain block copolymers from phosphonated and fluorinated monomers is approved. The next work will relate to the synthesis of high molecular weight block copolymers in order to perform proton exchange membranes

2 Further Investigation

Lots of further investigations can be realized in short and long term. Although most of the potential of the poly(CTFE-*alt*-VEPA) has been demonstrated, different points can be also improved, especially for the pseudo semi-IPN membranes. Indeed, the proton conductivity of the pseudo semi-IPN membrane is twice lower than the blend membrane. The crosslinking reaction increases the densification of the polymer network, so the accessibility of the phosphonic acid groups is decreased. In order to enhance the proton conductivity of these membranes, we could perform the synthesis of the terpolymers with only 2 or 3 mol% of cross-linkable monomer in the composition of the poly[(CTFE-*alt*-DEVEP)-*co*-(CTFE-*alt*-BVEMs)], in order to increase the access of the phosphonic acid groups.

Concerning the crosslinking reaction, the mechanism and the kind of bond which occurs during the reaction was not clearly identified. It will be necessary to continue our investigation. To do this, we must synthesize new models molecules, which possess higher thermal stability so a higher boiling point. For instance, we could use aromatic molecules such as the benzyl alcohol.

The RAFT strategy allowed us to synthesize new block copolymers with hydrophobic and hydrophilic parts. In this model study, the molecular weight of the synthesized polymer is too small to consider their use as PEMFC. Future work will therefore be devoted to the production of copolymers having higher molecular weight. To do this, during the polymerization of DEVBP, incorporating small amounts of styrene monomer could be used to obtain higher M_w while maintaining control of the polymerization as well as the living character of the CRP.

A graft copolymer synthesis is also in progress by using a click strategy from a phosphonated copolymer and a fluorinated grafting group. In order to do this, the phosphonated copolymer will be obtained by the copolymerization between a phosphonated styrene monomer and a styrene monomer carrying an alkyne function. The use of the Huisgen cycloaddition between this copolymer and a poly(VDF) carrying azide group allows us to obtain graft copolymer.

Equipment used

Nuclear magnetic resonance (NMR)

^{1}H, ^{19}F, ^{31}P NMR spectra were realized at room temperature on a Brüker AC 400 MHz in chloroform ($CDCl_3$), acetone (Acetone-d_6) and dimethylsulfoxide (DMSO-d_6) as deutered solvent. All ^{19}F and ^{31}P have been recorded with proton decoupling. Chemical shift (δ) were expressed in parts-per-million (ppm). The intern reference in ^{1}H NMR is the tetramethylsilane (TMS); in ^{19}F is trichlorofluoromethane ($CFCl_3$); and in ^{31}P is the orthophophosric acid.

Fourier transform infrared spectroscopy

The FTIR instrument used was a Nicolet Nexus. The polymers are analyzed in theform of very thin membranes. The analysis is performed in absorbance mode.

Thermal analysis

The thermal stability of the different blend membranes was evaluated from thermogravimetric analysis (TGA) on a Q50 analyzer from TA Instruments. The data were collected from 25 to 600°C. The samples were analyzed both under a nitrogen atmosphere at a heating rate of 20°C.min^{-1}. Differential scanning calorimetry (DSC) measurements were carried out using a Perkin-Elmer Pyris 1 apparatus. Scans were recorded at a heating/cooling rate of 20°C min^{-1} from -100 to 150°C. A second scan was required for the assessment of the Tg, defined as the inflection point in the heat capacity jump.

Mechanical properties

Dynamic-mechanical analysis (DMA) was conducted with a METRAVIB DMA 25. Uniaxial stretching of samples were performed while heating at a rate of 2°C/min from -100 to 150°C,

keeping frequency at 1 Hz (viscoelastic region) and a constant deformation rates. The glass transition temperature was obtained from tanδ determination. It has been shown that tanδ maximum relates much better to the value obtained by DSC. Furthermore, the mechanical behavior was studied versus the RH range between 0 and 80% and in the temperature range between 25 and 70°C.

Proton conductivity

The proton conductivity was evaluated by electrochemical impedance spectroscopy (EIS) using MATERIALS MATES 7260 dielectric analyzer with high and low frequencies compensations in order to take into account cables and connections effects. The temperature and humidity were controlled by FUMATEC MK3 device with three heating areas. The FUMATEC cell was composed by two parallel wires electrodes of platinum separated by 10mm.

Before conductivity measurements, membranes were previously stored 24 hours in deionised water at room temperature. Measurements were carried out in wet state membranes (5 x 20 mm). The proton conductivity was measured between 20 and 80°C with sample completely immerged in water. Impedance data were gathered over the frequency range of 10^{-1} – 10^{7} Hz at voltage amplitude of 100 mV and were analyzed with the MATERIALS MATES software. A typical impedance diagram measured with the EIS cell is presented below. The proton conductivity (σ) was calculated following the equation:

$$\sigma = \frac{d}{e \times L \times R}$$

Where d is the distance between the two electrodes

e is the thickness of the wet membrane

L is the larger of the wet membrane

R is the diameter of the half-circle in the impedance diagram Z', -Z"

SYNTHESIS AND CHARACTERIZATIONS OF NEW FLUORINATED MEMBRANES BEARING PENDANT PHOSPHONIC ACID GROUPS FOR PEMFC APPLICATION

Résumé

Ce travail de thèse s'inscrit dans la continuité des travaux de recherche réalisés sur le développent de nouvelles membranes échangeuses de protons pour piles à combustibles de type PEMFC, porteuses de groupements protogènes acides phosphoniques. L'objectif de ces travaux est d'apporter des solutions permettant l'amélioration des propriétés physico-chimiques d'un copolymère phosphoné, le poly(CTFE-*alt*-VEPA) obtenu à partir de la polymérisation radicalaire de vinyl éthers et de CTFE. La première stratégie employée est une stratégie Blend. Elle consiste à ajouter un polymère fluoré commercial, le poly(VDF-*co*-CTFE), lors de la mise en forme de la membrane. Les membranes ainsi obtenues montrent d'excellentes propriétés mécaniques et des valeurs de conductivité protonique acceptables. Cependant, lors de l'acidification du polymère phosphoné, une légère dégradation est observée. Une nouvelle technique de réticulation a alors été mise en place afin d'augmenter la stabilité vis-à-vis des acides. La réticulation de ces membranes blend a de plus permis d'améliorer la miscibilité entre le polymère fluoré et le polymère phosphoné. Enfin, les derniers travaux de cette thèse concernent la synthèse de copolymères à bloc à partir d'une stratégie RAFT. Ainsi la polymérisation radicalaire contrôlée de monomère phosphoné a pu être réalisée.

Mots Clé :

Pile à combustible, blend, réticulation, acide phosphoniques, polymérisation RAFT.

Abstract

This work is a continuation of research conducted on the development of new proton exchange membrane fuel cell (PEMFC), bearing phosphonic acid as protogenic groups. The aim of this work is to provide solutions with a view to improving the physicochemical properties of a phosphonate copolymer, poly(CTFE-*alt*-VEPA) obtained from the radical polymerization of vinyl ethers and CTFE. The first strategy used is a Blend strategy. It consists of adding a commercial fluorinated copolymer, poly(VDF-*co*-CTFE), during the casting of the membrane. The membranes thus obtained show excellent mechanical properties and acceptable values of proton conductivity. However, during the acidification of membrane, a slight degradation of the phosphonate copolymer is observed. A new technique of crosslinking was then established to increase the stability versus acids. The crosslinking of the blend membranes has also helped to improve the miscibility between the fluorinated copolymer and phosphonate polymer. Finally, the last work of this thesis relate to the synthesis of block copolymer from a RAFT strategy. Thus, the controlled radical polymerization of phosphonated monomer was achieved.

Key words:

Fuel cell, blend, crosslinking, phosphonic groups, RAFT polymerization.